UNIVERSIDAD DE SEVILLA

DEPARTAMENTO DE QUÍMICA INORGÁNICA

Procesos de oxidación selectiva catalizados por complejos metálicos en medios no convencionales: hacia una química sostenible

DOCTORANDO

MATTHEW HERBERT

Sevilla, 2009

Procesos de oxidación selectiva catalizados por complejos metálicos en medios no convencionales: hacia una química sostenible

por

Matthew Herbert

Trabajo presentado para aspirar al
Título de Doctor por la Universidad de Sevilla

FDO: MATTHEW HERBERT

Los directores:

FDO.: Francisco Montilla Ramos
Profesor Titular de Universidad

FDO.: Agustín Galindo del Pozo
Catedrático de Universidad

Índice

Índice

Lista de abreviaturas utilizadas

AcO	Acetato
acac	Acetilacetonato
bpy	2,2’-Bipiridina
$bpyO_2$	2,2’-Bipiridina-N,N’-dióxido
col	2,4,6-Colidina (2,4,6-trimetilpiridina)
colO	2,4,6-Colidina-N-óxido
Cp	Ciclopentadienilo
DMF	Dimetilformamida
dmpz	3,5-Dimetilpirazol
DMSO	Dimetilsulfóxido
GO	Galactosa oxidasa
HMPA	Hexametilfosforamida
IL	Líquido iónico
im	Imidazol
LDA	Diisopropilamiduro de litio
lut	2,6-Lutidina (2,6-dimetilpiridina)
lutO	2,6-Lutidina-N-óxido
mCPBA	Ácido *meta*-cloroperbenzoico
3mpz	3-Metilpirazol
MTO	Metiltrioxorenio
NHC	Carbeno N-heterocíclico
2pc	2-Picolina (2-metilpiridina)
2pcO	2-Picolina-N-óxido
3pc	3-Picolina (3-metilpiridina)
3pcO	3-Picolina-N-óxido
4pc	4-Picolina (4-metilpiridina)
4pcO	4-Picolina-N-óxido
PDMS	Polidimetilsiloxano
phen	1,10-Fenantrolina
PTC	Agente de transferencia de fase
py	Piridina

pyO	Piridina-N-óxido
pz	Pirazol
RTIL	Líquido iónico a temperatura ambiente
salen	2,2'-Etileno-bis(nitrilometilideno)difenol
salox	Salicilaldoxim
$scCO_2$	Dióxido de carbono supercrítico
SCF	Fluido supercrítico
scH_2O	Agua supercrítica
TBHP	Terbutil hidroperóxido
TEA	Trietilamina
THF	Tetrahidrofurano
TOF	Frecuencia del cíclo catalítico “Turnover frequency”
TON	Número de cíclos catalíticos “Turnover number”
TSIL	Líquido iónico con función específica
UHP	Aducto urea-peróxido de hidrógeno
VOC	Compuesto orgánico volátil
4VP	4-Vinilpiridina
XRD	Difracción de Rayos X

Abreviaturas empleadas para las sales de imidazolio

$C_n$mim-X

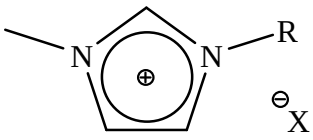

R = *n*-$C_nH_{(2n+1)}$

X = Anion

Ejemplos:

C_4mim-BF_4	Tetrafluoroborato de 1-*n*-butil-3-metilimidazolio
C_8mim-Br	Bromuro de 1-*n*-octil-3-metilimidazolio
C_{12}mim-PF_6	Hexafluorofosfato de 1-*n*-dodecil-3-metilimidazolio

Abreviaturas empleadas en los espectros de RMN

s	singlete	q	cuartete
d	doblete	a	ancho
t	triplete	m	multiplete

Objetivos

La presente memoria pretende efectuar una contribución en el área de la Química Verde o Química Sostenible en lo que se refiere a la utilización de medios no convencionales como disolventes en Catálisis Homogénea. En concreto, se ha investigado el empleo de dióxido de carbono supercrítico y de líquidos iónicos en las reacciones de oxidación selectiva de olefinas y alcoholes catalizadas por complejos metálicos fácilmente accesibles. En este contexto se plantearon los siguientes objetivos generales del proyecto de Tesis:

- Desarrollar procedimientos de síntesis que permitan la incorporación de grupos "*CO_2-fílicos*" a ligandos de tipo N-heterociclo. Esto conllevaría una modificación de la solubilidad de los complejos metálicos a los que se coordinara. En particular, se favorecería la solubilización de los mismos en disolventes de baja polaridad como el dióxido de carbono supercrítico.
- Evaluar la actividad catalítica de complejos metálicos del tipo oxoperoxomolibdeno u oxoperoxorenio con ligandos N-heterociclo modificados en reacciones de oxidación selectiva de olefinas usando H_2O_2 como oxidante terminal y dióxido de carbono supercrítico como disolvente.
- Evaluar la actividad catalítica de complejos metálicos de Pd(II) o Cu(II) con ligandos N-heterociclo modificados en reacciones de oxidación selectiva de alcoholes usando O_2 como oxidante terminal y dióxido de carbono supercrítico como disolvente.
- Explorar las condiciones idóneas para llevar a cabo la epoxidación de olefinas en líquidos iónicos utilizando precursores comerciales de molibdeno o renio o complejos de estos metales con ligandos comerciales o poco elaborados.

Relación completa de los compuestos preparados en la presente Memoria:

4-(Polidimetilsiloxaniletil)piridina (**A**)

4-Tridecilpiridina (**B**)

4-(2,2-Bis-trimetilsilanil-etil)piridina (**C**)

2,6-Bis-trimetilsilanilmetil-piridina (**D**)

4,4'-Ditridecil-2,2'-bipiridina (**E**)

4,4'-Bis-(bis-trimetilsilanil-metil)-2,2'-bipiridina (**F**)

4,4'-Bis-(2,2-bis-trimetilsilanil-etil)-2,2'-bipiridina (**G**)

4-Metil-4'-tridecil-2,2'-bipiridina (**H**)

Cloruro de 1-(3,5-dimetilpirazol-1-ilmetil)-3-metilimidazolio (dpmim-Cl)

$[Re(CH_3)(O)_3(\mathbf{A})]$ (**1a**)

$[Re(CH_3)(O)_3(\mathbf{B})]$ (**1b**)

Aducto de $[Mo(O)(O_2)_2(H_2O)_n]$ y **A** (**2a**)

$[Mo(O)(O_2)_2(H_2O)(\mathbf{B}O)]$ (**2b**)

$[Mo(O)(O_2)_2(H_2O)(\mathbf{E})]$ (**2e**)

$[Mo(O)(O_2)_2(H_2O)(\mathbf{F})]$ (**2f**)

$[Mo(O)(O_2)_2(H_2O)(\mathbf{G})]$ (**2g**)

$[Mo(O)(O_2)_2(H_2O)(\mathbf{H})]$ (**2h**)

$[Mo(O)(O_2)_2(H_2O)(2pcO)]$

$[Mo(O)(O_2)_2(H_2O)(3pcO)]$

$[Mo(O)(O_2)_2(H_2O)(lutO)]$

$[Mo(O)(O_2)_2(H_2O)(colO)]$

$[Mo(O)(O_2)_2(H_2O)(pz)]$

$[Mo(O)(O_2)_2(pz)_2]$

$[Mo(O)(O_2)_2(bpyO_2)]$

$[Mo(O)(O_2)_2(phen)]$

$[(O)(O_2)_2Mo(\mu^2\text{-}O)Mo(O)(O_2)_2]^{2-} \cdot 2[colH]^+$

$[Mo_8(O)_{22}(O_2)_4(dmpz)_2]^{4-} \cdot 4[(dmpzH)]^+ \cdot 2H_2O$

$[\{[Mo(O)(O_2)(dmpz)]_2(\mu^2\text{-}O)_2\{Mo(O)_2(O_2)(dmpz)_2\}_2] \cdot CH_2Cl_2$

$[Cu_2(\eta^2\text{-}AcO)_4(4VP)_2]$

$[Cu_2(\eta^2\text{-}AcO)_4(\mathbf{A})_2]$ (**3a**)

$[Pd(OAc)_2(4VP)_2]$

$[Pd(OAc)_2(\mathbf{A})_2]$ (**4a**)

$[Pd(Cl)_2(\mathbf{A})_2]$ (**5a**)

Durante la realización de la Tesis se han publicado los siguientes artículos:

- Catalytic epoxidation of cyclooctene using molybdenum(VI) compounds and urea-hydrogen peroxide in the ionic liquid [bmim]PF_6.
  Catal. Commun., 2007, **8**, 987.
- The use of pyridine-functionalised polydimethylsiloxane polymers as a supercritical carbon dioxide solubilising support for copper compounds.
  Inorg. Chem. Commun., 2007, **10**, 735.
- Methyltrioxorhenium Complexes of Polydimethylsiloxane Functionalised Pyridine as Efficient Olefin Epoxidation Catalysts in Solventless and Low Polar Solvent Conditions.
  Organometallics, 2009, **28**, 2855.
- Olefin epoxidations in the ionic liquid [C_4mim][PF_6] catalysed by oxodiperoxomolybdenum species *in-situ* generated from molybdenum trioxide and urea-hydrogen peroxide. The synthesis and molecular structure of [Mo(O)$(O_2)_2$(4-MepyO)$_2$]$\cdot H_2O$
  Polyhedron, en prensa. (http://dx.doi.org/10.1016/j.poly.2009.09.003)
- Supercritical carbon dioxide, a new medium for aerobic alcohol oxidations catalysed by copper-TEMPO
  Dalton Trans., 2010, **3**, 900.

1 Introducción

1 Introducción

La producción de residuos en los procesos industriales es uno de los problemas ambientales más preocupantes que existen hoy en día en el área de la química. El desarrollo de nuevas metodologías sintéticas, que eliminen o en su caso reduzcan estos residuos, es uno de los objetivos de la llamada *Química Verde* o "*Green Chemistry*",[1] también denominada *Química Sostenible*.

Dentro de los residuos cabe diferenciar entre aquellos que se originan junto con los productos deseados de un proceso químico, como productos secundarios o indeseados,[2] y aquellos que no se recuperan de forma eficiente, como por ejemplo los disolventes orgánicos volátiles que se utilizan en el proceso. El impacto ambiental que tienen estos últimos es considerable. Se ha estimado que aproximadamente el 85% del total de la masa de los productos químicos involucrados en la industria farmacéutica son disolventes y que la eficacia de su reciclado está comprendida en un rango del 50-80%.[3] Por tanto, el rediseño y la sustitución progresiva de aquellos procesos que utilizan disolventes orgánicos por procesos menos contaminantes debe ser otro objetivo básico que se plantee la química en nuestros días[4]. Entre las posibles soluciones al problema de la creación de residuos debidos a los disolventes orgánicos se encuentran las reacciones realizadas en ausencia de disolvente o la utilización de disolventes no convencionales.

1.1 Medios No Convencionales en Química Sostenible

Un disolvente no convencional que pueda considerarse como alternativa al empleo de los disolventes orgánicos típicos (VOCs, *volatile organic compounds*) debe ser poco (idealmente nada) peligroso. Es decir, relativamente no tóxico, no inflamable, no corrosivo, etc. Por otro lado, no puede ser diseminado al medio ambiente en ninguno de los puntos o fases del proceso químico, por lo que además deber ser fácil de reciclar. La eliminación del disolvente del medio de reacción se realiza generalmente por evaporación o destilación y por consiguiente el disolvente debe ser volátil. Esta característica es perjudicial porque el vertido y evaporación de los disolventes orgánicos típicos conduce inevitablemente a fenómenos de polución. Los disolventes no

convencionales, por tanto, tienen que proporcionar procedimientos alternativos que conduzcan a una separación eficiente de los productos de la reacción (y del catalizador en procesos catalizados) y a su reutilización eficaz.

Entre las distintas opciones que se están investigando en la actualidad como alternativa "*verde*" o "*limpia*" a los disolventes orgánicos se encuentran los fluidos supercríticos (SCFs) y los líquidos iónicos (ILs), en algunas ocasiones denominados "disolventes verdes",[5] que constituyen dos de las áreas de estudio más importantes y que más desarrollo están teniendo en las últimas décadas.[6]

En la presente introducción analizaremos en primer lugar brevemente y de forma genérica las características de estos disolventes no convencionales y su aplicación en catálisis homogénea como medios de reacción, para a continuación ir revisando una selección de los antecedentes que existen en la bibliografía sobre reacciones de oxidación de alcoholes y epoxidación de olefinas en fase homogénea y catalizadas por complejos metálicos.

1.1.1 Los fluidos supercríticos (SCFs)

Los SCFs son gases altamente comprimidos que se caracterizan por tener propiedades intermedias entre los gases y los líquidos (Tabla 1.1).[7] En general, presentan densidades propias del estado líquido que les permiten, en muchas ocasiones, disolver sustancias líquidas y sólidas; pero a la vez presentan propiedades típicas del estado gaseoso como, por ejemplo, la alta difusividad o la capacidad de disolver gases en cualquier proporción.

Tabla 1.1.

Fase	**Densidad (kg m^{-3})**	**Viscosidad (cP)**	**Difusividad (mm^2 s^{-1})**
Gas	1	0,01	1-10
SCF	100-800	0,05-0,10	0,01-0,10
Líquido	1000	0,5-1,0	0,001

Entre las ventajas que poseen los SCFs sobre los disolventes típicos se incluyen la posibilidad de ajuste de sus propiedades como disolventes por medio de la temperatura y la presión, su fácil recuperación debido a su volatilidad y la capacidad de extraer compuestos de alto punto de ebullición a bajas temperaturas. Entre las

desventajas se incluyen las altas presiones de trabajo y la energía necesaria para producirlas, que implican la necesidad de un equipamiento especializado y por tanto caro. Se han empleado una gran variedad de sustancias como SCFs,[8] pero por varias razones su uso en la mayoría de los casos no se encuentra todavía muy extendido. Los SCFs usados más frecuentemente son el agua en estado supercrítico, scH_2O, y, sobre todo, el dióxido de carbono en estado supercrítico, scCO_2.[9]

Tabla 1.2. Parámetros supercríticos de varias sustancias

Medio	Temperatura crítica (K)	Presión crítica (bar)
Dióxido de carbono	304,1	73,8
Metano	190,4	46,0
Metanol	512,6	80,9
Etano	305,4	48,8
Etileno	282,4	50,4
Etanol	513,9	61,4
Propano	369,8	42,5
Propileno	364,9	46,0
Acetona	508,1	47,0
Trifluorometano	299,3	48,6
Triclorometano	302,0	38,7
Triclorofluorometano	471,2	44,1
Amoniaco	405,5	113,5
Agua	647,3	221,2
Ciclohexano	553,5	40,7
n-Pentano	469,7	33,7
Tolueno	591,8	41,0

1.1.1.1 El dióxido de carbono supercrítico, scCO_2

El scCO_2 presenta una serie de características que permiten su uso como sustituto de los disolventes orgánicos convencionales. Presenta unas condiciones críticas fácilmente accesibles (T_c = 31,06 ºC, P_c = 73825 bar), es inerte, barato, no presenta toxicidad, no es inflamable, tiene una baja reactividad química, es apolar, y posee una alta dependencia de su capacidad como disolvente con respecto a la densidad. Este hecho puede proporcionar un control preciso sobre las condiciones de reacción y potencialmente altas selectividades, elevadas velocidades de reacción y la posibilidad de una fácil separación de los solutos por simple descompresión.[10]

Estas propiedades le permiten ser utilizado como disolvente no contaminante en diferentes procesos de interés como la extracción (p.e. de principios activos en productos naturales), la preparación y purificación de materiales de alto valor añadido[11] o como medio de reacción. En este último aspecto, son interesantes las aplicaciones en catálisis homogénea,[12] sobre todo aquellas reacciones que involucran gases que, como ya se ha mencionado, son totalmente solubles en el $scCO_2$. Por ejemplo, se ha empleado con éxito en los denominados procesos de oxidación "*limpios*", especialmente en sistemas homogéneos que utilizan catalizadores metálicos y oxígeno o peróxidos como reactivos oxidantes.[13] Las ventajas de estos procesos radican en la total substitución de los disolventes orgánicos, la completa miscibilidad de oxidantes como el oxígeno en $scCO_2$, eliminando problemas de transporte, y la alta resistencia del CO_2 a la oxidación.

No obstante, un problema que se plantea en el desarrollo de compuestos de los metales de transición que pueden actuar como catalizadores homogéneos en $scCO_2$ es la solubilización de dichos complejos en el medio supercrítico. Por esta razón, a pesar de la abundancia de estudios acerca de las reacciones heterogéneas de oxidación y de otras reacciones homogéneas en $scCO_2$, el número de trabajos sobre reacciones homogéneas de oxidación catalizadas en medio $scCO_2$ es bastante reducido.[14] La solución más común para este problema es la incorporación de grupos "*CO_2-fílicos*" en la esfera de coordinación del metal, destacando la funcionalización de los ligandos con grupos fluorados (p.e. cadenas alquílicas perfluoradas).[15] Sin embargo, esta solución puede presentar algunos inconvenientes como son el elevado precio y la difícil preparación de algunos de estos derivados, de ahí que la búsqueda de nuevas alternativas sea hoy día una de las líneas de investigación de mayor interés. A este respecto, cabe citar los trabajos desarrollados recientemente en nuestro grupo de trabajo en los que se introducen grupos trimetilsililo[16] o dendrímeros basados en carbosilanos[17] a ligandos de tipo triarilfosfina o ciclopentadienilo. Esta alternativa origina un aumento de la solubilidad de los correspondientes complejos metálicos sin perturbar esencialmente sus características electrónicas.

1.1.2 Los líquidos iónicos (ILs)

Los ILs son sales con un punto de fusión por debajo de 100 ºC y en particular los denominados RTILs (*Room Temperature Ionic Liquids*) son sales cuyo estado de agregación es líquido a la temperatura ambiente. Esta propiedad los convierte en compuestos potencialmente útiles como disolventes. En particular, los que se han investigado como disolventes para procesos químicos se encuentran típicamente constituidos por un catión orgánico (Figura 1.1, alquilimidazolio, N-alquilpiridinio, tetraalquilamonio, tetraalquilfosfonio, etc.) y un anión inorgánico (por ejemplo, $[PF_6]^-$, $[BF_4]^-$, $[(CF_3SO_2)_2N]^-$, $[CF_3SO_3]^-$, $[CH_3CO_2]^-$, $[CF_3CO_2]^-$, $[NO_3]^-$, $[Al_2Cl_7]^-$, etc.).[18]

Figura 1.1. Cationes comúnmente empleados en los ILs

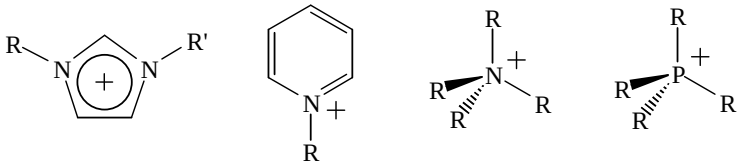

Muchos de los ILs de este tipo presentan propiedades que los hacen idóneos como sustitutos de los disolventes orgánicos convencionales, constituyendo una alternativa "*limpia*" a estos en procesos de catálisis homogénea.[19] La característica más importante es que presentan una presión de vapor muy baja (prácticamente no se evaporan bajo las condiciones típicas de reacción), y por consiguiente se elimina el problema de emisiones de compuestos orgánicos volátiles (VOCs) que conllevan generalmente los procesos que emplean disolventes orgánicos. Los ILs pueden presentar una gran variedad de combinaciones catión-anión con un rango diverso de propiedades, pero generalmente son estables y no son explosivos ni muy inflamables. Cuando actúan como disolventes varias de sus propiedades como la polaridad y la hidrofilia/hidrofobia pueden ser moduladas a través de la adecuada elección de la combinación catión-anión, lo que les permite ser disolventes muy efectivos con capacidad para disolver una gran variedad de especies orgánicas o inorgánicas. En bastantes ocasiones, se observa que muestran una buena capacidad para disolver compuestos inorgánicos, que son insolubles en los disolventes orgánicos comunes. Esta propiedad es muy interesante ya que ofrece la posibilidad de "*inmovilizar*" un catalizador (p.e. complejo metálico) en el seno del líquido iónico. El catalizador inmovilizado en el IL puede actuar en procesos

de catálisis homogénea de substratos orgánicos que posteriormente pueden ser extraídos del sistema, permitiendo el reciclado del catalizador. Sin embargo, el uso en la industria de los ILs como disolventes es todavía poco frecuente. Entre los problemas que presentan se pueden citar los precios relativamente elevados de obtención de cantidades industriales de estos disolventes, los resultados de estudios recientes sobre sus toxicidades, los problemas de su pobre biodegrabilidad y su impacto en el medioambiente.[20] En los últimos años han aparecido en la bibliografía numerosas publicaciones sobre la aplicación de los ILs como medio de reacción en diversos procesos catalíticos,[21] incluso en el área de la catálisis enantioselectiva.[22] Un objetivo de gran importancia en este campo para el futuro es el desarrollo de sistemas viables a escala industrial.[23]

1.1.3 Sistemas bifásicos $scCO_2$-ILs

Los líquidos iónicos presentan una característica que puede ser muy atractiva desde el punto de vista práctico: son altamente insolubles en $scCO_2$, mientras que el $scCO_2$ presentan una solubilidad notable en algunas de estas sales.[24] Este comportamiento ofrece interesantes posibilidades en procesos catalíticos de naturaleza bifásica, en los cuales los substratos orgánicos sean solubles en $scCO_2$, mientras que el catalizador sea soluble en el líquido iónico. De esta forma, la especie metálica, que actúa como catalizador, podría ser recuperada tras la reacción por simple trasvase de la fase supercrítica, que contendría los productos de la reacción. Con la recuperación y posible reutilización del catalizador, el proceso sería atractivo desde un punto de vista económico y medioambiental. Por otro lado y de forma adicional, estos medios bifásicos IL/$scCO_2$ ofrecen la posibilidad de desarrollar un sistema de reacción en flujo continuo, en el que el catalizador en el IL constituye la fase fija, mientras que el conjunto $scCO_2$/substrato constituye la fase móvil. Una ventaja que tendría dicho sistema en flujo continuo sobre una reacción más convencional empleando un catalizador heterogéneo es la mejor velocidad y selectividad de la reacción homogénea.

1.1.4 Reacciones en ausencia de disolvente

Considerando los principios de la Química Verde, la realización de una reacción química en ausencia de disolvente debería ser la opción más adecuada desde el punto de vista medioambiental. De esta manera se eliminarían los riegos asociados a la toxicidad del disolvente y se mejoraría la economía atómica del proceso. Aunque en la industria química abundan los ejemplos de reacciones en fase gaseosa o que transcurren sin la necesidad de la adición de un disolvente, la utilización de disolventes ha sido práctica habitual en los dos últimos siglos de química sintética, de manera que generalmente en el desarrollo de un nuevo proceso sintético siempre se tiene en mente su realización en disolución. En general, un proceso químico en disolución presenta una serie de características que facilitan la reacción, tales como permitir la homogenización del sistema, controlar la velocidad de la reacción o distribuir uniformemente el calor de reacción, de manera que, en muchos procesos, la eliminación del disolvente no sería práctica. En cualquier caso, la búsqueda de nuevas estrategias y tecnologías que permitan la realización de reacciones en ausencia de disolventes es un objetivo de gran importancia en la química de nuestros días.[25]

El concepto de reacción en ausencia de disolvente presenta algunas controversias.[26] Técnicamente, un proceso en el que uno de los reactivos o catalizador se disuelve en otro reactivo origina una disolución, de manera que dicho reactivo podría considerarse como disolvente de la reacción, en cuyo caso resulta discutible la consideración de reacción en ausencia de disolvente. Igualmente, existen reacciones químicas en las que uno de los componentes se adiciona necesariamente en un disolvente (p. e., el peróxido de hidrógeno en disolución acuosa). En ninguno de estos dos procesos se adiciona un componente cuya única función sea actuar como disolvente. Por consiguiente, en la discusión que se presenta a continuación se considerará que la reacción transcurre en ausencia de disolvente si en ningún momento se adiciona un componente cuya única función sea la de actuar como disolvente.

Dependiendo de la naturaleza de la reacción pueden emplearse diferentes tecnologías y estrategias para facilitar el proceso en ausencia de disolvente. En el caso de reacciones entre productos sólidos suele acudirse al tratamiento mecánico mediante el uso de molinos de bolas[27] entre otras tecnologías[28] (‘*mechanochemistry*’), dando lugar a excelentes resultados en una gran variedad de procesos.[29]

El uso de microondas,[30] ultrasonidos[31] y fotoactivación[32] constituyen otros tipos de tecnologías empleadas con el objeto de facilitar las reacciones en la ausencia de un disolvente.

Se conocen numerosos ejemplos en síntesis orgánica de reacciones que proceden adecuadamente sin la adición de un disolvente.[33] En catálisis, también se han descrito ejemplos de sistemas en ausencia de disolvente que emplean catalizadores heterogéneos, incluyendo complejos de metales de transición soportados en un sólido,[34] aunque el número de ejemplos de sistemas homogéneos que emplean un catalizador metálico es mucho más limitado.[35]

1.2 Oxidaciones y Catálisis Homogénea en Medios No Convencionales

Entre los procesos químicos que más residuos generan se hallan las oxidaciones selectivas de compuestos orgánicos. Muchas oxidaciones hechas en la industria no son catalíticas sino estequiométricas y emplean oxidantes fuertes y generalmente nocivos. Los oxidantes convencionales en estos procesos no son satisfactorios debido, entre otras razones, a la baja economía atómica, a la formación de productos secundarios desfavorables desde el punto de vista medioambiental y a su coste. Las alternativas a dichos oxidantes convencionales son el oxígeno, el peróxido de hidrógeno[36] y los alquilhidroperóxidos. Estos oxidantes presentan las ventajas generales de ser menos costosos y de generar productos secundarios no contaminantes. Desafortunadamente estos oxidantes no son suficientemente eficientes para usarlos en muchas transformaciones si no son activados, por ejemplo empleando un catalizador. También, en reacciones que emplean un reactivo gaseoso como el O_2, la baja solubilidad de gases en disolventes convencionales implica que la disolución del gas en el medio de reacción normalmente representa la etapa limitante del proceso.

La catálisis homogénea mediada por compuestos de los metales de transición es esencial en multitud de procesos sintéticos, ya que los procesos catalíticos pueden conseguir que la reacción química tenga lugar de una forma eficiente y quimioselectiva. Dentro de estos procesos, la catálisis oxidativa representa un campo de investigación de gran importancia.[37] En particular, de entre todos los procesos de oxidación se examinarán en los apartados siguientes dos tipos de reacciones: la epoxidación de olefinas y la oxidación selectiva de alcoholes a aldehídos. Para ambas transformaciones se conocen una gran variedad de sistemas catalíticos que emplean compuestos de diversos metales como precursores catalíticos. En esta introducción centraremos la atención en aquellos sistemas que se encuentran directamente relacionados con los resultados obtenidos en el presente trabajo.

1.3 Epoxidación de Olefinas

La epoxidación directa de olefinas mediante el uso de oxígeno molecular y de manera catalítica es un proceso posible, pero éste se realiza a escala significativa tan sólo en el caso del etileno.[38] La epoxidación de olefinas más pesadas se consigue generalmente mediante el uso de compuestos de naturaleza peroxídica en cantidades estequiométricas, por ejemplo el ácido peracético o el ácido *m*-cloro-perbenzoico.[39] Empleando compuestos metálicos en alto estado de oxidación (por ejemplo compuestos de Ti,[40] V,[41] W,[42] Re,[43] y Mo[44,45]) la epoxidación se puede conseguir de manera catalítica, con oxidantes más benignos desde el punto de vista medioambiental como el peróxido de hidrógeno e hidroperóxidos orgánicos.[37(a),46] En estos sistemas las conversiones y las selectividades dependen mucho de factores como la temperatura, el pH y la polaridad del medio de la reacción, además evidentemente de la naturaleza del catalizador empleado.

A continuación se analizarán con detalle los precedentes descritos en la bibliografía en dos sistemas catalíticos: el metiltrioxorenio (MTO) y sus derivados y los oxobisperoxo complejos de molibdeno.

1.3.1 Epoxidación de olefinas catalizada por MTO y complejos derivados

1.3.1.1 Antecedentes

La actividad que presentan los compuestos de renio en una gran variedad de procesos químicos es excelente y su potencialidad como catalizadores en diversas áreas de la síntesis es notable, tanto a nivel industrial como académico.[47] De entre todos estos procesos sintéticos, en este apartado se centrará la atención exclusivamente en las reacciones de epoxidación de olefinas que conducen a la síntesis de los correspondientes epóxidos. Los óxidos de renio, Re_2O_7 y ReO_3, muestran por si mismos una actividad, aunque sea limitada, como catalizadores en estos procesos, y aunque el desarrollo de sistemas catalíticos que emplean estos compuestos continúa en la actualidad,[48] el descubrimiento del complejo metiltrioxorenio (MTO)[49] y su alta actividad en la

epoxidación catalítica de olefinas[43] constituyó un hito en este campo, ya que se trata de un catalizador muy activo en la oxidación de olefinas hasta sus epóxidos.[50]

Figura 1.2. Metiltrioxorenio (MTO)

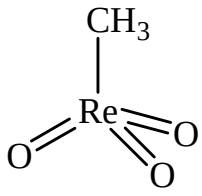

En los primeros resultados publicados, en la reacción se empleaba peróxido de hidrógeno como oxidante y ésta se llevaba a cabo en disolventes orgánicos polares, típicamente ^{t}BuOH, y en ausencia de agua. En estas condiciones el MTO no descompone el H_2O_2. Los substratos eran olefinas que generaban los correspondientes epóxidos, si éstos eran estables en el medio de reacción (p.e. en el caso de olefinas cíclicas). La catálisis era efectiva en un gran rango de temperaturas debido a la alta estabilidad del catalizador, la conversión era generalmente completa y la reacción rápida. Estas observaciones preliminares del grupo Herrmann por las que demostraban que el MTO y compuestos relacionados podían funcionar como catalizadores muy potentes en la epoxidación de olefinas representaron unos trabajos de excepcional importancia en el campo de las epoxidaciones catalíticas. Sin embargo, estos primeros sistemas estaban limitados por el problema de la hidrólisis del producto final. En los casos de epóxidos menos estables se encontró que dicha hidrólisis conducía a la formación del correspondiente *trans*-dialcohol y, por consiguiente, en estos casos era necesario asegurar la ausencia de agua. La necesidad de excluir la presencia de agua del medio de reacción implicaba la imposibilidad de uso de H_2O_2 en medio acuoso y además presentaba el inconveniente de que en la reacción se produce agua como producto secundario.

Una de las alternativas estudiadas que tratan de resolver este problema consiste en la utilización del aducto urea-peróxido de hidrógeno (UHP) anhidro.[51] De esta forma se facilita la epoxidación en disolventes poco polares (diclorometano, tolueno) y, por otro lado, la urea presente puede servir para regular el pH del sistema con objeto de inhibir la apretura del epóxido, reacción que se encuentra catalizada por ácidos. No obstante, el uso de UHP como oxidante no evita completamente la presencia de agua debido a su formación como producto secundario. Debido a ello, también se ha

investigado la utilización de tamiz molecular o agentes desecantes (p.e. Na_2SO_4) para secar *in-situ* el medio de reacción, pero en estos casos se observó una disminución de la velocidad de la reacción.[48,52] Además, aunque la epoxidación transcurre bien en los disolventes no polares, la UHP no es soluble en los mismos con lo que el sistema se transforma en heterogéneo. A modo de ejemplo, Teixeira y colaboradores investigaron la combinación de UHP y bases heterocíclicas N-donadoras en diclorometano con objeto de obtener mejores conversiones de los alquenos menos activos.[53] Empleando además como aditivo pirazol se obtuvieron conversiones buenas para *trans*-alquenos y alquenos terminales, que previamente eran poco activos en los sistemas que empleaban exclusivamente UHP. Sin embargo, las velocidades de conversión aún eran bajas. El empleo de líquidos iónicos en este sistema fue considerado por Owens, Abu-Omar y colaboradores. El líquido iónico tetrafluorborato de 1-etil-3-metilimidazolio (C_2mim-BF_4) permite la disolución del aducto UHP y con ello se alcanza un sistema homogéneo que es activo en la epoxidación de diversas olefinas.[54] Tras la reacción los productos se extraen con éter dietílico, observándose rendimientos generalmente comparables con otros sistemas de epoxidación. En este trabajo no se contempla el reciclado del conjunto catalizador/líquido iónico tras de la extracción de los productos, probablemente debido a los problemas inherentes a la eliminación de urea y el UHP no consumido tras finalizar la reacción. Además, el líquido iónico C_2mim-BF_4 es relativamente polar y se observaron problemas en la epoxidación de sustratos de muy baja polaridad (p.e. 1-deceno), debido a su baja solubilidad en el medio de reacción. Asimismo, como resultado de su alta miscibilidad con agua este líquido iónico no proporciona protección al epóxido producido con respecto a la reacción de hidrólisis por lo que la formación del mismo es muy pobre cuando se emplea H_2O_2 acuoso.

El uso de bases nitrógenadas terciarias se consideró en los primeros trabajos del grupo de Herrmann, pero se observó un efecto negativo sobre la actividad del catalizador aunque simultáneamente se producía una mejor selectividad al correspondiente epóxido. Igualmente, la descomposición del MTO por disoluciones básicas[55] hizo que el empleo de estas bases quedara temporalmente fuera de estudio. Sin embargo, en el año 1997 una publicación de Sharpless y colaboradores describe el uso de piridina con objeto de mejorar tanto la selectividad como la actividad y la estabilidad del catalizador.[56] Se observó que mientras las aminas terciarias saturadas no aromáticas inhiben fuertemente la actividad del catalizador en un variado rango de condiciones (disolventes diversos, distintas relaciones amina/catalizador y en la presencia o ausencia

de agua), la piridina y algunos de sus derivados pueden usarse para acelerar la velocidad de la reacción, inhibir la hidrólisis del epóxido y, en concentraciones suficientes, mejorar la vida del catalizador. Se percibió también que en presencia de bajas concentraciones de la base la descomposición del MTO se acelera pero en concentraciones más altas se inhibe notablemente, un efecto que depende en parte de la naturaleza del disolvente. La inhibición de la hidrólisis de los epóxidos llega a ser tan eficiente en presencia de la base, que es posible emplear H_2O_2 acuoso en un sistema bifásico con diclorometano. Por ejemplo, el empleo de un exceso de piridina (12 mol %) inhibe completamente la apertura de un amplio rango de epóxidos incluso algunos de ellos bastante sensibles (p.e. los óxidos de isopropenilbenceno, ciclohex-1-enilbenceno, 1-indeno). Desafortunadamente, este sistema no se muestra activo en epoxidaciones de olefinas terminales y *trans*-disustituidas, aunque haciendo uso de la piridina sustituida 3-cianopiridina si se observan buenas conversiones para olefinas terminales, incluso con sustratos difíciles de convertir selectivamente, como el estireno,[57] y los terpenos.[58] Sin embargo, los sistemas de 3-cianopiridina aún exhiben limitaciones en la epoxidación de algunos sustratos que conducen a epóxidos sensibles. De manera similar, Deloffre y colaboradores demostraron que el uso de bipiridina y sus derivados proporcionan resultados análogos.[59] En este trabajo se investigó la posibilidad de hacer epoxidaciones enantioselectivas, empleando bipiridinas funcionalizadas, pero sin éxito.

Herrmann y colaboradores demostraron que la razón por la que se necesita en estas reacciones de un exceso de base (piridina y derivados) es la conversión simultánea que se produce en el medio de la base a su correspondiente óxido.[60] Si la concentración inicial de piridina es baja, se transforma rápidamente al óxido de forma completa y de esta manera los efectos beneficiosos de la piridina no se observan. En una comparación utilizando de forma común un sistema bifásico cloroformo/agua, MTO como catalizador, H_2O_2 como oxidante y cicloocteno como sustrato, se observó que un 12 % de piridina acelera la velocidad de conversión al epóxido con respecto al mismo sistema sin piridina, mientras que la epoxidación es más lenta si se emplea el óxido de piridina. En el caso en el que se utiliza piridina el catalizador reside en la fase orgánica, mientras que sin piridina éste se halla en la fase acuosa. Esta observación justifica mejor la estabilización del catalizador en el primer sistema debido a la protección de la fase orgánica con respecto a la descomposición por hidrólisis. Si el sustrato es una olefina activada (p.e. cicloocteno) su epoxidación será el proceso dominante hasta que

prácticamente todo el sustrato sea convertido en el epóxido. En los casos de sustratos menos activos (p.e. estireno) la piridina se convertirá a su óxido antes de que se complete la epoxidación.

Para evitar el problema de la oxidación del ligando, Herrmann y colaboradores investigaron el uso de un base más resistente a la oxidación. Encontraron que el pirazol y algunos de sus derivados proporcionan resultados mucho mejores que los que se encontraban en la bibliografía para las epoxidaciones de diversos sustratos olefínicos (conversiones y selectividades casi completas).[61] En la Tabla 1.3 se recoge el resultado del estudio de varios pirazoles en la epoxidación de estireno.

Tabla 1.3.

Entrada	Ligando [b]	Conversión (%)[a]	Selectividad (%)[a]
1	Pirazol	> 99	> 99
2	Pirazol (6 mol %)	90	95
3	3-Metilpirazol	71	> 99
4	3,5-Dimetilpirazol	27	> 99
5	2-[3(5)-Pirazolil] piridina	95	> 99
6	4-Bromopirazol	92	2[c]
7	-	89	4[c]

[a] Determinado en una escala de 2-4 mmol por GC o ^{1}H-RMN calibrado (tiempo = 3h). [b] 0.5 mol % MTO y 12 mol % ligando (excepto entrada 2). [c] Producto dominante: 1-feniletano-1,2-diol (selectividad 70 %)

En este estudio se concluye que la conversión de estireno es más rápida para el pirazol no sustituido, mientras que los pirazoles N-alquilados, y en menor grado los alquilados en las posiciones 3 y/o 5, exhiben una peor actividad y estabilidad. Como continuación de este trabajo, Sharpless y colaboradores compararon la eficacia relativa de la piridina, la 3-cianopiridina y el pirazol en la epoxidación de varios alquenos.[62] Se observó que el pirazol es generalmente efectivo para la mayoría de los alquenos, incluso en algunos casos de olefinas que conducen a epóxidos sensibles a la hidrólisis y, por consiguiente, es el mejor para epoxidaciones difíciles. Sin embargo, para muchos alquenos ricos en electrones el uso de la piridina produce el mismo resultado por lo que no justifica el uso de una base más cara. La 3-cianopiridina también demostró ser eficaz con respecto a la piridina en la epoxidación de alquenos terminales, aunque algunos de estos resultados estaban en contradicción con lo observado previamente por Herrmann. Su grupo de trabajo continuó la investigación sobre el efecto de varias bases empleando un rango de piridinas sustituidas y estudiando la correlación entre el valor del pK_a y las propiedades de los sistemas catalíticos (Tabla 1.4).[63] Se encontró que las piridinas que

contienen grupos donadores de electrones, que poseen basicidad más alta, protegen al epóxido de la apertura vía hidrólisis acídica y, aunque inicialmente pueden acelerar la conversión, tienen un impacto negativo en la vida del catalizador. Por el contrario, las piridinas que contienen grupos atractores de electrones y basicidad más baja, permiten una conversión más alta debido a la larga vida del catalizador pero con menos selectividad por hidrólisis del producto.

Tabla 1.4.

Aditivo	**pK_a**	**Conversión (Rto. del epóxido) (%)[a]**	
Sin aditivo	-	100	(5)
2-Cianopiridina	-0,26	99	(3)
3-Cianopiridina	1,45	100	(1)
4-Cianopiridina	1,9	100	(7)
3-Cloropiridina	2,81	95	(87)
3-Fluoropiridina	2,97	98	(97)
Picolinato de metilo	2,65	85	(13)
Nicotinato de metilo	3,25	93	(86)
Isonicotinato de metilo	3,26	94	(90)
Quinolina	4,87	62	(62)
Piridina	5,17	70	(70)
2-Picolina	5,97	14	(14)
3-Picolina	5,60	58	(58)
4-Picolina	6,03	63	(63)
4-tert-Butilpiridina	5,99	69	(69)
4-Metoxipiridina	6,62	63	(63)

[a] *30 % H_2O_2 acuoso, estireno, aditivo y MTO en un razón molar de 400:200:20:1. Se determina la conversión por GC con respecto a un estándar.*

En los casos correspondientes a las bases más fuertes (*p*K_a más alto), se supone que se produce una coordinación más estable de la misma al centro metálico de Re y se bloquea de este modo la coordinación del epóxido, inhibiéndose su descomposición catalítica. Sin embargo, también se acelera la descomposición del MTO a través de la rotura del enlace Re-metilo y produciendo el aducto del ácido perrénico y la base más metanol (Esquema 1.1). Las bases menos fuertes tienen una coordinación más débil, con lo que la hidrólisis catalítica del epóxido se encuentra favorecida, debido a la coordinación más favorable del epóxido al renio. El catalizador no se descompone por lo que la vida del mismo se hace más duradera y resultan conversiones más elevadas.

Esquema 1.1.

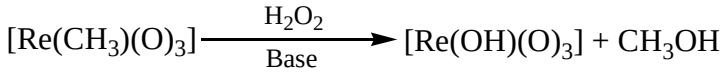

La mejora de la velocidad de la epoxidación mediante el empleo de piridina y sus derivados, y otras bases de tipo N-heterocíclicas, no se ha explicada completamente racionalizada. Claramente estas bases actúan como agentes que transfieren el catalizador de la fase acuosa a la fase orgánica. Ello resulta evidente desde el punto de vista experimental simplemente por la observación del color amarillo de la especie peroxo, que actúa como catalizador, en la fase orgánica en la presencia de un aditivo y en la fase acuosa en su ausencia. Este comportamiento como agente de transferencia entre las fases se ha visto confirmado al comprobar en otros estudios que un aumento de la velocidad de agitación conduce a una conversión más rápida. Del mismo modo, la velocidad de conversión se observa que está relacionada con la basicidad del aditivo. La presencia de una base más fuerte produciría una concentración más alta del anión hidrogenoperóxido HOO^-, lo que conllevaría a la formación más rápida de las especies renio-peroxo. También esto explicaría la alta velocidad de descomposición ya que ésta se produce por medio de esta especie HOO^-. Igualmente, es posible que la coordinación de una base al centro metálico debilitara el enlace Re–O_{peroxo} y como resultado de ello originara una disminución la barrera energética para la formación del epóxido.[64] El Esquema 1.2 resume la influencia de la base en las velocidades de conversión y descomposición del catalizador.

Esquema 1.2.

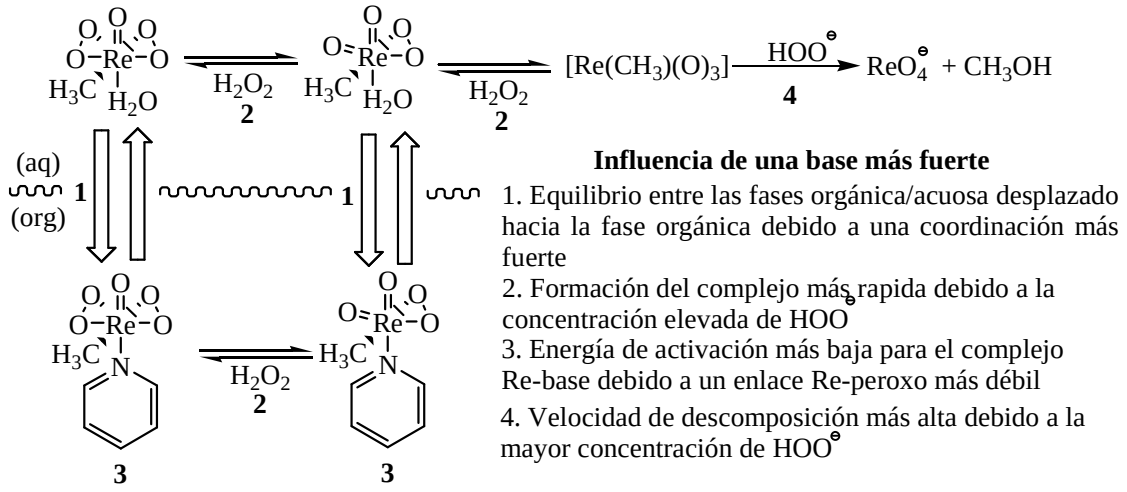

Como continuación de los resultados prometedores obtenidos mediante el empleo de pirazol como aditivo, Yamazaki ha desarrollado recientemente un sistema que emplea 3-metilpirazol como base y que quizás sea el más efectivo entre las epoxidaciones con MTO.[65] Para la epoxidación de cicloocteno ha descrito un TON de 20000 en 6 horas empleando MTO (0.001 %), pirazol (10 %) y H_2O_2 acuoso (200 %) en un sistema bifásico con diclorometano como disolvente, lo que constituye el valor más elevado de TON en la literatura para las epoxidaciones homogéneas realizadas con MTO/H_2O_2. En general, el uso del 3-metilpirazol conduce a mejores actividades y TONs con respecto a los valores observados para la piridina o el pirazol y además la selectividad hacia el epóxido en un amplio rango de productos sensibles también eran excelentes. El autor supone que la mejor actividad que se observa para este sistema empleando 3-metilpirazol resulta de su valor de pK_a (3,3) que es mayor que los del pirazol y la 3-cianopiridina (2,5 y 1,5 respectivamente), pero menor que el de la piridina (5,2). Con respecto al trabajo anterior de Adolfsson y colaboradores (ver Tabla 1.4) se observa que para las especies con un valor de pK_a comprendido en el rango aproximado 2.8–3.3 (3-cloropiridina, 3-fluoropiridina, nicotinato de metilo, isonicotinato de metilo), se obtienen altas conversiones combinadas con altas selectividades. Aditivos más o menos básicos dieron pobres conversiones y pobres selectividades, respectivamente, por las razones ya comentadas. Se puede concluir que este rango de pK_a representa el óptimo para el aditivo a emplear en las epoxidaciones, constituyendo un balance entre la conversión hacia el epóxido y, simultáneamente, la protección del mismo.

A pesar de la gran labor realizada en el estudio de la reacción de epoxidación catalizada por MTO cuyo objetivo ha sido el mejorar las conversiones y la selectividad de la reacción, las investigaciones que han analizado la posibilidad de controlar la enantioselectividad de la reacción han tenido poco éxito.[66] Entre las publicaciones en este campo destaca el trabajo de Corma y colaboradores en el que se describe la epoxidación de varios sustratos con una selección de aminas quirales, en el mejor caso con un enantioselectividad del 36 % (para el *cis*-β-metilestireno empleando (R)-(+)-feniletilamina).[67] Sin embargo, las conversiones en este trabajo eran bajas y se encontraron problemas con la selectividad aún con el empleo de temperaturas de reacción muy bajas. Por otro lado, empleando UHP como oxidante para evitar el problema de hidrólisis, de Palma Carreiro y colaboradores obtuvieron enantioselectividades modestas (2-12%) a temperatura ambiente con una selección de ligandos que incorporan heterociclos nitrogenados.[68] Haider y colaboradores han tenido

un éxito moderado empleando ligandos quirales de pirazol y dialcohol, en los mejores casos con excesos enantioselectivos superiores al 40 %.[69] Hasta el momento estos resultados representan los mejores enantioselectividades para una epoxidación catalizada por MTO, pero la reacción necesita temperaturas muy bajas, exceso de ligando y las velocidades de reacción y los rendimientos eran pobres. Se espera que en un futuro cercano el desarrollo de nuevos métodos permita realizar con mejores resultados las epoxidaciones enantioselectivas empleando el MTO.

1.3.1.2 Mecanismo de la epoxidación

El estudio de los mecanismos de los procesos de oxidación en los que participa el MTO ha sido una constante desde que se descubrió la potencialidad de este compuesto en catálisis.[70] En este apartado describiremos algunos detalles del mecanismo de la reacción de epoxidación. En primer lugar, la interacción del H_2O_2 con el MTO produce los complejos denominados mono- y bis-peroxo (Figura 1.3), que participan en un equilibrio que depende de la concentración del oxidante.[71]

Figura 1.3. Los complejos mono- y bis-peroxo

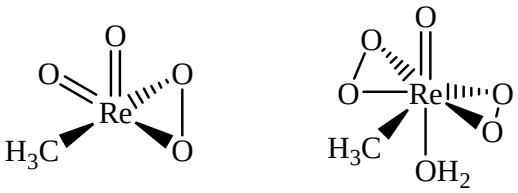

Se propone que el ligando η^2-peroxo se forma a través de un complejo intermedio de tipo σ-hidroperoxo (Esquema 1.3).[72] Sin embargo, parece descartado que la actividad de los sistemas MTO/H_2O_2 resulte simplemente de la activación del H_2O_2 por el MTO. De hecho no es posible aislar un complejo de renio de este tipo y en mezclas MTO/H_2O_2 no se encuentra evidencia de su presencia. Si existe, nunca se halla en una concentración apreciable y claramente este intermedio no participa en ningún proceso salvo en el de la transformación rápida al peroxo-compuesto. No obstante, la velocidad de la formación de este intermedio puede tener consecuencias en la velocidad de la reacción catalítica.

Esquema 1.3.

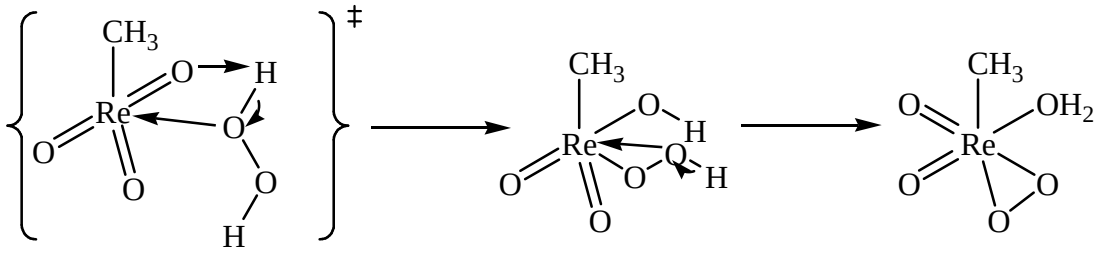

Se ha demostrado que ambos complejos mono- y bis-peroxo pueden conseguir la epoxidación de olefinas. La reacción entre el bisperoxo y la olefina produce el epóxido y el monoperoxo y la reacción con el monoperoxo deja el epóxido y MTO, como se representa en el Esquema 1.4. Obviamente las velocidades relativas de los procesos que se muestran en este esquema dependen de las concentraciones de las propias especies. Se debe hacer notar que en general el mono- y el bis-peroxo epoxidan las olefinas con prácticamente la misma velocidad, aunque existen ejemplos específicos de epoxidaciones en los cuales el complejo mono-[73] o el bis-peroxo[74] ha mostrado una mejor actividad uno con respecto el otro.

Esquema 1.4.

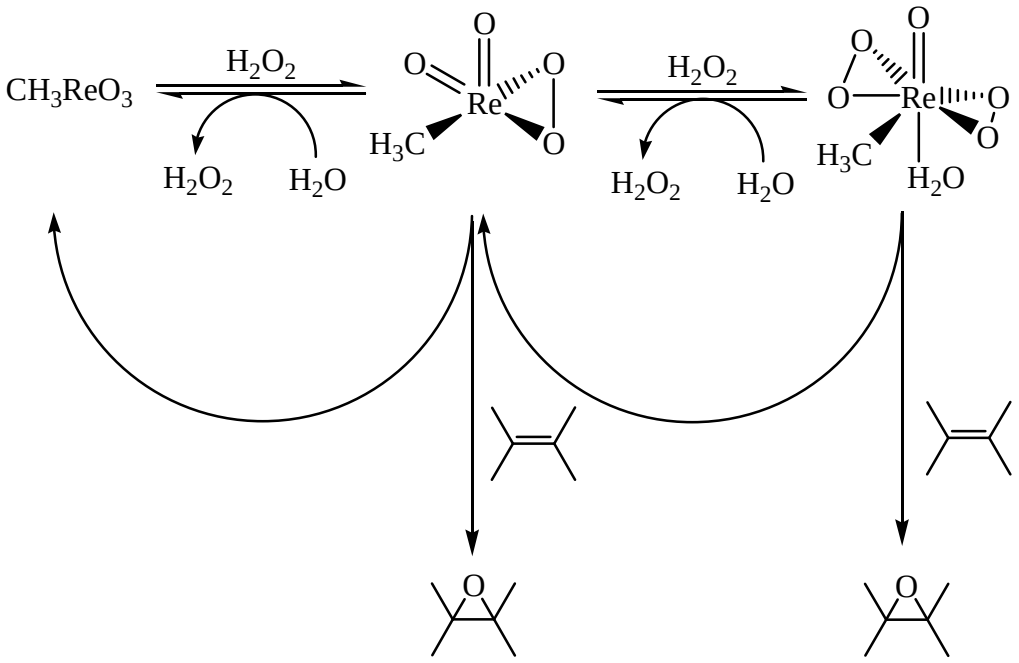

Existe todavía controversia sobre el mecanismo concreto por el que transcurren las reacciones de epoxidación. En oxidaciones catalizadas por el conjunto MTO/H_2O_2, se ha probado mediante estudios que emplean RMN de ^{18}O que se transfiere al producto final uno de los átomos de oxígeno de los ligandos peroxo (y no los átomos de los grupos oxo),[75] y se supone que esto ocurre igualmente en las reacciones de epoxidación de olefinas. Dentro del mecanismo más aceptado para esta tipo de reacción, generalmente se considera que ésta procede a través de la formación de un intermedio bicíclico producido por un ataque nucleófilo de la olefina sobre uno de los átomos de oxígeno del grupo peroxo seguido de la formación del epóxido y un oxo-complejo (Esquema 1.5).

Esquema 1.5.

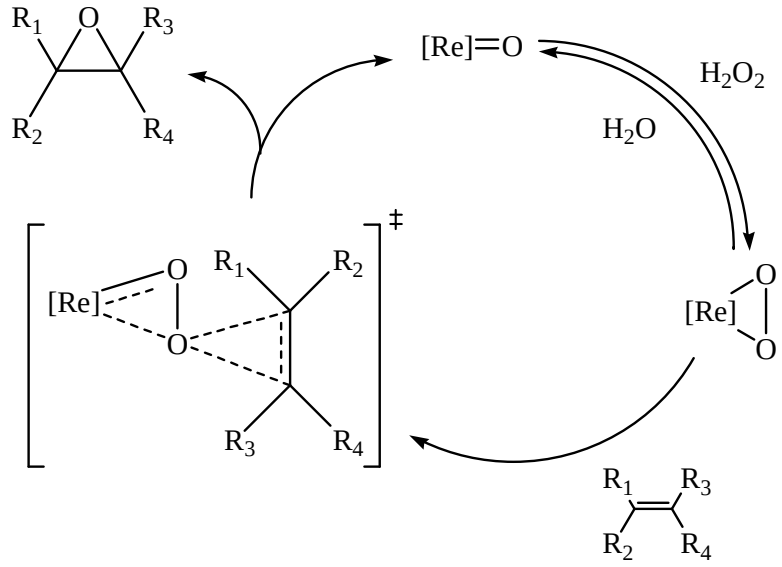

[Re] = [Re(CH_3)(O_2)] o [Re(CH_3)(O_2)(O)]

Con respecto al estado de transición bicíclico del Esquema 1.5 existen dos estructuras posibles, que se representan en el Esquema 1.6. La primera muestra una configuración plana y la segunda una estructura espirocíclica. Sobre la base de estudios dedicados a analizar la influencia sobre la velocidad de la reacción de epoxidación que producen los efectos estéricos de varios estirenos sustituidos, parece que la segunda es la más probable aunque la conclusión no parece definitiva.[94]

Esquema 1.6.

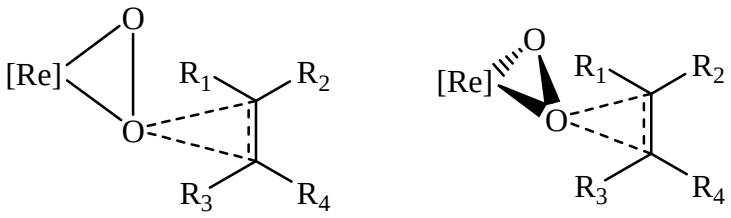

La transformación no deseada, a través de la reacción de hidrólisis, de los epóxidos que se producen en la reacción al correspondiente dialcohol puede ocurrir por medio de dos mecanismos: hidrólisis no catalizada e hidrólisis catalizada por el renio. Se ha observado que el primero es demasiado lento para ser significativo durante el curso de una reacción, por lo que la descomposición catalítica por renio representa la ruta por la cual ocurre la hidrólisis y la pérdida del epóxido. En la primera etapa de este mecanismo, se da la coordinación del epóxido al renio y se forma un complejo con un diol coordinado. En condiciones anhidras es posible detectar la formación de este complejo por reacción entre el óxido de estireno y MTO.[71] En ausencia de agua estos complejos son estables pero el agua contribuye a su descomposición irreversible generando el dialcohol libre. De esta manera, en una epoxidación empleando el H_2O_2 acuoso como oxidante, el complejo de renio también cataliza la hidrólisis del producto (Esquema 1.7).

Esquema 1.7.

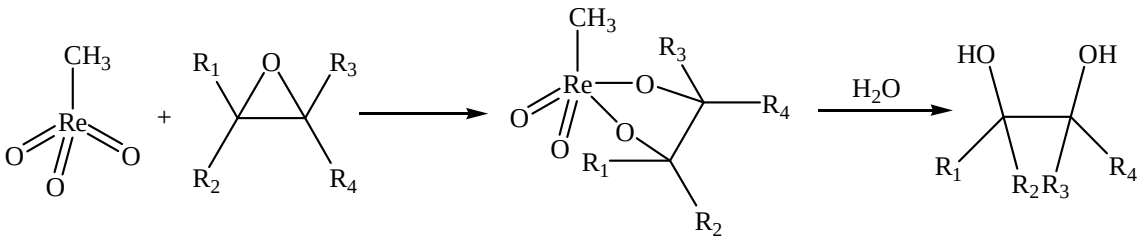

Conviene hacer notar que el renio no cataliza la conversión directa de un alqueno al dialcohol correspondiente, sino que ésta tiene que proceder vía el epóxido. Como se ha discutido anteriormente, el uso de bases coordinantes de tipo N-heterociclo es muy efectivo para inhibir este proceso ya que se produce el bloqueo de la coordinación del epóxido al centro metálico. Concretamente, el MTO forma aductos de

geometría bipirámide trigonal con bases monodentadas N-donadoras, mientras que la geometría es octaédrica distorsionada con bases bidentadas (Esquema 1.8).[76]

Esquema 1.8.

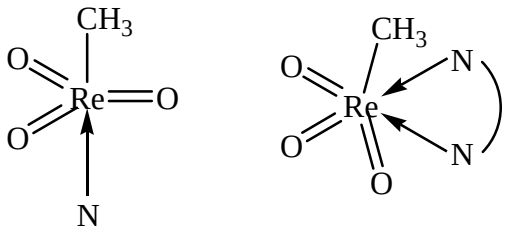

Los complejos con las bases monodentadas pueden formar los complejos de tipo mono y bisperoxo de la misma manera que en el caso del MTO, pero con la base coordinada en lugar del agua. Para los ligandos monodentados se observa una correlación lineal entre el valor del pK_a y la fuerza de coordinación al centro metálico. Así por ejemplo, se observa una correlación lineal entre el constante de Hammett σ de los sustituyentes y la fuerza de coordinación en un ligando de tipo piridínico, detectándose una desviación de esta relación en los casos de ligandos en los que la coordinación se afecta por factores estéricos (p.e. piridinas substituidas en las posiciones 2- o 2,6-).[77]

1.3.2 Oxobisperoxocomplejos de molibdeno como catalizadores en la epoxidación de olefinas

La epoxidación de olefinas realizada por oxidantes de tipo peroxo se ha llevado a cabo empleando como precursores compuestos de molibdeno en alto y bajo estado de oxidación, como por ejemplo $[Mo(CO)_6]$, $[\eta^5\text{-}(C_5H_5)Mo(O)_2(Cl)]$, $[Mo(O)_2(Cl)_2]$, $[Mo(O)_2(acac)_2]$, diversos compuestos tipo clúster de molibdeno o molibdeno metálico.[46(b),78]

Entre los distintos derivados de molibdeno con actividad demostrada para esta reacción, la familia de compuestos de tipo oxobisperoxo, $[Mo(O)(O_2)_2(L)_n]$, presenta especial interés desde un punto de vista económico, así como por su simplicidad. El $[Mo(O)(O_2)_2(H_2O)_n]$ en disolución acuosa, se puede preparar fácilmente mediante la reacción entre el trióxido de molibdeno y el peróxido de hidrogeno (Esquema 1.9).[45]

Esquema 1.9.

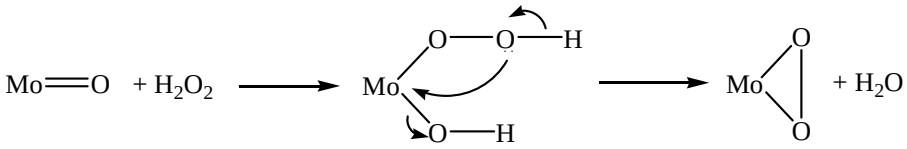

A partir de este precursor simple se han sintetizado una gran variedad de complejos que contiene coordinados ligandos de naturaleza mono- (a) y bidentada (b) (Figura 1.4). Sin embargo la baja solubilidad de un buen número de estos compuestos, en particular los que contienen ligandos bidentados, puede representar una barrera en su uso en reacciones de oxidación catalizadas en fase homogénea.

Figura 1.4. Oxobisperoxocomplejos de molibdeno

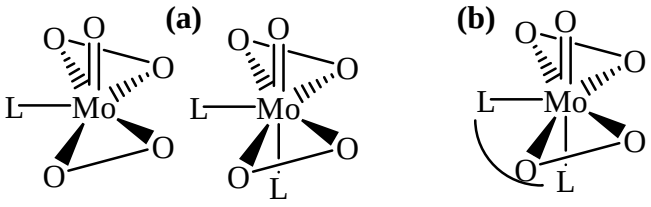

En 1969 el grupo de trabajo de Mimoun describió la preparación de oxobisperoxocomplejos de molibdeno[44] y su uso consiguiente en la oxidación de olefinas.[79] Empleando, por ejemplo, el complejo $[Mo(O)(O_2)_2(HMPA)]$ (HMPA = hexametilfosforamida), se consiguió la epoxidación de ciclohexeno de manera estequiométrica (Esquema 1.10). La adición al sistema de H_2O_2 como oxidante terminal permite regenerar el oxobisperoxocomplejo de partida de manera que se consigue cerrar el ciclo catalítico.

Esquema 1.10.

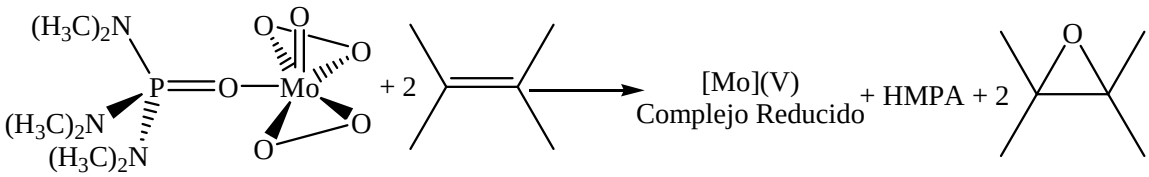

Conviene hacer notar que la mayoría de sistemas descritos en la bibliografía para la reacción de epoxidación de olefinas catalizada por complejos de molibdeno emplean alquilhidroperóxidos, y en particular terbutilhidroperóxido (TBHP), como oxidante terminal. Como ejemplo significativo, Thiel y colaboradores consiguieron buenas conversiones en la reacción de epoxidación de una amplia variedad de olefinas cíclicas, lineales y funcionalizadas mediante el uso de un catalizador de molibdeno y TBHP como oxidante.[80] El sistema permite buenas selectividades hacia epóxido, sin observarse procesos de apertura del epóxido para dar el diol o el correspondiente *tert*-butil éster. El mecanismo de esta reacción resulta de interés dado que podría aplicarse a reacciones de epoxidación empleando H_2O_2 como oxidante (ver Apartado 1.3.2.1). En la presente discusión no se tratará con más detalle este tipo de reacciones que usan hidroperóxidos orgánicos, centrando la atención en los procesos que emplean H_2O_2 como un oxidante menos contaminante.

Un problema en el diseño de catalizadores de oxobisperoxocomplejos de molibdeno es la capacidad que muestran para oxidar catalíticamente muchas clases de compuestos, incluyendo algunos ligandos como los de tipo fosfina que se oxidan a sus correspondientes óxidos, de manera simultánea a la oxidación del pretendido sustrato. La síntesis y el uso de complejos de este tipo con fosfinas no oxidadas se inhiben por esta razón. Sin embargo, Jiménez y colaboradores demostraron la eficacia en la epoxidación de olefinas de un rango de oxobisperoxocomplejos de molibdeno con varios óxidos de fosfinas como ligandos.[81] Se observó que complejos que contenían óxidos de trialquil o trifenilfosfina como ligandos eran capaces de epoxidar olefinas en medios poco polares (diclorometano, cloroformo) de una manera estequiométrica y, en conjunto con oxidantes terminales como TBHP o H_2O_2, de forma catalítica. En un sistema bifásico empleando H_2O_2 acuoso como oxidante y un óxido de fosfina como surfactante, las conversiones fueron altas pero para un rango limitado de sustratos y empleando temperaturas altas (40-70 ºC).

El sistema más eficiente de los descritos dentro de esta línea de investigación fue descrito por Bhattacharyya y colaboradores, empleando complejos de molibdeno[82] y wolframio[83] como catalizador, especialmente oxobisperoxocomplejos de molibdeno,[84] con ligandos bidentados de tipo N,O-donador y bicarbonato de sodio como co-catalizador (Esquema 1.11). El sistema muestra una actividad catalítica excepcional en la reacción de epoxidación de una gran variedad de substratos olefínicos. Particularmente, los valores de TON y TOF de 9.900 y 19.800, respectivamente,

observados en la epoxidación del *cis*-cicloocteno representan los valores más altos descritos para una reacción de epoxídación utilizando un complejo metálico de molibdeno como catalizador. Los autores atribuyen la alta actividad a la presencia del bicarbonato de sodio que genera, vía reacción con el H_2O_2, el monoperoxocarbonato, HCO_4^-. La reacción con esta especie podría facilitar la fácil regeneración de los ligandos peroxo en el complejo metálico. La capacidad del hidrogenocarbonato de sodio para efectuar la epoxidación por sí solo es conocida,[85] pero en este caso es probable que su participación sea el facilitar la regeneración del catalizador.

Esquema 1.11.

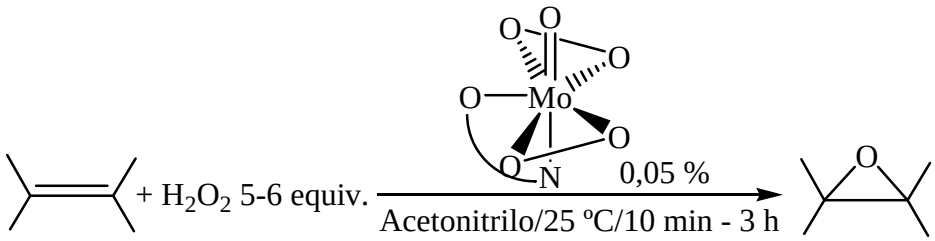

1.3.2.1 Mecanismo de la reacción de epoxidación catalizada por oxobisperoxocomplejos de molibdeno

Mimoun y colaboradores propusieron un mecanismo basado, en gran parte, en el comportamiento general que manifiestan los sustratos olefínicos en el proceso de activación por un centro metálico.[45] Transformaciones tales como la adición nucleofílica o la polimerización catalizadas por complejos metálicos comienzan con la coordinación reversible de la olefina al centro metálico, paso previo a la inserción en el enlace metal-ligando. (Esquema 1.12)

Esquema 1.12.

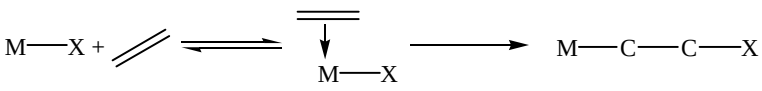

De ese modo, en el mecanismo propuesto el complejo $[Mo(O)(O_2)_2(HMPA)]$ pierde el HMPA coordinado generando una vacante en la esfera de coordinación del

complejo que es ocupado por la olefina en la etapa determinante de la reacción (Esquema 1.13). El derivado $Mo(O)(O_2)_2$ insaturado actúa como un ácido Lewis fuerte, de manera que la olefina coordinada al centro metálico pierde su naturaleza nucleofílica, adquiriendo un carácter electrofílico, lo que la hace susceptible de un ataque nucleofilico por parte del peroxo coordinado formando un intermedio peroxo-metaloheterocíclico de cinco miembros. Tras la eliminación del epóxido se genera un ligando oxo, que posteriormente regenera el ligando peroxo a través de la reacción con peróxido de hidrogeno completándose el ciclo catalítico.

Esquema 1.13.

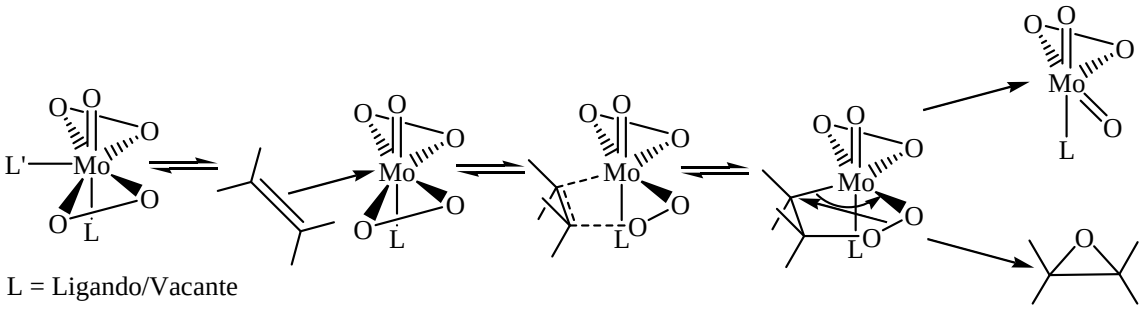

Se consideró probable que la olefina se coordinara en la posición ecuatorial, la posición ocupada previamente por el HMPA.[86] Los autores en su trabajo proporcionan evidencias que demuestran la sustitución del HMPA por la olefina y que sustentan este mecanismo, a través de estudios cinéticos y de RMN. Asimismo, se comprobó que ligandos σ-donadores fuertes inhiben considerablemente la epoxidación, ya que se vería impedida su sustitución por la olefina y se reduciría la acidez del centro metálico, disminuyendo la actividad del proceso.

En el caso de la reacción de epoxidación empleando un alquilhidroperóxido como oxidante terminal los autores consideraron que la reacción debería proceder por el mismo mecanismo descrito para los peroxocomplejos metálicos, pero vía inserción a un ligando metaloalquilperoxo formado por la reacción del alquilhidroperóxido con el complejo (Esquema 1.14). La posterior eliminación del epóxido generaría un ligando alcoxo coordinado (M-OR), que originaría el alcohol correspondiente.[45,90]

Esquema 1.14.

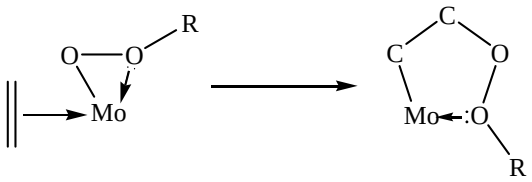

Complejos de este tipo se han aislado, por ejemplo, en la reacción de diversos complejos de compuestos de iridio[87] y paladio[88] con alquilperóxidos, igualmente, se han descrito alqulihidroperoxocomplejos de vanadio,[89] pero un compuesto similar de molibdeno no ha sido aislado hasta la fecha, a pesar de que estas especies serían intermedios en la reacción con alquilhidroperóxidos. Mimoun y sus colaboradores prepararon varios complejos de tipo M-O-NR_2 mediante el uso de derivados de hidroxilamina, que son análogos a los alquilperoxos propuestos, observando que el alquilhidroperóxido Ph_3COOH conseguía oxidar el ligando oxo a peroxo en la esfera de coordinación del molibdeno,[90] determinando, mediante el uso de oxidantes marcados isotópicamente con ^{18}O, que los dos átomos de oxígeno del ligando peroxo provenían del oxidante.

La transferencia a la olefina de uno de los átomos de oxígeno del ligando peroxo para formar el epóxido fue confimada por Sharpless y colaboradores, mediante el uso de oxobisperoxocomplejos de molibdeno con el ligando oxo marcado isotópicamente con ^{18}O.[91] Como continuación, en el mismo trabajo, suministraron evidencias que cuestionaban el intermedio cíclico de cinco miembros propuesto en el mecanismo de Mimoun et. al. A través de la revisión de otros trabajos, comprobaron que era posible correlacionar las velocidades relativas de las epoxidaciones de norborneno y ciclohexeno con el mecanismo de la reacción.[92] En el caso de las reacciones de epoxidación que proceden a través de un anillo de cinco miembros (p.e. con óxido de benzonitrilo o con OsO_4) la reactividad del norborneno es mucho más alta, pero en el caso de las epoxidaciones que proceden por un anillo de tres miembros (p.e. con ácido peracético o con compuestos de Cr(VI)) las reactividades son similares.[93] Se demostró que la epoxidación catalizada por oxobisperoxocomplejos de molibdeno entra en esta segunda categoría y así se concluyó que el mecanismo por el que uno de los átomos de oxígeno del grupo peroxo se transfiere a la olefina procede vía un intermedio cíclico de tres miembros, como el peroxometalaciclo espirocíclico representado en la Figura 1.5.

Figura 1.5.

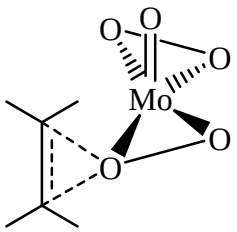

De igual forma que en el mecanismo propuesto por Mimoun, tras la epoxidación se regenera el peroxo a través de la reacción con el oxidante terminal.

Este mecanismo tiene precedentes para otros catalizadores que consiguen la epoxidación por transferencia de un oxígeno-peroxo,[94] pero la evidencia de que este mecanismo es activo para peroxocomplejos de molibdeno no es concluyente. Chong y Sharpless observaron en sus estudios de epoxidaciones, catalizadas por complejos de Mo y V, utilizando el terbutilhidroperóxido (TBHP) como oxidante terminal un mecanismo alternativo que procede vía activación del oxidante por el centro metálico del complejo es también operativo. Los autores apreciaron que, aunque la síntesis de complejos peroxo de molibdeno es posible empleando alquilperóxidos como fuente de oxígeno, se necesita generalmente condiciones muy extremas.[95] Así, en la reacción de epoxidación en presencia de agua enriquecida en ^{18}O no se detectó producto enriquecido, de lo que se deduce que el átomo de oxígeno transferido a la olefina proviene del TBHP. Se consideró un mecanismo en el que el alquilperóxido se activase por coordinación al metal vía el oxígeno distal al grupo alquílico (Figura 1.6).[96] El átomo de oxígeno hidroxi se transfiere a la olefina y se elimina el alcohol como subproducto. Estas observaciones y los trabajos posteriores que apoyan este mecanismo son de trascendencia ya que la mayor parte de los trabajos que emplean compuestos de molibdeno como catalizador epoxidativo emplean alquilperóxidos, en particular el TBHP, como oxidante.

Figura 1.6.

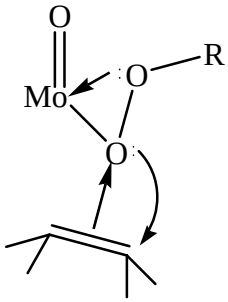

El mejor estudio sistemático del mecanismo de la epoxidación con un catalizador oxobisperoxocomplejos de molibdeno y el *tert*-butilhidroperóxido (TBHP) como oxidante se ha realizado en una serie de publicaciones de Thiel y colaboradores utilizando oxobisperoxocomplejos de molibdeno con ligandos bidentados de tipo N,N-donador tales como pirazolil-piridina sustituidas (ver Figura 1.7). Este tipo de complejos, que pueden dar lugar a mezclas de los dos isómeros posibles, presentan buenas actividades en la reacción de epoxidación. La presencia de una cadena N-alquílica como el N-sustituyente proporciona solubilidad al derivado resultante en disolventes poco polares (incluyendo tolueno, disolventes halogenados y alcanos) y en los primeros estudios realizados se demostró una buena actividad catalítica en la epoxidación trabajando en estos disolventes.[97]

Figura 1.7.

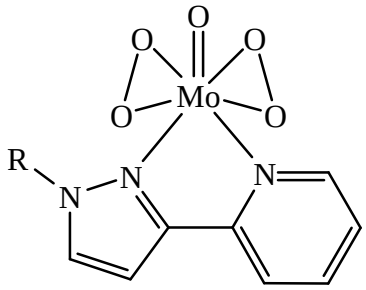

Mediante la modificación de la estructura del ligando pirazolil-piridina coordinado al centro de molibdeno, el grupo de Thiel realizó varias investigaciones del mecanismo de la reacción de epoxidación con TBHP.[98] En primer lugar, investigaron la disociación del ligando, para determinar si el mecanismo de la reacción era similar al propuesto por Mimoun. Se observó que la protólisis de los complejos era lenta incluso con ácido trifluoroacético y se concluyó que la disociación del ligando no sería la etapa determinante en el proceso catalítico. Esto indicaría que la epoxidación no podría transcurrir por un mecanismo que requiriera la coordinación del sustrato al metal. Sin embargo, en una publicación más reciente de este mismo grupo, estudios de RMN y teóricos indicaron que mediante la disociación del ligando sería posible la transformación de un isómero en otro.[99] Estos resultados sugieren que la disociación podría ser también factible.

Como se ha descrito anteriormente, se propone que estos oxobisperoxocomplejos de molibdeno epoxidan olefinas a través de la transferencia de

un oxigeno peroxo a la olefina. De esta manera, se podría predecir que complejos que contengan una funcionalización de tipo olefínico podrían auto-oxidarse como oxidantes estequiométricos. Para investigar esta posibilidad sintetizaron complejos N-funcionalizados con grupos alilo y ciclooctenilo (Figura 1.8).

Figura 1.8.

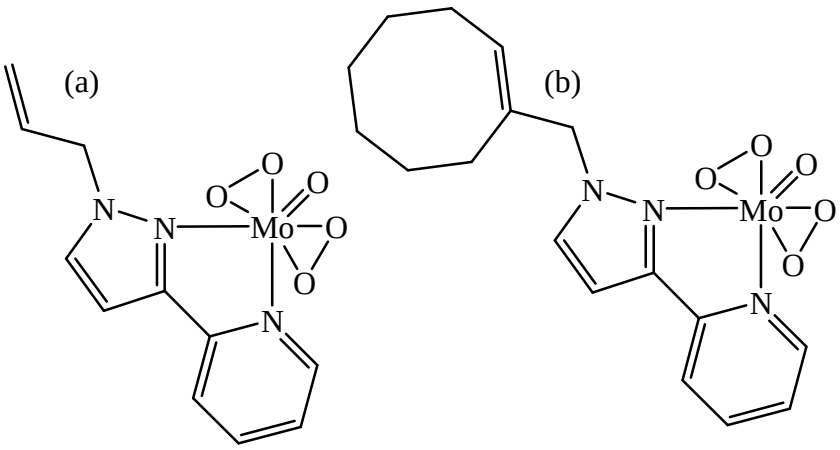

A través de la estructura del complejo alilo (a), determinada mediante difracción de rayos-X de monocristal, no observaron ninguna interacción inter- o intramolecular entre el fragmento olefínico y el centro metálico o los átomos de oxígeno. Un estudio mediante RMN del complejo de ciclooctenilo (b) en cloroformo deuterado demostró que el compuesto es extremamente estable, sin observarse la reacción de autoepoxidación tras calentamiento a 65 ºC durante una hora. De esta forma se demostró que, a diferencia de otros complejos descritos previamente capaces de donar un oxígeno del ligando peroxo a un sustrato olefínico, los grupos peroxo de este complejo no son activos para esta reacción. No obstante, cuando se adiciona TBHP a la disolución se observó la rápida epoxidación de la función olefínica. Se puede concluir que la epoxidación catalítica, al menos en este complejo, tiene que transcurrir vía la transferencia de uno de los átomos de oxígeno del oxidante a la olefina y no de los ligandos peroxo tal y como habían demostrado Sharpless y Chong.[96] Esto demuestra que los complejos oxobisperoxocomplejos de molibdeno pueden oxidar a las olefinas a través de dos mecanismos alternativos, dependiendo de la actividad de los ligandos peroxo y la presencia de oxidante. La observación de la existencia de un tiempo de activación a temperaturas de 50 ºC indica la formación de un complejo intermedio en que el TBHP es activado para la epoxidación. Se encontró evidencia adicional a esta

propuesta mediante un estudio de la modulación de la basicidad del ligando por el efecto atractor o donador de electrones de los grupos sustituyentes en los anillos.[100] Una reducción en la basicidad del ligando resultará en un centro metálico más ácido. Se observaron mejores actividades empleando ligandos con grupos atractores de electrones, hecho que apoya un mecanismo en que el alquilperoxo básico coordina mejor a un catalizador más ácido.

En el mecanismo propuesto por los autores (Esquema 1.15), la activación del oxidante procede a través de la transferencia del átomo de hidrógeno del hidroperóxido a uno de los átomos de oxígeno del grupo peroxo, formando un hidroperoxo y dejando libre una vacante de coordinación en la que se puede coordinar el nuevo ligando alquilperoxo. El ligando oxo no tiene tendencia a aceptar protones por lo que se descarta la posibilidad que se produzca a este grupo la transferencia del protón. En la reacción con la olefina se produce la transferencia de uno de los átomos de oxígeno para generar el peróxido y dejar un complejo alcoxo-hidroperoxo. Este se descompone vía la salida de alcohol dejando nuevamente un ligando peroxo por lo que la epoxidación puede transcurrir de manera catalítica.

Esquema 1.15.

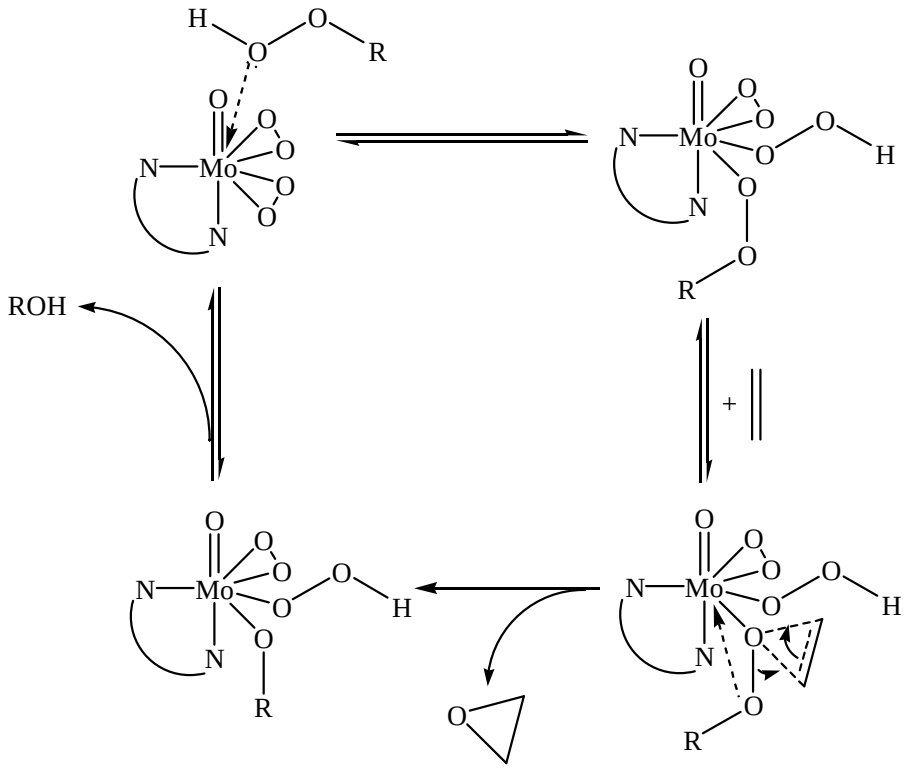

Se debe hacer notar que, aunque en todas sus experiencias se empleaba el TBHP como oxidante, en sus conclusiones los autores asumen que la epoxidación con otros oxidantes hidroperoxos, incluyendo el H_2O_2, procedería por el mismo mecanismo. Algunos complejos metálicos reaccionan con H_2O_2 para formar ligandos hidroperoxos,[101] pero no existe evidencia experimental de la existencia de hidroperoxocomplejos de molibdeno.

1.3.2.2 Epoxidación empleando catalizadores de molibdeno en ILs

En los últimos años, se ha introducido en el estudio de las reacciones de epoxidación que emplean catalizadores de molibdeno la utilización como medio de reacción de líquidos iónicos. Hasta la fecha no son muchas las contribuciones realizadas y, en particular, el grupo de Romão ha investigado el proceso de epoxidación con TBHP en diversos ILs utilizando como catalizador bien ciclopentadienilcomplejos de molibdeno [102] o bien dioxo-derivados de molibdeno.[103] Se ha demostrado que es posible el reciclado del conjunto catalizador-IL en este tipo de sistema, aunque en algunos casos la selectividad no es muy alta debido a la apertura del epóxido. Aún más reciente es otro estudio relacionado, que analiza la epoxidación de cicloocteno usando dioxotiocianatocomplejos de molibdeno como catalizador.[104]

1.4 Oxidación Selectiva de Alcoholes

La oxidación catalítica de alcoholes primarios y secundarios a sus correspondientes derivados carbonílicos es una reacción clásica en síntesis orgánica (Esquema 1.16).[37(a)] La producción mundial de aldehídos es del orden de 10^7 toneladas cada año y en su mayor parte se producen por oxidación de los alcoholes correspondientes.[105] Estas oxidaciones se hacían tradicionalmente empleando oxidantes en cantidades estequiométricas, por ejemplo compuestos de cromo,[106] permanganatos,[107] óxido de rutenio(VIII),[108] perrutenato de tetrapropilamonio/N-óxido de N-metil-morfolina,[109] reactivos activados de dimetilsulfóxido[110] y reactivos Dess-Martin.[111] Los problemas asociados a estos reactivos son fundamentalmente sus costes y la producción de grandes cantidades de residuos tóxicos, es decir económicos y medioambientales. Resulta por tanto de extraordinario interés el conseguir procesos que efectúen la oxidación de manera catalítica y empleen oxidantes "*verdes*".

Esquema 1.16.

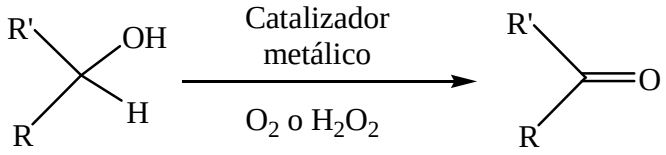

(R, R' = alquilo, arilo o H)

Se conocen muchos ejemplos de catalizadores heterogéneos y homogéneos que consiguen esta síntesis y ambas modalidades de catálisis tienen sus respectivas ventajas. En el caso de la catálisis homogénea, por ejemplo, una mejor selectividad y el empleo de temperaturas de reacción más bajas representan ventajas muy importantes. En estas reacciones cabe diferenciar dos categorías dependiendo si el reactivo oxidante es el H_2O_2[112] (o un hidroperóxido orgánico) o el oxígeno[113] (o el aire). En este resumen se centrará la atención en el segundo tipo de procesos.

1.4.1.1 Oxidación selectiva de alcoholes empleando dioxígeno como oxidante

En las oxidaciones aeróbicas de alcoholes se dan mecanismos de reacción distintos (Esquema 1.17) que proceden vía un intermedio de tipo hidroperoxo (a) o de

tipo peroxo (b). La mayoría de los ejemplos de oxidación de alcoholes con oxígeno molecular emplean catalizadores de los grupos 8-10, Pd(II), Ru(II), Rh(III), etc., siendo los más numerosos los catalizadores de rutenio.[114]

Esquema 1.17.

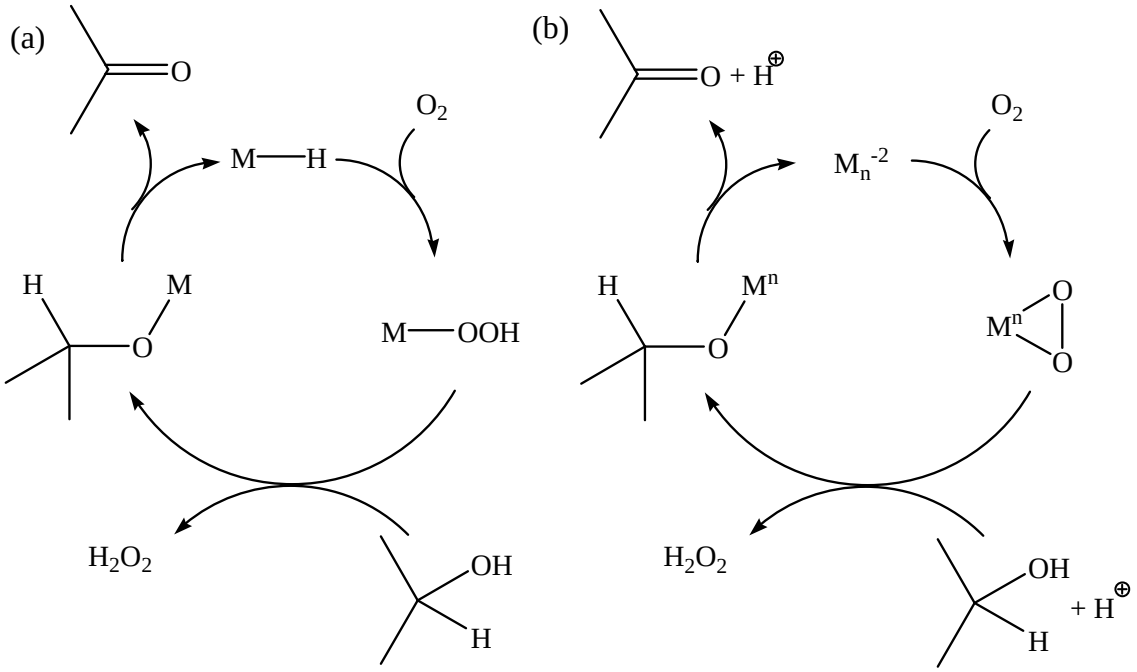

1.4.1.2 Oxidación de alcoholes en $scCO_2$

El número de ejemplos de oxidación de alcoholes en $scCO_2$ usando catalizadores metálicos en fase homogénea es reducido. Como ejemplo se halla la investigación de Busch y colaboradores sobre el proceso de autooxidación de fenoles con oxígeno empleando compuestos de Co(II) con ligandos tipo salen modificados, [Co(salen*)].[115] Más reciente es la contribución de Leitner, que describe la oxidación aeróbica de alcoholes catalizada por un polioxometalato de Mo y V.[116] Recientemente, el grupo de Asensio en Valencia ha descrito un sistema en continuo en $scCO_2$ que permite la oxidación de alcoholes en un medio heterogéneo en el que el catalizador es óxido de cromo CrO_3 depositado en SiO_2.[117] Como última novedad a reseñar se encuentra el reciente trabajo de Pagliaro y colaboradores,[118] que hacen uso de ILs soportados en sílica.[119] La idea original consiste en incorporar el catalizador de rutenio ($KRuO_4$) en el IL soportado en sílica, y efectuar la oxidación con oxígeno en $scCO_2$. En el medio

supercrítico se recuperan los productos de la reacción. De esta forma se propone un sistema integrado de oxidación que emplea un medio de reacción "*verde*", un disolvente (de la reacción y de extracción) "*verde*" y un catalizador que se puede recuperar.

1.4.1.3 Oxidación de alcoholes en ILs

En el campo de los ILs, es necesario citar que, en comparación con otras reacciones catalíticas, la oxidación de alcoholes ha recibido poca atención, hecho que ya apuntaban Seddon y Stark en 2002.[120] Estos autores observaron mejores resultados para la oxidación del alcohol bencílico a benzaldehido con oxígeno y un catalizador de Pd cuando el proceso se llevaba a cabo en un líquido iónico en comparación con la misma reacción en un medio convencional (dimetilsulfóxido como disolvente). Se ha descrito igualmente la oxidación en ILs de alcoholes a aldehídos o cetonas mediante el empleo de $[^{n}Pr_4][RuO_4]$ y el óxido de la N-metilmorfolina como co-oxidante.[121]

Existen un número limitado de ejemplos de oxidación de alcoholes catalizados por complejos de cobre en ILs. En 2002 Ansari y Gree presentaron un sistema catalítico empleando [CuCl]-TEMPO en C_4mim-PF_6. El sistema era efectivo en la oxidación de diversos alcoholes pero la reacción era lenta para los sustratos menos activos y el catalizador no podía ser reciclado al término de la reacción.[122] En 2005, Jiang y Ragauskas publicaron detalles de un sistema empleando $[Cu(ClO_4)_2]$–TEMPO(acetamida) (un análogo funcionalizado de TEMPO) en hexafluorofosfato de 1-butil-4-picolina. A temperatura ambiente este sistema era activo en la oxidación de un rango de alcoholes primarios mientras era inactivo para los secundarios. En este caso el catalizador era reciclable.[123]

Recientemente se ha descrito la funcionalización del TEMPO mediante la inclusión de un fragmento a modo de apéndice que contiene los grupos funcionales característicos de un líquido iónico.[124] Estos derivados serían ejemplos representativos de los denominados TSILs ("task-specific ionic liquids").[119(a)] Mediante la utilización de estos compuestos es posible realizar la oxidación de alcoholes catalizada por [CuCl] y el propio TEMPO, que se encontraría inmovilizado en el IL y por consiguiente puede ser reciclado con efectividad.[125]

1.4.2 Oxidaciones selectivas de alcoholes empleando como catalizador compuestos de cobre

El primer sistema práctico para la oxidación de alcoholes utilizando cobre como catalizador fue descrito por Semmelhack y colaboradores en 1984.[126] Desde la publicación de este trabajo, se han efectuado numerosos estudios en este campo, de los cuáles discutiremos algunos ejemplos seleccionados.

La mayoría de los sistemas que se detallarán emplean complejos de cobre como catalizador conjuntamente con un co-catalizador que incrementa la eficiencia del sistema. No obstante, merece la pena destacar las investigaciones realizadas con la metaloproteína galactosa oxidasa (GO), cuyo centro activo es un átomo de cobre(II). La GO cataliza selectivamente la oxidación aeróbica de alcoholes primarios a sus correspondientes aldehídos con la formación de un equivalente de H_2O_2 bajo condiciones suaves.[127] El mecanismo propuesto para la oxidación del sustrato consiste en la abstracción de un protón del alcohol coordinado, la transferencia de un radical H y la transferencia de electrones (Esquema 1.18).[128]

Esquema 1.18.

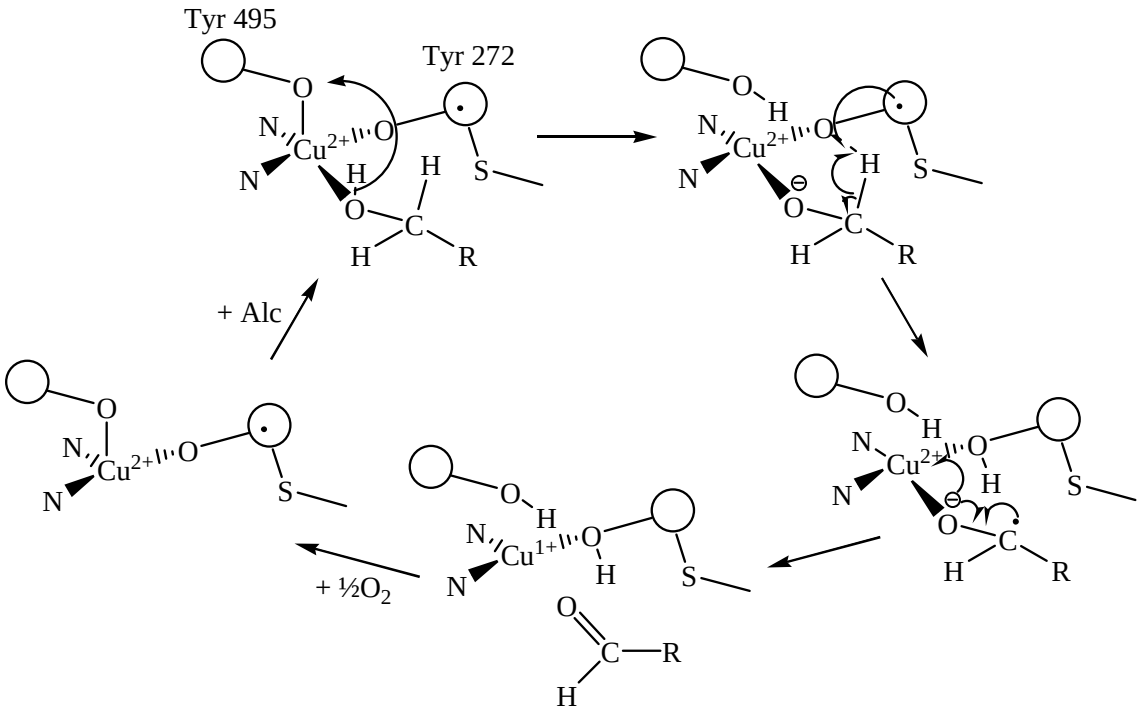

Se han sintetizado una gran variedad de compuestos que poseen una distribución de ligandos en torno al centro metálico de Cu(II) similar a la estructura de la GO y que muestran la capacidad de conseguir la oxidación de alcoholes primarios de la misma manera.[129] Sin embargo, la catálisis es lenta, se necesita una base y en la mayoría de los casos es limitada solamente a alcoholes primarios activos (alcoholes bencílicos y alílicos). En el mecanismo de esta reacción el oxígeno es activado por una especie de Cu(I), por lo que este tipo de compuestos debe ser potencialmente activos en dicha catálisis. En particular, los trabajos del grupo de Markó[130] han demostrado la eficiencia de los derivados de Cu(I) como catalizadores en estas reacciones. Por ejemplo, se ha descrito la oxidación de alcoholes primarios por oxígeno aeróbico empleando el complejo [CuCl(phen)] (phen = 1,10-fenantrolina) como catalizador. Este sistema ha sido muy bien estudiado, pero desafortunadamente su acción se ve limitada a sustratos activos ya que para alcoholes no activos y secundarios las conversiones eran relativamente bajas, incluso en presencia de grandes cantidades de catalizador.

1.4.2.1 Oxidaciones selectivas de alcoholes empleando sistemas Cu-TEMPO

El uso de radicales nitroxilo como catalizadores en procesos de oxidación es bien conocido tanto a escala de laboratorio como a nivel de la industria.[131] Entre los radicales más estudiados se encuentra el N-oxil-2,2,6,6-tetrametilpiperidina (TEMPO) (Figura 1.9) que ha demostrado comportarse como un catalizador versátil y eficaz.

Figura 1.9. N-Oxil-2,2,6,6-tetrametilpiperidina (TEMPO)

TEMPO

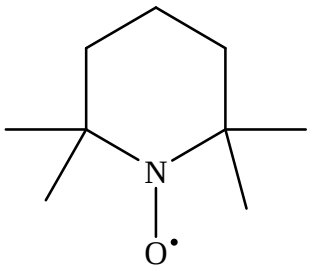

Por ejemplo, empleando TEMPO (1 %) como catalizador y una cantidad estequiométrica de hipoclorito de sodio como oxidante, se da la oxidación de varios alcoholes a los correspondientes compuestos carbonílicos con rendimientos superiores al 95%.[132] La especie oxidante en este proceso es el catión de tipo oxo-piperidinio que

se forma por la acción del hipoclorito sobre el TEMPO. Este catión oxida al grupo alcohol reduciéndose a una especie de tipo hidroxilpiperidina (TEMPOH); posteriormente, ésta regenera el catión oxidante mediante la re-oxidación con el hipoclorito (Esquema 1.19).

Esquema 1.19.

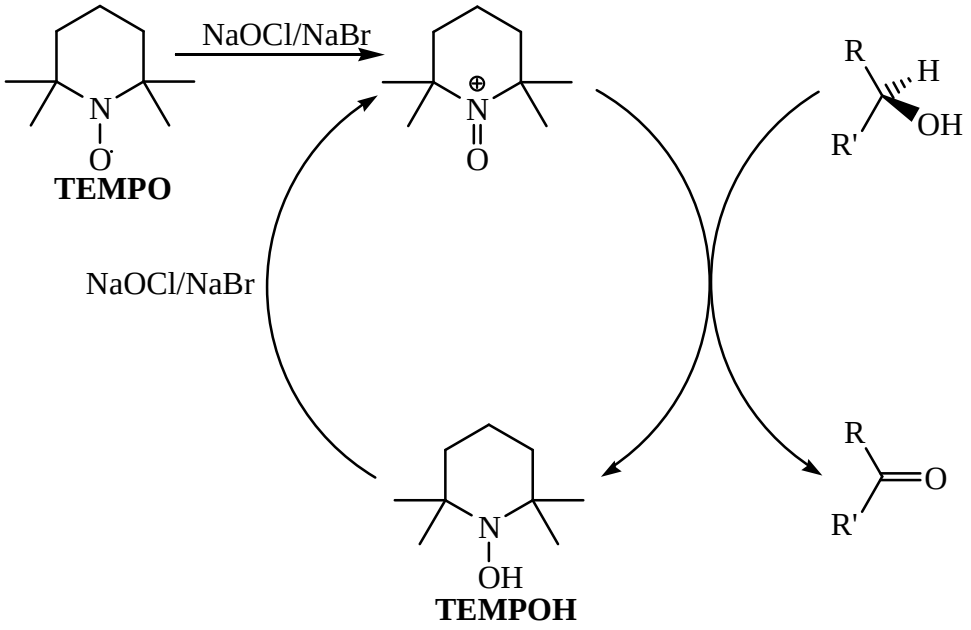

El sistema que se muestra en el Esquema 1.19 emplea bromuro de sodio como co-catalizador porque en la reacción con el hipoclorito se forma hipobromito que funciona mejor como oxidante del TEMPOH, permitiendo un ciclo catalítico más rápido. Desde un punto de vista medioambiental el uso en este sistema de hipoclorito como oxidante y grandes cantidades de bromuro de sodio y base no es ideal, ya que los reactivos son nocivos y resulta una baja economía atómica. Por ello, el desarrollo de sistemas catalíticos metal-TEMPO que empleen oxígeno como oxidante es un objetivo de gran interés. En este campo de investigación destacan en particular los sistemas empleando catalizadores de rutenio[133] y de cobre conjuntamente con TEMPO. A causa de la escasez y del precio del rutenio, los sistemas que emplean cobre tienen ventajas obvias.

Como se mencionó con anterioridad, en 1984, Semmelhack y colaboradores observaron la oxidación de alcoholes primarios de tipo bencílico, alílico y alifático, empleando [CuCl] (10 %) y TEMPO (10 %) como co-catalizadores y oxígeno como

oxidante.[126] En esta publicación también se propuso la secuencia catalítica para la oxidación que se muestra el Esquema 1.20.

Esquema 1.20.

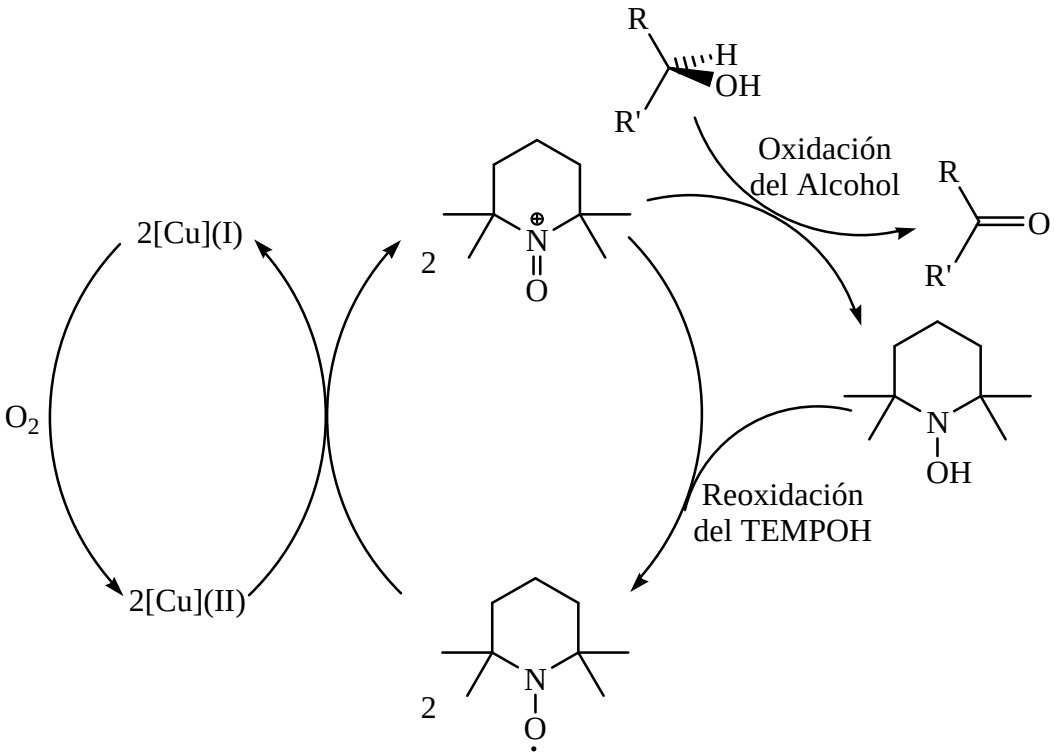

Tras la contribución mencionada, el grupo de investigación de Endo publicó en 1985 sus resultados empleando compuestos análogos de TEMPO junto con una selección de derivados de Cu(II).[134] La actividad del catalizador era proporcional a la capacidad coordinante del contra-anión. La catálisis era más rápida cuanto menor fuera la capacidad coordinante, aunque no proporcionaron una explicación específica a este comportamiento.

En 2003, Sheldon y colaboradores describieron la oxidación de alcoholes primarios empleando el conjunto $[Cu(Br)_2(bpy)]$/TEMPO (bpy = 2,2'-bipiridina) como catalizador.[135] El mecanismo propuesto para esta reacción está basado en el propuesto para la oxidación catalizada por GO descrita con anterioridad. En primer lugar, por sustitución de uno de los ligandos del complejo de cobre, el alcohol reacciona para formar un complejo Cu-alcóxido (complejo (a), Esquema 1.21). Éste interacciona con el TEMPO para formar el intermedio (complejo (b), Esquema 1.21), y abstracción del hidrógeno por parte del TEMPO produce el compuesto con el grupo carbonilo. El cobre

se reoxida por acción del TEMPO y éste se regenera por reacción con oxígeno completando el ciclo catalítico (ver Esquema 1.21).[136]

Esquema 1.21.

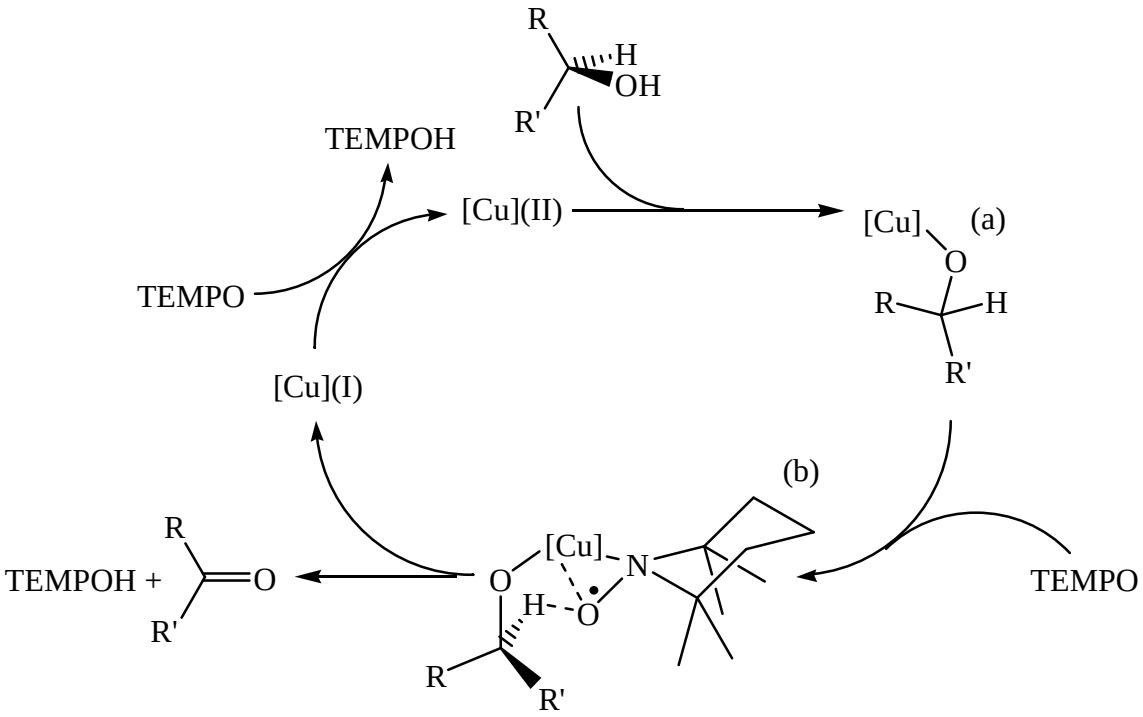

Sobre la base de este esquema es posible racionalizar la observación comentada anteriormente relativa al aumento de la velocidad de la oxidación cuando los contra-aniones no son muy coordinantes (p.e. Br^- ó ClO_4^-). La formación del intermedio alcóxido se verá impedida si existen especies con una buena capacidad coordinante al centro metálico. En el caso de alcoholes secundarios no se da la reacción de oxidación y, aunque no hay una explicación completamente establecida, se propone que en estos casos existe un impedimento estérico que previene la formación del intermedio (b). También, en el caso de un alcohol primario es probable que el oxígeno de la nueva especie TEMPOH pueda estabilizar el intermedio radical ((c), Esquema 1.22) por formación de un enlace intramolecular con el segundo hidrogeno del alcohol. En el caso de un alcohol secundario esta estabilización no es posible.

Esquema 1.22.

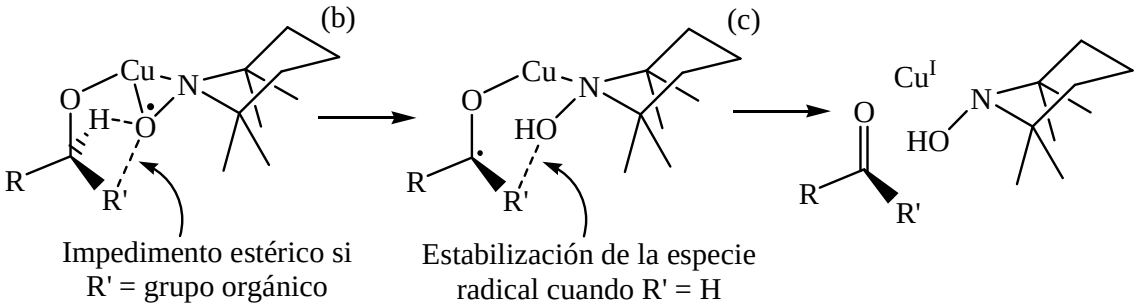

En el 2006 Punniymurthy y colaboradores también observaron la misma actividad catalítica para un sistema constituido por un complejo de cobre con un ligando modificado del tipo 'salen'.[137] En este caso es posible realizar varias veces de forma eficaz el reciclado del catalizador, pero se necesita una temperatura de reacción relativamente alta.

Recientemente se encontró que se mejoran las propiedades catalíticas de este sistema empleando una temperatura de reacción más alta en condiciones bifásicas.[138] Por ejemplo, el grupo de trabajo de Fish empleaba un sistema constituido por una fase orgánica (clorobenzeno) sobre una fase de perfluoroheptano a temperatura ambiente. El catalizador, una especie acetato de cobre(II) modificada con sustituyentes de cadenas alquílicas perfluoradas, se disuelve en la fase de perfluoroheptano mientras que en la fase orgánica se hallan el sustrato y el TEMPO. Cuando se calienta el sistema las dos fases son perfectamente miscibles y de esta manera se obtenía la oxidación catalítica eficiente del alcohol primario a su correspondiente aldehído. El catalizador se podía reciclar con la separación de las fases, que ocurre a temperatura ambiente, y usar en más ciclos catalíticos, aunque termina por desactivarse por reducción a una especie de [Cu](I).[139]

1.4.3 Oxidación selectiva de alcoholes empleando paladio(II) como catalizador

La utilización de catalizadores de paladio en la reacción de oxidación de alcoholes tiene precedentes que se remontan a fechas tan lejanas como 1977,[140] pero es a partir de los años noventa cuando este campo comienza a recibir una mayor atención. Schwartz y Blackburn desarrollaron el primer sistema viable para la oxidación aeróbica

de alcoholes, empleando diacetato de paladio junto con acetato de sodio. De los numerosos estudios que han aparecido desde esta publicación, se mencionan en este apartado los que destacan por su importancia en el desarrollo y en la interpretación de esta reacción catalítica. Peterson y Larcock desarrollaron un sistema empleando [$Pd(AcO)_2$] en DMSO con oxígeno como oxidante que mostró una buena actividad en la oxidación de alcoholes alílicos y bencílicos a sus correspondientes compuestos carbonilos.[141] Se consideró que el DMSO podría participar en la química redox de la reacción, hecho que contaba con diversos precedentes,[142] pero Stahl y colaboradores comprobaron que no era así. Estos autores propusieron el mecanismo que se muestra en el Esquema 1.23 en que el DMSO actuaba como inhibidor de la desactivación del catalizador a nanopartículas de Pd(0) mediante la coordinación a la especie intermedia de Pd(0) que se forma después de la oxidación del alcohol.[143] Igualmente, se investigó el destino final del H_2O_2 producido como subproducto de la reacción, encontrándose que éste se descompone catalíticamente por el paladio. Sobre la base de esta observación se concluye que no es posible utilizar peróxido de hidrógeno como oxidante en presencia de paladio en este tipo de sistemas y que el mecanismo de reacción procede por un intermedio tipo peroxo de acuerdo al propuesto en el mecanismo (b) del Esquema 1.17.

Esquema 1.23.

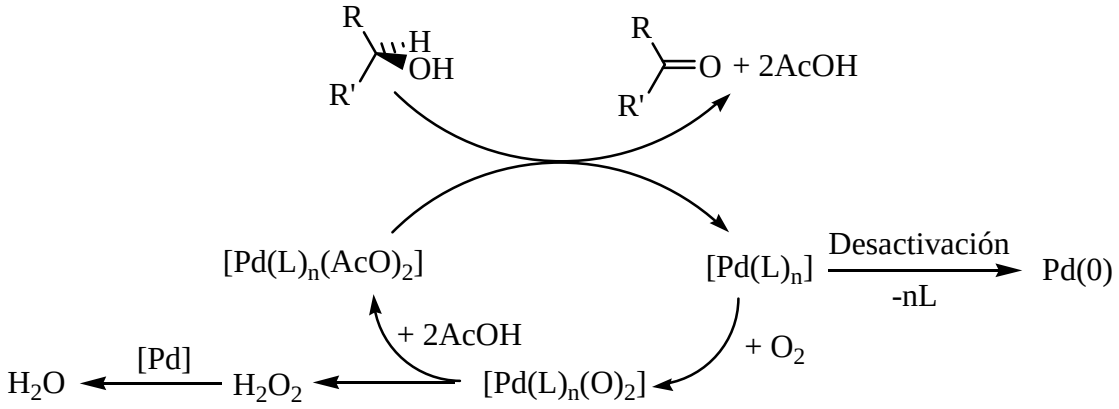

De manera similar, en un sistema empleando [$Pd(AcO)_2$]/piridina, el mismo grupo de trabajo observó que la piridina tiene la misma función.[144] Se encontró que en un disolvente orgánico la presencia de la piridina era esencial para facilitar oxidación del Pd(0) producido hasta Pd(II). En su ausencia ocurre tan sólo la oxidación

estequiométrica por el Pd, que se reduce a nanopartículas de Pd(0) inactivas. A este respecto, la piridina es superior al DMSO y un equivalente de piridina conduce a una velocidad de reacción 10 veces mayor que si la reacción se hace en DMSO puro. Si se emplean concentraciones más alta de piridina se inhibe mejor la desactivación del catalizador, pero tiene un efecto negativo en la velocidad de la reacción resultado de la competición con el sustrato en las vacantes de coordinación del centro metálico.

En 1998, Uemura y colaboradores desarrollaron un sistema empleando [$Pd(AcO)_2$], piridina y tamiz molecular, que mostraba una actividad considerable más alta que las descritas anteriormente (Esquema 1.24).[145] Como Peterson y Stahl se observó que la presencia de una base era esencial para la catálisis, aunque concentraciones elevadas inhibían la misma como resultado de la competición con el alcohol para coordinarse al centro metálico.

Esquema 1.24.

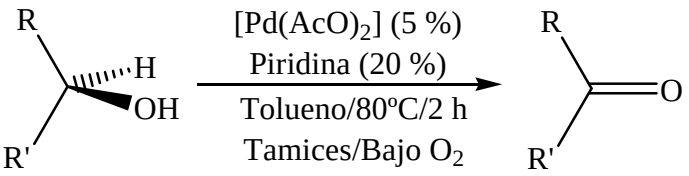

Alcoholes 1º, 2º y cíclicos

Este sistema muestra una alta actividad en la oxidación de una gran variedad de alcoholes, aunque se encontraron limitaciones en algunos casos. Como continuación, el mismo grupo ha publicado detalles de la aplicación de este sistema en otras oxidaciones.[146] También, en otros estudios demostraron que la adición de ligandos piridina con sustituyentes perfluorados convierte el sistema en bifásico con la posibilidad de reciclar el catalizador, pero con limitaciones con respecto a los sustratos a los que se aplica.[147] En este sistema se propone un mecanismo, que se muestra abajo (Esquema 1.25), en el que se forma como intermedio un hidroperoxocomplejo en el que el paladio conserva su estado de oxidación, de acuerdo con el mecanismo general (a) descrito en el Esquema 1.17.[148] La función de la piridina es estabilizar la especie intermedia hidruro-Pd(II) y evitar su descomposición a Pd(0) a través de la pérdida de AcOH. Este hidruro de paladio reacciona con oxígeno para formar un hidroperóxido, que en su interacción con el alcohol genera de nuevo el alcoxocomplejo y una molécula

de peróxido de hidrógeno. La reacción inversa reduce la velocidad de la catálisis y por esta razón se pueden emplear el tamiz molecular que ayuda en el proceso mediante la descomposición del H_2O_2.

Esquema 1.25.

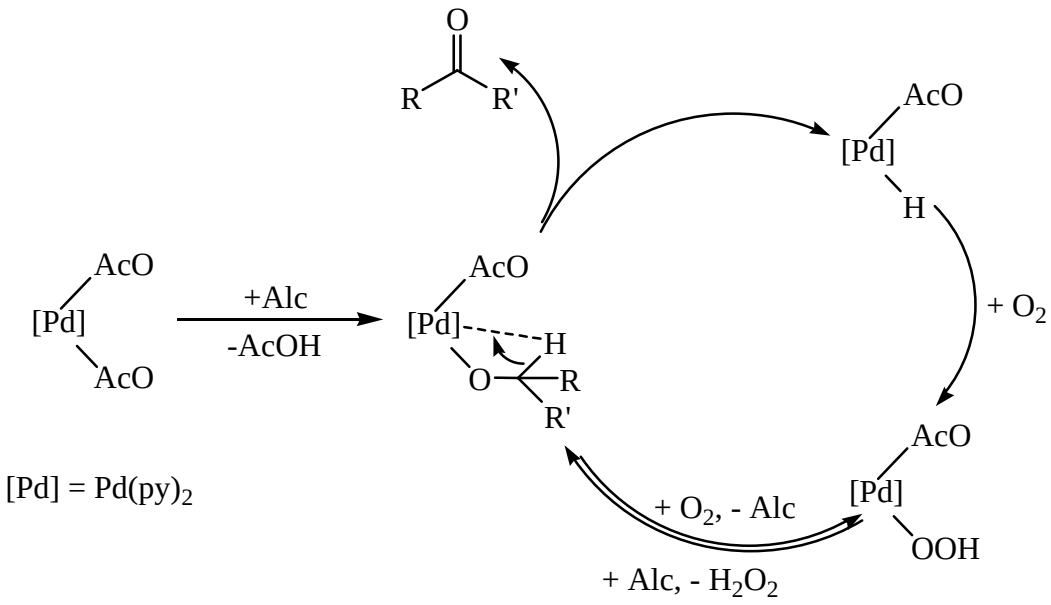

En todos los sistemas mencionados, la reacción catalítica emplea altas temperaturas de reacción. A este respecto, el desarrollo de sistemas que operen a temperaturas menores sería deseable y en este punto podemos citar el trabajo de Sigman y colaboradores, que describe la primera oxidación aeróbica de alcoholes catalizada por paladio a temperatura ambiente, empleando trietilamina (TEA) como base.[149] Se estudió el efecto que tiene la concentración del TEA sobre el mecanismo de la reacción mediante la técnica de RMN, observándose que los complejos $[Pd(AcO)_2]$, $[Pd(AcO)_2(TEA)]$ y $[Pd(AcO)_2(TEA)_2]$ existen en equilibrio. Una mayor concentración de TEA desplaza el equilibrio hacia el complejo $[Pd(AcO)_2(TEA)_2]$ con un efecto negativo en la velocidad de la reacción, que se encuentra relacionada con la concentración reducida del complejo $[Pd(AcO)_2(TEA)]$. Esto demuestra que la especie activa en el proceso catalítico es el complejo $[Pd(AcO)_2(TEA)]$ a diferencia del mecanismo propuesto para los sistemas que emplean piridina como ligando en los que se observa el complejo $[Pd(AcO)_2(py)_2]$ como única especie presente.

Tras este trabajo el mismo grupo describió un sistema que emplea como catalizador un complejo de paladio con un ligando carbeno heterocíclico nitrogenado (NHC).[150] Se observaron buenas actividades para una gran variedad de sustratos

empleando aire a presión ambiente como oxidante a una temperatura de 60 ºC. El ligando NHC enlaza fuertemente con el centro metálico, estabilizando las especies de Pd(II) y Pd(0) formadas en disolución, de manera que permite realizar la reacción catalítica sin la necesidad de un exceso de base adicional (Esquema 1.26). De esta forma es posible realizar un estudio mecanístico en la ausencia de base que permite determinar la naturaleza "no inocente" del ligando acetato, que no solo actúa como ligando sino que también lo hace como base que desprotona el alcohol en una reacción intermolecular tras su coordinación al paladio.

Esquema 1.26.

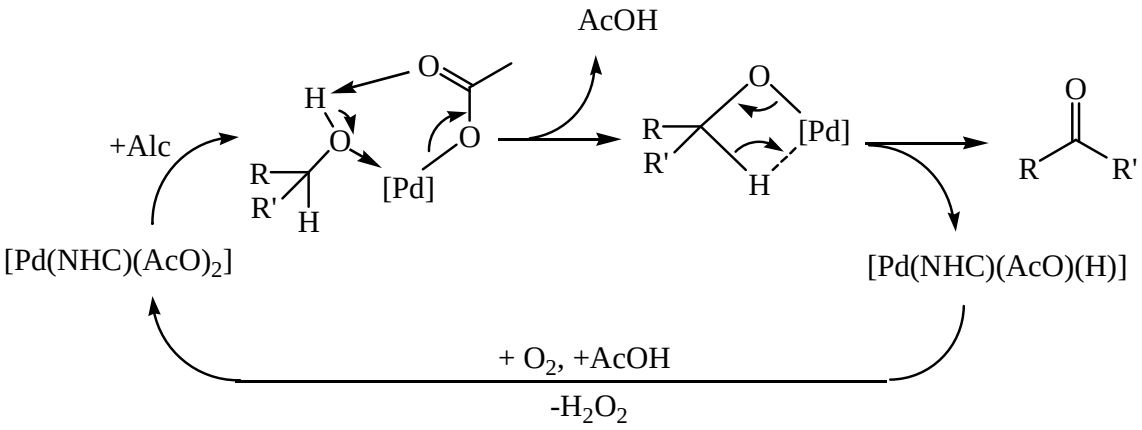

Esta observación explicaría las bajas actividades de otras especies de paladio (p.e. $[PdCl_2]$, $[PdCl_2(AcN)_2]$, $[Pd(dba)_2]$, $[Pd(PPh_3)_4]$, etc.). Se propone un mecanismo en el que el alcohol coordinado es desprotonado por el acetato, eliminándose como ácido acético, y el paladio por eliminación del hidrógeno-β formando como intermedio un hidruro-complejo con la formación del producto carbonilado, como se había propuesto en el mecanismo de Uemura. Sin embargo, por aquí el mecanismo procede en la manera propuesto por Stahl et. al. (Esquema 1.23), eliminación de ácido acético reduciéndose la metal a Pd(0), que se haya estabilizado por el ligando NHC. La oxidación por O_2 da el peróxido, que por reacción con ácido acético regenera el complejo inicial de diacetato (mecanismo (b), Esquema 1.17).

Como continuación de este trabajo, se investigaron carboxilatos más básicos alternativos al acetato y se encontró que la sustitución por pivalato ($t\text{-}BuCOO^-$) ofrece otro sistema efectivo en la oxidación aeróbica a temperatura ambiente.[151] Se realizó una comparación extensa investigando las ventajas de los tres sistemas mencionados. Se

demostró que el sistema con TEA era efectivo para una gran variedad de sustratos en condiciones suaves, pero se necesita bastante catalizador. El sistema con acetato era más ajustable, empleaba menos paladio, pero se necesitaba una temperatura de reacción más alta, mientras que con pivalato las condiciones eran más suaves, pero hay más limitaciones en los sustratos.

Finalmente, entre los estudios de esta reacción, cabe destacar los realizados por el grupo de Sheldon. Mediante el empleo de un ligando derivado de la fenantrolina que contiene grupos sulfonato es posible preparar un complejo de [$Pd(AcO)_2$] soluble en agua.[152] De este modo es posible realizar la catálisis en un sistema bifásico, el catalizador se encuentra disuelto en la fase acuosa y el alcohol forma la otra fase. La velocidad de la catálisis está limitada por la solubilidad del sustrato en agua y al término de la reacción el producto se puede separar del catalizador en la fase acuosa por simple decantación. El mecanismo propuesto del proceso, que procede en la fase acuosa, es similar al descrito por Stahl. Este trabajo destaca como un buen ejemplo de un proceso catalítico *verde*, ya que emplea condiciones suaves, disolvente y oxidante no nocivos y un catalizador que proporciona buenos TON.

2 Results and Discussion

2 Results and Discussion

2.1 A Methyltrioxorhenium Complex of Polydimethylsiloxane Functionalised Pyridine as an Efficient Olefin Epoxidation Catalysts in Solventless and Low Polar Solvent Conditions

The first of the studies that will be discussed here concerns the development of a method for carrying out the solventless epoxidation of olefin substrates using methyltrioxorhenium complexes as catalyst precursors and the green oxidant hydrogen peroxide. Detailed descriptions of the experimental procedures employed in the study can be found in the experimental section and the reaction conditions employed for comparative catalytic investigations are given in the sub-texts of the relevant results tables.

2.1.1 Preparation of 4-(polydimethylsiloxanyl-ethyl)pyridine (A)

Low molecular weight polysiloxanes are liquids at room temperature, chemically and thermally stable, inert, non volatile and display relatively good solubility in nearly all organic solvents including even highly non polar media such as $scCO_2$.[153] Despite this, although the use of other types of polymer substituents in such a capacity has been commonly reported,[154] the use of PDMS functional groups in the design of novel catalysts that make use of these properties has not been described until relatively recently.[155] Over the last few years however, a number of reports detailing their application in catalytic systems have appeared.[156] Systems where the catalyst (Jacobsen[157] or Grubbs[158]) is incorporated in a polydimethylsiloxane (PDMS) membrane have been reported, and Kerton, Rayner and co-workers synthesised PDMS tagged arylphosphines which were subsequently employed as $scCO_2$ solubilising ligands in homogeneous catalysis.[159]

One of the objectives of part of the studies described here was to develop catalytic systems in low polar media; $scCO_2$ and solventless conditions where the organic substrate/product serves as the reaction medium. With the potential of PDMS

functionalisation to solubilise catalyst complexes in non-polar media recognised, PDMS functionalised coordinating species thus became a synthetic target. To this end the PDMS functionalised pyridine, 4-(polydimethylsiloxanyl-ethyl)pyridine (**A**) was synthesised and characterised as discussed below. Subsequently, catalytic transition metal complexes of **A** were prepared and investigated appropriately.

Figure 2.1. 4-(Polydimethylsiloxanyl-ethyl) pyridine (**A**)

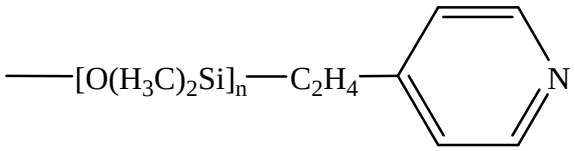

Transition metal coordination compounds of **A** could be considered as either metal complexes possessing short chain PDMS functions or as metal complexes supported on a liquid PDMS polymer, similar to how one might view heterogeneous catalysts where the catalytic complex is bound to the surface of a solid support. In contrast to solid supported materials, the metal complexes of **A** were intended for use in homogeneous rather than heterogeneous catalytic systems and the [catalyst]:mass ratio was thus the important measure for its quantification, rather than any surface area related measurements. Similarly though, in catalytic experiments the complex could be viewed as being supported in solution. In discussions of metal complexes of compound A, the complexes will be described as being "PDMS functionalised", but clearly they could equally be described as "PDMS supported".

Compound **A** was synthesised by the reaction of hydride terminated polydimethylsiloxane, $H[Si(CH_3)_2(OSi(CH_3)_2)_n]$, with 4-vinylpyridine (a hydrosilylation) using Kardstedt's catalyst.[160] *In-situ* IR spectra of the reaction mixture were used to monitor the progress of the reaction, as the hydride was consumed the Si-H peak of the hydride terminated PDMS at 2126 cm^{-1} gradually disappeared. Its absence indicated that the reaction was complete. After appropriate workup, **A** was obtained as clear oil. NMR analysis indicated that the product consisted of a mixture of two isomers resulting from the α and β (Markovnikoff and anti-Markovnikoff) addition of the Si-H to the vinyl group in a ratio of 1:2 (Scheme 2.1).[161] Attempts at controlling the ratio of isomers by adjusting the reaction conditions were unsuccessful. Chromatographic separation of the isomers was also attempted but results were

unsatisfactory. The resulting product mixture was characterised by analytic and spectroscopic methods.

Scheme 2.1. Hydrosilylation of 4-vinylpyridine with hydride terminated PDMS

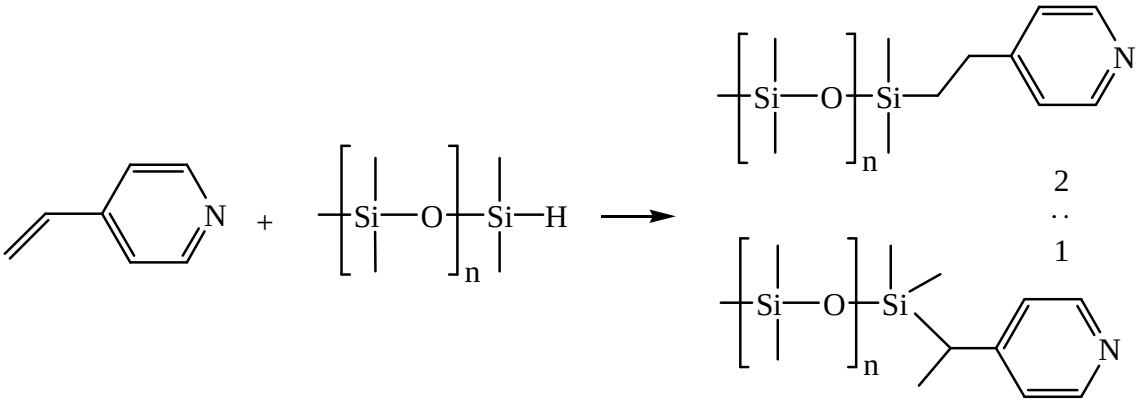

The number average molecular weight of $H[Si(CH_3)_2(OSi(CH_3)_2)_n]$ was determined by ^{1}H-NMR integration of Si-C*H*$_3$ versus Si-*H*. A M_n of ~525 was calculated, corresponding to $n \approx 6.3$. It was necessary to synthesise several samples of **A** during the course of the work. In each case, the ratio $Si(CH_3)_2$:pyridine was determined using ^{1}H-NMR integrals and it was thus possible to calculate the average M_n. The number average molecular weight of **A** varied between preparations, probably as a result of concurrent action of the platinum catalyst on the siloxane polymer during the hydrosilylation reaction. The ratio $Si(CH_3)_2$:pyridine was found to vary within a range of 5 to 10 (M_n = 530-900), although the α to β isomer ratio remained constant at around 1:2. Spectroscopic data for a representative product are collected together in the Appendices. For this sample, ^{1}H-NMR integrals indicate a ratio of approximately 5.5 $Si(CH_3)_2$ to every terminal pyridine (i.e. M_n = ~500). The ^{1}H-NMR spectrum displays a broad singlet at approximately 0 ppm produced by the Si(C*H*$_3$)$_2$ protons and appropriate alkyl signals corresponding to the -CH(CH$_3$)- and -CH$_2$-CH$_2$- protons in a 2:1 ratio, respectively. The pyridyl protons clearly differentiate into separate peaks corresponding to the two isomers. In the ^{29}Si{^{1}H}-NMR spectrum several signals are observed in the 21.6-22.1 ppm range corresponding to the non-terminal O-*Si*(CH$_3$)$_2$-O silicon atoms of the PDMS and the peak occurring at –12.9 ppm can be attributed to the silicon atoms adjacent to the -C$_2$H$_4$- moiety.[162] The absence of any peaks corresponding to tertiary or indeed quaternary silicon links indicates that there is no significant branching of the

polymer so that the product should be constituted from entirely linear chains terminated at both ends by pyridine functions.

2.1.2 Preparation of $[Re(CH_3)(O)_3(A)]$ (1a)

The hydrosilylative addition of PDMS to coordinated 4VP has been reported in the preparation of some iridium complexes.[163] However, having observed that the direct hydrosilylation of coordinated 4VP in a copper acetate complex was not possible (see Section 2.3.1), probably due to deactivation of the Pt catalyst, direct hydrosilylation of the 4-vinylpyridine complex of MTO was not investigated as a synthetic route to the desired product. The preparation of the coordination compound of MTO and compound **A** was thus achieved via reaction of the latter with MTO in dichloromethane. The PDMS functionalised MTO compound **1a** was obtained as a brown oil which was appropriately characterised. Clearly apparent in the ^{1}H and $^{13}C\{^{1}H\}$-NMR spectra are signals corresponding to $Si(CH_3)_2$, $-CH_2-CH_2-$ and one pyridine isomer, but signals from the α isomer present in the spectra of **A** are no longer apparent. This isomeric purification was also observed in the preparation of Pd complexes of **A**, **3a** and **4a** (see Section 2.4) via a similar experimental procedure (see Section 2.4.1). The most likely explanation for the elimination of the α isomer during work-up seems to be the lower solubility of its complexes in non polar media leading to their removal by filtration.

2.1.3 MTO catalysed epoxidation reactions

Several studies were carried out to investigate the relative effectiveness of MTO-**A** and MTO-pyridine catalysed systems as well as any advantages that the PDMS functionality might confer upon the former system. Investigations of relative epoxidative efficacy depending on experimental conditions initially employed the relatively active *cis*-cyclooctene as the olefin substrate, which for both steric and electronic reasons is highly susceptible to epoxidation and therefore commonly used for such studies. An excess 30 % aqueous H_2O_2 (3.0 equiv.) was used as oxidant and the catalyst:substrate ratio was 1:40. Initially catalytic performance depending on the reaction solvent was investigated before the focus shifted to solventless systems where the olefin itself comprised the organic phase. The success of the MTO-**A** catalyst under

these conditions led to generalisation of the study to investigate its effectiveness applied to a more diverse range of olefin substrates. Also particularly interesting were the results obtained in the solventless epoxidation of *cis*-cyclooctene with very low loadings of MTO catalyst (0.005 %), where **A** was seen to enhance the achievable TON considerably more than the other bases tested.

2.1.3.1 Influence of the reaction conditions on the epoxidation and comparisons with the MTO-pyridine system

The epoxidation of *cis*-cyclooctene in both chlorophorm and hexane, in the absence of base and in the presence of pyridine or **A** in a ratio of 4:1 to MTO was investigated (Table 2.1). The effect of temperature was also investigated by performing reactions at room temperature and at 60 ºC. The exact reaction conditions are given in the footnotes.

Scheme 2.2. MTO catalysed epoxidation of *cis*-cyclooctene

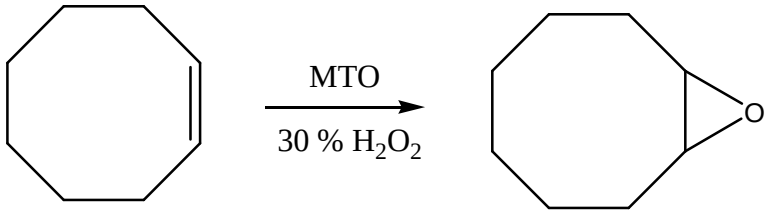

Table 2.1. *cis*-Cyclooctene epoxidations in chlorophorm or hexane, in the presence of no base, pyridine or compound **A**, at r.t. or 60 ºC [a]

Entry	Solvent [b]	Ligand	T	Conversion	(Yield) (%)[c]
1	Chlorophorm	-	Room temperature	100	(97)
2		Pyridine		100	(90)
3		**A**		100	(92)
4	Hexane	-		88	(82)
5		Pyridine		97	(89)
6		**A**		90	(82)
7		Pyridine	60 ºC	29	(29)
8		Pyridine[d]		29	(29)
9		**A**[d]		99	(99)

[a] MTO (0.025 mmol), 30 % H_2O_2 (3.0 mmol), cis-cyclooctene (1.0 mmol), ligand (0.1 mmol), $t_{reaction}$ = 18 h. [b] V = 10 mL. [c] Determined by GC analysis. [d] Coordination compound MTO-ligand previously prepared.

Examination of the results shown in Table 2.1 does not reveal any particularly significant differences in conversion which is always complete for the reactions in chlorophorm and nearly complete for those in hexane. Somewhat oddly, in chlorophorm the selectivity was slightly higher when no base was employed (entry 1, Table 2.1) than when it was (entries 2 and 3, Table 2.1). This makes little sense as while it could be argued that the bases might compete for coordinative sites on the metal and inhibit the rate of catalysis, thus lowering the conversion (though previous studies indicate that N-bases actually accelerate conversion, although formation of N-O oxides has been observed to lower the conversion rate), they should have a positive impact on selectivity due to their capacity to inhibit hydrolysis. The differences are sufficiently minor to be attributable to experimental variation in any case. In hexane it was anticipated that the MTO catalysts might have poor solubility, leading to low conversions, when no base or pyridine were used, whilst **A** might solubilise the catalyst and permit normal homogeneous catalysis consequently giving higher conversions. However, conversions were approximately the same in all cases, suggesting there was no difference in the mechanism of catalysis in any of the experiments. Notably, the PDMS containing catalyst MTO-**A** is entirely compatible with the use of the aqueous H_2O_2, in contrast to some existing examples where the catalyst is occluded in a PDMS membrane which acts as a barrier for H_2O_2 precluding the oxidation catalysis.[157c]

The results had therefore established that **A** did not offer any notable advantage over unsubstituted pyridine in these systems, presumably because of complete homogeneity in all cases. With **A** offering little advantage by way of solubility, the possibility that the PDMS functionalisation might lead to greater resistance to decomposition of the organometallic MTO was therefore examined. Under the basic oxidising conditions used for the epoxidation MTO is known to undergo decomposition via loss of its methyl group by which it converts to largely inactive oxide species.[55,164] The experiments in hexane were therefore repeated at 60 ºC to see if any differences would be observed.

The results clearly show that the coordination complex of **A** allows a very significantly higher yield under these conditions than if unsubstituted pyridine is used. The retarded yields observed using pyridine (entries 7 and 8, Table 2.1) compared with the analogous reaction employing **A** (entry 9, Table 2.1) or pyridine at room temperature (entry 5, Table 2.1) seem likely to result from decomposition of the MTO complex under the harsher conditions. Additional evidence for this comes from visual

observations of the reaction mixtures after reaction. For entries 5 and 9 they were yellow due to the presence of catalytically active rhenium peroxide complexes, but for entries 7 and 8 the mixture were colourless, indicating that the rhenium complex had likely decomposed to catalytically inactive inorganic oxide species. The identical conversions observed in entries 7 and 8 provide evidence that the complex had no problem forming *in-situ*. It can be concluded that complex **1a** (MTO-**A**) possesses superior resistance to decomposition under the oxidative conditions of the catalytic system compared to MTO-pyridine.

2.1.3.2 Solventless epoxidation reactions

The potential capacity of PDMS to solubilise MTO-**A** in non-polar media did not lead to any observable benefit in the experiments so far described. However, the study was extended to see if any advantages would be evident in solventless reactions, where the olefin substrate and reaction products alone comprise the organic phase. Table 2.2 shows the results obtained for a series of reactions investigating the solventless epoxidation of *cis*-cyclooctene.

Table 2.2. Solventless *cis*-cyclooctene epoxidations with different ligand additives [a]

Entry	Compound	Ligand	t (h)	Conversion (%)[b]	Yield (%)[b]
1	MTO	-	2	40	30
2	MTO	Pyridine	2	84	76
3	**1A**	-	1	45	45
4	**1A**	-	2	97	97
5	**1A**	-	18	100	100

[a] MTO (0.025 mmol), 30 % H_2O_2 (3.0 equiv.), cis-cyclooctene (0.5 mL, 3.65 mmol), ligand (0.1 mmol), r.t. [b] Determined by GC analysis.

It was found that in the absence of base (entry 1, Table 2.2) the conversion after 2 h was significant, though well less than complete, with some hydrolysis of the product to the diol taking place. It is likely that in this reaction the MTO catalyst resided mainly in the aqueous phase, separated from the substrate, thus inhibiting the rate of the reaction, and making the catalyst more vulnerable to decomposition, limiting the maximum obtainable yield. In the absence of base hydrolysis of the product would also be less inhibited. The results observed support these hypotheses. When pyridine was employed (entry 2, Table 2.2) the conversion was doubled and selectivity was

improved, although some hydrolysis still took place. Better solubility of the catalyst in the organic substrate due to the coordinated pyridines and inhibition of the hydrolytic epoxide decomposition may explain these improvements. For both entries 1 and 2 the post-reaction mixture was observed to be colourless, indicating an absence of rhenium peroxide species and implying that the catalyst had decomposed over the course of the reaction and was thus now inactive. When compound **1a** was employed as catalyst (entries 3-5, Table 2.2) faster conversion with complete selectivity for the epoxide product was observed. Practically complete conversion was observed after 2 h (entry 4, Table 2.2) and the strong yellow colour of the rhenium peroxide complex could be clearly seen in the organic phase, indicating that the catalyst remained active. The superior activity and selectivity observed in this system may be due to several factors. These include superior catalyst solubility in the organic substrate than in the two analogue systems with unfunctionalised catalysts, and concurrent insolubility in the aqueous phase, which should lead to more rapid epoxidation whilst hydrolysis is inhibited, since this reaction would best prevail in the aqueous phase. Reduced contact with the aqueous phase should also lead to greater catalyst stability and it would thus be logical to predict that higher TONs would be achievable using this catalyst (see below).

The reactions described up until this point all employed the *cis*-cyclooctene substrate, which is relatively activated to epoxidation for both steric and electronic reasons. However it was important that the scope of the study was extended to a greater range of olefin substrates to investigate how factors, such as the different solvent environments, susceptibilities to epoxidation and presence of other functional groups, that other substrates present would affect the activity of the catalyst. Terminal alkyl olefins are less electron rich and therefore less easily epoxidised than many other alkenes, as is regularly observed in catalytic epoxidation studies. The epoxidation of 1-octene would therefore be expected to proceed more slowly than that of *cis*-cyclooctene. A comparison between the activities of systems employing **1a** and MTO-pyridine as catalysts in the epoxidation of 1-octene was therefore made. Additionally, to investigate any difference in the stabilities of the catalysts when exposed to aqueous H_2O_2, the catalytic tests were repeated after the catalysts had been stirred with the oxidant for 2 hours prior to the reaction. The results are summarised below in 0.

Scheme 2.3. MTO catalysed epoxidation of 1-octene

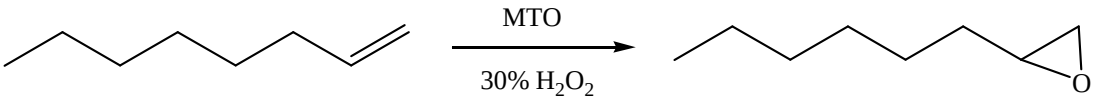

Table 2.3. Solventless 1-octene epoxidations with and without catalyst pre-treatment with H_2O_2 [a]

Entry	Ligand	Time stirred with H_2O_2 prior to commencing reaction (h)	Yield (%)[b]
1	Pyridine	0	50
2	**A**	0	58
3	Pyridine	2	23
4	**A**	2	56

[a] MTO (0.025 mmol), 30 % H_2O_2 (3.0 equiv.), 1-octene (0.585 mL, 3.65 mmol), ligand (0.1 mmol), r.t, $t_{reaction}$ = 18 h. [b] Determined by GC analysis.

Comparison of entries 1 and 2 shows that the two catalysts had relatively similar activities, the yield obtained employing **1a** only slightly greater than that obtained with MTO-pyridine. This would seem to indicate that a difference in the catalyst solubilities is not a factor affecting the conversion rates here. A more likely explanation is a slight difference in the activities of the catalysts or their stability to decomposition during the course of the reaction. Entries 3 and 4 provide evidence supporting the latter. A comparison of the yields observed in entries 2 and 4 reveals only a negligible difference, indicating that compound **1a** underwent no significant decomposition during 2 hours stirring with aqueous H_2O_2. In contrast, yield was observed to decrease by over 50 % between entries 1 and 3. Stirring the catalyst with hydrogen peroxide produced a change which was highly detrimental to the activity of the system, with decomposition of the catalyst the most probable explanation. Note that H_2O_2 decomposition by the MTO is unlikely to be responsible for the diminished yield; previous studies have shown that MTO compounds do not in fact decompose H_2O_2 so this should not be a factor.[94] Compound **1a** therefore appears to possess a far greater stability to decomposition by aqueous hydrogen peroxide than its pyridine analogue, which indicates a potential for higher yields and TONs, and subsequently this was appropriately investigated as will later be discussed.

Attention then shifted to the investigation of the range of olefin substrates to which the solventless **1a**/H_2O_2 epoxidation system might be applied. A selection of olefins were thus tested, the results summarised in Table 2.4.

Table 2.4. Solventless olefin epoxidations employing MTO-**A** as catalyst [a]

Entry	Olefin		Yield (%)
1	*cis*-Cyclooctene	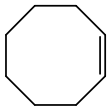	100 [b]
2	1-Octene	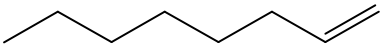	55 [b]
3	*trans*-2-Octene	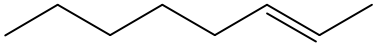	100 [c]
4	*trans*-4-Octene	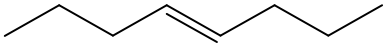	95 [c]
5	Cyclohexene	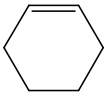	100 [b]
6	Styrene	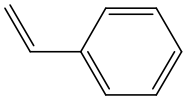	95 [c]
7	Allylic alcohol	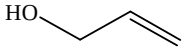	80 [c]
8	Ethyl acrylate	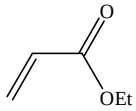	<5 [c]

[a] *MTO (0.025 mmol), **A** (0.1 mmol), 30 % H_2O_2 (3.0 equiv.), olefin (3.65 mmol), r.t., $t_{reaction}$ = 18 h.*
[b] *Determined by GC analysis.* [c] *Determined by ^{1}H NMR integral analysis.*

The cyclic olefins, *cis*-cyclooctene and cyclohexene were found to convert completely within 18 h (entries 1 and 5 respectively, Table 2.4), as expected for these activated substrates. Amongst the alkyl olefins, the inactive primary olefin 1-octene converted slowly, giving only a 55 % yield (entry 2, Table 2.4) whilst the more active secondary *trans*-2- and *trans*-4-octene substrates converted almost completely (entries 3 and 4 respectively, Table 2.4). In many epoxidation systems styrene has a tendency to hydrolyse, undergo C-C splitting reactions and over oxidise, leading to products such as benzoic acid and benzaldehyde, though there was no evidence of such products here and

almost complete conversion to the epoxide was seen (entry 6, Table 2.4). The oxidation of allylic alcohol (entry 7, Table 2.4) was chemoselective and a good conversion to the epoxide was observed, indicating that the close proximity of the alcohol group did not present a problem. However, only trace evidence of the epoxide was observed in the epoxidation of ethyl acrylate (entry 8, Table 2.4).

2.1.3.3 Attempted epoxidation of propylene with the MTO catalysts

Having observed from the results shown in Table 2.4 that the MTO-**A** catalyst was capable of catalysing the epoxidation of a variety of even relatively inactive substrates, the possibility that it might be capable of catalysing the industrially important epoxidation of propylene was considered. Propylene oxide is an important chemical intermediate in the production of a range of products, including polyether polyols (used to produce polyurethane plastics), propylene glycols and propylene glycol ethers. Until recently it was generally produced via hydrochlorination,[165] but several oxidative processes now account for a significant proportion of propylene oxide production, including the Halcon process with organohydroperoxo oxidants[166] and the HPPO process which employs H_2O_2.[167] Since propylene is a gas under standard conditions the study of its oxidation was more complicated than the liquid substrates previously investigated. Reactions were therefore performed in octane, which was able to dissolve the propylene substrate, with the aqueous hydrogen peroxide oxidant forming a separate phase. The reactions were carried out in a special pressure reactor, applying initially a 4 bar pressure of propylene. Given the reactor volume (~160 mL) this was calculated to correspond to approximately a 28 mmol propylene loading. The pressure was observed to drop quickly to around 2 bar once stirring was initiated due to dissolution of the propylene in the organic solvent phase, which visibly expanded in volume. The epoxidation was attempted using MTO, MTO-pyridine and MTO-**A** as catalyst precursors. For these reactions an assessment in terms of TON relative to the catalyst loading was more appropriate than the reaction yield. The results of the study are shown below in Table 2.5.

Table 2.5. Propylene epoxidations with MTO catalysts [a]

Entry	Catalyst	TON
1	MTO	0
2	MTO-py [b]	0.2
3	MTO-**A** [c]	14.5

*[a] MTO (0.025 mmol), propylene (4.0 bar, 28 mmol), 30 % H_2O_2 (1.5 equiv., 42 mmol), r.t., $t_{reaction}$ = 12 h, yields determined by GC analysis. [b] Pyridine (0.1 mmol). [c] **A** (0.1 mmol).*

Comparing entry 1 (Table 2.5) with entries 2 and 3 (Table 2.5) it appears that the presence of a base species was required to induce an appreciable level of conversion, no epoxide being detected when only MTO was employed as catalyst. Visually, the behaviour of the system which employed **A** as base additive differed significantly to the other two reactions. In the absence of base and where pyridine was used (entries 1 & 2, Table 2.5), immediately after charging the system an intense yellow colour was observed in the lower aqueous phase, though within five minutes this colour faded and the reaction thereafter remained colourless throughout the course of the reaction (see Figure 2.2 (b)). In the system which employed **A** as additive (entry 3, Table 2.5) the yellow colour was instead observed in the organic phase, and the colouration did not appreciably fade even after 12 h of reaction (Figure 2.2 (a)). The reasons for these observations are likely hydrolytic decomposition of the catalyst in the former systems, due to dissolution of the MTO catalyst complex in the aqueous phase, and stabilisation of the MTO-**A** catalyst in the organic phase in the latter, where it was protected from substantial decomposition for the duration of the reaction. Moreover the rapid formation of a strong yellow colour indicates that the MTO was still easily able to react with the hydrogen peroxide to form the peroxo complex. In terms of TON the MTO-**A** system was indeed found to be very markedly more active than the other systems; in the absence of base no conversion was detectable and only a trace amount of epoxide product was produced by employing pyridine, resulting in an extremely poor turnover of just 0.2. However, the yield of propylene oxide measured after 12 h of reaction was still only 14.5, indicating that the latter system was still only fairly poorly active. Given that formation of the rhenium-peroxide complex in this system appeared to be fairly rapid it therefore seems likely that the poor activity resulted from the limited capacity of the peroxide complexes to transfer an oxygen atom to the substrate. The poor rate of the epoxidation in this system is put into context by considering the TOF for the reaction, which is only just over 1 h^{-1}. Further development of this system might be achievable through consideration of how the transfer of oxygen from the peroxo complex to the

substrate might be accelerated, perhaps achievable through the use of additives or a different PDMS functionalised ligand. However this was not further investigated as part of the studies presented here.

Figure 2.2. Colouration of the octane phase after 12 h of reaction when (a) MTO-**A** and (b) MTO-py was employed as the catalyst precursor

(a) 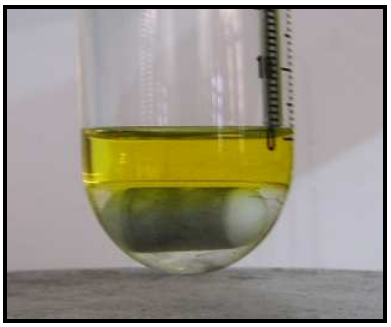 (b) 

2.1.3.4 Investigation of N-donor bases in solventless epoxidations in the presence of very low (0.005 %) MTO catalyst loadings

It was previously shown that in small scale reactions employing ~0.68 % MTO and ~2.7 % base in the epoxidation of *cis*-cyclooctene, only minor differences in activity are observable between systems employing **A** and pyridine as base (Table 2.1). However, a further study was conducted using a much lower MTO:substrate ratio, raising the maximum achievable TON to 20,000. Under these conditions, differences in the maximum achievable yields, resulting from the catalyst lifetimes, for the systems tested should become apparent. A series of reactions employing only 0.005 % MTO and 1 % of the selected N-donor base were thus run (see Table 2.6).

Table 2.6. Solventless *cis*-cyclooctene epoxidations with a very low catalyst loading [a]

Entry	Ligand	Yield (≈ conversion) [b]	TON
1	Pyridine	0.23 %	45
2	3-Methylpyrazole	0.30 %	61
3	3-Methylpyrazole [c]	0.66 %	133
4	4-Tridecylpyridine	0.06 %	12
5	**A**	11.60 %	2320

[a] MTO ($7.3 \cdot 10^{-4}$ mmol, 0.00005 equiv. 11 mM in CH_2Cl_2), ligand (0.146 mmol, 0.01 equiv.), 30 % H_2O_2 (3 equiv.), cis-cyclooctene (2 ml, 14.6 mmol), r.t, $t_{reaction}$ = 17 h. [b] Determined by GC analysis. [c] 0.1 equiv. of ligand.

A comparison of entries 1 and 5 now shows a clear difference between the conversions achieved using unsubstituted pyridine (entry 1, Table 2.6) and **A** (entry 5, Table 2.6), with a far higher yield and thus TON obtained in the MTO-**A** system. A trial was also performed using 4-tridecylpyridine (entry 4, Table 2.6), but this system also performed poorly. The highest TON yet observed in an MTO catalysed olefin epoxidation was 20,000, employing 10 % 3-methylpyrazole in the oxidation of *cis*-cyclooctene in chlorophorm.[65] Under solventless conditions, this reaction was attempted using both 1 % (entry 2, Table 2.6) and 10 % (entry 3, Table 2.6) 3-methylpyrazole, but in neither case were the TONs observed even nearly of the magnitude of those with MTO-**A**. Thus, in the solventless epoxidation of *cis*-cyclooctene by MTO, the addition of just 1 % of **A** resulted in yields many times higher than those observed for simple bases typically employed in these reactions. Notably the yield was considerably higher than that observed even when 10 % of 3-methylpyrazole was employed, established as an optimal system when carrying out this epoxidation in chlorophorm.[65] The greater activity of the MTO-**A** system seems to result from the catalysts high resistance to decomposition compared to other MTO-base systems.

Such a stabilisation of the catalyst could conceivably arise due to the ligand having a relatively high resistance to oxidation to its N-oxide. For reasons already discussed in the introduction section, this would likely result in both higher catalytic activity and resistance to irreversible decomposition of the Re-CH_3 bond and would explain the superior results observed for the MTO-**A** system. Elevated yields observed in epoxidation systems employing **A** in conjunction with oxobisperoxomolybdenum (see Section 2.2.7.1) also lend some credence to this hypothesis. The oxidation resistance of the ligand might result from protection that its emulgent nature accords. However, actual experimental evidence regarding the oxidation of **A** in such catalytic systems remained elusive, and this theory as such remains speculative. Evidence for another manner in which such a stabilisation might arise was provided by a theoretical study conducted independently of the work covered here.[168] DFT calculations were carried out for several model MTO complexes which are shown below in Figure 2.3 The studied models correspond to **1a** complexes of both the α and β hydrosilylation products with short PDMS chains (models **1i** and **1ii** respectively). These were also compared with the (4-heptylpyridine)methyltrioxorhenium complex (**1iii**), appropriate

since in **1iii** the alkyl chain function has the same number of atoms as the PDMS chains in **1i$_2$** and **1ii$_2$**.

Figure 2.3. Models used in the DFT study

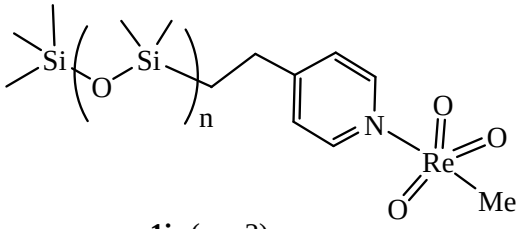

1i$_2$ (n = 2)
1i$_4$ (n = 4)

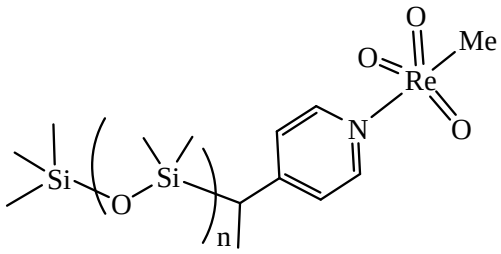

1ii$_2$ (n = 2)
1ii$_4$ (n = 4)

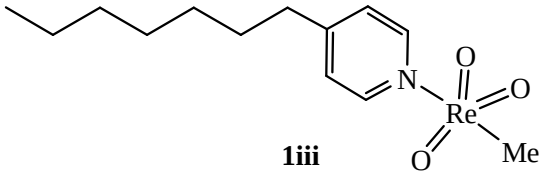

1iii

Optimised structures for **1i$_2$**, **1ii$_2$** and **1iii** are shown below in Figure 2.4. No significant energetic differences between the α and β isomers were calculated. However, when the optimised geometries and structural parameters of **1i$_2$** and **1ii$_2$** were compared with **1iii** interesting differences were observed. In both **1i$_2$** and **1ii$_2$** the PDMS chains are observed to have moved into proximity with the oxo ligands of the rhenium, indicating C-H$^{\cdots}$O interactions. In contrast such an interaction is not observable in **1iii**. The importance of such interactions in MTO has been previously investigated,[169] and the computed C-H$^{\cdots}$O lengths of 2.749 and 3.581 Å (**1i$_2$**) and 2.673 and 2.789 Å (**1ii$_2$**) are in the range of those previously calculated[169] and observed experimentally via diffraction methods[170] for MTO. The electronic energy calculated for the C-H$^{\cdots}$O interactions is small but significant (*ca*. 2 kcal·mol^{-1}) and these interactions may be a factor in the catalyst stability of the MTO-**A** system.

Figure 2.4. Optimised structures of model compounds **1i$_2$**, **1ii$_2$**, and **1iii**

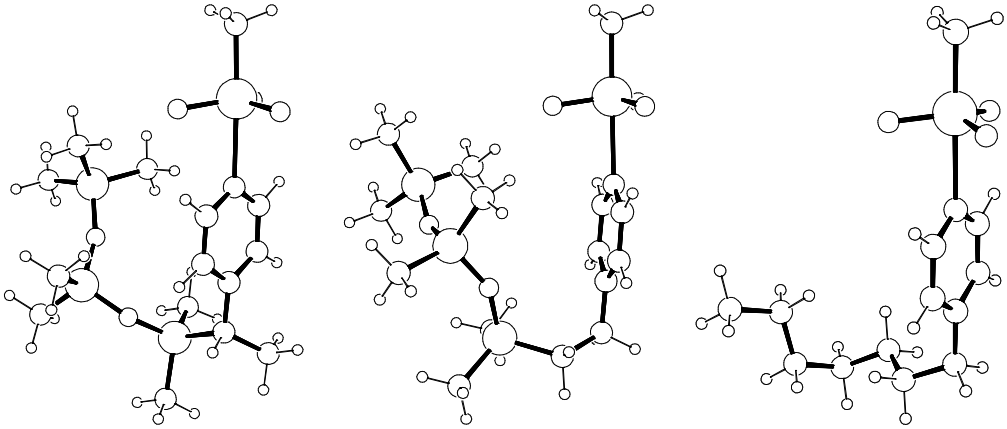

1i$_2$ **1ii$_2$** **1iii**

In summary, the activity of **1a** was compared with that of MTO-pyridine and in several cases the PDMS functionalised catalyst was observed to possess significant advantages. For the epoxidation of *cis*-cyclooctene with 30 % aqueous H_2O_2 as oxidant, the influence of the solvent and temperature were investigated, concluding that whilst the PDMS did not confer any solubility advantages even in hexane, it did result in the catalyst being more resistant to decomposition at higher temperatures. It is also notable that, unlike PDMS membranes which can act as a barrier to H_2O_2 and preclude oxidative catalysis, the PDMS supported catalyst is compatible with the aqueous 30 % H_2O_2 oxidant. In studies of catalytic activity in the absence of solvent, compound **1a** was found to offer faster, more selective conversion than the MTO-pyridine analogue, with the catalyst also much more resistant to decomposition. It was concluded that this is due, at least in part, to the capacity of the PDMS to solubilise the coordinated MTO in the olefin more effectively than unfunctionalised analogues. This solventless epoxidation system was successfully applied to a variety of olefins achieving good epoxide yields in many cases. Additionally, the catalyst also performed well when the MTO-base:substrate ratio was lowered in order to investigate the maximum attainable yields in the epoxidation of *cis*-cyclooctene. Apparently as a result of superior catalyst stability a far higher TON was achievable using the MTO-**A** catalysed system compared to other typical MTO-base combinations. In the oxidation of propylene performed in octane, **1a** was markedly more active than non PDMS functionalised analogue catalysts apparently due to higher stability probably resulting from stabilisation of the catalyst in the organic phase. However, the activity was still relatively poor apparently due to the low rate at which peroxo oxygens transferred to the substrate.

2.2 Oxobisperoxomolybdenum(VI) Complex Catalysed Epoxidations Part A: in Ionic Liquids

2.2.1 Molybdenum trioxide as an olefin epoxidation catalyst precursor in 1-butyl-4-methylimidazolium hexafluorophosphate (C_4mim-PF_6)

As was previously discussed in the introduction, olefin epoxidations can be accomplished employing compounds of a variety of transition metals as catalysts/catalyst precursors.[40-43] From an economic and environmental perspective, the use of simple, cheap and commercially available molybdenum compounds in such a capacity would offer significant advantages over many other known processes. On this basis, this study of homogeneous oxobisperoxomolybdenum catalysed olefin epoxidations using molybdenum compounds such as the trioxide or ammonium molybdate as catalyst precursors was initiated. Molybdenum catalysed epoxidations often employ organohydroperoxides, particularly *tert*-butyl hydroperoxide (TBHP) as oxidants. Preferable however would be the use of hydrogen peroxide, which is cheaper and generates only benign oxygen and water as waste by-products. Problematic in the use of many oxo-molybdenum compounds as homogeneous catalysts is their poor solubilities in commonly used reaction solvents. Because of their excellent solubilising properties, the use of an ionic liquid as the reaction medium is one way in which this problem could potentially be solved. 1-Butyl-3-methylimidazolium hexafluorophosphate (C_4mim-PF_6) is a very commonly used, relatively low cost ionic liquid which interestingly has only a fairly low miscibility with water.

2.2.1.1 Investigation of MoO_3 as a catalyst precursor

As in the previous study of MTO catalysed epoxidations, *cis*-cyclooctene was selected as the olefin substrate. To begin with the readily available molybdenum(VI) compounds molybdenum trioxide, MoO_3 and ammonium dimolybdate $(NH_4)_2Mo_2O_7$, and several solvent and oxidant combinations were investigated. With the objective being to use hydrogen peroxide as the oxidant, two H_2O_2 sources were investigated, 30 % aqueous solution and the urea-hydrogen peroxide adduct (UHP). Several commonly used solvents were tested in order to make comparisons with the ionic liquid

C_4mim-PF_6. The results obtained in this study are shown below in Table 2.7. Detailed descriptions of the experimental procedures can be found in the experimental section and the reaction conditions are given in the sub-text to the relevant results tables.

Scheme 2.4. *cis*-Cyclooctene epoxidation system

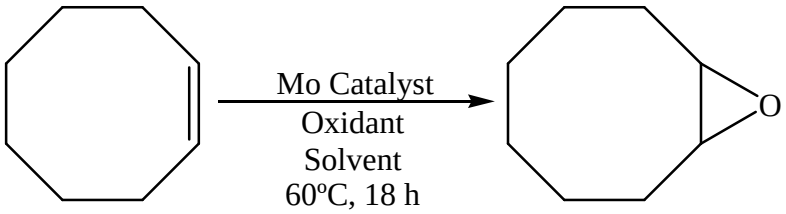

Table 2.7. Molybdenum catalysed cyclooctene epoxidations [a]

Entry	Solvent	Precatalyst	Oxidant	Conversion (Yield) [b]	
1	C_4mim-PF_6	-	UHP	<5	(<5)
2		$(NH_4)_2Mo_2O_7$	UHP	>90	(>90)
3		MoO_3	UHP	>90	(>90)
4		MoO_3	H_2O_2	100 [c]	(0) [c]
5		[Mo(O)$(O_2)_2$(bpy)]	UHP	>90	(>90)
6	MeOH	$(NH_4)_2Mo_2O_7$	UHP	0	(0)
7		MoO_3	UHP	1	(1)
8	H_2O	$(NH_4)_2Mo_2O_7$	UHP	0	(0)
9		MoO_3	UHP	<5	(<5)
10		MoO_3	H_2O_2	<5	(<5)
11	CH_2Cl_2	$(NH_4)_2Mo_2O_7$	UHP	0	(0)

[a] T = 60ºC, t = 18 h, cis-cyclooctene (1.0 mmol), UHP (1.5 mmol) catalyst (0.025 mmol), $V_{solvent}$ = 5 ml. [b] Conversion and yield were calculated by weight and NMR of product. [c] Conversion to cyclooctane-1,2-diol was observed.

The only solvent/oxidant combination in which significant conversion to the epoxide was observed was C_4mim-PF_6 with UHP. The conventional solvents H_2O, MeOH and CH_2Cl_2 (entries 6–11, Table 2.7) gave, at best, extremely low yields (<5 %) of the epoxide product. It is likely that an important factor which limited conversion in these cases was the inability of these solvents to dissolve all of the reaction components (i.e., UHP is insoluble in Cl_2CH_2 whilst cyclooctene is insoluble in water). In C_4mim-PF_6 almost complete reaction was seen after approximately 18 h using both $(NH_4)_2Mo_2O_7$ (entry 2, Table 2.7) and MoO_3 (entry 3, Table 2.7) as catalytic precursors. Compared to the other systems tested, the capacity of the C_4mim-PF_6 to sufficiently solubilise all of the component compounds of the reaction seems the likely explanation for the activity of this system. Epoxidation clearly proceeded via a metal catalysed mechanism since no conversion was observed in the absence of a molybdenum species

(entry 1, Table 2.7). The use of aqueous hydrogen peroxide as the oxidant resulted in complete conversion of the olefin but with no yield of epoxide (entry 4, Table 2.7). This is attributable to ring opening hydrolysis of the epoxide, giving cyclooctane-1,2-diol. The acidic molybdenum centre catalyses this reaction,[102,171] which would have been facilitated in this system by the high concentration of water. Using the dry hydrogen peroxide source UHP seems to sufficiently limit the availability of water to prevent this reaction. Additionally, it is worth noting at this point the low basicity of the urea by-product (pK_a = 0.18); it can be considered unlikely that urea has any important influence as a coordinative species in the system. The best result obtained is shown by entry 3, where the reaction in C_4mim-PF_6 using UHP catalysed by the cheap and commercially available molybdenum trioxide gave an excellent conversion. Note also the equally high conversions seen in entries 2 and 5 for the dimolybdate and [Mo(O)$(O_2)_2$(bpy)] species. In the former case it is likely that the molybdate is a precursor for the same catalytic species as is active when the trioxide is employed, and largely identical results are thus observed. It is assumed that the catalytic species is an oxobisperoxomolybdenum, as employed in the latter, where such a species was observed to give a similarly high conversion. In this case, the bipyridine had no discernible effect upon the rate of reaction, though it should be noted that this contrasts the results of later studies presented here (see Table 2.11, Table 2.12 & Table 2.23), where bipyridyls were determined to have an inhibitory effect on the rate of epoxidation. This will be discussed in more detail later on.

The results presented in Table 2.7 are notable in that they are the first reported examples of an oxobisperoxomolybdenum catalysed olefin epoxidation in an ionic liquid.[172] Use of MoO_3 as a convenient and cheap catalyst precursor in this transformation has been recently reported, though using *tert*-butyl hydroperoxide as oxidant in toluene.[173] It should be noted that the system described here requires a rather long reaction time and high temperature when compared to optimal examples of Mo catalysed olefin epoxidation, for example compare with the work of Bhattacharyya and co-workers.[84]

2.2.1.2 Recycling the catalytic system

In continuation, the recyclability of the catalyst/ionic liquid mixture left after product extraction was then investigated. This is a well known advantage for many catalysed reactions in ionic liquids with reported precedents.[174] Recycling the system could lead to several advantages such as a better turnover number and atom economy. A problem in the case of this system is that the use of UHP as oxidant results in an accumulation of urea in the reaction medium which is not eliminated in the extraction. Two possibilities exist for its removal; a water wash or its precipitation and removal by filtration. Washing with water would likely be very effective in removing the urea but catalyst leaching could be a problem. It was found that dissolving the ionic liquid in dichloromethane caused the dissolved urea to precipitate and reduced the solvent viscosity, allowing its removal by filtration. Simultaneous precipitation of the catalyst was considered a potential problem, but visually there was no evidence of this as the filtered urea was colourless whilst the ionic liquid retained the yellow colouration of the catalyst. Dichloromethane was subsequently removed under reduced pressure and after the new addition of UHP and cyclooctene further catalytic cycles were attempted (Table 2.8).

Table 2.8. Recycling catalytic ionic liquid systems [a]

Catalyst	**MoO_3**					**$Mo_2O_7(NH_4)_2$**					**MTO**	
Run	1	2	3	4	5	1	2	3	4	5	1	2
Conversion (%)	>90	>90	75	30	-	>90	50	10	5	-	>90	-

[a] T = 60ºC, t = 18 h, cis-cyclooctene (1.0 mmol), UHP (1.5 mmol), catalyst (0.025 mmol), C_4mim-PF_6 (5.0 mL). [b] Conversion and yield were calculated by weight and NMR of product.

For the two simple molybdenum species tested it was found that effective re-use of the catalyst/ionic liquid system was feasible, active catalyst clearly remaining in the ionic liquid after product extraction and removal of residual urea. However after several cycles yields were seen to decline significantly, likely due to leaching of the catalyst either when the product was extracted with diethyl ether or possibly with the urea during filtration. Leaching was significantly faster when using the molybdate precursor rather than the trioxide, though a reason for this is not apparent. For comparison a study was also carried out using MTO, a very active epoxidation catalyst (as seen in Section 2.1), in place of a molybdenum precursor. In this case a complete conversion was observed for the first cycle but thereafter the system became inactive. This is probably

due either to decomposition of the catalyst or its complete extraction along with the product. In a previous investigation employing MTO as an olefin epoxidation catalyst in an IL similar results were reported.[54] Whilst the recyclability of the molybdenum based systems was admittedly limited, with at best a TON of under 150 for even the MoO_3 system, by the new addition of MoO_3 it was found that the system could be reactivated again, without the need for fresh ionic liquid.

2.2.1.3 Application to other substrates

With an effective epoxidation system now established its efficiency in the epoxidation of a greater range of substrates, beyond the relatively activated *cis*-cyclooctene was investigated. This study employed the same experimental set up as previously described for entry 3, Table 2.7, but with several different olefin substrates in place of cyclooctene. The results are shown below in Table 2.9.

Table 2.9. Molybdenum catalysed epoxidations of several olefins in C_4mim-PF_6 [a]

Entry	**Substrate**		**Conversion (Yield)** [b]
1	Cyclohexene	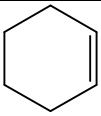	73 (73)
2	1-Octene	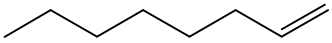	4 (3)
3	*trans*-2-Octene	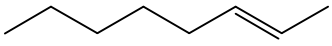	21 (13)
4	*trans*-4-Octene	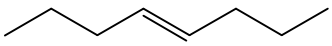	21 (12)
5	*cis*-2-Heptene	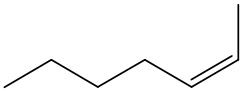	57 (39)
6	Styrene	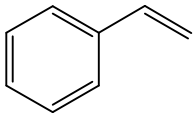	57 (10)
7	Cyclohexen-1-ol	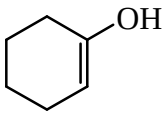	0 (0)

8	Allylamine	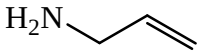	0	(0)

[a] *T = 60 ºC, t = 18 h, C_4mim-PF_6 (2 ml), olefin substrate (1.0 mmol), MoO_3 (2.5 % equiv.), UHP (150 % equiv.).* [b] *Conversion and yield were calculated by weight and NMR of product.*

A relatively high conversion with complete selectivity for the epoxide was observed for the cyclic olefin cyclohexene (entry 1, Table 2.9), although the conversion was significantly short of complete, demonstrating that the system was somewhat less active toward this substrate compared to *cis*-cyclooctene. Only a very low level of conversion was seen for the terminal aliphatic olefin 1-octene (entry 2, Table 2.9) which is electronically a poorly activated substrate. Higher, though still relatively poor, yields were obtained for the secondary aliphatic *trans*-alkenes 2- and 4-octene (entries 3 & 4, Table 2.9), with hardly any difference in the isolated yields in either case. There was also evidence of a significant level of epoxide hydrolysis for these substrates. It could seem odd that these epoxides would be quite so highly vulnerable to hydrolysis given that only low levels of water, generated as a byproduct from the UHP oxidant, should have been present in the system. *cis*-2-Heptene (entry 5, Table 2.9) was found to convert slightly better than the *trans* substrates perhaps indicating that it was more activated towards epoxidation in this system. Again the discrepancy between yield and conversion indicated that some product might have been lost to hydrolysis. A moderate conversion, but poor yield was recorded for styrene (entry 6, Table 2.9), this epoxide is known to be very susceptible to hydrolysis in the presence of an acidic catalyst and this result would appear to indicate that even the reduced level of moisture present in this system was still sufficient to destroy the majority of the product soon after it formed. The enol substrate, cyclohexen-1-ol (entry 7, Table 2.9) did not convert appreciably and allylamine likewise showed no evidence of conversion (entry 8, Table 2.9), probably as a result of interference by its highly coordinating amine group. In summary, the system showed itself to be active in the epoxidation of several classes of olefin substrate. However the yields obtained were always incomplete after 18 h and despite the very reduced levels of water in the system due to the use of a dry oxidant, there was substantial evidence of hydrolysis in many cases.

2.2.2 Influence of coordinating N-bases and elongated IL N-alkyl chains on oxobisperoxomolybdenum epoxidation with aqueous H_2O_2

The initial study (Section 2.2.1) had demonstrated that using UHP as oxidant in oxobisperoxomolybdenum catalysed cyclooctene epoxidations in C_4mim-PF_6, complete conversion could be achieved after 18 h at 60 ºC. However, there are several respects in which this system could be significantly improved. The reaction is slow, particularly when compared to the optimum examples of molybdenum catalysed epoxidations[84,80] or epoxidations employing more active catalysts.[175] Additionally, the UHP adduct is not an ideal oxidant for this reaction firstly due to the accumulation of urea residue which must be removed from the system, which consumes solvents and is work intensive, and secondly since it is a solid reagent and would be incompatible in any continuous flow type system, the development of such a system being an ideal objective for a catalytic investigation such as that here. Aqueous hydrogen peroxide would be a preferable oxidant, it is cheaper than UHP and it is a liquid solution which leaves only water as a by-product, which is more easily removed than urea and carries a lower environmental risk. However in the system previously discussed, whilst its use resulted in complete conversion of the olefin, the product was completely hydrolysed to the diol (see entry 4, Table 2.7). Investigations therefore proceeded by examining strategies by which these issues might be addressed and permit the use of aqueous H_2O_2 as oxidant.

2.2.2.1 Effects of N-alkyl chain length and presence of pyridine when using aqueous H_2O_2 as oxidant

By employing a reaction medium with a lesser water miscibility, the concentrations of water available for hydrolysis would be reduced and epoxide opening should thus be inhibited. One way of reducing the water miscibility is to increase the length of the 1-alkyl chain on the imidazolium cation of the IL reaction medium. Concurrently, the solubility of some olefin substrates might increase, improving the versatility of the epoxidation system. Also, the addition of coordinating base species was investigated, starting in this preliminary study with the effect of pyridine. As will latterly be discussed, coordinating base species might potentially induce both rate and selectivity enhancements in such an oxidation system.

Table 2.10 shows the conversions and epoxide yields observed in imidazolium type ILs with varying 1-alkyl chain lengths, hexafluorophosphate or tetrafluoroborate anions and with the two different H_2O_2 oxidants (aqueous and UHP adduct). Also shown are the results obtained where 20 mol % pyridine had also been added to the system, to see what effect this simple coordinating base species might have on the reaction.

Table 2.10. Effects of varying alkyl chain lengths, aqueous H_2O_2 and addition of pyridine [a]

Entry	Solvent	Oxidant	Base	Conversion (Yield)	
1	C_4mim-BF_4	H_2O_2	-	31	(9)
2		H_2O_2	Pyridine	31	(10)
3	C_4mim-PF_6	UHP	-	99	(99)
4		H_2O_2	-	97	(0)
5		H_2O_2	Pyridine	75	(48)
6	C_8mim-PF_6	UHP	-	77	(77)
7		H_2O_2	-	97	(21)
8		H_2O_2	Pyridine	97	(97)
9	C_{12}mim-PF_6	H_2O_2	-	95	(95)
10		H_2O_2	Pyridine	93	(93)
11	C_{18}mim-PF_6/	H_2O_2	-	32	(15)
12	C_8mim-PF_6	H_2O_2	Pyridine	31	(15)

[a] *Aqueous $[Mo(O)(O_2)_2(H_2O)_n]$[*] 0.025 mmol, pyridine (where relevant) 0.20 mmol, oxidant (30 % $H_2O_{2\,(aq)}$ or UHP) 3.0 mmol, cis-cyclooctene 1.0 mmol, solvent 2.0 mL, 18 h, 60ºC. Extraction with pentane (3 x 3 mL), yields and conversions calculated by GC.*

As a result of its smaller, slightly more polar tetrafluoroborate anion, the C_4mim-BF_4 ionic liquid (entries 1 & 2 Table 2.10) is significantly more miscible with water than its hexafluorophosphate counterpart. It was thus able to solubilise the aqueous H_2O_2 along with all of the other reaction components in the quantities present in the epoxidation system, leading to a completely homogeneous reaction. In spite of this, after 18 h conversion of the olefin was far short of complete (31 % in each case), in contrast to the equivalent reactions in the hexafluorophosphate IL (entries 4 & 5, Table 2.10) where effectively complete conversion was achieved after this time. The addition of pyridine to the BF_4 system apparently had no effect either on conversion or selectivity. The factor inhibiting efficient conversion is not clear, though the slightly more strongly (though still relatively very weakly) coordinating BF_4 anion may interfere

[*] The aqueous solution resulting from the dissolution of MoO_3 in aqueous H_2O_2 actually consists of several molybdenum species in equilibrium (see Ref. 224) but will hereon be referred to simply as aqueous $[Mo(O)(O_2)_2(H_2O)_n]$. For details on the preparation of this solution see Section 3.6.1.

unfavourably with the catalytic mechanism or the *in-situ* IL-H_2O medium may constitute a poor media for the reaction for some reason. When the results obtained using aqueous H_2O_2 in the absence of pyridine in the C_4mim-BF_4 and PF_6 ILs are compared it appears strange that hydrolysis of the epoxide product is complete in the PF_6 media, which has a lower miscibility with water, but incomplete in the BF_4 media. It is possible that this is due to the faster rate of epoxidation in the former, where the substrate completely converted after a short time and thus vulnerable to hydrolysis for the remainder of the 18 h reaction time. In the latter much of the epoxide that was detected was likely more recently formed and thus had been able to survive until the end of the reaction time.

Moving on to the results obtained in the hexafluorophosphate ILs and considering first the reactions performed without pyridine, in the 1-butyl ionic liquid, conversion was complete when utilising either H_2O_2 and UHP as oxidant (entries 3 & 4, Table 2.10) but when the aqueous oxidant was employed there was complete hydrolysis of the epoxide to the di-alcohol. In contrast, UHP gave no hydrolysis and complete selectivity for the epoxide. When using aqueous H_2O_2 in the 1-octyl ionic liquid, complete conversion was again observed (entry 7, Table 2.10), but this time hydrolysis of the product was not complete and a low yield of the epoxide product was obtained. This result clearly indicates that the longer alkyl chain of the C_8mim-PF_6 was having some effect in preventing hydrolysis, presumably by lowering the solubility of water in the medium relative to the C_4mim-PF_6. Employing UHP in this solvent resulted in a lower rate of reaction than observed in the other reactions, though selectivity for the product was again 100 % (entry 6, Table 2.10), perhaps due to UHP having a lower solubility in C_8mim-PF_6. Finally, in the 1-dodecyl medium, nearly complete conversion with complete selectivity for the epoxide was observed, despite using aqueous H_2O_2 (entry 9, Table 2.10). To summarise, in the absence of a coordinating base additive, conversion was always high (>95 %). However, as the alkyl chain length was increased from C_4 to C_8 to C_{12} the selectivity toward the epoxide increased from 0 % to 100 % (entries 4, 7 & 9 respectively, Table 2.10). Longer alkyl chain lengths in these ILs result in a reduced capacity to solvate water, which might lead to a lower rate of hydrolysis of the epoxide product to the di-alcohol, which would be supported by the results observed here.

Having observed the better results obtained in the longer chain ILs a composite media consisting of a 1:1 wt % mixture of C_{18}mim-PF_6 and C_8mim-PF_6 was also

investigated. C_{18}mim-PF_6 itself has a melting point well above the 60 ºC employed for the epoxidations and is thus unsuitable to use in these reactions on its own. Mixed with C_8mim-PF_6 though, the melt point falls below 60 ºC permitting its employment as art of a composite reaction media. In contrast to the monospeciatic ILs however, the results obtained in this medium were poor, with conversions of only approximately 30 % even after 18 h (entries 11 & 12, Table 2.10). The addition of pyridine affected neither the conversion nor the selectivity, with yields of 15 % recorded in both cases. Visually, these reactions were extremely clouded in appearance and it may well be that the media was unable to solubilise some of the reaction components as effectively.

The addition of pyridine was shown to greatly increase selectivity for the epoxide product (entries 5, 8 and 10, Table 2.10) compared to equivalent reactions in its absence (entries 4, 7 & 9, Table 2.10). This would seem to indicate that pyridine inhibits hydrolysis to the di-alcohol, the possible mechanism of which will be discussed later (see Section 2.2.4.1).

Following this study it was concluded that the optimal reaction medium was the C_{12}mim-PF_6, with the $C_n$mim-PF_6 type monospeciatic IL media generally providing the best reaction conditions. In the BF_4 IL the rate of epoxidation was very significantly reduced which dissuaded its continued study as media for this reaction. Increasing the alkyl chain length improved selectivity, but in the composite IL which contained a proportion of the octadecyl species, poor results were observed, maybe due to poor solubility, which would suggest that the dodecyl species was close to optimum. The addition of pyridine had a strongly positive effect on the selectivity for the epoxide.

2.2.2.2 Comparison of base additives

Having established that the addition of pyridine apparently inhibits unwanted hydrolysis of the product, this aspect of the study was extended to investigate a range of coordinating N-donor bases in this capacity. The majority of species tested were nitrogen-heterocyclic bases common to chemical laboratories. The principle objective of the investigation was to look for patterns in catalytic activity and selectivity related, for example, to the pK_a/donor strength or steric factors. Since complete conversion would be undesirable for the purposes of making comparisons, the reaction time was reduced to 2 hours. Table 2.11 shows the results obtained in this study.

Table 2.11. Molybdenum catalysed epoxidations of cyclooctene in the presence of selected N-donor base additives [a]

Entry	Base Additive [pK_a]	Solvent	Conversion	(Yield)
1	None	Cl_3CH	17	(1)
2		C_4mim-PF_6	29	(9)
3		C_8mim-PF_6	38	(25)
4		C_{12}mim-PF_6	40	(40)
5	Benzonitrile	C_8mim-PF_6	41	(16)
6		C_{12}mim-PF_6	44	(34)
7	Pyridine [5.25]	C_8mim-PF_6	29	(29)
8		C_{12}mim-PF_6	49	(49)
9	4-Picoline [5.98]	C_4mim-PF_6	31	(18)
10		C_8mim-PF_6	54	(54)
11		C_{12}mim-PF_6	46	(46)
12	4-Picoline-N-oxide [1.4]	C_4mim-PF_6	32	(23)
13		C_8mim-PF_6	39	(39)
14		C_{12}mim-PF_6	48	(48)
15	2,2'-Bipyridine [4.30] [b]	C_4mim-PF_6	18	(5)
16		C_{12}mim-PF_6	19	(1)
17	4,4'-Dimethyl-2,2'bipyridine [5.9] [b]	C_4mim-PF_6	16	(6)
18		C_{12}mim-PF_6	19	(4)
19	Pyrazole [2.5]	Cl_3CH	16	(3)
20		C_8mim-PF_6	63	(63)
21		C_{12}mim-PF_6	73	(73)
22	3-Methylpyrazole [3.3]	C_8mim-PF_6	62	(62)
23		C_{12}mim-PF_6	78	(78)
24	3,5-Dimethylpyrazole [4.2]	Cl_3CH	23	(8)
25		C_8mim-PF_6	84	(84)
26		C_{12}mim-PF_6	99	(99)
27	Imidazole [6.95]	C_8mim-PF_6	48	(48)
28		C_{12}mim-PF_6	43	(43)
29	1-Methylimidazole [6.95]	C_8mim-PF_6	48	(48)
30		C_{12}mim-PF_6	44	(44)
31	4-Methylimidazole [7.40]	C_8mim-PF_6	45	(45)
32		C_{12}mim-PF_6	44	(44)

[a] *Aqueous $[Mo(O)(O_2)_2(H_2O)_n]$ 0.025 mmol, base additive 0.10 mmol (where appropriate), 30 % $H_2O_{2\,(aq)}$ 3.0 mmol, cis-cyclooctene 1.0 mmol, solvent 2.0 mL, T = 60 ºC, t = 2 h. Extraction with pentane (3 x 3 mL), yields and conversions calculated by GC.* [b] *0.05 mmol base additive.*

The results shown in Table 2.11 allow several observations regarding the effects of the different classes of N-donor species on catalytic activity of these epoxidation systems to be made. Note that for monodentate N-donors 0.1 molar equivalents of the additive were employed, whilst for bidentate species 0.05 was used with 0.025 equivalents of [Mo] in all cases.

Benzonitrile: Benzonitrile did not notably affect the rate of conversion, and comparison with the corresponding results in the absence of any additive (compare entries 3 & 4 with 5 & 6, Table 2.11) indicates that hydrolysis was actually slightly more rapid in its presence, leading to lower selectivity. This may have resulted from a slightly increased concentration of water in the IL phase due to the presence of the relatively polar benzonitrile, it is unlikely that such a weakly coordinating species would have significantly affected the mechanisms of epoxidation or hydrolysis.

Pyridyls: The addition of pyridine (entries 7 & 8, Table 2.11) inhibited hydrolysis, as previously observed over 4 hours (Table 2.10), and complete selectivity for the epoxide was observed in the longer chain ILs. No dramatic effect on catalyst activity was observable, conversions were approximately the same as those observed in the absence of base (entries 3 & 4, Table 2.11). Interestingly, 4-picoline gave results largely similar to those of pyridine (entries 9-11, Table 2.11), despite the notable difference in the pK_a of the two species (5.25 and 5.98 respectively). Additionally the results obtained when 4-picoline oxide was added (entries 12-14, Table 2.11) were also approximately the same as those for 4-picoline. Molybdenum catalysts with coordinated N-donor or N-oxide ligands should have fairly different electronic properties and noticeable differences in catalytic activity might thus be expected. The fact that there is little difference might indicate that the catalyst is the same species in both cases: an N-oxide complex. Such metal-peroxo complexes are known to efficiently convert N-bases to their oxides,[176,177] and consequently it seems likely that prior to substantial catalytic epoxidation taking place both pyridine and 4-picoline were quickly oxidised to their N-oxides, which were subsequently the only coordinating species present during the respective catalytic epoxidations. Addition of pyridine to oxobisperoxomolybdenum solutions in hydrogen peroxide results only in the formation of N-oxide complexes,[178] and analogous observations were made in this study when attempting to prepare molybdenum-peroxo complexes of picolines, lutidine and collidine (see Section 3.6). N-oxides are much weaker donors than nitrogen bases and this would explain the similarity in the activities observed with either pyridine or 4-picoline. The catalytic oxidation of pyridine species with oxobisperoxomolybdenum and H_2O_2 seems to proceed under facile conditions, indicating that this conversion is fairly likely to take place *in-situ* in the catalytic reactions. To demonstrate this, 4-tridecylpyridine-N-oxide was successfully isolated after mixing a solution of 4-tridecylpyridine in chlorophorm with a catalytic amount of $[Mo(O)(O_2)_2(H_2O)_n]$ in aqueous hydrogen peroxide for only

a few minutes at room temperature (see Scheme 2.5 below). Unfortunately the higher solubilities of pyridine and 4-picoline in water made them more difficult to isolate in the same way, but it is not unreasonable to assume on the basis of their chemical similarity to 4-tridecylpyridine that they would likewise undergo oxidation.

Scheme 2.5. Molybdenum catalysed oxidation of 4-tridecylpyridine with H_2O_2

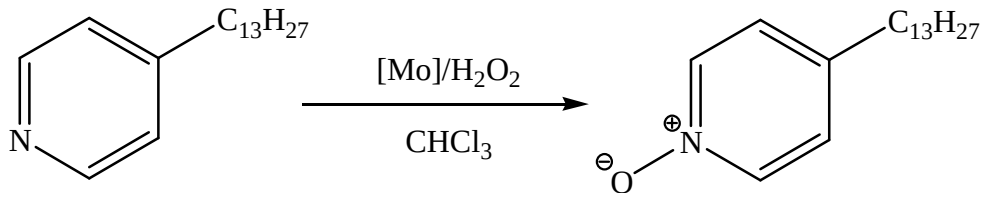

Bipyridyls: The bidentate bipyridyl ligands (entries 15-18, Table 2.11) were found to actually inhibit catalysis, leading to lower conversions than those observed in their absence (entries 2 & 4, Table 2.11). It may be noted that this leads to a discrepancy with one of the results previously obtained in the C_4mim-PF_6/UHP system (entry 5, Table 2.6), though this will be discussed later. In contrast to the monopyridyls it is probable that the bipyridyls would coordinate to the molybdenum as bidentate N-donors, rather than N-oxides.[179] A more extended study of oxobisperoxomolybdenum-bipyridine catalysed epoxidations and the reasons for their apparently retarding effect was subsequently conducted, which will be discussed in Section 2.2.2.4.

Imidazolyls: Fairly consistent results were obtained for the imidazolyls. The imidazole species tested (entries 27-32, Table 2.11) were found to inhibit hydrolysis giving complete selectivity for the epoxide. Conversions were comparable to those observed for pyridyls, at around 40 % (entries 7 & 8, Table 2.11). The fact that the results were always similar despite the significant differences in the pK_a values between the different imidazole species tested would seem to indicate that the catalytic species was similar in each case. Consequently, an obvious conclusion is that similar to the pyridyls, in each case an imidazole-N-oxide species formed *in-situ* prior to any significant oxidation taking place, and the activity of each system was thus very similar due to the ligands no longer being significantly different in behaviour and donor strength. However, the reactivity of imidazoles with solutions of oxobisperoxomolybdenum in aqueous H_2O_2, was later studied further in an attempt to

isolate such complexes. The results revealed that imidazoles are actually prone to oxidative decomposition making the presence of stable imidazole-oxide species in the reaction for any significant length of time unlikely. This would still explain the similarity in the results, since with the imidazole decomposed the active catalytic species would consequently have been the same in each case. These results are discussed further in Section 2.2.2.3 below.

Pyrazolyls: Remarkable amongst the results shown in Table 2.11 were those recorded for the pyrazole species (entries 19-26, Table 2.11). In ILs, all of the pyrazoles were found to significantly improve catalytic activity, giving superior conversions when compared with all of the other N-donor species tested. Selectivity for the epoxide was also complete in all cases. Additionally, whilst pyrazole and 3-methylpyrazole gave markedly elevated conversions, 3,5-dimethylpyrazole was observed to produce an even more active system. With the addition of dimethylpyrazole, complete conversion to the epoxide was observed in the dodecyl ionic liquid within the two hours, the optimal result encountered by this study. The use of oxobisperoxopyrazolylmolybdenum type complexes as catalysts for oxidation reactions has a limited number of precedents, though apparently not in olefin epoxidation. Supported $[Mo(O)(O_2)_2(H_2O)(pz)]$ has been used to catalyse the heterogeneous oxidation of sulfides,[180] though advantages resulting from coordinated pyrazole went undiscussed. Additionally, $[Mo(O)(O_2)_2(dmpz)_2]$ has been previously described as a homogeneous alcohol oxidation catalyst, [181] although the authors of this study again gave no reason for their selecting this specific complex as the catalyst.

Reaction media: The final observation to be made from these results regards the relative activities and selectivities observed depending on the solvent used. Firstly, in every case where chlorophorm was used (entries 1, 19 and 24, Table 2.11) conversion was very markedly lower than in the ionic liquid media with which it was compared. Additionally, little better than trace yields of the epoxide were isolated from these reactions leading to the conclusion that chlorophorm is a very unsuitable solvent for these reactions. It is likely that this is due to the poor solubility of the molybdenum species in chlorophorm which leaves them unable to function effectively as catalysts. Of the ionic liquids, in Table 2.11 a general trend, whereby conversion increased as the length of the N-alkyl chain was increased was observed clearly in the absence of base (entries 1-4, Table 2.11), for pyridyls/pyridyl-N-oxides (entries 7-14, Table 2.11), bipyridyls (entries 15-18, Table 2.11) and pyrazoles (entries 19-26, Table 2.11).

Additionally selectivity for the epoxide also improved with the chain length. The better selectivity in the longer alkyl chain ILs should be due to the lower solubility of water in these media, which reduces that available for hydrolysis. All reactions employing aqueous H_2O_2 with the $C_n$mim-PF_6 ILs were biphasic, with a separate aqueous phase, so the ionic liquid reaction medium would have been saturated with water in all cases and water solubility was thus very important. The higher conversions, and thus catalytic activities, are less easily explained however. Higher solubilities of one or more of the substrate, catalyst or base additive in the less polar longer chain ILs should be considered possibilities for this observation, although the cyclooctene was apparently fully miscible with all of the ILs tested and the yellow colouration of the molybdenum catalyst was observed exclusively in the IL (as opposed to the aqueous phase) in all cases. It is also possible that the lower concentration of water not only results in reduced hydrolysis but faster epoxidation. Water may be able to inhibit the reaction mechanism in some way, perhaps in its capacity as an O-donor ligand. The possibility that the ionic liquids' role in these reactions is more than that of a merely spectatorial solvent, with a more active participation in the reaction mechanism should also remain open to consideration. However, examination of any reasons for the activating effect of the ionic liquids on the catalysis was not attempted in the study described here.

2.2.2.3 Further investigation of the reaction between aqueous $[Mo(O)(O_2)_2(H_2O)_n]/H_2O_2$ and imidazoles

In order to better understand the imidazole oxidation systems that had been investigated, the isolation of the catalytic complexes that were likely to form *in-situ* in these reactions was attempted. Through characterisation of the catalysts, their activities might be better explained. Based on the similarities in the catalytic activities of all of the systems employing imidazolyl species as base additives, it was considered possible that the imidazoles would first undergo oxidation to their N-oxides before coordinating to the metal to give imidazole-N-oxide complexes of oxobisperoxomolybdenum.[182] Also considered possible was that the imidazoles might simply coordinate as N-donors, as in the complex characterised by Martín-Zarza et al.[183]

When 4-methylimidazole was reacted with the an aqueous solution of $[Mo(O)(O_2)_2(H_2O)_n]/H_2O_2$ several different products were obtained depending on the

reaction conditions. When the reaction was carried out at a low temperature and the solution maintained at around 4 ºC, a yellow solid was observed to precipitate. However, rather than an imidazolyl oxobisperoxomolybdenum complex, characterisation by microanalysis, ICP, ESI-MS, IR and ^{1}H-NMR indicated that the species formed was a monometallic oxobisperoxomolybdenum complex with an empirical formula of $MoO_5N_5H_{10}$, thus implying the coordination and/or co-precipitation of one or more species containing only partially unsaturated nitrogen and hydrogen. In spite of considerable effort, full characterisation was not achieved however.

When the solution resulting from the reaction of 4-methylimidazole was heated for a while different products were obtained. By maintaining the solution at a low temperature for a period of weeks yellow crystals were formed in the yellow solution. These were not crystals of the compound described above however, with elemental analysis and ICP indicating an empirical formula of approximately $MoO_5C_2N_2H_6$. Analysis by XRD[196] identified a heptamolybdate salt, the anion consisting of a heptamolybdate with several peroxo ligands but no coordinated organic fragments. At the time of writing the cationic species were unidentified due to disorder problems.

When this solution was evaporated more quickly at room temperature, a strong smell of formaldehyde was notable and once the solution had evaporated down to a yellow oil, crystals of 1-acetylurea began to form. The molybdenum was therefore able to facilitate the oxidative decomposition of 4-methylimidazole to these products. Scheme 2.6 below shows the oxidative decomposition of 4-methylimidazole, amongst the "other oxidation products" at least one fragment containing only unsaturated nitrogen and hydrogen seems to occur under certain conditions and it seems that several coordination compounds with molybdenum may form, though these remain unconfirmed speculations.

Scheme 2.6. Oxidative decomposition of 4-methylimidazole by oxobisperoxomolybdenum

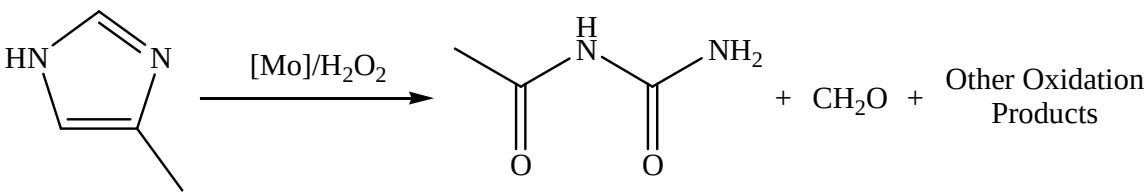

Similar results were observed when imidazole was reacted with an aqueous solution of $[Mo(O)(O_2)_2(H_2O)_n]/H_2O_2$. This reaction was heated in the same manner as described for 4-methylimidazole and by maintaining a low temperature yellow crystals, with an apparently identical empirical composition, were obtained in the same manner. Assuming that the products were identical the similarity in the breakdown products from each type of imidazole explains the similarity in the catalytic activities. An odour of formaldehyde was again noted, though no urea type decomposition product was isolated. It does seem likely that imidazole had been oxidatively decomposed in a similar manner to its 4-methyl analogue however.

Full synthetic procedures and analytical data for the reactions described here is provided in the Experimental (Sections 3.6.22 & 3.6.24).

2.2.2.4 Further investigation of the apparently inhibitory effect of bipyridyl species on the epoxidation

The inhibitory effect of the bipyridyls (see entries 15-18, Table 2.11) is an interesting anomaly amongst the results and these reactions thus merited further investigation. Considering first the likely catalytic species in this reaction, it would seem probable that the bipyridyl species coordinated to the oxobisperoxomolybdenum centre *in-situ* as bidentate N-donors. Reaction between aqueous oxobisperoxomolybdenum and bipyridine is known to produce such a complex,[184] the coordinated bipyridine being unoxidised, unlike in analogous complexes of monopyridyls synthesised via similar procedures.[178] Bipyridyl compounds are more difficult to oxidise than monopyridyls and although oxidation of bipyridine to the N-oxide has been observed in MTO catalysed oxidations[59] and peroxomolybdenum catalysts could well be capable of catalysing this oxidation under some conditions, it can probably be considered unlikely in this case. Additionally, in these investigations (see Sections 2.2.8 & 3.6) several substituted bipyridyls were observed to form bipyridyl complexes rather than undergo oxidation and form the respective N-oxide complexes.

In the preliminary study conducted in C_4mim-PF_6 (Table 2.7) where previously synthesised $[Mo(O)(O_2)_2(bpy)]$ was used to catalyse an epoxidation with UHP (entry 5, Table 2.7), almost complete conversion had been observed after 18 h, in common with

the results for the other catalyst precursors. When contrasted with the poor results observed in Table 2.11, it was considered that this result might be erroneous. However, when this reaction was repeated the high conversion was found to be reproducible. There are however several significant differences between the experimental setups of the reactions in Table 2.7 and Table 2.11. Firstly, the former employs UHP as the oxidant, the latter aqueous H_2O_2. Secondly in the former the ratio of Mo:bpy is 1:1 with the bipyridine coordinated to the molybdenum centre prior to the reaction, in the latter an excess of bipyridine (Mo:bpy = 1:2) was present. Thirdly the former employs 5 % [Mo] and the reaction time is 18 h, in the latter only 2.5 % [Mo] is employed and the reaction time is only 2 h, apparently insufficient to allow significant conversion to take place. For these reasons a study was conducted in order to observe any differences in the results depending on the oxidant used and whether excess base was available. Since bipyridine apparently inhibits the epoxidation a reaction time of 18 h was allowed. The results are presented below in Table 2.12.

Table 2.12. Investigation of the effect of the bipyridyl ligand on epoxidation [a]

Entry	Catalyst	Oxidant	Conversion (Yield)
1	$[Mo(O)(O_2)_2(bpy)]$	H_2O_2 (aq) [b]	61 (23)
2		UHP [c]	59 (57)
3	$[Mo(O)(O_2)_2(bpy)]$ + bpy [d]	H_2O_2 (aq) [b]	57 (57)
4	$[Mo(O)(O_2)_2(bpyO_2)]$	H_2O_2 (aq) [b]	65 (65)

[a] $[Mo(O)(O_2)_2(bpy)]$ (0.025 mmol), cis-cyclooctene (1.0 mmol), C_8mim-PF_6 (2.0 mL), T = 60 ºC, t = 18 h. [b] 30 % H_2O_2 (3.0 mmol). [c] UHP (1.5 mmol). [d] 2,2'-Bipyridine (0.025 mmol).

Entry 1 (Table 2.12) shows the result obtained using aqueous hydrogen peroxide oxidant together with $[Mo(O)(O_2)_2(bpy)]$ complex as catalyst. Comparing the result with entries 15 & 16, Table 2.11, the extended reaction time (18 as opposed to 2 h) allowed a far more significant level of conversion to take place. However, a large proportion of the product subsequently underwent hydrolysis and selectivity was thus poor. Comparing with the results obtained using other base additives (Table 2.11) this seems to indicate that bipyridine offers poorer protection from hydrolytic epoxide opening than the *in-situ* catalysts formed when using pyrazoles, imidazoles or even pyridine-N-oxides. Entry 2 (Table 2.12) shows the result for the same reaction but with dry UHP as oxidant. In this case, whilst conversion was approximately equal to that obtained with the aqueous H_2O_2, selectivity for the epoxide is now effectively complete, as might be expected since the only water available for hydrolysis is that produced as a

by-product of the oxidation. Entry 3 (Table 2.12) is interesting in that it represents the same reaction as that in entry 1 (Table 2.12) but this time in the presence of 1 extra equivalent of bipyridine per [Mo]. Conversion in this case was again roughly equivalent to those recorded in entries 1 and 2 at around 60 %, but in contrast to entry 1 the excess base apparently completely inhibited hydrolysis, resulting in complete selectivity for the epoxide. Finally, entry 4 (Table 2.12) shows the result obtained when the complex of bipyridine-N,N'-dioxide, rather than the unoxidised bipyridine was used. A similar conversion was again observed, but this time with complete selectivity for the epoxide. This seems to demonstrate that the dioxide complex suffers the same retardation in the rate of epoxidation as the complex of unoxidised bipyridine, but differs in behaviour with respect to hydrolysis which is effectively inhibited.

2.2.3 $[Mo(O)(O_2)_2]$/dmpz/IL catalysed olefin epoxidation

The comparison of oxobisperoxomolybdenum/N-base systems described in Section 2.2.2.2 had established 3,5-dimethylpyrazole to be the most activating of the base additives tested, with the optimum performance observed in C_{12}mim-PF_6. The likely reasons for this observation will be covered later (Section 2.2.4), discussion here will now move to the further investigations of this catalytic system.

2.2.3.1 Progression of the $[Mo(O)(O_2)_2]$/dmpz/C_{12}mim-PF_6 epoxidation over time

The optimum results were obtained employing 3,5-dimethylpyrazole in the longer chain ILs (entries 25 & 26, Table 2.11), making further study of these systems pertinent, and investigations thus proceeded to try to define a highly efficient epoxidation system. To this end the progress of the epoxidation in C_{12}mim-PF_6 was followed over two hours. Samples were taken from the system every twenty minutes and the conversion plotted.

Table 2.13. Progress of the $[Mo(O)(O_2)_2]$/dmpz/C_{12}mim-PF_6 catalysed epoxidation of *cis*-cyclooctene over 120 min [a]

Time (min)	20	40	60	80	100	120
Yield	29 %	47 %	62 %	74 %	81 %	85 %

[a] *Aqueous $[Mo(O)(O_2)_2(H_2O)_n]$ 0.025 mmol, 3,5-dimethylpyrazole 0.1 mmol, 30 % $H_2O_{2\ (aq)}$ 3.0 mmol, cis-cyclooctene 1.0 mmol, C_{12}mim-PF_6, 2.0 mL, T = 60 ºC. Samples taken by pipette and extracted by mixing with pentane (1.5 mL), yields calculated by GC.*

As can be seen, the reaction did not reach completion after 120 minutes as in the initial 2 hour study (entry 26, Table 2.11) which subsequently creates some problems in assessing the results. It may be reasonable to attribute this discrepancy to retardation arising for various reasons when the reaction was halted every twenty minutes for sampling. The complete conversion previously obtained in a single two hour run was shown to be reproducible. Figure 2.5 thus shows conversion plotted against time over the course of the experiment and also a modified set of data, factored to produce complete conversion.

Figure 2.5. Conversion plotted against reaction time in the epoxidation of *cis*-cyclooctene with the $[Mo(O)(O_2)_2]$/dmpz/C_{12}mim-PF_6 system

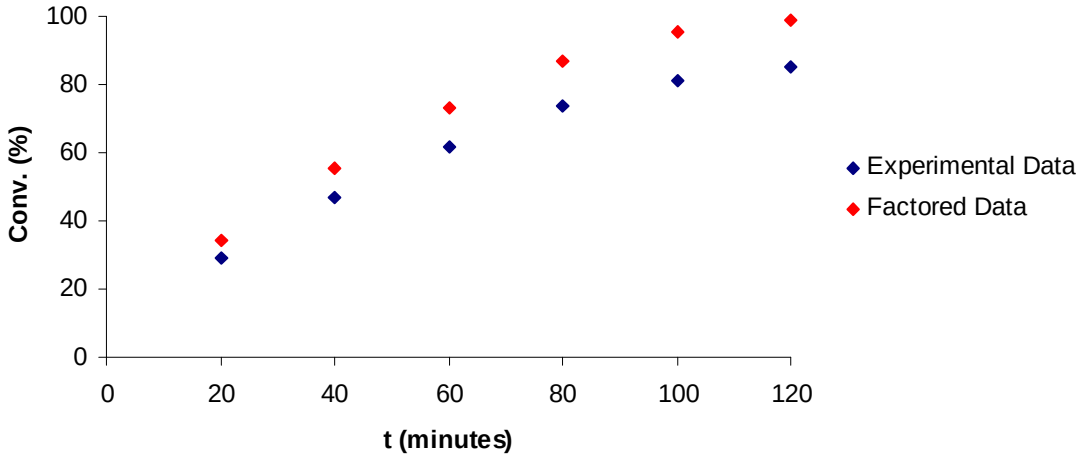

The curve of the graphs and the fact that the oxidant was present in excess might indicate that in this experiment the reaction rate was first order dependent on the concentration of the olefin substrate (the possibility that the reality was more complicated will be discussed subsequently). Therefore in the rate equation:

$$v = k_{(333\ K)}[cis\text{-cyclooctene}]^1[H_2O_2]^n[Mo]^m$$

the concentrations of both the oxidant (in excess) and catalyst (constant, 0.0125 mol L^{-1}) can be ignored and a pseudo first order rate coefficient, $k'_{(333\ K)}$ with respect to [*cis*-cyclooctene] for the reaction calculated. Thus, values of $k'_{(333\ K)} = 4.04 \times 10^{-4}\ s^{-1}$ for the experimental data and $k'_{(333\ K)} = 6.56 \times 10^{-4}\ s^{-1}$ for the factored data were calculated (concentrations in mol L^{-1}).

The assumption that the only influence on the reaction rate was the changing substrate concentration may well be a fair one, since the oxidant was present in excess. However, three equivalents of H_2O_2 was not a large excess and its tendency to spontaneously decompose and the capacity of [Mo] to decompose H_2O_2 should also be considered. The possibility that changes in the concentration of the oxidant were also markedly affecting the rate of the reaction cannot therefore be discounted in this experiment. Experiments employing larger excesses of oxidant in order to eliminate this possibility were attempted but the large volume of the aqueous phase complicates such reactions, making sampling difficult and no useful results were obtained. However, it is interesting to provide these rate coefficients on the basis that they are approximately representative of the likely actual value.

2.2.3.2 Recyclability of the $[Mo(O)(O_2)_2]$/dmpz/C_8mim-PF_6 system

The results obtained in the 1-dodecyl ionic liquid were excellent, with a higher rate of conversion observed than in the other ILs. However, the use of this compound as a reaction medium is made difficult by its high melt point, the compound being a solid at room temperature. This complicates both product extraction with solvents and its general usage in the laboratory, as it can be manipulated as a liquid only when heated. For this reason the 1-octyl ionic liquid, C_8mim-PF_6, was preferred in the model system subsequently used in further studies.

In the interests of developing a system more compliant with the principles of sustainable chemistry, the recyclability of the system was examined. By re-using the catalyst the TON per mol of catalyst might be increased. Re-use of the ionic liquid reaction solvent was also important, given its expense and undesirable chemical constitution as a waste product. It had previously been shown that the MoO_3/C_4mim-PF_6/UHP system was recyclable in the epoxidation of cyclooctene (see Table 2.8 and the relevant discussion). In this case the addition of new substrate and

oxidant following product extraction had allowed a number of successful cycles before catalytic efficiency was seen to fall, presumably due to catalyst leaching. A disadvantage in this system was the removal of the urea, which was done by filtration, requiring the use of solvent solely to reduce the viscosity of the reaction medium. The catalytic system defined here was advantageous in this respect since the only by-product left by the oxidant, water, could be easily removed simply by evaporation. This in turn would reduce the use of solvents in a catalytic cycle and reduce the potential for catalyst loss due to leaching. It is still the case that the use of an extraction solvent was necessary in order to separate the product from the reaction medium. However, were systems such as these ever to be used practically, in batch, it is reasonable to hypothesise that an epoxide product might actually be separated by distillation, or that the extraction solvent would at least serve as medium for a subsequent synthetic reaction. Solvent extraction was far more practical under lab conditions and since this study was focused on conversion and yield this practice was maintained, though it should be acknowledged that it is not ideal. To investigate recyclability, two $[Mo(O)(O_2)_2(H_2O)_n]$/dmpz/H_2O_2(aq)/C_8mim-PF_6 cyclooctene epoxidation systems were thus investigated over several cycles. Catalytic runs lasted 4 hours, which was found sufficient to produce effectively complete conversion on the first run. The epoxide product was extracted from the IL with pentane between each cycle, before eliminating residual water and pentane at 60ºC under vacuum over 1 hour. Fresh oxidant and substrate were then added, to one of the systems fresh dimethylpyrazole was also added, as it was hypothesised that the base species might leach during the product extraction. Ten catalytic cycles were carried out in each case and the results are shown in Table 2.14 below.

Table 2.14. Catalytic cycles with the dimethylpyrazole system in C_8mim-PF_6 [a]

Run	+ 10 % dmpz after every run (yield) [b]	No new base added between runs (yield) [c]
1	>95 %	>95 %
2	>95 %	>95 %
3	>95 %	93 %
4	>95 %	86 %
5	>95 %	77 %
6	>95 %	70 %
7	>95 %	70 %
8	>95 %	67 %
9	>95 %	66 %
10	>95 %	62 %

[a] *Initially: Aqueous $[Mo(O)(O_2)_2(H_2O)_n]$ 0.025 mmol, 3,5-dimethylpyrazole 0.1 mmol, 30 % $H_2O_{2\,(aq)}$ 3.0 mmol, cis-cyclooctene 1.0 mmol, C_8mim-PF_6 2.0 mL. Extraction with pentane (3 x 3 mL) after each cycle, yields calculated by GC. T = 60 ºC, t_{run} = 4 h.* [b] *30 % $H_2O_{2\,(aq)}$ 3.0 mmol, cis-cyclooctene 1.0 mmol, 3,5-dimethylpyrazole 0.1 mmol added prior to each successive run.* [c] *30 % $H_2O_{2\,(aq)}$ 3.0 mmol, cis-cyclooctene 1.0 mmol added prior to each successive run.*

In the experiment where fresh dimethylpyrazole was added before each cycle (column 2, Table 2.14) the yields remained almost complete even after ten cycles. This implies that any loss of the molybdenum catalyst that had occurred due to leaching was still not high enough at this point to affect negatively the level of conversion under these conditions. This is not surprising, as it is unlikely that the molybdenum complex would have any substantial solubility in pentane. Incidentally, after ten catalytic runs just 0.025 mmol of molybdenum had converted over 95 % of 10.0 mmol *cis*-cyclooctene to its epoxide, equating to a TON of ≥380 with the TOF over 9.5 h^{-1}. Interestingly, in the experiment where no fresh dimethylpyrazole was added in between cycles (column 3, Table 2.14), a slow but marked decrease in the catalytic efficiency was observed after two cycles and the conversion continued to drop slowly with each successive cycle until the experiment was halted after ten cycles. It is unlikely that the loss in efficiency was due to leaching of the molybdenum species since no such reduction was apparent in the other experiment where dimethylpyrazole was added before each cycle (column 2, Table 2.14). It is likely however that dimethylpyrazole has limited solubility in pentane and was thus slowly leaching from the IL solution with every extraction. An interesting conclusion that could be reached from this experiment is that the excess dimethylpyrazole may produce an enhancement in the epoxidation rate.

2.2.3.3 Green metrics for the recycled system

When examining this system from a sustainability perspective it is interesting to evaluate it in terms of some green metrics, in this case atom economy (AE) and the E-factor, to give some idea of where inefficiencies may be arising. The chemical compounds utilised in the epoxidation of 1 mmol of *cis*-cyclooctene where fresh dimethylpyrazole was added prior to each catalytic cycle are all depicted below in Scheme 2.7. All calculations pertaining to this section appear in the appendices.

Scheme 2.7. Recycled system for the epoxidation of 1 mmol *cis*-cyclooctene

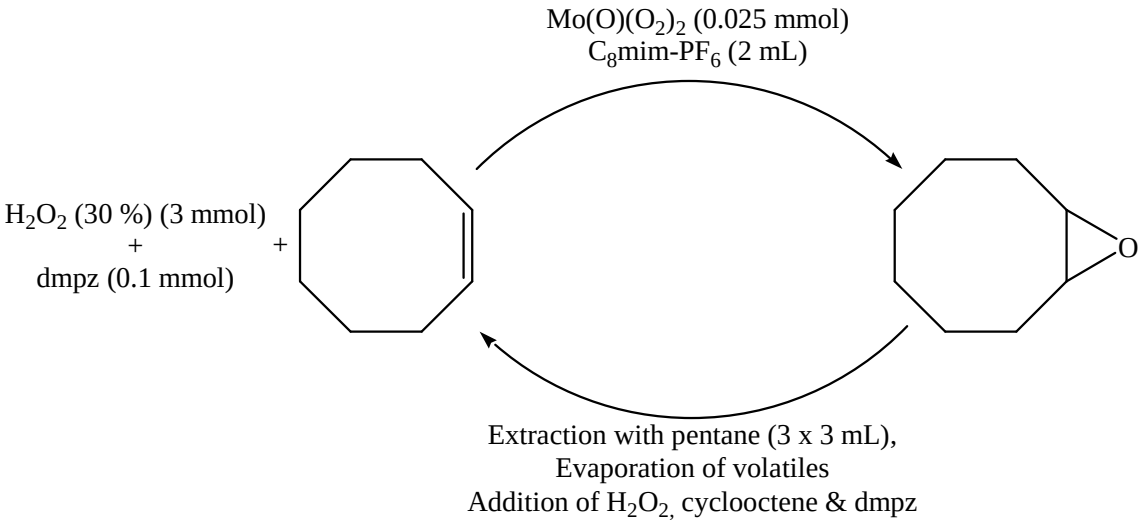

Atom Economy: AE assesses the efficiency of the reaction step with regard to the incorporation of reactants' atoms in the product and in a long synthetic process may be calculated over several reaction steps to allow comparison of the efficiency of reaction pathways. It is calculated from the weight of the products divided by the weight of the reactants and is expressed as a percentage, with 100 % representing a perfect reaction where all of the atoms of the reactants are incorporated in the product molecule and none leaves the system as by-product.[2] In the epoxidation of *cis*-cyclooctene four reactions will be considered, oxidation by one equivalent of the commonly used stoichiometric oxidant *meta*-chloroperoxybenzoic acid (mCPBA), one of the organic hydroperoxide *tert*-butylhydroperoxide (TBHP), one of hydrogen peroxide and half an equivalent of oxygen (Figure 2.8). The atom economy calculated for the reaction with each of the four reactants is shown in Table 2.15.

Scheme 2.8. Oxidation of *cis*-cyclooctene by four common oxidants

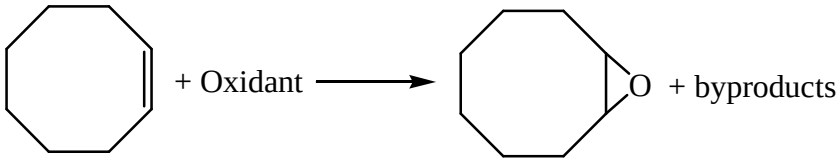

Oxidant = mCPBA, TBHP, H_2O_2, ½O_2

Table 2.15. Atom economies in the epoxidation of *cis*-cyclooctene by four common oxidants

Entry	Oxidant	AE (%)
1	mCPBA	45
2	TBHP	63
3	H_2O_2	88
4	½O_2	100

mCPBA is an excellent oxidant for the epoxidation of olefins[185] and is advantageous in that it is used as a stoichiometric reagent without the need for any catalyst or special conditions. However, for every equivalent of substrate oxidised one equivalent of the undesirable by-product 3-chlorobenzoic acid is produced. As a chlorinated organic acid compound this is a highly undesirable waste and as a large molecule it also means that for the epoxidation under discussion the weight of the by-products exceeds the weight of the product, leading to an AE of 45 % (entry 1, Table 2.15). In comparison TBHP produces much more benign waste in *tert*-butyl alcohol and its use also leads to an improvement in the AE to 63 % (entry 2, Table 2.15). This is still far from ideal however, organic waste still accounting for more than a third of the weight of the reaction products and TBHP does not oxidise olefins so readily, requiring the use of a catalyst. Using H_2O_2 leaves only benign water as a by-product and gives a good AE of 88 % (entry 3, Table 2.15). This desirable reaction is the object of the studies in this section, but as seen this oxidation must be carried out catalytically and in such systems the issue of product hydrolysis must also be addressed. Lastly, the use of dioxygen leads to a perfect AE of 100 % (entry 4, Table 2.15). Unfortunately this ideal epoxidation is only yet known in the epoxidation of ethylene.[186] Clearly then, in terms of atom economy the epoxidation being studied here using the "green" H_2O_2 oxidant results in an efficient epoxidation, with relatively little by-product waste when compared with commonly used alternatives. However, in practice the vast majority of the waste resulting from a reaction is not derived from the reactants but made up of

solvents and additives used in the process. To obtain a perspective on the efficiency of the reaction in practice these must therefore be accounted for.

E factor: The E-factor is calculated by dividing the mass of the waste produced by a process by the mass of the product.[187] Clearly, an ideal process would produce no waste, resulting in an E-factor of 0. The lower the E-factor, the more efficient a process. Table 2.16 below shows several E-factors calculated for theoretical systems and the experimental system under discussion. Catalyst refers both to the [Mo] complex which was added only once and did not need to be renewed between cycles, and to the dimethylpyrazole which was added prior to each successive run. Solvents refers to the IL which was added only prior to the first catalytic cycle and re-used thereafter, the water added as a solvent for the hydrogen peroxide and the pentane used to extract the products after reaction.

Table 2.16. E-factors in the epoxidation of *cis*-cyclooctene

Entry	System	E-factor
1	Theoretical: 1:1 Reaction of pure H_2O_2 with *cis*-cyclooctene (entry 1, Table 2.15)	0.14
2	Theoretical: Reaction of 3 equiv. aqueous H_2O_2 with *cis*-cyclooctene	2.6
3	Experimental: 1st cycle only, including catalyst but excluding solvents, 95 % yield	0.84
4	Experimental: 1st cycle only, including catalyst and solvents, 95 % yield	73
5	Experimental: 10 cycles including catalyst & solvents, 95 % overall yield	52
6	Theoretical: Infinite cycles including catalyst & solvents, 100 % overall yield	47
7	Experimental: 10 cycles incl. catalyst & solvents but excl. pentane, 95 % overall yield	5.1

Entry 1 (Table 2.16) shows the E-factor for the complete epoxidation of *cis*-cyclooctene by 1 equivalent of hydrogen peroxide taking into account no solvents or catalysts, as in the reaction described for the AE calculations (entry 3, Table 2.15). This

reaction could not of course be carried out in practice, but the value represents a theoretical optimum efficiency. The very low value (0.14) reflects the fact that the mass of the waste is only 14 % that of the product. Entry 2 (Table 2.16) shows another theoretical value but this time calculated for the epoxidation of *cis*-cyclooctene if an excess, 3 equivalents, of H_2O_2 is employed and taking into account the additional water resulting from the use of 30 % aqueous H_2O_2. Since H_2O_2 can only be safely handled in aqueous solutions of not much higher concentration the inclusion of water into the equation makes the target more realistic. Also, 3 equivalents of H_2O_2 were employed in the experimental system largely to avoid significant experimental variations resulting from reasonable variations in the concentration of the oxidant solution, rather than through experimental necessity for a large excess of oxidant. Were this system to be utilised practically it is likely that the proportion of oxidant could be lowered significantly with little negative effect on its efficiency. Therefore a fairer comparison is made between the experimental E-factors and this theoretical value of 2.6, which thus represents a perfect system where the only waste was from unavoidable by-products of the oxidant. Entries 3 and 4 (Table 2.16) describe the actual experimental system and show E-factors calculated for the first run only. In entry 3 solvents are discounted, whilst in entry 4 they are included, giving the real E-factor for the reaction. E-factors of 0.84 and 73 were calculated respectively, making immediately evident how solvents account for the vast majority of the waste from this reaction. Entry 3 is only just over 1 % of that of entry 4, illustrating how solvents account for nearly a hundred times more waste mass than other by-products. Entry 5, like entry 4, takes into account all reactants and compounds employed but this time over ten catalytic cycles, reducing the relative waste from metal catalyst and IL. As a result of recycling the system the E-factor improves markedly to 52 indicating that almost a third less waste was produced per equivalent of product than over one cycle only. Moving on to entry 6 (Table 2.16) the theoretical e-factor has been calculated for s system run an infinite number of times as depicted in Scheme 2.7 obtaining 100 % yield. The value of 47, is found to be little lower than that of entry 5 demonstrating that the efficiency of the system in this respect had almost plateaued. This optimal E-factor of almost 50 demonstrates that significant improvements to the level of waste generated by the process should be desirable and, with it having earlier been shown that solvents account for most of this waste, entry 6 (Table 2.16) shows the E-factor calculated over ten cycles when the pentane used to extract the product is omitted, 5.1. This value is therefore approximately ten times lower

than the best attainable if the pentane extraction step is maintained and shows how the pentane accounts for the vast majority of the waste. Thus, an alternative method of extraction, for example distillation of the epoxide from the IL rather than solvent extraction, could lead to a large reduction in the mass of waste produced by the process and greatly improve the E-factor.

In reviewing the values discussed here the limitations of atom economy and E-factor in assessing a process should be aknowledged. As an example, the energy required to heat and vacuum dry the system are ignored and whilst a distillation would improve the E-factor it would necessitate a higher consumption of energy. These metrics also completely ignore factors such as the hazards and environmental impacts presented by waste streams, concentrating only on quantities.

2.2.3.4 Substituting dimethylpyrazole for a phase stabilised ionic N-donor ligand to facilitate better recyclability

Having considered in terms of AEs how best to reduce the quantity of waste produced by the reaction it is also pertinent to review the by-products leaving the system as waste. Aside from the epoxide product and any unreacted olefin, water, unreacted H_2O_2, pentane and 3,5-dimethylpyrazole will all leave the system shown by Scheme 2.7. Water can be considered very benign waste and dilute H_2O_2 is neither particularly hazardous nor difficult to decompose. Pentane is obviously an undesirable waste product but as previously discussed might be eliminated by employing an alternative means of product extraction. This leaves the dimethylpyrazole, which imparts a degree of hazard to waste streams and in addition leaves the system in solution with the product, which in practice might necessitate purification. Even were a distillation to be employed to separate the product, sublimation of dimethylpyrazole which would then leave with the product could remain a problem. The question is therefore raised whether there might be any alternative to dimethylpyrazole which would be equally activating, yet at the same time better stabilised in the ionic liquid medium to eliminate the problem of leaching. In this respect, an interesting option was to investigate bases with ionic functional groups which could be expected to show decent solubility in the IL reaction medium whilst having such low solubility in any

apolar extraction media that losses from leaching during extraction should be insignificant.

Wang et al. described the synthesis of the ligand 1-(pyrazol-1-ylmethyl)-3-methylimidazolium chloride from which were prepared interesting complexes of palladium which proved to be good Heck catalysts in ionic liquids.[188] As an ionic compound, this pyrazole N-donor ligand could be anticipated to possess poor solubility in apolar solvents but good solubility in ILs and also very low volatility. For these reasons, in the system investigated here such a ligand had interesting potential as a substitute for dimethylpyrazole, able to activate the system in its capacity as a pyrazole type N-donor ligand, whilst being far more resistant to leaching during product extraction. A potential problem that was envisaged is that N-substitution of the pyrazole in such a manner results in a considerable reduction in pK_a. For this reason the ligand used here was prepared from dimethylpyrazole rather than pyrazole, obtaining the dimethyl substituted analogue 1-(3,5-dimethylpyrazol-1-ylmethyl)-3-methylimidazolium chloride (dpmim-Cl, see Figure 2.6) in order to try and obtain an analogous structure with as high a pK_a as possible. Having synthesised and characterised the compound it was then used in an epoxidation system with repeated catalytic cycles without adding fresh base in the same way as previously described.

Figure 2.6. 1-(3,5-dimethylpyrazol-1-ylmethyl)-3-methylimidazolium chloride

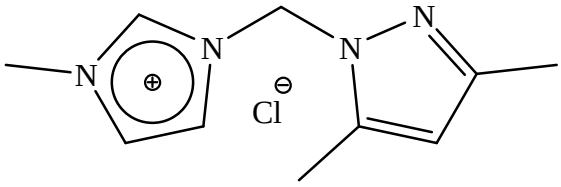

Table 2.17. Catalytic cycles with the $[Mo(O)(O_2)_2]$/dpmim-Cl/C_8mim-PF_6 system [a]

Cycle	1	2	3	4	5
Isolated Yield	≥90 %	≥90 %	88 %	85 %	84 %

Start : Aqueous $[Mo(O)(O_2)_2(H_2O)_n]$ 0.025 mmol, dpmim-Cl 0.1 mmol, 30 % $H_2O_{2\ (aq)}$ 3.0 mmol, cyclooctene 1.0 mmol, C_8mim-PF_6 2.0 mL, 60ºC, 18 h. After 18 h : Extraction with pentane (3 x 3 mL), volatiles eliminated (vacuum, 60 ºC, 1 h), addition of cyclooctene 1.0 mmol & H_2O_2 3.0 mmol, cycle repeated. Yields calculated by GC.

Whilst the results (Table 2.17) showed that it was indeed possible to obtain good conversion of cyclooctene using this system, no significant advantages over the dimethylpyrazole system were observed (see Table 2.14). Activity was markedly inferior to that of the dimethylpyrazole system, which may me attributable to the lower

basicity of the N-functionalised pyrazole ring in dpmim-Cl, which may consequently be less activating. The lower activity required catalytic cycles to be run over 18, rather than 4 hours in order to obtain high conversions. The catalytic activity also diminished over successive cycles, which could be attributable to leaching during the product extraction, which it had been anticipated might be avoided by using the ionic ligand. The catalyst and/or pyrazolyl ligand may therefore be slightly soluble in pentane. The possibility that the pyrazolyl species was decomposing in some way, probably oxidatively, should also not be discounted however.

2.2.3.5 Application of the 3,5-dimethylpyrazole system to other olefin substrates

The general applicability of the dimethylpyrazole system was investigated by testing its activity in the epoxidation of a selection of other interesting olefin substrates. The results of this study are shown below in Table 2.18.

Table 2.18. Application of the dimethylpyrazole system to other olefin substrates [a]

Entry	Olefin Substrate		Conversion (Yield) (%)
1	1-Octene	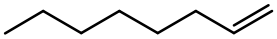	<1 (<1)
2			2 (2) [b]
3	*trans*-2-Octene	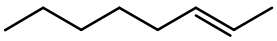	5 (5)
4			20 (20) [b]
5	*cis*-2-heptene	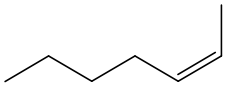	15 (15) [b]
6	*trans*-4-Octene	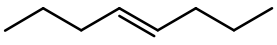	20 (20)
7	Styrene	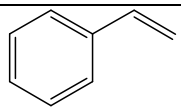	60 (4)
8	Ethyl acrylate	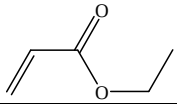	0
9	Allyl amine	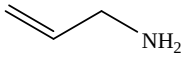	0
10	Cyclohexen-1-ol	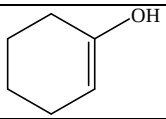	66 (34)

[a] *Aqueous $[Mo(O)(O_2)_2(H_2O)_n]$ 0.025 mmol, 3,5-dimethylpyrazole 0.1 mmol, 30 % $H_2O_{2\ (aq)}$ 3.0 mmol, olefin substrate 1.0 mmol, C_8mim-PF_6 2.0 mL, T = 60ºC, t = 4 h. Extraction with pentane (3 x 3 mL), yields and conversions calculated using GC.* [b] *t = 18 h.*

Perhaps surprisingly, given the excellent activity seen for the *cis*-cyclooctene substrate, the results show very poor activity in the epoxidation of all of the alternative substrates tested. The terminal alkyl olefin, 1-octene, is a poorly activated substrate and was here epoxidised to only an insignificant extent in 4 hours (entry 1, Table 2.18), and even after 18 hours only around 2 % conversion was observed (entry 2, Table 2.18). Several secondary olefins, *trans* 2- and 4-octene and *cis*-2-heptene were investigated (see entries 3-6, Table 2.18). The double bond in these substrates is more electron rich than in a terminal aliphatic alkene and they are thus more active to epoxidation. It was interesting to observe whether there would be any difference in activity towards *trans* and *cis* substrates as in some catalytic epoxidation processes significant differences are observable, presumably due to differences in conformational hindrance between the two types of substrate,[56(b)] and the previously described MoO_3/UHP system (Table 2.7) had demonstrated a slightly higher reactivity towards a *cis* substrate. Presumably due to their greater activation to epoxidation slightly better conversions were observed for the secondary alkenes than for 1-octene, but the results were still relatively poor. *trans*-2-Octene reached only 5 % conversion after 4 hours which increased to a still low 20 % after 18 hours. The *cis*-2-heptene substrate converted to a similar 15 % after 18 hours, indicating there was little difference in activity towards the epoxidation of *trans*- or *cis*- alkenes in this system. The *trans*-4-octene substrate was found to convert notably faster than the 2-alkenes, but the 20 % conversion observed after 4 h still compared very poorly with the rates of conversion observed in the epoxidation of *cis*-cyclooctene. Styrene apparently converted well, with a 60 % conversion observed, however selectivity was poor indicating poor protection from hydrolysis and only a low yield (4 %) of the epoxide was recovered. Two functionalised substrates, ethyl acrylate (entry 8, Table 2.18) with its ester function, and allyl amine (entry 9, Table 2.18) with the potentially coordinative amine showed no sign of any conversion. This is presumably explained by interference from the functional groups inhibiting the epoxidation mechanism or simply inactivity of the substrate. The enol substrate cyclohexen-1-ol appeared to convert fairly well at 66%, although only a moderate, 34 % yield of the epoxide was recovered. In comparison with the MoO_3/UHP system, the dmpz/H_2O_2 system was less active for the *cis*-2-heptene substrate but displayed similar activity

toward the two secondary *trans* substrates (in fact a better yield was obtained in only 4 hours for the 4-octene). The results for styrene are similar in both systems but notably the dimethylpyrazole system displays activity toward the enol whilst no conversion was observed toward this substrate in the MoO_3/UHP system.

2.2.4 Discussion of the mechanism of the epoxidation with regard to studies in ILs

From the results obtained in the catalytic studies several interesting trends were observed which provide evidence regarding the nature of the catalytic epoxidation. Whilst any inferences made are largely speculative, the discussion of patterns in the results with respect to the current understanding of this particular epoxidation process would seem to be relevant.

2.2.4.1 Inhibition of hydrolysis

Hydrolysis was clearly limited by reducing the availability of water, either by using UHP as oxidant or lowering the solubility of water in the reaction medium. The use of donor ligands can also apparently inhibit hydrolysis, both N-donor ligands and, generally to a lesser extent, N-oxide ligands were observed to increase selectivity for the epoxide product when using aqueous H_2O_2 as oxidant (see Table 2.11 and subsequent discussion). The monodentate ligands were only ever tested at a 4:1 ratio with molybdenum, but for 2,2'-bipyridine it was also found that, whilst a 1:1 ratio resulted in partial hydrolysis, a 2:1 ratio completely prevented any hydrolysis of the product during an 18 h epoxidation in the presence of water (entries 1 & 3, Table 2.12).

It is likely that the mechanism of hydrolysis of the epoxide proceeds firstly via coordination of the epoxide to the metal centre followed by reaction with water (coordinated or uncoordinated) forming the diol, which then leaves the metal. The observations made here would seem to support such a mechanism, since competition for free coordinative sites on the metal apparently reduces the rate of this process. The ligands examined here could block coordinative positions on the metal complex and in this manner block the epoxides access to the metal centre, thus preventing this step of

the hydrolytic mechanism. N-donors are stronger donors than N-oxides, thus they bind more strongly to the active sites and are more effective in preventing hydrolysis. Similarly, for bipyridine, the use of excess base should have increased competition for active sites and in this manner reduced hydrolysis. Results which did not conform to this theory were observed however, for example $[Mo(O)(O_2)_2(bpyO_2)]$, with the coordinated dioxide gave more protection to hydrolysis than $[Mo(O)(O_2)_2(bpy)]$ (entries 1 & 4, Table 2.12). It may be that the oxide actually bonds more easily to the metal centre than bipyridine for steric reasons, though there is no direct evidence on which to base a discussion of this. Interestingly though, better yields when using bipyridine-dioxide rather than bipyridine have been observed in other metal catalysed epoxidations and it has been shown to be effective in inhibiting hydrolysis in such systems.[189]

2.2.4.2 Oxygen donating intermediate complexes in oxobisperoxomolybdenum catalysed epoxidations

To summarise the important mechanistic studies of this reaction from the literature which were previously reviewed in the introduction (Section 1.3.2), oxobisperoxomolybdenum complexes have been studied as olefin epoxidation catalysts in reactions employing both H_2O_2[82-84] and organohydroperoxides[97] as oxidants and the complexes themselves are also known to serve as stoichiometric oxidants.[79] Studies have indicated fairly conclusively that molybdenum catalysed epoxidations employing relatively basic organohydroperoxides, such as TBHP, proceed via a hydroperoxo-organoperoxo-molybdenum intermediate (mechanism (a), Scheme 2.9).[45,96,98] As a result some authors have assumed that epoxidations employing H_2O_2 will proceed analogously via a dihydroperoxo species,[90] despite the lack of any direct evidence for such an intermediate. Other authors have speculated on a mechanism whereby the complex donates a peroxo oxygen to the substrate before being re-oxidised to the bisperoxo form (mechanism (b), Scheme 2.9).[82] In the latter mechanism the oxidant plays no active part in the oxidation step and instead serves to regenerate the oxidative metal species.

Scheme 2.9. Hypothesised mechanisms of epoxidation via: (a) an organoperoxohydroperoxo intermediate; (b) peroxo oxygen transfer

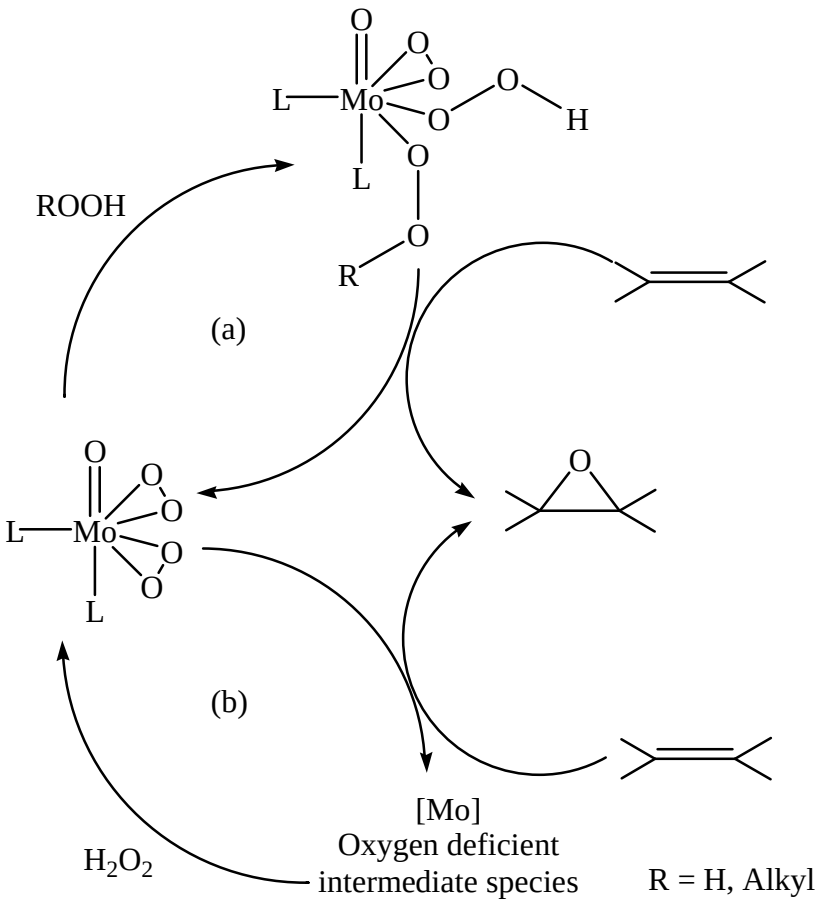

In oxomolybdenum catalysed epoxidations which proceed by mechanism (a) it has been shown that a more acidic metal centre improves the reaction, presumably since this helps facilitate coordination of the basic organoperoxide. Thiel et al. in their studies of olefin epoxidation by TBHP showed that electron withdrawing groups on the ligands of the oxobisperoxomolybdenum complex, which will result in increased acidity at the metal centre, increased the rate of catalysis.[98] It has also been observed that more basic oxidants are preferable in this mechanism, for example Mimoun noted that triphenylmethyl hydroperoxide (Ph_3COOH) was an inferior oxidant to TBHP in certain catalytic systems.[90] The role of the peroxo ligands in this mechanism is to abstract the peroxo proton upon coordination of the oxidant, but the peroxo oxygen atoms are not transferred to the substrate. Thiel et al. demonstrated that when olefinic functions were affixed to the ligands on their oxobisperoxomolybdenum catalysts, the resulting complexes were unable to auto-epoxidise, but when TBHP was added the epoxide was

rapidly formed.[98] Extending the scope to oxomolybdenum catalysed epoxidations in general, Trost and Bergman found that whilst [Mo(Cp)(Cl)$(O)_2$] was an efficient epoxidation catalyst when using organohydroperoxide oxidants, the corresponding monoperoxo complex, [Mo(Cp)(Cl)(O)(O_2)], was catalytically inactive and its formation during catalysis resulted in deactivation of the system.[190] The peroxo complex was found to form rapidly in the presence of less basic oxidants, such as H_2O_2 and Ph_3COOH, with only more basic organohydroperoxide oxidants permitting efficient catalysis. The observations made in both of these systems seem to indicate that whilst the more acidic metal centres benefit mechanism (a) by facilitating formation of the organoperoxohydroperoxo intermediate complex, they deactivate peroxo ligands, which are inhibited from donating an oxygen atom to the substrate (see Figure 2.7).

Figure 2.7. Effect of a more acidic metal centre on mechanisms of epoxidation

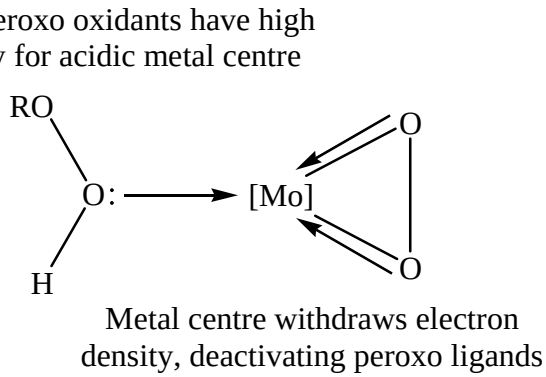

Moving on to systems proceeding via mechanism (b), it is useful to note that this mechanism is similar to that of MTO/H_2O_2 catalysed epoxidation systems which are fairly well understood. In such epoxidation systems MTO is converted by the oxidant to its mono- and subsequently bisperoxo complexes which are both capable of transferring peroxo oxygen atoms to an olefin substrate. MTO is an excellent olefin epoxidation catalyst precursor when H_2O_2 is used as oxidant, but is completely unable to activate TBHP, presumably since TBHP cannot generate MTO-peroxo ligands. Similarly, it has long since been noted that, whilst trioxomolybdenum is relatively easily converted to the bisperoxo complex by H_2O_2 or less basic organoperoxides such as Ph_3COOH, it is difficult to carry out the same transformation with TBHP.[96,90] In contrast to oxobisperoxomolybdenum/organohydroperoxide systems which function best with more basic oxidants and a more acidic metal centre, the activity of MTO/H_2O_2 systems is actually improved by strong donor ligands, which will reduce the acidity of the metal

centre.[56,57] Particularly effective are pyrazole ligands,[56(b),65] which have a higher *in-situ* donor strength than many stronger bases such as pyridines due to their resistance to oxidation. As previously discussed, although pyridines generally possess markedly higher pK_a values than pyrazoles, they convert to much more facile N-oxides under oxidising conditions and are thus weaker ligands for the purposes of oxidations. The more electron rich metal centre apparently activates the peroxo ligands, the reason for which is not completely understood, although Espenson et al. postulated upon electronic activation of the Re-O_{peroxo} bond.[64] Figure 2.8 shows how a more electron rich metal centre may favour oxidation reactions proceeding via peroxo oxygen donation rather than oxidant activation.

Figure 2.8. Effect of a more basic metal centre on the mechanisms of epoxidation

Basic peroxo oxidants less attracted to metal centre

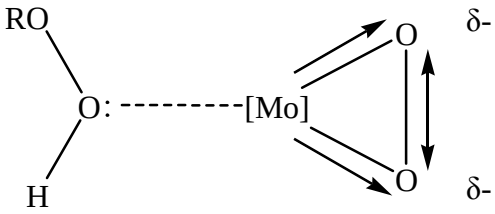

More electron rich metal centre results in more polar, more activated peroxo ligands

Considering the oxobisperoxomolybdenum/IL systems under discussion it seems fairly probable that oxygen transfer to the olefin substrate occurred via mechanism (b). It would be logical to conclude that the enhancement in catalytic activity induced by pyrazoles arises for the same reasons in both MTO and these oxobisperoxomolybdenum epoxidation systems. The effectiveness of pyridine and particularly imidazole species as donor ligands was limited due to their oxidation so, as in related MTO systems, pyrazoles were identified as the most effective ligand species. 3-Methylpyrazole has been proposed as the most activating pyrazole additive in MTO systems,[65] the author speculating that 3-methylpyrazole possesses an optimal pK_a value (3.3), slightly higher than that of pyrazole (2.5) thus rendering 3-methylpyrazole a stronger, more activating ligand, but at the same time lower than that of more basic pyrazoles, such as 3,5-dimethylpyrazole (4.2), which in MTO/H_2O_2 systems facilitate more rapid decomposition of the Re-CH_3 bond, deactivating the catalyst, to the extent that any

higher activating effect is cancelled out. Since oxobisperoxomolybdenum complexes are not vulnerable to any such type of deactivation it makes sense that the best additive is simply the strongest donor ligand under the catalytic conditions - dimethylpyrazole which has the highest pK_a of the oxidation resistant pyrazoles that were tested here.

To further understand the oxygen transfer to the substrate the pyrazolyl complexes were subsequently investigated as stoichiometric epoxidising reagents, in the absence of oxidant. The reactions of both $[Mo(O)(O_2)_2(pz)_2]$ and $[Mo(O)(O_2)_2(dmpz)_2]$ with *cis*-cyclooctene in C_8mim-PF_6 were subsequently investigated for this reason. A 1:2 oxidant complex:substrate ratio was employed, this corresponded to a 1:1 ratio between peroxo ligands and the substrate. $[Mo(O)(O_2)_2(bpy)]$ was also investigated as a stoichiometric oxidant to investigate reasons for the poor catalytic results obtained in catalytic studies. The stoichiometric oxidation of a selection of other, apparently much less activated, olefin substrates by the $[Mo(O)(O_2)_2(dmpz)_2]$ was also attempted. The influence of excess base on the oxidation was also investigated, epoxidation with $[Mo(O)(O_2)_2(dmpz)_2]$ carried out both in the presence and absence of two equivalents (with respect to the Mo complex) of the corresponding base (two equivalents were already coordinated to the metal in both instances). These reactions were carried out under completely anhydrous conditions under an inert atmosphere to eliminate any possibility of hydrolysis.

Table 2.19. Stoichiometric oxidation of olefins with oxobisperoxomolybdenum complexes in C_8mim-PF_6 [a]

Entry	Oxidant	Substrate	Conversion (Yield) [b]
1	$[Mo(O)(O_2)_2(pz)_2]$	*cis*-Cyclooctene	58 (51)
2	$[Mo(O)(O_2)_2(pz)_2]$ + pz [c]	*cis*-Cyclooctene	63 (56)
3	$[Mo(O)(O_2)_2(bpy)]$	*cis*-Cyclooctene	10 (10)
4	$[Mo(O)(O_2)_2(dmpz)_2]$	*cis*-Cyclooctene	58 (51)
5	$[Mo(O)(O_2)_2(dmpz)_2]$	1-Octene	0 (0)
6	$[Mo(O)(O_2)_2(dmpz)_2]$	*trans*-4-Octene	0 (0)
7	$[Mo(O)(O_2)_2(dmpz)_2]$	Styrene	0 (0)

[a] T = 60 °C, t = 12 h, C_8mim-PF_6 (2.0 mL), [Mo] (0.50 mmol), olefin substrate (1.0 mmol). [b] Conversion/yield calculated by GC, product(s) extracted with pentane (3 x 3 mL). [c] Pyrazole (1.0 mmol).

The first observation to highlight from the results obtained is that both $[Mo(O)(O_2)_2(pz)_2]$ and $[Mo(O)(O_2)_2(dmpz)_2]$ were quite clearly able to epoxidise the *cis*-cyclooctene substrate despite the absence of oxidant (entries 1 & 4, Table 2.19), confirming that the complexes could transfer coordinated oxygens (presumably peroxo)

to the substrate. The epoxidation step of mechanism (b), Scheme 2.9 would thus appear the probable mechanism in catalytic reactions. The yields obtained in the epoxidation of *cis*-cyclooctene with $[Mo(O)(O_2)_2(pz)_2]$ and $[Mo(O)(O_2)_2(dmpz)_2]$ (entries 1, 2 & 4, Table 2.19) were all approximately 50 %, seeming to indicate that oxobisperoxomolybdenum is capable of epoxidising 1 equivalent of olefin. This differs from the well studied MTO epoxidation system where the oxobisperoxo complex is able to donate 2 of its peroxo oxygen atoms in order to oxidise 2 equivalents of olefin, undergoing reduction to the dioxoperoxo and, sequentially, the trioxo complex in doing so.[94,71] An excess of pyrazole was not found to affect the final yield of the stoichiometric reaction after 12 h (entry 2, Table 2.19), any acceleratory effect the excess base might induce over a shorter reaction period was not investigated. For $[Mo(O)(O_2)_2(bpy)]$ (entry 3, Table 2.19), a low yield was observed (10 %) as in the catalytic studies. However, $[Mo(O)(O_2)_2(bpy)]$ was not completely soluble and so the reasons for the low yield are not clear. It is possible that the coordinated bipyridine in some way inhibits (though not totally) transference of the peroxo oxygen to the olefin, though the possibility that the poor conversion resulted simply because the undissolved complex was unable to react with the substrate cannot be discounted (note that the small amounts of complex employed in catalytic reactions were always observed to be completely dissolved so insolubility should not explain the poor catalytic results).

Having demonstrated in isolation the epoxidation step the regeneration of the bisperoxo complex by reaction of the reduced complex with H_2O_2 was also carried out. After the stoichiometric oxidation of *cis*-cyclooctene with $[Mo(O)(O_2)_2(dmpz)_2]$ (entry 1, Table 2.19), following extraction of products and evaporation of remaining volatiles, a small excess (1.2 equiv.) of aqueous H_2O_2 was added and the mixture stirred at 60 ºC for 30 mins. Excess water and hydrogen peroxide were then removed by evaporating under vacuum for several hours. When cyclooctene was added to the mixture and the epoxidation repeated the same result was obtained (approx. 50 % conversion), indicating that the bisperoxo species must have been regenerated. A control was also run where the complex was not reoxidised which, as expected, produced no significant conversion of the product on the second run, showing that treatment with H_2O_2 was necessary to restore the epoxidative potential. It was thus shown that both the epoxidation and peroxo regeneration reactions depicted in mechanism (b), Scheme 2.9 occur very readily under the reaction conditions leaving little reason to doubt that this is the catalytic mechanism of the reaction.

Visually, clear colour changes were apparent both when the complex reacted with the olefin and when the oxygen deficient species was regenerated with H_2O_2. 0.5 mmol of either $[Mo(O)(O_2)_2(pz)_2]$ or $[Mo(O)(O_2)_2(dmpz)_2]$ dissolved readily in 2 mL of C_8mim-PF_6 to give a clear yellow solution. When reacted with the olefin the colouration distinctly shifted to orange. Notably, this colour was visually similar to that of a dioxoperoxomolybdenum complex of dimethylpyrazole that was isolated during these studies (see Section 2.2.6.3), providing some indication that this type of complex is formed and is stable following transference of the peroxo oxygen to the olefin. When the orange solution was treated with H_2O_2 the yellow colour was restored within minutes.

Scheme 2.10. Colour changes during stoichiometric epoxidation with $[Mo(O)(O_2)_2(pz)_2]$

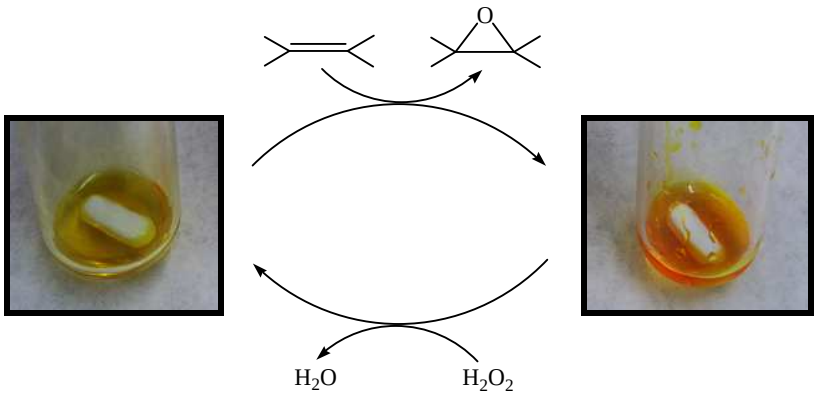

Interestingly, if the orange solution was heated for a longer period of time a very dark green colour evolved (see Scheme 2.11). For $[Mo(O)(O_2)_2(dmpz)_2]$ this occurred very quickly, within hours, whilst for $[Mo(O)(O_2)_2(pz)_2]$ heating had to be continued for several days to bring about the same change. The green colour would seem likely to correspond to a molybdenum(V) compound, with reduction of the metal species, indicating that corresponding oxidation of the substrate might have taken place. However, no more than the 1:1 epoxidation ratio observed once the orange species had evolved was detected, indicating that the reduction results from decomposition of the metal species, rather than a redox reaction wherein further substrate was oxidised. It should be noted that the green solution could be reoxidised to a yellow colour in the same manner as the orange precursor, so this decomposition would not kill a catalytic

system. It is significant to point this out, as in many catalytic systems, maximum TON is dependent on the average lifetime of the catalyst species prior to its deactivation. In these oxobisperoxomolybdenum systems however, the active catalytic species represents an oxidative extreme for the metal, which should always be regenerated simply by ensuring that oxidant is available, thus catalyst deactivation by chemical means within the catalytic system would be improbable.

Scheme 2.11. Progressive colour changes in C_8mim-PF_6/[Mo] solutions

Lastly, the results obtained in the attempted stoichiometric epoxidation of some other substrates should be discussed (entries 5-7, Table 2.19). For none of the substrates, 1-octene, *trans*-4-octene and styrene, was any conversion observed. Interestingly, the colour change from yellow to orange was still observed after the solution was heated for a while, seeming to indicate that the catalyst simply decomposed. Having obtained good results in the epoxidation of *cis*-cyclooctene the complete inertness towards these substrates could seem somewhat surprising. Seemingly the oxobisperoxomolybdenum species is unable to oxidise these substrates due to inability to transfer an oxygen to these types of substrate, though it is not obvious why. Interestingly however, for these non-cyclic substrates, whilst the results for stoichiometric oxidations, where mechanism (b) in Scheme 2.9 is the only available epoxidation route, were completely negative, in the catalytic systems (Entries 1, 2, 6 & 7, Table 2.18) low, but significant, levels of conversion were observed, the presence of the oxidant apparently making low conversions feasible. Perhaps then, these low epoxide yields are attributable to an alternative mechanism: activation of the H_2O_2 in a dihydroperoxomolybdenum intermediate as shown in mechanism (a), Scheme 2.9. This alternative mechanism appears to be much slower than the peroxo oxygen transfer (mechanism (b), Scheme 2.9) which should dominate for *cis*-cyclooctene. However, for these non-cyclic substrates where mechanism (b) is for some reason impossible, mechanism (a) becomes the only viable epoxidation mechanism and a slow but

significant level of oxidation takes place in this manner. As already discussed, with a more basic metal centre and a relatively less basic oxidant in H_2O_2 the oxidative intermediate does not form readily and mechanism (a) is thus very slow. By employing different coordinating species and/or oxidants a more efficient [Mo]/IL epoxidation system might be developed, capable of effectively oxidising non-cyclic substrates such as those appearing in Table 2.19. However, the work here was not extended to such a study.

2.2.4.3 Discussion of the Mimoun and Sharpless mechanisms

In the epoxidation of olefins by oxobisperoxomolybdenum complexes, independently of whether the oxygen atom is transferred from a peroxo or alkylperoxo ligand, the mechanism of the transfer itself is considered most likely to follow one of two pathways (Scheme 2.12), via a spirocyclic intermediate associated prominently with publications from Sharpless and co-workers,[91,96] or coordination of the olefin substrate to the metal in an equatorial position followed by formation of a five membered peroxometallocyclic intermediate, as proposed in the preliminary publications discussing this reaction from Mimoun and co-workers.[89,191] Scheme 2.12 shows the olefin receiving an oxygen derived from a peroxo ligand, but these mechanisms are also postulated as operative where oxygen is transferred to the substrate from an organoperoxo or hydroperoxo ligand.

Scheme 2.12. Olefin epoxidation via the Sharpless and Mimoun type mechanisms

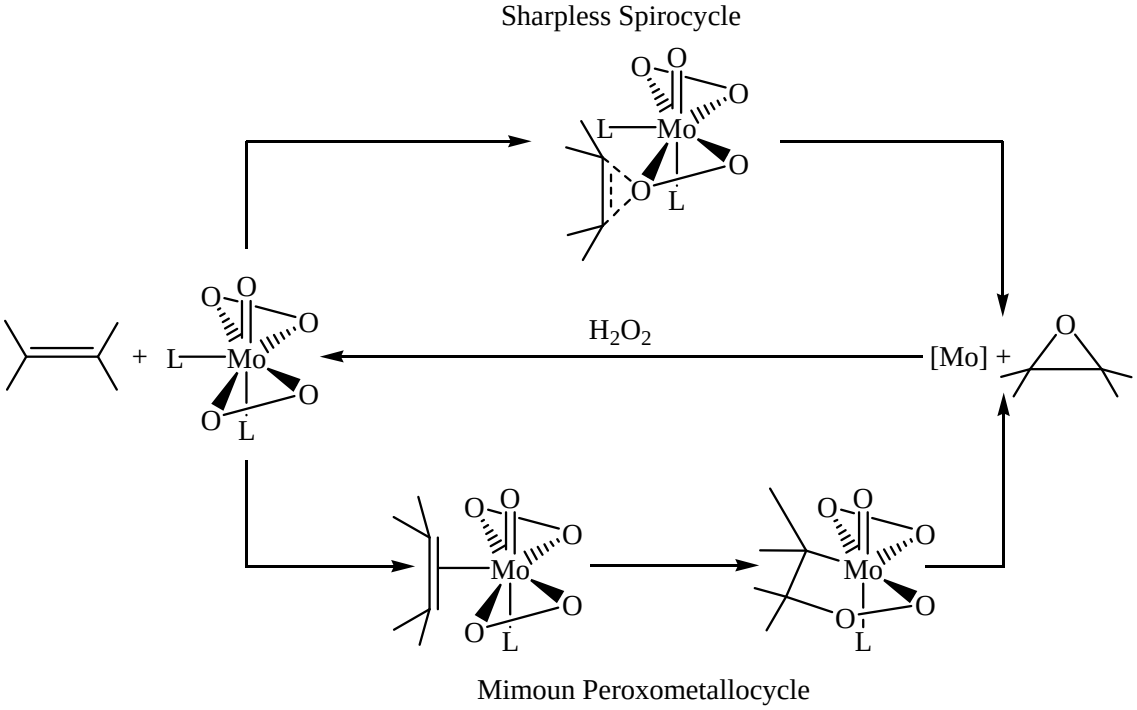

Peroxometallocycles of the type proposed by Mimoun are indeed isolable from the reactions of certain metal-peroxo complexes with olefins,[192] although it is notable that no such complex with a d^0 centre has yet been isolated. However, whilst some experimental evidence indicates that coordination to the metal centre might occur, the alternative mechanism proposed by Sharpless is now often considered the more likely.[71] In this mechanism, external nucleophilic attack of the olefin on the electrophilic peroxy oxygen results in a spirocyclic three membered ring transition state which breaks down, liberating the epoxide product. The original argument for this was based on a detailed study of relative rates of epoxidation reactions proceeding via 5- and 3-membered ring transition states, which indicated that epoxidations by oxobisperoxomolybdenum species should proceed via the latter.[91,96] Theoretical studies have also indicated that this three membered ring transition state should be more favourable than the five membered metallocycle for d^0 peroxo complexes of chromium, molybdenum and tungsten.[46(b),193] In spite of this, the probability of either mechanism is still considered an unresolved debate[84(a),178(b),190] and as such it would seem pertinent to discuss what indications the results obtained here give as to the mechanism active in these epoxidations.

Observations from monodentate ligands: Fundamental evidence which led Mimoun to propose a mechanism requiring coordination of the olefin substrate to the metal centre at some stage was the observation that, under certain conditions, basic solvents and strongly coordinating ligand species such as DMF and HMPA reduced the rate of the epoxidation.[90] This would infer that coordination to the metal centre was a necessary step and that such species were retarding the reaction by blocking this coordination. In this study, if the epoxidation were to proceed by such a mechanism, it would be expected that the investigations into the effect of the coordinating species on the reaction should have concluded that the more coordinating the additive species, the slower the conversion of the substrate, irrespective of any benefits to the selectivity. However, the results showed that none of the monodentate coordinating species investigated inhibited conversion at all and some additives actually enhanced the rate of conversion. 3,5-Dimethylpyrazole was more activating than pyrazole which in turn was more activating than pyridine-N-oxides. This runs contrary to the trend that would be expected were coordination to the metal centre necessary, since the more strongly coordinating species should block the catalysis more effectively. The only process that any of the additives were shown to inhibit was the hydrolysis of the epoxide, which should require access to the metal centre. From these results a mechanism not involving any direct coordination of the substrate to the metal centre during the epoxidation would appear to be favoured, making the Sharpless mechanism therefore seem more likely. Having previously noted the similarities between this system and reported MTO/H_2O_2 epoxidation systems it is worth remarking that the catalytic mechanism of MTO epoxidation is thought to proceed via a spirocyclic intermediate.[71] The analogies observed between the two types of system could indicate that the mechanisms are the same.

Observations from bidentate ligands: 2,2'-Bipyridyl ligands were found to very markedly reduce the catalysts activity, inhibiting conversion to the epoxide. This contrasts all of the monodentate species tested, which either had no effect on the conversion or actually increased it. This observation could be seen to support the Mimoun mechanism requiring coordination to the metal centre, since the bidentate bipyridyl ligands might well dissociate less easily than monodentates, leading to blockage of active sites on the metal.[194] However, further study of the effect of 2,2'-bipyridine indicated that blocking of active sites may well not explain the poor

conversion. Employing an excess of the base over [Mo] should have increased competition for, and reduced access to, the metal centre. Indeed, when an excess of bipyridine was used, as opposed to only one equivalent, selectivity for the epoxide improved from partial to complete, indicating that metal catalysed hydrolysis was being more effectively inhibited for this reason. At the same time however, no signifiant change in the rate of conversion was observed. This would seem to indicate that access to the metal centre was not important to the rate of the epoxidation mechanism and consequently this observation does not favour the mechanism postulated by Mimoun. In addition, the N,N'-dioxide, which is more weakly coordinating than unoxidised bipyridine, should block access to the metal centre less effectively. However, approximately equal conversions were observed with the dioxide complex and the unoxidised bipyridine complex. This would suggest that inhibited access to the metal centre was not responsible for the poor conversions. Exactly why the bipyridyls would inhibit the epoxidation is not clear however. As mentioned previously, poor solubility was not considered likely to be a problem in the catalytic reactions. The fact that bipyridine and its dioxide both gave similar conversions may indicate that the reason is steric, rather than electronic, since the strength of electron donation to the metal centre should vary significantly between the two. The best explanation that can therefore be offered for the poor conversions observed for bipyridyl complexes is that they produce an inhibitory steric effect, though specifically not by blocking access of the olefin substrate to the metal centre.

Note that coordination of a bidentate ligand does not necessarily lead to poor catalytic activity in oxobisperoxomolybdenum complexes: most notably, in the highly active systems described by Bhattacharyya et al. coordination of bidentate N, O donor ligands has produced very active complexes.[82-84] Also of interest, Thiel et al. showed that coordination of a bidentate N-donor ligand from oxobisperoxomolybdenum complexes was unlikely to inhibit access to the metal centre.[99] It is important to note that this describes a pyrazolyl-pyridine, rather than bipyridine type ligand, although despite their higher basicity, experimentally there is no precedential basis for arguing that bipyridyl ligands would necessarily be more poorly dissociating in these complexes.

2.2.5 IR study of oxobisperoxomolybdenum complexes

As was disussed in the preceding section, it is possible that coordination of certain species such as pyrazoles can activate the Mo-O_{peroxo} bond, rendering it more reactive and thus accelerating the rate of the epoxidation. If this were the case, one manner in which this activating effect might be observed is in the relevant bands in the IR spectra of appropriate oxobisperoxo complexes. Having synthesised a range of such complexes, the energies of the distinctive M=O, O-O and Mo-O_{peroxo} bands[181] (these are highlighted for $[Mo(O)(O_2)_2(dmpz)_2]$ in Figure 2.10) were recorded and are shown in Table 2.20 below.

Figure 2.9. The IR spectrum of $[Mo(O)(O_2)_2(dmpz)_2]$

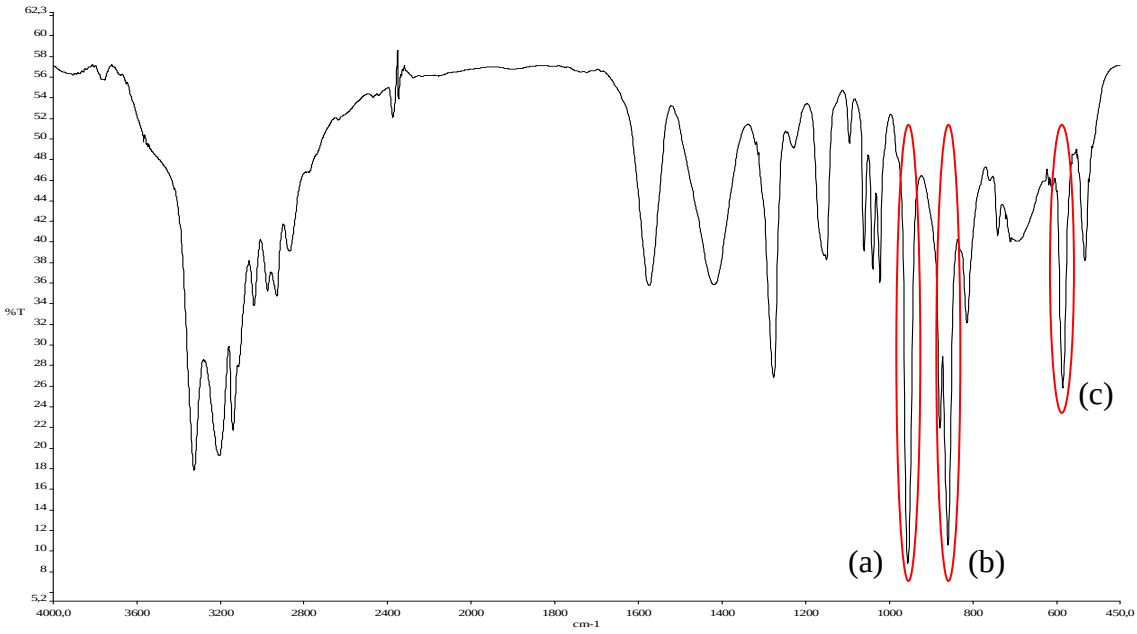

Highlighted peaks: (a) M=O, (b) O-O, (c) M-O_{peroxo}

Table 2.20. Energies of M=O, O-O and M-O_{peroxo} bands (cm^{-1}) for oxodiperoxmolybdenum complexes

Entry	Complex	M=O	O-O	Mo-O_2, sym.
1	$[Mo(O)(O_2)_2(pz)_2]$	963	852	580
2	$[Mo(O)(O_2)_2(dmpz)_2]$	957	860	586
3	$[Mo(O)(O_2)_2(phen)]$	949	847	Not Recorded [a]
4	$[Mo(O)(O_2)_2(bpy)]$	939	858	581
5	$[Mo(O)(O_2)_2(bpyO_2)]$	952	859	580
6	$[Mo(O)(O_2)_2(H_2O)(pz)]$	951	860	577
7	$[Mo(O)(O_2)_2(H_2O)(colO)]$	959	851	577
8	$[Mo(O)(O_2)_2(H_2O)(lutO)]$	961	856	Not Recorded [a]
9	$[Mo(O)(O_2)_2(H_2O)(2pcO)]$	973	848	Not Recorded [a]
10	$[Mo(O)(O_2)_2(H_2O)(3pcO)]$	951	852	Not Recorded [a]
11	$[Mo(O)(O_2)_2(H_2O)(pyO)]$	960	859	Not Recorded [a]

[a] In these cases the longer wavelengths were not recorded.

Overall the results indicate that there is hardly any change in the energies of these bonds irrespective of the coordinating species. The Mo-O_{peroxo} bands all fall within a very narrow 15 cm^{-1} range, too small to indicate any significant energetic difference. It was noted that $[Mo(O)(O_2)_2(dmpz)_2]$ fell at the top of this range, with $[Mo(O)(O_2)_2(pz)_2]$ also relatively high, but the differences with the other complexes are basically insignificant and well within reasonable experimental variation. Likewise the O-O bands fell into a narrow range with no discernible trend. Perhaps surprisingly there was also no attributable pattern in the M=O bands. In the monoaqua compounds the water molecule usually coordinates in the free axial position, trans to the M=O and as such a general difference between the values for these complexes and the other complexes, particularly those with N-donors in the axial position might have been expected. However all of the results fall into a relatively narrow range with the exception of one or two slightly anomalous results (i.e. entries 3 & 8 Table 2.20). Taking into account natural experimental variation there seems therefore to be hardly any significant energetic difference in these bands between the various complexes.

In discussing the IR spectra the possibility of erroneous assignments should be considered. In all cases the best possible effort was made to avoid such any such mistakes but it is sometimes difficult to rule this possibility out. In particular, in the case of the N-oxide complexes strong signals appear in the 600-650 cm^{-1} region, leading to the possibility for misassignment of the Mo-O_{peroxo} band. All spectra can be viewed in the appendices.

2.2.6 Structural data for some molybdenum-peroxo complexes

Oxobisperoxomolybdenum complexes generally conform to the configuration shown in Figure 2.10, with the axial oxo ligand, the two peroxo ligands occupying equatorial positions and coordinating ligands, if present, occupying the free positions, one on the equatorial plane and one *trans* to the oxo ligand.

Figure 2.10. Oxobisperoxomolybdenum complex

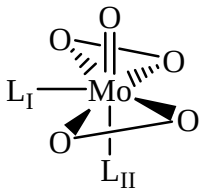

Despite their relative simplicity, structural data regarding the oxobisperoxomolybdenum complexes of simple N-heterocyclic bases is surprisingly scarce.[195] Many of these complexes, particularly those of bidentate ligands, such as 2,2'-bipyridines, have very poor solubilities which makes them difficult to recrystallise, although recrystallisation of some such complexes from polar media including DMF[184] and water:propanol[178(b)] has been described. Presumably as a result of this, despite the relative ease of their synthesis XRD studies have been reported for only a few of the simple oxobisperoxomolybdenum complexes, limited to pyridine N-oxide,[178] imidazole[183] and 2,2'-bipyridine.[184] For the purposes of this catalysis centred study the data obtained by XRD analysis of crystalline forms of these compounds would be interesting since it would potentially allow for analysis of any relationships which exist between the structure and catalytic activity of the complexes. The crystallisation of a range of these compounds was thus attempted. Via a range of methods (detailed in Section 3.6) several crystalline products suitable for structural analysis were obtained. The crystal structure analysis of these compounds was conducted independently of the studies discussed here and does not form part of this work.[196] However, some interesting findings will be discussed here qualitatively in relation to the previous catalytic studies.

The majority of crystalline products obtained were found in preliminary analysis to be oxoperoxo-polymolybdate salts of organic cations derived from protonation and in some cases decomposition of the N-heterocyclic base species. In these cases the bases

were not coordinated to the molybdenum atoms and the interest provoked by resolving these structures would thus be rather limited. As an example, a product crystallised from the reaction of $[Mo(O)(O_2)_2(H_2O)_n]$ with collidine was identified as $[\{Mo(O)(O_2)_2\}_2(\mu^2\text{-}O)]^{2-}\cdot 2[colH]^+$.

Figure 2.11. $[\{Mo(O)(O_2)_2\}_2(\mu^2\text{-}O)]^{2-}\cdot 2[colH]^+$ [196]

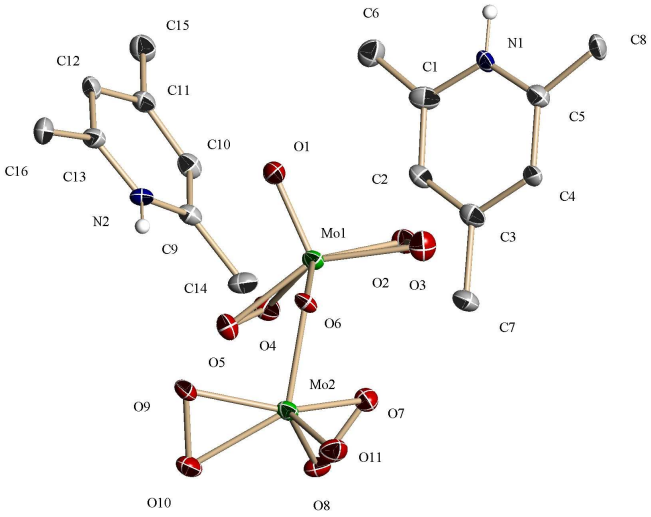

2.2.6.1 $[Mo(O)(O_2)_2(pz)(H_2O)]$ and $[Mo(O)(O_2)_2(pz)_2]$

$[Mo(O)(O_2)_2(H_2O)(pz)]$ and $[Mo(O)(O_2)_2(pz)_2]$ were synthesised simply by the reactions of 1 and 2 equivalents respectively of pyrazole with a solution of $[Mo(O)(O_2)_2(H_2O)_n]$ in hydrogen peroxide. After filtration of any precipitates, slow crystallisation of the filtrates yielded the products as yellow crystals from which their structures were determined. Both were found to adopt the trigonal bipyramidal conformation that would be anticipated for these compounds. The axial positions are occupied by the oxo ligand and either a water (in $[Mo(O)(O_2)_2(H_2O)(pz)]$) or pyrazole (in $[Mo(O)(O_2)_2(pz)_2]$) ligand whilst the two peroxo ligands and the pyrazole are coordinated equatorially. The equatorial ligands are bent slightly away from the oxo ligand so that the angles formed are greater than 90º. The equatorial pyrazole rings are angled approximately perpendicular to the equatorial plane, although in

$[Mo(O)(O_2)_2(pz)_2]$ the ring is twisted more considerably off from a right angle, and both are angled so that the NH is in proximity to the oxo ligand. The structures are shown below in Figure 2.12 and Figure 2.13.

Figure 2.12. $[Mo(O)(O_2)_2(pz)(H_2O)]$ [196]

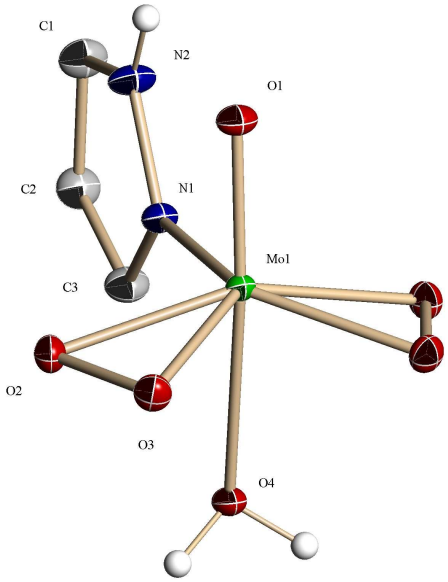

Figure 2.13. $[Mo(O)(O_2)_2(pz)_2]$ [196]

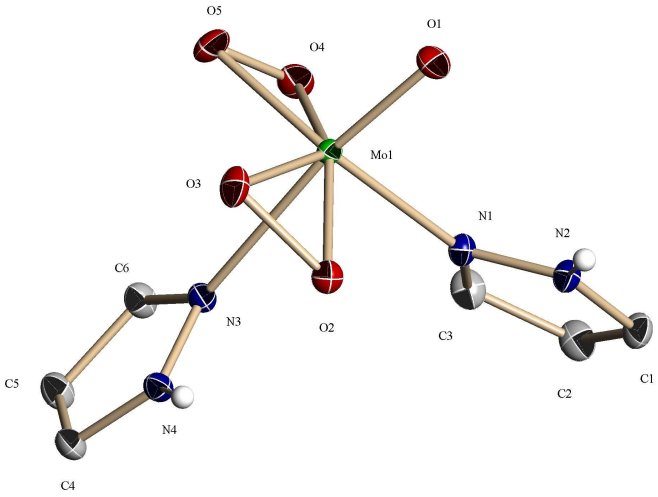

2.2.6.2 $[Mo_8(O)_{22}(O_2)_4(dmpz)_2]^{4-} \cdot 4[dmpzH]^{+} \cdot 2H_2O$

Given the exceptional catalytic activity observed for the 3,5-dimethylpyrazole complex of oxobisperoxomolybdenum, structural characterisation of this complex would clearly have been highly desirable. Unfortunately this complex was never isolated in crystalline form and so this was not ultimately achieved. Reaction between dimethylpyrazole and an aqueous solution of oxobisperoxomolybdenum gave the target compound in a yellow, microcrystalline form. However attempts to obtain crystals of the complex from the remaining liquors in the same way as for the pyrazole complex met with no success. The bis(3,5-dimethylpyrazolyl) complex was identical in appearance to the dipyrazolyl equivalent but notably, whilst the latter is stable for months under atmospheric conditions at room temperature, the former decomposes to dark solids within days. Recrystallisation of the complex from water and propanol yielded yellow crystals, however these were not the oxobisperoxo complex but rather an octamolybdate species with the formula $[Mo_8(O)_{22}(O_2)_4(dmpz)_2][Hdmpz]_4 \cdot 2H_2O$. Interestingly, an octamolybdate structure bearing peroxo ligands in this manner has yet to appear in literature. Unlike the oxobisperoxo complex this compound was stable under air even over a period of months. The anion is shown below in Figure 2.14.

Figure 2.14. The $[Mo_8(O)_{22}(O_2)_4(dmpz)_2]^{4-}$ anion [196]

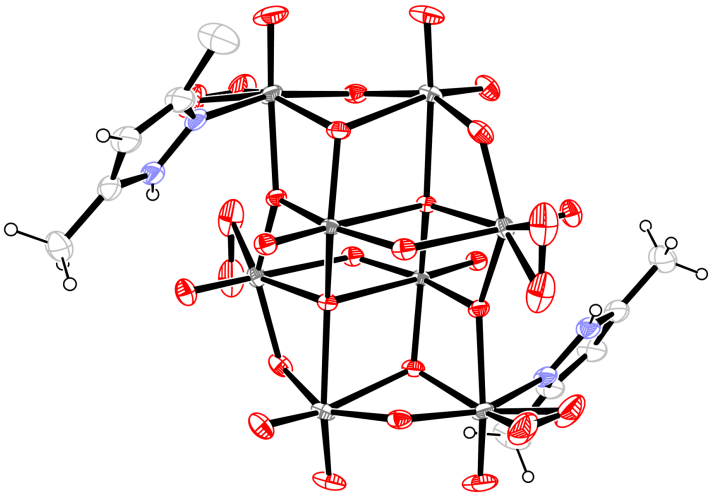

2.2.6.3 [{[Mo(O)(O_2)(dmpz)]$_2$(μ^2-O)$_2${Mo(O)$_2$(O_2)(dmpz)$_2$}$_2$]·CH_2Cl_2

Further efforts to crystallise the oxobisperoxomolybdenum complex of 3,5-dimethylpyrazole led to a another interesting discovery. When solutions of oxobisperoxomolybdenum in aqueous hydrogen peroxide and 3,5-dimethylpyrazole in dichloromethane were mixed, the distinctive yellow of the bisperoxo complex was seen to rapidly cross over into the organic phase. Furthermore however, within minutes the distinctive yellow colouration darkened to orange. When carefully crystallised this solution yielded orange crystals which were characterised as a polymetallic complex comprised of four dioxoperoxo configured molybdenum(VI) centres with general formula $Mo_4O_{16}(dmpz)_6$ (see Figure 2.15). The compound consists of a symmetrical chain with four molybdenum atoms. The middle two metal atoms in the chain are connected to each other through two bridging oxygen atoms and each possesses an oxo and a peroxo ligand along with one dimethylpyrazole donor ligand. The terminal molybdenum atoms are dioxoperoxo, possessing two oxo ligands, a peroxo and two dimethylpyrazole donor ligands and are bound to the central molybdenum atoms through one of their oxo ligands acting as a donor. Remarkably, this compound is the first dioxoperoxomolybdenum(VI) compound to be characterised in the solid state.

Figure 2.15. [{[Mo(O)(O_2)(dmpz)]$_2$(μ^2-O)$_2$}{Mo(O)$_2$(O_2)(dmpz)$_2$}$_2$] [196]

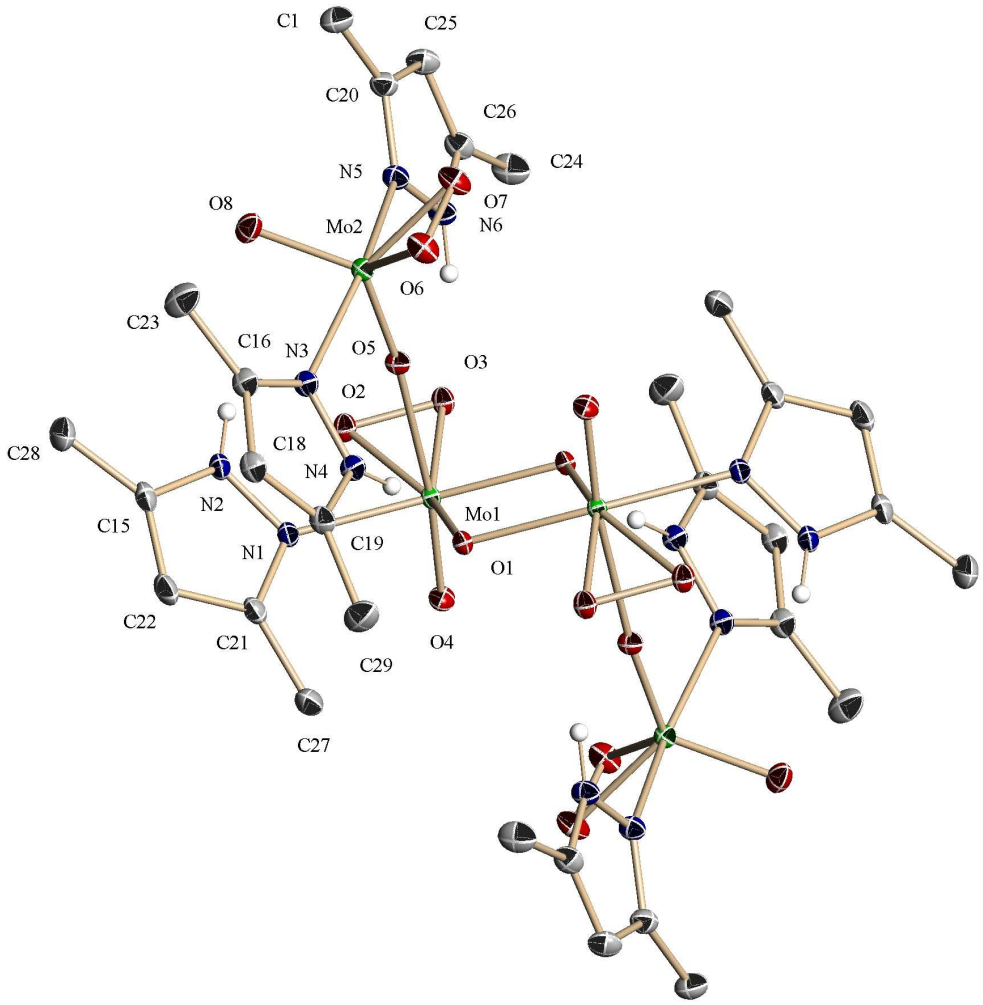

One final item of interest regarding the dioxoperoxo complex, which has already received mention when discussing the catalytic epoxidations in ILs, concerns the colour of the compound and the dichloromethane solution from which it was crystallised. Both show a distinctive orange colouration which was also observed in stoichiometric epoxidations by the oxobisperoxo complex in IL after 1 equivalent of olefin had been oxidised. This provides an indication that in catalytic reactions an intermediate dioxoperoxo complex forms after oxidation of the substrate which is subsequently re-oxidised to the oxobisperoxo form by H_2O_2. At the time of writing this had not been successfully confirmed however.

2.2.6.4 Relationship between catalytic activity and structural data

It was unfortunate that an oxobisperoxomolybdenum complex of dimethylpyrazole was not isolated for structural analysis in the solid state as this was the optimum catalyst identified during the catalytic studies. Nevertheless, the pyrazole complex had also demonstrated an enhanced activity and comparison of its structural parameters with those of related structures was therefore interesting in examining reasons for the catalytic enhancement that coordinated pyrazoles apparently induce. In particular the bond lengths relating to the peroxo ligands, both the Mo-O_{peroxo} and O-O bonds, might give some indication if the peroxo ligands of this complex were more reactive, thus facilitating more rapid epoxidation. Heightened polarity in the peroxo ligands might well induce greater epoxidative activity both due to the lesser stability of the ligand, which should cause it to release the oxygen atom more readily, and the increased capacity for nucleophilic attack by the oxygen atom during the epoxidation mechanism. Pyrazole ligands may facilitate increased electron donation by the metal centre to the peroxo ligands due to their previously discussed properties as stronger *in-situ* ligands. A strong donor ligand results in a more basic metal centre and thus increased donation to the peroxo ligands. In this manner the coordination of a pyrazole in an equatorial position on the oxobisperoxo complex may render the peroxo ligands more reactive.

Table 2.21 below lists bond lengths determined by XRD analysis of the oxobisperoxomolybdenum complexes of pyrazole synthesised in this work along with those of all oxobisperoxomolybdenum complexes of simple N-heterocyclic bases and their oxides so far described in literature.

Table 2.21. Structural data for relevant $[Mo(O_2)_2(O)(L_I)(L_{II})]$ complexes

Complex	Bond Lengths (Å)[a]		
	Mo-O_{oxo}	**Mo-O_{peroxo}**	**O-O**
Aqua-monodentate			
$[Mo(O)(O_2)_2(pyO)(H_2O)]$[178(b)]	1.670	1.955, 1.919, 1.955, 1.919	1.470, 1.470
$[Mo(O)(O_2)_2(pz)(H_2O)]$[196]	1.6819(15)	1.9482(11), 1.9450(10), 1.9482(11), 1.9450(10)	1.4796(3)
$[Mo(O)(O_2)_2(im)(H_2O)]$[183]	1.670(3)	1.949(2), 1.935(2)	1.468(4)
Di-monodentate			
$[Mo(O)(O_2)_2(pyO)_2]$[178(a)]	1.676(3)	1.942(3), 1.926(3), 1.944(2), 1.913(2)	1.460(3), 1.458(4)
$[Mo(O)(O_2)_2(pz)_2]$[196]	1.6778(12)	1.9620(12), 1.9357(12), 1.9401(13), 1.9189(13)	1.4807(16), 1.474(2)
Bidentate			
$[Mo(O)(O_2)_2(bpy)]$[184]	1.682(4)	1.953(4), 1.912(5), 1.948(4), 1.908(4)	1.459(6), 1.465(5)

[a] *Standard deviations given in brackets when available.*

An examination of the data presented in Table 2.21 shows that there is little significant variation between the Mo-O_{oxo} bond lengths of any of the complexes, all being within a range of 1.670-1.685 Å. Mo-O_{peroxo} bond lengths vary depending on whether the oxygen is adjacent to the equatorial ligand. If adjacent, bond lengths fall generally between 1.945 and 1.960 Å, but are shorter and more variable for the non-adjacent bond. Bond lengths between the metal centre and the non-adjacent peroxo oxygen are slightly longer in the pyrazole complexes than in the other examples, particularly in the aqua-pyrazole complex. The O-O bond lengths do seem to be slightly longer in the pyrazole complexes than in the other examples. Amongst the complexes described in literature these distances fall into a range of around 1.455-1.470 Å whilst for the pyrazole complexes values of around 1.480 Å are observed. Longer O-O bond lengths may indicate that this bond is weakened due to higher polarity in the O_2 ligand, resulting from electron donation to antibonding O_2 orbitals by the metal centre.[197] Shorter Mo-O_{peroxo} bond lengths might also have been anticipated as a result,[198] though this is not evident. The differences (0.010 – 0.025 Å) are not very significant however, so the inference of this observation is limited.

It should be aknowledged that amongst the complexes described in Table 2.21 the complexes with a coordinated bipyridine or imidazole ligand actually have more basic ligands than pyrazole coordinated at the equatorial site, and in theory these should therefore induced greater destabilisation of the peroxo ligands than pyrazole. Sterically, the bidentate bipyridine may be inhibited from bonding effectively, but imidazole is

structurally very similar to pyrazole (the authors even confused the two when resolving the structure[183]) and would be expected, as a stronger base, to donate more electron density to the metal. If the slight differences observed in O-O bond lengths are attributable to activation by a bound pyrazole ligand it is not clear why these other species would have a lesser activating effect.

It is also interesting to look briefly at the peroxo bond lengths determined for the dioxoperoxomolybdenum structure that was discussed in Section 2.2.6.3. As previously discussed, oxobisperoxomolybdenum is capable of epoxidising only one equivalent of substrate and may well form a dioxoperoxo intermediate subsequent to losing a peroxo oxygen. For this reason the peroxo ligands of this structure might be expected to be notably deactivated compared with those of the oxobisperoxo compounds. The structural data are thus shown below in Table 2.22.

Table 2.22. Bond lengths for $[\{[Mo(O)(O_2)(dmpz)]_2(\mu^2\text{-}O)_2\{Mo(O)_2(O_2)(dmpz)_2\}_2]$ [196]

Position of Mo	**Bond Lengths (Å)**[a]	
	Mo-O_{peroxo}	**O-O**
Terminal	1.9255(17), 1.9240(17)	1.451(2)
Central	1.9560(16), 1.9547(16)	1.447(2)

[a] *Standard deviations given in brackets*

There is some evidence of differences in the bond lengths both in comparison with the oxobisperoxo complexes and between the two peroxo ligands, though the observations are probably not highly remarkable. Looking first at the Mo-O_{peroxo} bond lengths, the peroxo ligand affixed to the terminal molybdenum atom exhibits bond lengths of approximately 1.925 and 1.924 Å. In oxobisperoxo complexes these bond lengths are typical for the oxygen atom which is not adjacent to the equatorial ligand. However, they are notably shorter than bond lengths typical for the adjacent oxygen atoms, where bond lengths fell between 1.940 and 1.962 Å. This might indicate that in an oxobisperoxo complex, the peroxo oxygen atom adjacent to the equatorial ligand is less strongly bound to the metal centre, with this perhaps resulting in higher reactivity, whilst in a dioxoperoxo complex both the peroxo oxygen atoms have relatively strong bonding with the molybdenum atom and thus are not easily transferred from the complex. In contrast however, the Mo-O_{peroxo} bond lengths for the central metal atom are of approximately 1.956 and 1.955 Å. Both of these bond lengths are typical of those observed with the oxygen atom postioned adjacent to the equatorial ligand in an

oxobisperoxomolybdenum complex. According to the logic of the prior speculation this should make them fairly activated, which is not anticipated for this relatively oxygen deficient compound and is thus contradictory. The O-O bonds are both of a similar magnitude, at approximately 1.451 and 1.447 Å. These values are actually somewhat shorter than the range observed for the oxobisperoxo complexes, between 1.458 - 1.480 Å, which could be interpreted as corresponding to reduced polarity and thus deactivation. However, the differences are not large enough to be considered particularly significant.

2.2 Oxobisperoxomolybdenum(VI) Complex Catalysed Epoxidations Part B: in Apolar Media

The studies of molybdenum catalysed olefin epoxidations covered up until this point were conducted in ILs in order to achieve homogenisation of the catalyst and substrate. As already discussed, these media have the novel capacity to dissolve the otherwise often poorly soluble molybdenum catalyst complexes of simple base ligands. In terms of sustainability and "greenness", the use of ILs incurs various advantages and disadvantages compared to similar processes in conventional solvents. In continuation of this study of oxobiperoxomolybdenum catalysed epoxidations focus was next switched onto reactions in low polar organic solvents and solventless conditions.

2.2.7 Solubilisation of oxobisperoxomolybdenum complexes with solubilising substituents

Oxobisperoxomolybdenum complexes generally have particularly poor solubilities in apolar media, so in order to more easily achieve a homogeneous catalytic system the first step was the design of catalyst complexes with enhanced solubility in such solvents. In this study this was achieved by appropriate functionalisation of some standard ligands. This strategy does have successful precedents[16,17,159] and has even been employed for oxobisperoxomolybdenum catalysts.[97,80] The use of the PDMS functionalised/supported pyridine ligand 4-(polydimethylsiloxanyl-ethyl)pyridine (**A**) and its application in a similar context with MTO,[199] palladium and copper[200] catalysts is discussed elsewhere in the results section. Its potential to form coordination complexes with oxobisperoxomolybdenum which would be both catalytically active and soluble in conventional apolar organic solvents was also studied and these results will be covered here. Additionally, several alkyl and TMS functionalised coordinating N-heterocyclic base species were synthesised and investigated in a similar capacity.

2.2.7.1 Epoxidations in apolar solvents

By dissolving oxobisperoxomolybdenum catalysts in this manner, homogeneous reaction systems wherein the catalyst and olefin substrate are dissolved in an apolar organic reaction solvent solvent could be envisaged, with aqueous hydrogen peroxide serving as oxidant and forming a separate phase. With the substrate and product remaining separated from the aqueous oxidant in the organic phase, hydrolysis could hopefully be avoided whilst catalytic conversion to the epoxide could take place. Table 2.23 shows a selection of results obtained in chlorophorm, toluene and hexane for a selection of the substituted bases and their unsubstituted analogues.

Table 2.23. Oxobisperoxomolybdenum catalysed *cis*-cyclooctene epoxidations in apolar organic solvents with a selection of base additives [a]

Entry	Solvent	Ligand	Conversion	(Yield)
1	Chlorophorm	-	0	(0)
2		Pyridine	2	(2)
3		4-(Polydimethylsiloxanyl-ethyl)-pyridine (**A**)	86	(86)
4		2,2'-Bipyridine	12	(2)
5		4,4'-Ditridecyl-2,2'-bipyridine (**E**)	17	(17)
6		4,4'-Dinonadecyl-2,2'-bipyridine	27	(16)
7		4,4'-Bis(bistrimethylsilanylmethyl)2,2'bipyridine (**F**)	17	(17)
8		2,6-Bis-trimethylsilanylmethyl-pyridine (**D**)	38	(38)
9		4-Tridecylpyridine (**B**)	99	(99)
10		4-(2,2-Bis-trimethylsilanyl-ethyl)-pyridine (**C**)	72	(71)
11	Toluene	4-(Polydimethylsiloxanyl-ethyl)-pyridine (**A**)	2	(2)
12	Hexane	Pyridine	5	(1)
13		4-(Polydimethylsiloxanyl-ethyl)-pyridine (**A**) [b]	4	(2)
14		2,2'-Bipyridine	0	(0)
15		4,4'-Ditridecyl-2,2'-bipyridine (**E**)	0	(0)
16		4,4'-Ditridecyl-2,2'-bipyridine (**E**) [b]	0	(0)
17		2,6-Bis-trimethylsilanylmethyl-pyridine (**D**)	9	(1)

[a] *Aqueous $[Mo(O)(O_2)_2(H_2O)_n]$ 0.025 mmol, ligand 0.05mmol, 30 % $H_2O_{2\ (aq)}$ 3.0 mmol, cis-cyclooctene 1.0 mmol, solvent 10 mL, 18 h, 60ºC. Yields and conversions calculated by GC.* [b] *Coordination compound prepared prior to the reaction (as opposed to formation in-situ).*

The first observation to be made from the results of these studies is that significant conversion in hexane was never achieved (entries 10-15, Table 2.23). Visually solubilisation of the catalyst was not observable in any of these reactions, the complex instead precipitating as a a colloidal yellow solid, which would indicate that the lack of any catalytic conversion stems from the insolubility of the catalyst which is

thus unable to catalyse the reaction. The possibility that a soluble catalytic species was unable to form *in-situ* due to insolubility of the molybdenum precursor was considered, but when reactions were carried out using previously synthesised coordination compounds (entries 13 & 16, Table 2.23) significant conversions were still not achieved. A reaction carried out in toluene gave a similarly poor result with no observable catalyst solubility, indicating the same problem (entry 11, Table 2.23). The lack of activity observed in these systems, dissuaded any further investigation of the potential for epoxidations in very non-polar environments, such as $scCO_2$, where the catalyst complexes would very likely also be insoluble and inactive. Additionally, when no base (entry 1, Table 2.23) or the unsubstituted analogue bases (entries 2, 4, 10 & 12, Table 2.23) were employed there was never any significant conversions. Again in these instances it seems probable that the insolubility of the catalyst complexes explains the lack of catalytic activity. In chlorophorm low, but significant conversions were observed when the 4,4'-dialkyl substituted bipyridines were used (entries 5 & 6, Table 2.23). This represented a slight improvement over the yields observed using unsubstituted bipyridine in ionic liquids (entries 5 & 6, Table 2.23), but when direct comparison was made with 4-alkyl substituted monopyridines in chlorophorm (compare entries 5 & 9, Table 2.23), utilising the bidentate ligands was found to result in activities far deficient of their monodentate counterparts. Reasoning for this observation has previously been discussed in detail (see Section 2.2.4.3) and these results are probably explicable in the same manner.

Considering now the instances where relatively good activities were observed, in chlorophorm the two 4-substituted monopyridyl ligands 4-(polydimethylsiloxanyl-ethyl)pyridine (**A**) (entry 3, Table 2.23) and 4-tridecylpyridine (**B**) (entry 9, Table 2.23) afforded high yields within the 18 hours, with complete conversion to the epoxide observed in the latter. It seems likely that in both of these systems coordination of the solubilising ligands to the metal centre resulted in a soluble catalyst, with effective homogeneous catalysis subsequently resulting in good conversion. Additionally the selectivity to the epoxide was found to be complete in both cases. This indicates that the epoxide product is effectively protected from hydrolysis within the system, most likely due to its separation from the aqueous phase. These results are highly interesting as the low solubility of most oxobisperoxomolybdenum complexes renders homogeneous catalysis in conventional media very difficult. Here, effective solubilisation and

efficient, selective catalysis have been achieved employing only common pyridine rings with relatively simple polymeric solubilising structures.

The other functionalised monopyridyl species that were examined were the structural isomers 2,6-bis(trimethylsilanylmethyl)pyridine (entry 8, Table 2.23) and 4-(2,2-bis-trimethylsilanyl-ethyl)pyridine (entry 10, Table 2.23). Interestingly, whilst both species apparently completely inhibited hydrolysis of the epoxide and afforded significant epoxidation, there was a marked difference in the observed yields. It is likely that the 2,6-functionalised pyridine might encounter steric hindrance in its coordination to the metal centre, and this may explain the lower conversion compared with the 4-substituted isomer. However, the benefits from the solubilising methyl-trimethylsilanyl substituents still clearly outweigh any such hindrance that they impose (compare with unsubstituted pyridine (entry 2, Table 2.23), indicating that solubilisation of the catalyst complexes is vital in obtaining significant catalytic activity.

It is worth noting at this point that in the instances where monopyridyl coordinating species were employed (pyridine, **A**-**D**) it is likely that the *in-situ* coordinating species would actually be the corresponding N-oxides, which have been found to be less efficient both in limiting hydrolysis and activating the catalyst than N-donors. In the previous study of oxidations in ILs it was shown that pyridine was likely oxidised as such (Section 2.2.2.2), and reaction of pyridine with $[Mo(O)(O_2)_2(H_2O)_n]$ in the presence of H_2O_2 gives the N-oxide complexes (see literature Refs[178] and Section 3.6.8). The facile oxidation of **B** to its oxide was demonstrated in chlorophorm (Scheme 2.5) and reaction of $[Mo(O)(O_2)_2(H_2O)_n]$ with **B** gave the oxide complex, $[Mo(O)(O_2)_2(\mathbf{B}O)(H_2O)]$ (Section 3.6.3). In the case of **A** such an oxidation might also be considered probable, though it is worthy of note that it was considered possible that this particular ligand possesses a higher resistance to oxidation, explaining the higher epoxidative activities witnessed for MTO-**A** compared with MTO-**B** and MTO-pyridine systems (Section 2.1.3.4).

2.2.7.2 Epoxidation of other olefin substrates in chlorophorm

Having established that the systems employing **A** and **B** (Table 2.23, entries 3 & 9) had high activity in the epoxidation of *cis*-cyclooctene, investigation of these systems was extended to other olefin substrates, shown below in Figure 2.16.

3,5-Dimethylpyrazole was also investigated, having produced a high activity in the previous study in ILs. In this prior study, a system employing dimethylpyrazole in 2 mL of chlorophorm produced a conversion of 23 % with an 8 % yield of epoxide for *cis*-cyclooctene (entry 24, Table 2.11) The results are shown below in Table 2.24.

Figure 2.16. Olefin Substrates used in extended studies

Cyclohexene 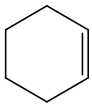

1-Octene 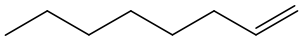

trans-2-Octene 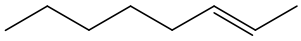

trans-4-Octene 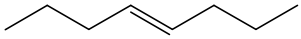

cis-2-Heptene 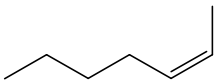

Styrene 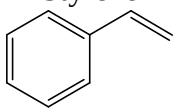

Table 2.24. Epoxidations in chlorophorm [a]

Entry	Base Additive	Olefin	Conversion (Yield)
1	3,5-Dimethylpyrazole 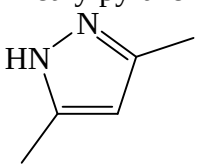	Cyclohexene	12 (12)
2		1-Octene	3 (1)
3		*trans*-2-Octene	20 (11)
4		*trans*-4-Octene	22 (9)
5		*cis*-2-Heptene	23 (23)
6		Styrene	17 (0)
7	**B** 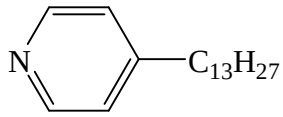	Cyclohexene	23 (5)
8		1-Octene	0 (0)
9		*trans*-2-Octene	15 (13)
10		*trans*-4-Octene	25 (22)
11		*cis*-2-Heptene	29 (29)
12		Styrene	60 (0)
13	**A** 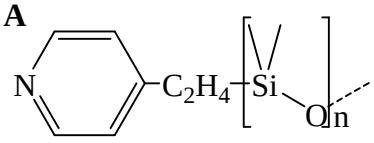	Cyclohexene	75 (75)
14		1-Octene	0 (0)
15		*trans*-2-Octene	2 (3)
16		*trans*-4-Octene	2 (2)
17		*cis*-2-Heptene	1 (1)
18		Styrene	100 (0)

[a] *Aqueous $[Mo(O)(O_2)_2(H_2O)_n]$ 0.025 mmol, base additive 0.10 mmol, 30 % $H_2O_{2\ (aq)}$ 3.0 mmol, olefin substrate 1.0 mmol, chlorophorm 10 mL, t = 18 h, T = 60 ºC. Yields and conversions calculated by GC.*

Six substrates were tested in this study, cyclohexene which is relatively active to epoxidation, the inactive terminal alkene 1-octene, one *cis* and two *trans* secondary alkenes which should be more active and also styrene, the oxide of which is very vulnerable to decomposition through hydrolysis. Brief examination of the results is sufficient to conclude that none of the base additives tested was able to produce a very

efficient system. Going on to look in more detail regarding the findings, for the epoxidation of cyclohexene, **A** produced the most active system, with 75 % yield after 18 h and no detectable hydrolysis (entry 13, Table 2.24). However, given the long reaction time, to have still obtained incomplete conversion for such an active substrate still indicates the efficiency of the system was limited. The performance of both dimethylpyrazole and **B** was very poor with very low isolated yields and poor selectivities (entries 1 & 7, Table 2.24). The latter result is surprising considering that **B** had previously produced the highest activity towards *cis*-cyclooctene (entry 9, Table 2.24), with complete conversion under exactly the same conditions. Efficient conversion of the terminal 1-octene was never achieved. No trace of any conversion was detectable for **A** or **B** (entries 8 & 14, Table 2.24), whilst dimethylpyrazole produced only a trace level of conversion (entry 2, Table 2.24). In contrast to the results obtained for the epoxidation of cyclohexene, in the conversion of the secondary alkenes **A** proved to be very inactive with little better than trace conversion of any of the substrates (entries 15-17, Table 2.24), whilst **B** and dimethylpyrazole produced slightly more active systems (entries 3-5 & 9-11, Table 2.24). In these cases the *cis* substrate (entries 5 & 11, Table 2.24) appeared to convert slightly more efficiently and with slightly better selectivities, although the difference is slight and should not be considered conclusive evidence that the *cis* substrate was chemically more reactive than the *trans*. In no case was any yield of styrene isolable after the reaction (entries 6, 12 and 18, Table 2.24). Although the substrate was completely consumed when **A** was used, the epoxide had apparently all been lost to hydrolysis. In the GC analysis, a peak corresponding to benzaldehyde was observable, though it was not quantified. The other additives produced inferior conversions, indicating that epoxidation was slower and the protection from hydrolysis similarly poor.

In summary, none of the three base additives tested was able to induce a highly active system in chlorophorm for any of the substrates, particularly when the long reaction time is taken into account. **A** gives fairly good activities when converting cyclic substrates but is otherwise very inactive. The dimethylpyrazole and **B** systems on the other hand were poorly active toward cyclohexene but markedly superior results were observed for secondary olefin substrates. Whilst all systems apparently had a measurable level of activity toward styrene no epoxide was ever recoverable.

2.2.7.3 Solventless epoxidations

Having established that several of the base additives could produce, albeit limited, epoxidation systems in an apolar media such as chlorophorm their efficacy in solventless epoxidations, similar to those previously examined in the studies of rhenium catalysed epoxidations was examined. To begin with, a selection of base additives were tested in the epoxidation of *cis*-cyclooctene. Bipyridyl type ligands were excluded from this study due to the generally inhibitory effect observed for bipyridyls in the studies conducted up to this point. The results are shown below in Table 2.25.

Table 2.25. Solventless epoxidation of *cis*-cyclooctene [a]

Entry	Base Additive	Conversion (Yield)
1	None	12 (5)
2	Pyridine	8 (8)
3	Pyrazole	16 (12)
4	3,5-Dimethylpyrazole	31 (31)
5	**B**	31 (31)
6	**A**	25 (23)

[a] *Aqueous $[Mo(O)(O_2)_2(H_2O)_n]$ 0.025 mmol, base additive 0.10 mmol, 30 % $H_2O_{2\ (aq)}$ 3.0 mmol, cis-cyclooctene 1.0 mmol, t = 18 h, T = 60 ºC. Yields and conversions calculated by GC.*

In the absence of any base additive (entry 1, Table 2.25) a conversion of 12 % was observed, contrasting the result obtained when the reaction was carried out in the presence of chlorophorm solvent, where there was no observable conversion (entry 1, Table 2.23). Surprisingly a significant yield of epoxide was also obtained (5 %), which indicates that under these conditions the epoxide was not highly vulnerable to hydrolytic decomposition. This may be due to the low miscibility of the cyclooctene/cyclooctene oxide phase with the aqueous, which limits chemical interaction, preventing hydrolysis. The unsubstituted N-heterocyclic bases pyridine and pyrazole (entries 2 & 3, Table 2.25) gave slightly higher selectivities but with similar catalytic activities. The pyrazole system was apparently slightly more active, which is in common with observations made during the study in ionic liquids. Higher conversions were seen for the functionalised heterocycles that were studied, 3,5-dimethylpyrazole, **B** and **A** (entries 4-6, Table 2.25), though it should be noted that despite the long reaction time (18 h) conversion was still never seen to progress much further than 30 %. It would seem logical to attribute the higher activity of these systems to the higher solubility of the molybdenum coordination complexes formed in the organic substrate, facilitating

more efficient catalysis. For all three of these additives the selectivities were effectively complete, dimethylpyrazole and **B** producing the slightly higher conversions. As the three most active systems the study progressed to an examination of their efficacy in the epoxidation of other olefin substrates.

2.2.7.4 Solventless epoxidation of other olefin substrates

The same six substrates as were employed for the extended study of epoxidations in chlorophorm (Figure 2.16) were tested under the solventless conditions for the 3,5-dimethylpyrazole, **B** and **A** base additive systems. The results of the study are shown below in Table 2.26.

Table 2.26. Solventless epoxidation of various olefin substrates [a]

Entry	Base Additive	Olefin	Conversion (Yield)
1	3,5-Dimethylpyrazole 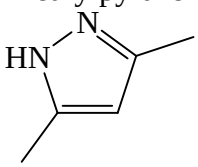	Cyclohexene	48 (26)
2		1-Octene	3 (1)
3		*trans*-2-Octene	5 (5)
4		*trans*-4-Octene	17 (10)
5		*cis*-2-Heptene	87 (1)
6		Styrene	15 (3)
7	**B** 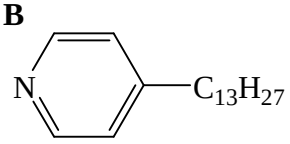	Cyclohexene	10 (3)
8		1-Octene	5 (1)
9		*trans*-2-Octene	44 (22)
10		*trans*-4-Octene	21 (18)
11		*cis*-2-Heptene	51 (12)
12		Styrene	62 (8)
13	**A** 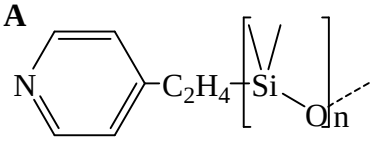	Cyclohexene	15 (15)
14		1-Octene	1 (1)
15		*trans*-2-Octene	4 (4)
16		*trans*-4-Octene	3 (3)
17		*cis*-2-Heptene	13 (6)
18		Styrene	23 (3)

[a] *Aqueous $[Mo(O)(O_2)_2(H_2O)_n]$ 0.025 mmol, base additive 0.10 mmol, 30 % $H_2O_{2\ (aq)}$ 3.0 mmol, olefin substrate 1.0 mmol, t = 18 h, T = 60 ºC. Conversions and yield calculated by GC.*

A quick overview of the results reveals that, in common with the study in chlorophorm, none of the systems tested had a particularly high activity towards any of the substrates. The yields from the epoxidation of cyclohexene obtained using dimethylpyrazole and **A** (entries 1 & 13 respectively, Table 2.26) were significant, if

slightly lower, than those obtained for cyclooctene (entries 4 & 6, Table 2.25). Similar to the results seen in chlorophorm, only a very low cyclohexene oxide yield was obtained for **B**. Only barely higher than trace yields were observed for the inactive 1-octene substrate in all of the systems (entries 2, 8 & 14, Table 2.26), which is unsurprising when the inactivity of any molybdenum based catalytic system previously tested here toward this substrate is considered. For the secondary *trans* olefin substrates the results varied. Dimethylpyrazole (entries 3 & 4, Table 2.26) gave low yields (5 and 10 % for 2 and 4-octene respectively) and for **A** (entries 15 & 16, Table 2.26) barely higher than trace epoxide yields were obtained. **B** (entries 9 & 10, Table 2.26) however produced relatively good yields of 22 and 18 % for the 2 and 4-octene respectively. In no case was a marked difference in activity towards the *trans* substrates and *cis*-2-heptene observed (entries 5, 11 & 17, Table 2.26) with low yields for dimethylpyrazole and **A** and relatively higher yield in the case of **B**. A very high conversion combined with a slightly unexpectedly low yield in the case of dimethylpyrazole (entry 5, Table 2.26) probably results from a poor extraction. The results regarding the relative activities of the systems towards secondary olefin substrates mirrored those previously observed in chlorophorm (see the relevant entries in Table 2.24), with **B** again showing the highest activities and **A** producing very low yields. Lastly, only very low yields of the epoxide were obtained in the epoxidation of styrene (entries 6, 12 & 18, Table 2.26), and in all cases conversion was significantly higher than the yield, indicating that the epoxide was vulnerable to hydrolysis. However, in chlorophorm no yield of epoxide was ever observed (entries 6, 12 & 18, Table 2.24) which infers that the hydrolysis was more inhibited in the solventless conditions. This would indicate that decreasing the polarity of the reaction medium is a good means of protecting styrene from hydrolysis, improving the selectivity of such reactions.

In summary, there was no marked improvement in the catalytic activities of these systems compared with those in chlorophorm (section 2.2.7.2), in both cases only rather dissapointingly low yields were obtained even after 18 h. The differences in activity toward secondary alkenes depending on the base additive were the same in solventless conditions as in chlorophorm solution, with **B** giving the most active system and **A** the least. Very small, but significant quantities of styrene oxide were produced, indicating that solventless conditions were slightly more favourable than chlorophorm solution for producing this product.

2.2.8 NMR spectra of substituted pyridyl oxobisperoxomolybdenum complexes

The oxobisperoxomolybdenum complexes of simple bases generally exhibit low solubilities which inhibits their analysis by NMR, as they cannot be dissolved. However, complexes of the functionalised bases used in the epoxidation study in apolar media generally possess good solubilities in many organic solvents thus facilitating their analysis in this manner. Some of the interesting results for the complexes of the functionalised monopyridine ligands are presented in this section. All of the NMR spectra collected for these complexes are available in the appendices.

2.2.8.1 Complex of 4-(polydimethylsiloxanylethyl)pyridine, (**2a**)

This compound was isolated as an oily yellow solid which possessed reasonable solubility even in very apolar media such as pentane. However, whilst palladium (**4a** & **5a**) and rhenium (**1a**) complexes of this ligand were easily and usefully characterised by NMR, in this case the data was poor and of extremely limited use. Aside from those corresponding to the polymer methyl groups, signals in the spectrum were so weak as to be almost invisible, and even when magnified showed very poor definition. The Mo content (5.18 % determined by ICP) correlates reasonably closely to a 1:2 molar ratio with the nitrogen content (1.36 % determined by elemental analysis), and the complex was thus predicted to be either that of **A** $[Mo(O)(O_2)_2(\mathbf{A})_2]$, or its oxide $[Mo(O)(O_2)_2(\mathbf{A}O)_2]$ with PDMS chain lengths or approximately 9 units per pyridine. The ^{1}H-NMR integrals are thus very inaccurate.

Figure 2.17. ^{1}H-NMR spectrum of **2a** with the faint pyridyl peaks expanded

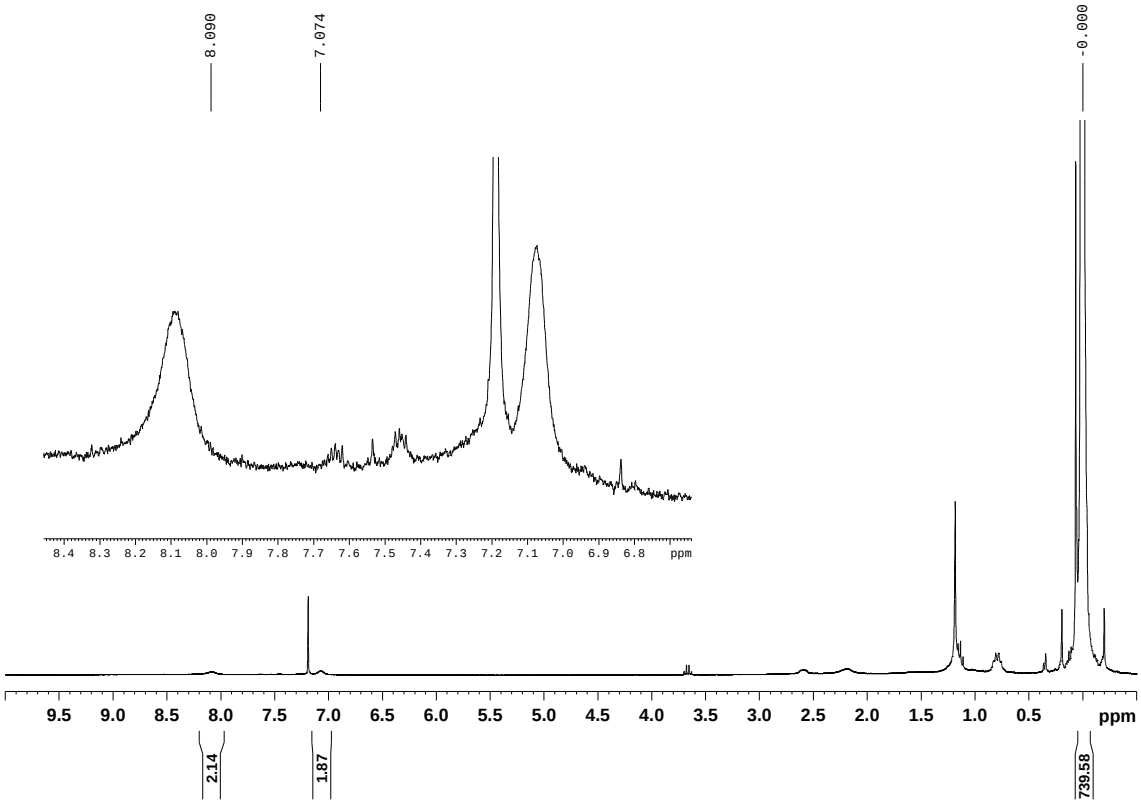

2.2.8.2 Complex of 4-tridecylpyridine, **2b**

Another oxobisperoxomolybdenum complex of a monodentate coordinating species, that formed from reaction with 4-tridecylpyridine was also prepared and characterised. In the NMR spectra of this compound, signals corresponding to the tridecyl alkyl function are clearly identifiable (see peaks in the range 0.5-3.0 ppm in Figure 2.18).

Figure 2.18. ^{1}H-NMR spectrum of **2b** with the pyridyl region expanded

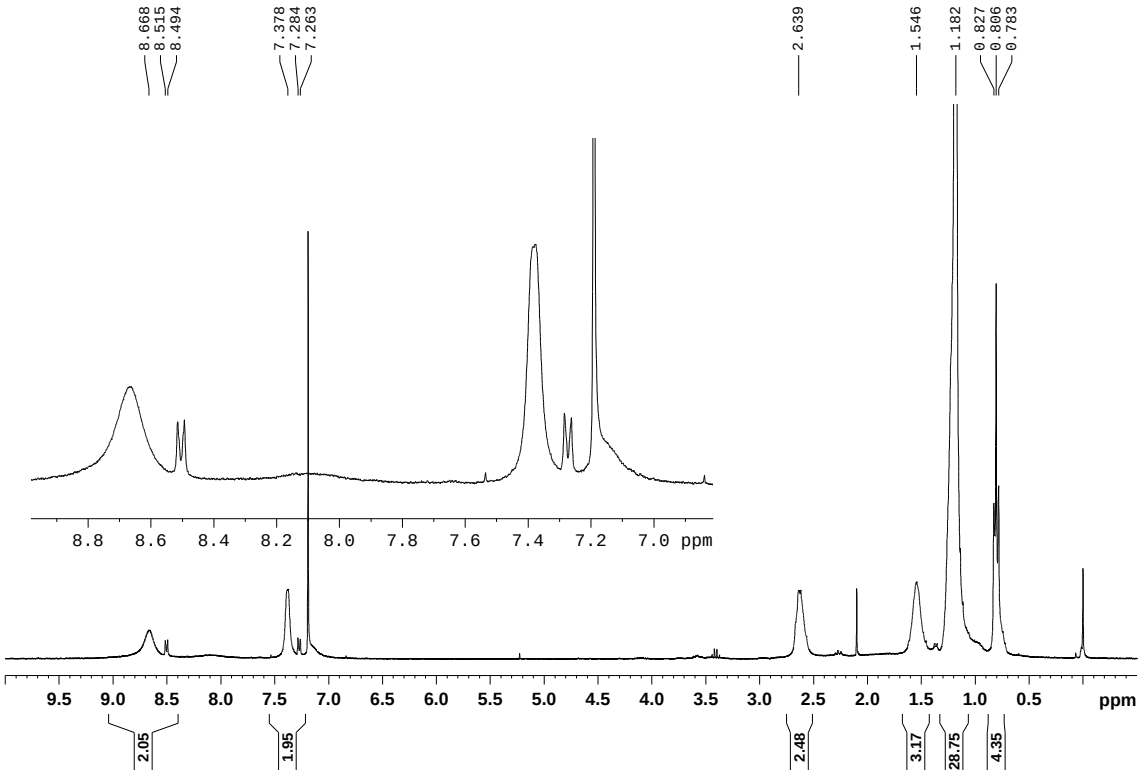

However, as was the case for **2a**, the pyridyl protons of the coordinated pyridine produced broad, poorly defined peaks. This is particularly highlighted by trace signals of uncoordinated **B** that was present in the sample, which in contrast are sharp and well defined. For this compound elemental analysis indicated that the compound formed was the aqua-N-oxide complex, [Mo(O)(O_2)$_2$(H_2O)(**B**O)].

2.2.9 NMR spectra of substituted bipyridyl oxobisperoxomolybdenum complexes

Oxobisperoxomolybdenum complexes of bidentate ligands, including 2,2'-bipyridine type ligands generally exhibit particularly poor solubilities in most media. The complexes formed with the functionalised bipyridine ligands **E**-**H** possessed very good solubilities in many apolar samples however, and their NMR spectra were thus easily recorded. Interestingly, unlike the spectra recorded for monopyridine ligands discussed in the previous section, oxobisperoxomolybdenum complexes of the functionalised bipyridines had excellent clarity in the pyridyl region. Whilst NMR spectra for oxobisperoxomolybdenum complexes with bidentate ligands have

previously been recorded[98] the ligands **E**-**G** are especially interesting in that they are symmetrical ligands and thus highlight electronic differences between the two rings resulting from coordination. Some of the interesting results for the complexes of the functionalised bipyridine ligands are presented in this section. All of the NMR spectra collected for these complexes are available in the appendices.

2.2.9.1 Complex of 4-(2,2-bis-tridecyl)-pyridine, **2e**

In complex **2e** distinct signals of equal area were clearly observed for each of the pyridyl protons. It is interesting to note that this difference extended even to the 4-alkyl substituents. Figure 2.19 shows the ^{1}H-NMR spectrum of **2e**, highlighting the paired signals in the alkyl region. The triplet of the CH_2 adjacent to the ring and the quintuplet for the neighbouring CH_2 clearly appear twice. At the resolution employed this difference was not discernible in the terminal triplet however. The environments of the two bipyridyl fragments are thus clearly shown to be distinct. There are several possible reasons why this might be the case, for example a polymetallic species with several **G** coordinated in two distinct manners or coordination of one pyridine ring but not the other, might both produce a pair of signals as observed. However, taking into account the other analytical data for **2e** (IR, elemental analysis) it would seem most likely that the distinction results from the difference between coordination at the axial and equatorial positions on an oxobisperoxomolybdenum complex

Figure 2.19. ^{1}H-NMR spectrum of **2e** with the alkyl region expanded

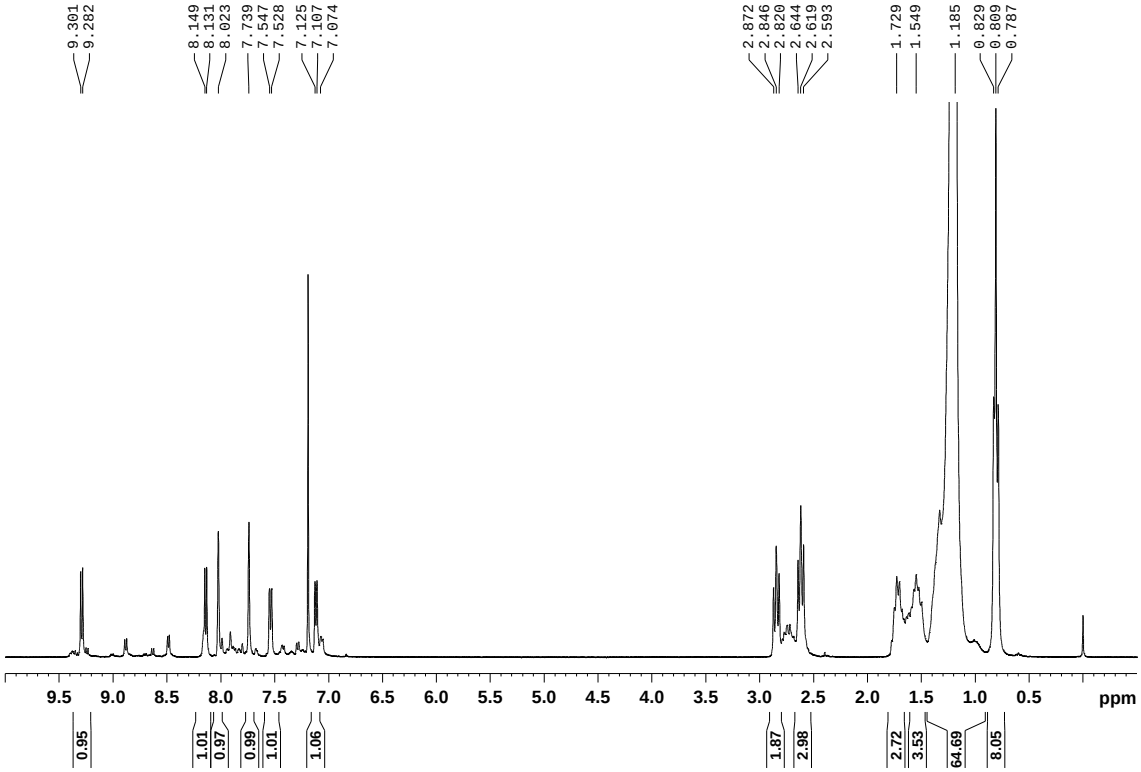

2.2.9.2 Complex of 4-(2,2-bis-trimethylsilanyl-ethyl)pyridine, **2g**

Similarly, in the spectrum of compound **2g**, two distinct signals of equal area were clearly observed for each of the pyridyl protons. To confirm that both signals are distinct to those of uncoordinated **G**, Figure 2.20 compares the ^{1}H-NMR spectra of **G** and **2g** demonstrating that both peak signals are clearly in distinct positions to those of uncoordinated **G**.

Figure 2.20. Comparison of the ^{1}H-NMR spectra of (a) **G** and; (b) **2g**

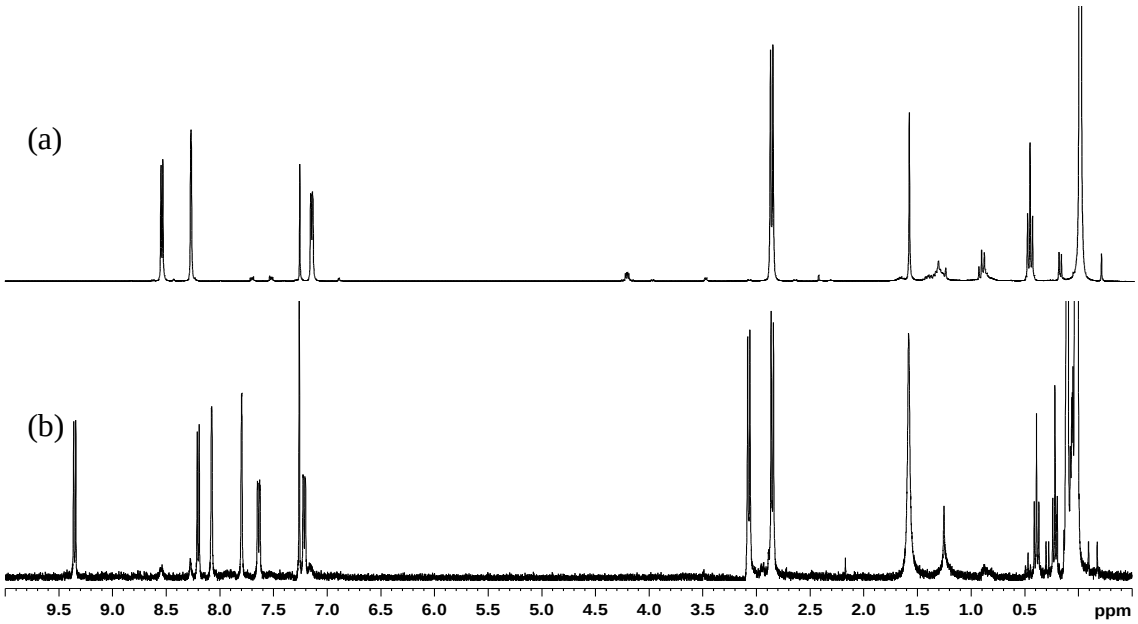

2.2.9.3 Complex of 4-methyl-4'-tridecylpyridine, **2h**

Lastly, it was interesting to observe the spectrum of the complex **2h**. In the bipyridyl complexes that were previously described the bipyridine ligands were symmetrical. **H** however is not, with a methyl at the 4 position on one ring and a tridecyl substituent on the other. This being the case, there are two possible isomers resulting from its complexation with oxobisperoxomolybdenum, depending on which ring coordinates to the axial and to the equatorial positions. From the NMR spectra it should be possible to determine whether one or both of the isomers is present and also determine the ratio between them from the integrals.

Figure 2.21. The ^{1}H-NMR spectrum of **2h**

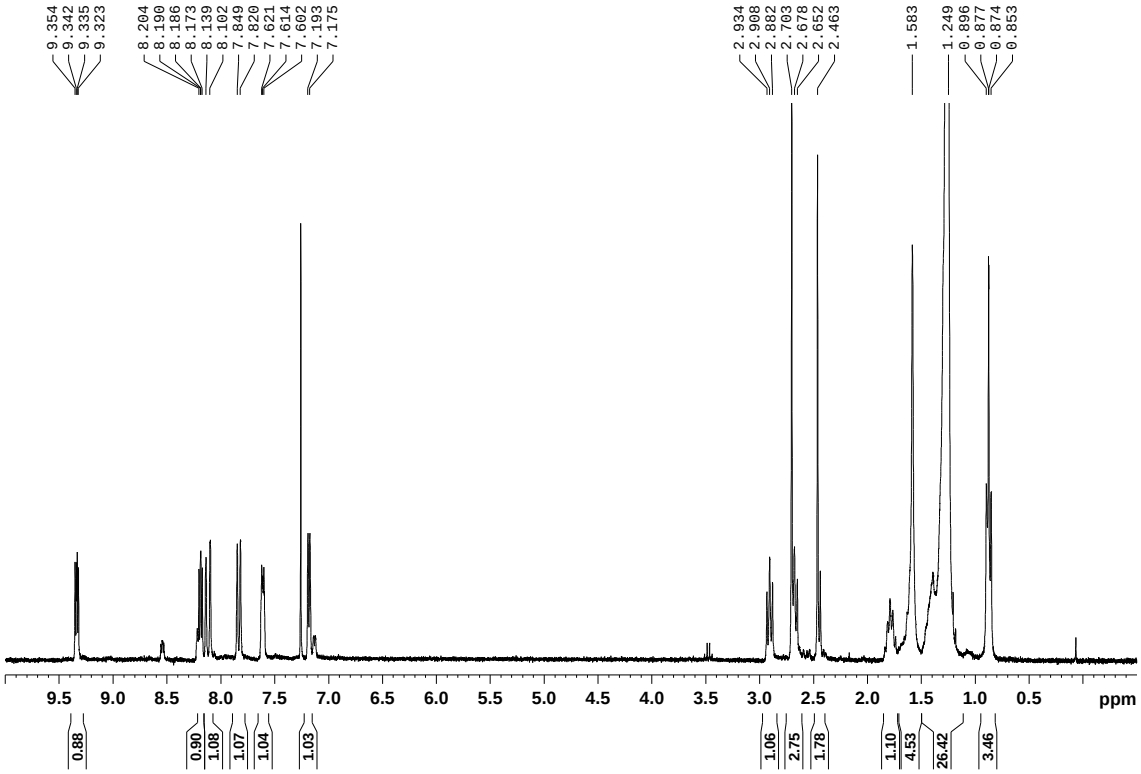

From Figure 2.21 it is easily determined that both of the possible coordinative isomers are present certainly in an approximately equal ratio, indicating that neither is particularly more favoured than the other. Thiel et al in their extensive studies of the oxobisperoxomolybdenum complexes of pyrazolylpyridine ligands determined that their ligands also coordinated so as to form the two possible isomers and that isomeric purification would not be possible since the complex was able to interchange between the two.[99] This conversion was determined to take place via decoordination of one of the coordinated nitrogen atoms, as opposed to a Berry type rotation. It might be predicted that **2h** would behave in the same way.

2.3 Cu(II)/TEMPO catalysed alcohol oxidation in supercritical carbon dioxide using soluble and insoluble copper acetate catalysts

The wide range of catalytic metal species active in the selective oxidation of alcohols to aldehydes was already discussed in the introduction (Section 1.4). From a sustainability perspective those systems which are capable of facilitating this transformation using dioxygen as the oxidant are clearly advantageous. Amongst the metal catalysts capable of catalysing this process copper catalysts represent a favourable option due to the high abundance and the relatively easy isolation of this element compared to many of the other active metals. A detailed review of the important examples and mechanistic understanding of this catalytic process has already been covered in the introduction (see Section 1.4.2). As discussed therein, alcohol oxidation by simple copper(II) compounds is usually achieved with a co-catalytic system employing the N-heterocyclic-oxyl radical 2,2,6,6-tetramethylpiperidine-1-oxyl (TEMPO), or related compounds, as the co-catalyst. In these systems it is believed that copper first complexes with the alcohol and a TEMPO then abstracts an α hydrogen from the coordinated alcohol.[136] The copper is then reduced by dissociation of the aldehyde product but subsequently re-oxidised by TEMPO, allowing the catalytic cycle to begin again. The reduced species TEMPOH reacts directly with oxygen regenerating TEMPO and producing only water as a side product. With regard to examples of Cu(II)/TEMPO catalysed alcohol oxidation in alternative media, recent publications have described this process being carried out successfully in fluorous biphasic systems[138,139,201] and ionic liquids.[122-125] As a reaction employing a gaseous reagent, $scCO_2$ would present obvious advantages as a media for this oxidation reaction, due to the perfect mixing of SCFs with gases.[25,202] In addition, general advantages of reactions in $scCO_2$ such as easy product separation and the potential for development of continuous flow processes would seem to make the development of a Cu(II)/TEMPO catalysed alcohol oxidation system in this media a potentially interesting objective. It is perhaps surprising then that such a system has not yet been described in literature.[203]

The study presented in this section details the development of a PDMS functionalised, $scCO_2$ soluble copper acetate type complex and the preparation of silica

supported copper acetate pyridine and the investigation of both of these as co-catalysts in conjunction with TEMPO in the oxidation of alcohols in $scCO_2$.

2.3.1 Preparation of $[Cu_2(AcO)_4(A)_2]$ (3a)

As was previously mentioned, the synthesis of PDMS functionalised transition metal complexes via the hydrosilylation of vinyl functions on coordinated ligands has precedent.[163] Following such a strategy, the hydrosilylation of the vinyl groups of the $[Cu(AcO)_2(4VP)]_2$, complex[204] with hydride terminated PDMS, $H[Si(CH_3)_2O]_n$, and Kardstedt's catalyst was attempted. However, no trace of the desired product was produced in this manner, probably due to deactivation of the platinum catalyst. The PDMS functionalised coordination complex was ultimately synthesised via reaction of $[Cu(AcO)_2(H_2O)]_2$ with 4-(polydimethylsiloxanyl-ethyl)pyridine (**A**), the synthesis and characterisation of which was discussed previously in the section on MTO catalysed epoxidations (see Section 2.1.1).

Scheme 2.13. The synthesis of compound **3a**.

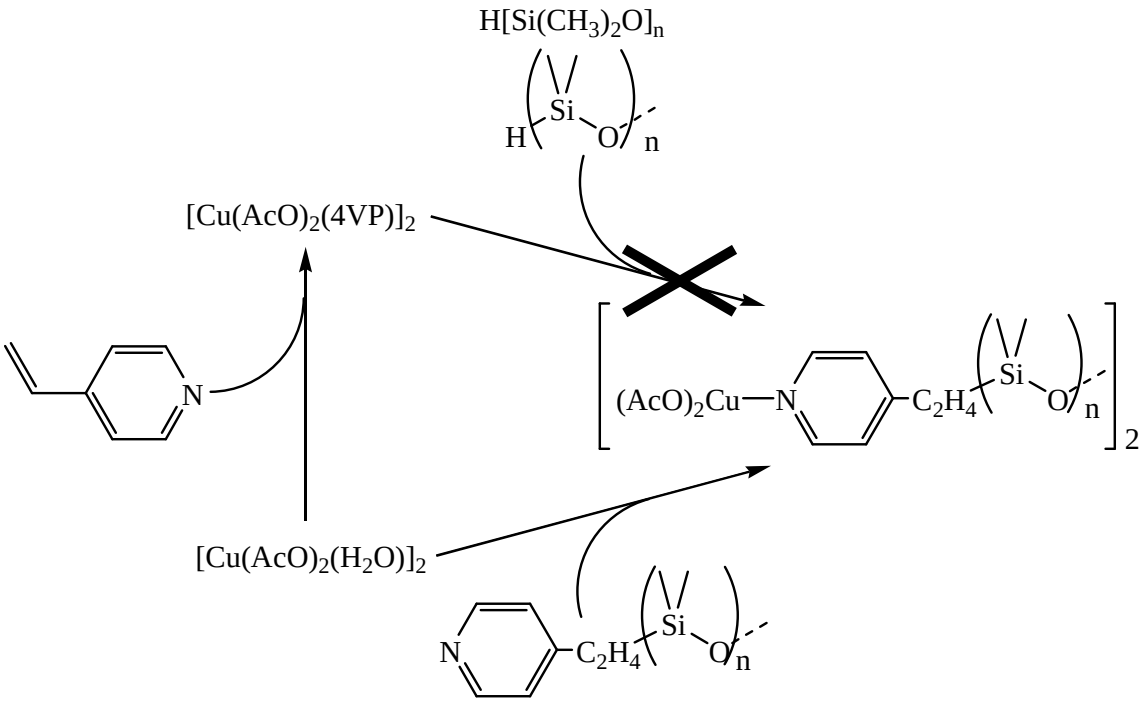

The copper acetate coordination compound of **A, 3a**, was a green oil (Figure 2.22; (a)), which was air-stable and soluble in low polar solvents, such as hexane. The functionalised pyridine was clearly coordinated to the copper centre; whilst **3a** was wholly soluble in hexane, when the dissolution of a dispersion of $[Cu(AcO)_2(py)]_2$ in PDMS (prepared by evaporating a dichloromethane solution of the two components to dryness) was attempted, only the polymer dissolved, leaving behind the undissolved $[Cu(AcO)_2(py)]_2$.

The IR spectrum of **3a** (Figure 2.22; (b)) clearly exhibits signals corresponding to the PDMS along with the pyridine and acetate fragments. From the positions of the IR peaks (υ_{asym}{COO} 1630 cm^{-1}, υ_{asym}{COO} 1430 cm^{-1}) [205] corresponding to the coordinated acetates and indeed the colour of the compound (blue-green as opposed to the violet colour that would probably be anticipated for a monometallic configuration),[206] the "chinese lantern" type dimetallic centre with four bridging μ_2-acetate ligands typical of many copper carboxylate complexes, including the synthetic precursor hydrate complex, would seem the probable configuration at the metal centres.

Figure 2.22. (a) Compound **3a**; (b) IR spectrum of **3a**.

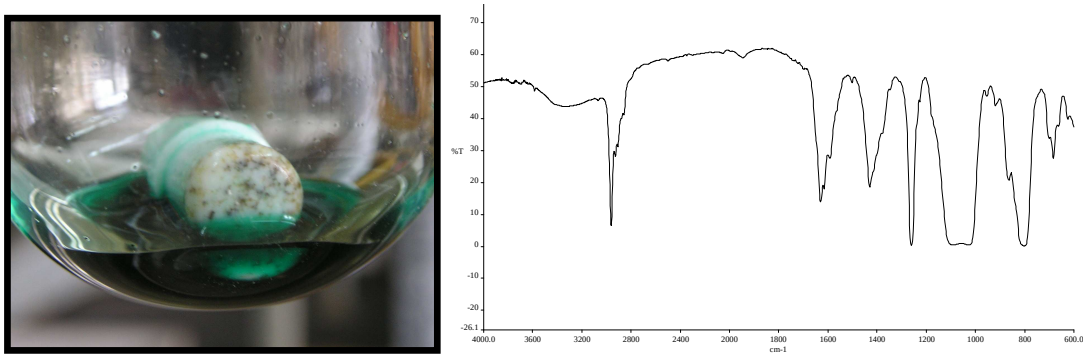

(a) (b)

Such a configuration would leave one free site per copper atom for coordination of the pyridine function of **A** and a 1:1 molar ratio of terminal pyridine:copper would thus be expected. A sample of **3a** determined to contain 5.31 wt. % Cu by ICP was found by elemental analysis to have a nitrogen content of 1.21 wt. %, which corresponds approximately to the anticipated 1:1 nitrogen:copper molar ratio. From the previously discussed analytical data compound **3a** was thus determined to be the μ^2-tetrakisacetato-bis(4-{polydimethylsiloxanyl-ethyl}pyridyl)dicopper complex shown

in Figure 2.23. The copper content in samples of **3a** prepared for catalytic studies was accurately and more conveniently determined using UV-Vis absorbance spectroscopy (see Experimental, Section 3.7.2.1), the accuracy of these measurements was confirmed by their collusion with results obtained by iodometric titration and ICP.

Figure 2.23. Compound **3a**, $[Cu_2(\mu^2\text{-}AcO)_4(\mathbf{A})_2]$

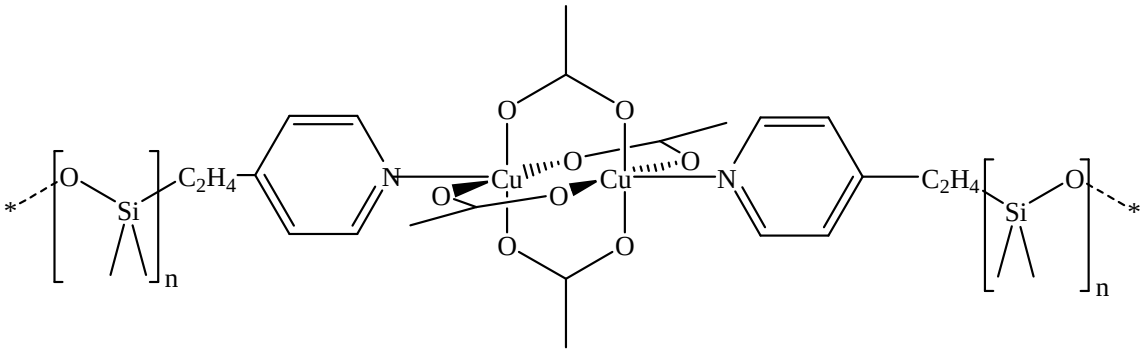

Interestingly, the sample of **A** from which this sample of **3a** was prepared had a calculated M_N of ~500, which corresponds to n = 5.3 (n being the number of siloxane units per terminal pyridine, $(Si(CH_3)_2\text{-}O)_n$). This sample of **3a** apparently had a significantly greater value, n = 11.7, indicating that the average polymer length was now considerably higher. It is likely that this results from the elimination of fractions of **3a** with lower n values during the product workup. Complexes with insufficiently long chain lengths are likely to be insoluble in very apolar solvents such as hexane and they thus precipitate and are eliminated. Similar observations were made in the synthesis of MTO (**1a**) and Pd (**4a** and **5a**) complexes of **A** (see Sections 2.1.2 and 2.4.1), where the values of n were also found to be markedly higher in the prepared coordination compounds. In addition, NMR analysis of these compounds demonstrated that the α-addition ($C_2H_4 = CHCH_3$) product was also eliminated during the workup, leading to complexes of the pure β-addition isomer ($C_2H_4 = CH_2CH_2$). This isomeric purification may also occur in the synthesis of **3a** but this would be difficult to confirm since the product is paramagnetic, prohibiting the use of NMR to investigate the possibility.

The solubility of the **3a** in $scCO_2$ was determined by UV-Visible analysis of solutions inside a high-pressure cell equipped with 2 sapphire windows. Concentrations were calculated using the Beer-Lambert law and a calibration plot of standard solutions in hexane. Hexane was used for the calibration as it is a very low polarity solvent,

similar to $scCO_2$, and thus exhibits a similar extinction coefficient and a negligible solvochromatic shift.[207] **3a** was observed to dissolve in $scCO_2$ giving a green solution (Figure 2.24), and a concentration of 1.7 mmol/dm^3 of Cu(II) was recorded at 40 ºC and 105 bar of pressure. On the contrary analogous Cu complexes with no PDMS functions, $[Cu(AcO)_2(py)]_2$ and $[Cu(AcO)_2(4VP)]_2$ had no detectable solubility.

Figure 2.24. (a) Solution of **3a** in $scCO_2$; (b) UV-Visible spectra of **3a** in different solvents.

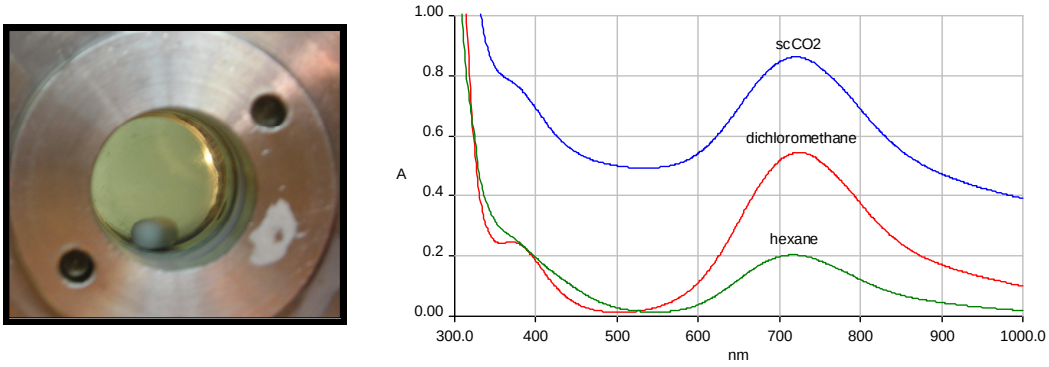

(a) (b)

The solubility of any potential catalyst precursor is an important criteria in assessing its suitability for homogeneous catalysis in $scCO_2$. However, literature concerning the solubility data of metal complexes in $scCO_2$ is sparse,[208] although some compilations have now appeared.[209] Amongst copper complexes, the solubilities of compounds incorporating β-diketonate,[207,210] dithiocarbamate[211] and hydrogenoarsenate ligands[212] have been determined. For all of these species the solubilities determined were lower than that measured for **3a**. Incorporation of fluorous groups into ligands is generally found to enhance the solubility of their coordination complexes in comparison with the non-fluorous analogues. Accordingly, fluorinated diiminates,[213] β-diketonates,[209a,210b,214] and dithiocarbamates[215] have been employed to solubilise copper complexes. As examples $[Cu(hfa)_2]$ (hfa = hexafluoropentane-2,4-dionate)[209a,210b] and $[Cu(fddc)_2]$ (fddc = bis(trifluoroethyl)dithiocarbamate)[209c,215] display solubilities of 1.3 mmol/dm^3 at 40 ºC and 110 bar, and 0.9 mmol/dm^3 at 50 ºC and 100 bar, respectively. The solubility of **3a** is thus found to be of a similar order of magnitude to such fluorinated complexes, demonstrating as such that PDMS functionalisation, a more economic and arguably

"greener" option than perfluorous functionalisation, can induce $scCO_2$ solubilisation to a comparable magnitude.

2.3.2 Copper/TEMPO catalysed alcohol oxidation reactions in $scCO_2$

It is possible to view compound **3a** either as a copper complex possessing a short chain PDMS function or as a copper complex supported on a liquid PDMS polymer, similar to how one might view heterogeneous catalysts where the catalytic complex is bound to the surface of a solid support. In contrast to solid supported catalysts however, **3a** is intended for use in homogeneous rather than heterogeneous catalytic systems. In catalytic experiments one might therefore view the complex as being supported in solution. The observed concentration of **3a** in $scCO_2$ fell into the concentration range (1 mM or higher) generally adopted for homogeneous catalytic processes, which made study of its catalytic activity in oxidation reactions feasible. Consequently, a study of the activity of **3a** in the Cu(II)/TEMPO co-catalysed oxidation of 4-nitrobenzyl alcohol with dioxygen was conducted (Scheme 2.14). This electron rich primary alcohol substrate is very active to oxidation, and its oxidation was therefore a good model to study before proceeding to less activated substrates.

Scheme 2.14. Copper-TEMPO catalysed oxidation of 4-nitrobenzylalcohol

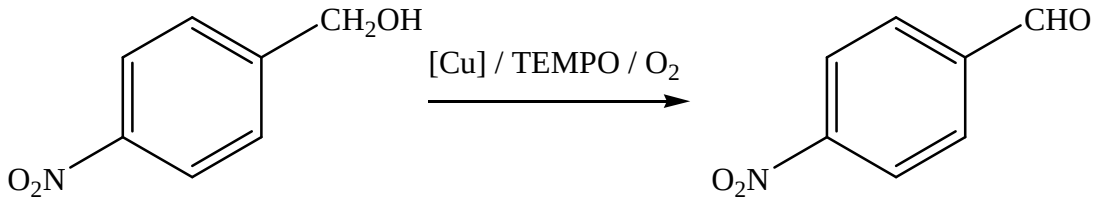

Above the "green" benefits associated with the reaction solvent, studying the activity of this system in $scCO_2$ was particularly interesting for two main chemical reasons:

- The very low polarity of the $scCO_2$ reaction solvent is often inhibitive to homogeneous catalysis due to the non solubility of the catalyst, however the adequate solubility of **3a** had been proven. This study might therefore demonstrate the efficacy of PDMS functionalisation in solubilising catalysts for use in homogeneous catalysis

- When using gaseous reagents the slow rate of their transfer into the reaction phase can be rate limiting, however gaseous O_2 is perfectly miscible with $scCO_2$ and the enhanced mixing could well lead to high reaction rates and selectivities.

The results obtained in the catalytic study are shown below in Table 2.27.

Table 2.27. Oxidation of 4-nitrobenzyl alcohol to aldehyde by dioxygen catalysed by [Cu]/TEMPO.[a]

Entry	Catalyst	Solvent	Time (h)	[Cu] (% equiv.)	TEMPO (% equiv.)	Yield (%)
1	None	$scCO_2$	4	3.5	7.0	2
2	$[Cu(AcO)_2(H_2O)]_2$	$scCO_2$	4	3.5	7.0	34
3	$[Cu(AcO)_2(py)]_2$	$scCO_2$	4	3.5	7.0	95
4	$[Cu(AcO)_2(4VP)]_2$	$scCO_2$	4	3.5	7.0	93
5	**3a**	$scCO_2$	4	3.5	7.0	100
6	$[Cu(AcO)_2(py)]_2$	$scCO_2$	2	3.5	7.0	80
7	$[Cu(AcO)_2(4VP)]_2$	$scCO_2$	2	3.5	7.0	93
8	**3a**	$scCO_2$	2	3.5	7.0	83
9	$[Cu(AcO)_2(py)]_2$	$scCO_2$	4	3.5	1.0	8
10	$[Cu(AcO)_2(py)]_2$	$scCO_2$	4	1.0	7.0	31
11	$[Cu(AcO)_2(py)]_2$	$scCO_2$	4	1.0	2.0	29
12	$[Cu(AcO)_2(py)]_2$	$scCO_2$	4	1.0	1.0	7
13	**3a**	$scCO_2$	4	1.0	2.0	27
14	$[Cu(AcO)_2(py)]_2$	Toluene	2	3.5	7.0	96
15	$[Cu(AcO)_2(py)]_2$	Hexane	2	3.5	7.0	67
16	**3a**	Toluene	2	3.5	7.0	86
17	**3a**	Hexane	2	3.5	7.0	33

[a] *4-Nitrobenzyl alcohol (1.0 mmol), 150 bar CO_2 (excluding entries 14-17), 60 ºC, 1 bar O_2.*

For the **3a**/TEMPO catalysed oxidation in $scCO_2$ co-catalyst loadings of [Cu] at 3.5 % equiv. and TEMPO at 7.0 % equiv. were found to represent the optimum ratio, facilitating conversion at a convenient rate for the purposes of the study with the reaction conditions fixed at 150 bar of CO_2, 60 ºC and 1 bar of O_2. After four hours, NMR analysis of the crude mixture indicated complete conversion of the alcohol to the corresponding aldehyde (entry 5, Table 2.27). A control where TEMPO alone was present produced practically no detectable conversion (entry 1, Table 2.27), demonstrating that the presence of the copper catalyst was essential for oxidation to take place. Notably then, these experiments had established, for the first time, a Cu(II) catalysed alcohol oxidation in $scCO_2$. In continuation of the study, comparisons with systems in which structurally analogous copper complexes lacking the solubilising PDMS substituent were made and the reaction was also attempeted in conventional solvents rather than $scCO_2$. The catalytic reaction in $scCO_2$ was therefore repeated, this

time using a selection of copper acetate compounds in place of **3a**, to allow direct comparison of the copper species as catalysts. The results clearly established that coordinated pyridine species increase the catalytic activity (compare entry 2 with 3-5, Table 2.27). More importantly however, and rather surprisingly, almost complete conversion to the aldehyde was observed for the simpler pyridyl analogues $[Cu(AcO)_2(py)]_2$ and $[Cu(AcO)_2(4VP)]_2$ (entries 3 and 4, respectively, Table 2.27), in spite of the non solubility of these copper compounds in $scCO_2$. Presumably in these cases, the oxidation reaction would have had to proceed via a heterogeneous mechanism. With the conversion observed for **3a** (entry 5, Table 2.27) only slightly exceeding that of the pyridyl analogues (entries 3 and 4), over the four hour reaction time solubilisation by the PDMS substituent present in **3a** did not lead to any remarkable increase in conversion. The reaction time was subsequently reduced to 2 hours in order to obtain incomplete conversions and better compare the relative rates of the reactions to see if catalysis with **3a** was via a faster mechanism than its analogues.

Acknowledging that the 4-vinylpyridine analogue (entry 7, Table 2.27) produced a slightly higher conversion than the other two species (though this can be considered to be within reasonable experimental variation), all conversions were found to be of the same order of magnitude. Comparison of entries 6-8 therefore strongly indicates that the reactions all proceeded by the same mechanism. Since this mechanism would almost certainly have to be heterogeneous in the case of entries 6 and 7, it is therefore inferred that, despite the demonstrable solubility of **3a** in $scCO_2$, dissolution of the catalyst was not necessary for effective catalysis. This is in contrast to precedent copper catalysed processes in $scCO_2$, for instance, in the Cu-promoted oxidative homocoupling of alkynes the presence of methanol as co-solvent was necessary to dissolve the inorganic salts.[216]

Certainly, for the reactions catalysed by the apparently insoluble analogues, heterogeneous catalysis seemed the most likely mechanism. However a feasible alternative is a homogeneous mechanism catalysed by an immeasurably low but significant concentration of [Cu] in the $scCO_2$. Possibly due to a higher activity they might then be able to give a conversion rate comparable to the far more soluble but less active catalyst **3a**. This hypothesis was easily tested by conducting a further series of experiments where the [Cu]:TEMPO ratios were varied. The results seem to disprove this possibility. Since $[Cu(AcO)_2(py)]_2$ has an immeasurably low solubility in $scCO_2$ there should be no difference in the concentration of dissolved [Cu] in reactions

employing 3.5 equivalents or 1.0 equivalent of copper, since a saturated solution would be achieved in both cases. Consequently no difference in the rate of catalysis would be anticipated. Clearly though, comparison of entries 3 and 10 (Table 2.27), shows that the rate of reaction is proportional to the amount of copper complex used. Since the vast majority of the catalyst in each case must be insoluble the reaction rate is therefore proportional to the amount of undissolved copper, very clearly inferring a heterogeneous mechanism. Entries 5 and 13 indicate that the quantitative dependency was exactly the same for **3a** as for its pyridine analogue. Varying the proportions of [Cu]:TEMPO also showed that optimum results are obtained at a ratio of 1:2, i.e. at this ratio, if the relative quantity of either of the co-catalysts is reduced the reaction rate will fall, apparently proportionally. Conversely, if either is raised without simultaneously raising the other, no improvement in the reaction rate will be observed. This is shown by the lack of any significant change in conversion between a 1:7 and 1:2 ratio (entries 10 and 11 respectively, Table 2.27), but a large drop in the reaction rate at 1:1 (entry 12, Table 2.27). Similarly, the identically low rates observed in entries 9 and 12 (Table 2.27), despite the much higher [Cu] concentration in the former, indicate that the low TEMPO concentration was limiting.

Thus, the solubility of **3a** in $scCO_2$ did not result in any catalytic advantage over insoluble analogues in this reaction. However, it remained conceivable that in conventional non polar solvents, such as hexane, in which the pyridine analogues are insoluble and **3a** is soluble, that **3a** might be observed to be more active. Using fixed parameters, the catalytic activities of compounds **3a** and $[Cu(AcO)_2(py)]_2$ in two different organic solvents, toluene and hexane were compared. However, the results again showed that no catalytic advantage resulted from the higher solubility of **3a**. In hexane (entries 15 and 17, Table 2.27) it was clearly observed that $[Cu(AcO)_2(py)]_2$ remained undissolved whilst **3a** gave a green solution, but the rate of reaction was actually much lower for the latter catalyst. In conclusion; insolubility of the copper catalyst does not appear to limit catalytic activity of [Cu]/TEMPO co-catalysed alcohol oxidations in apolar reaction media.

2.3.3 Silica supported Copper/TEMPO catalysed alcohol oxidation reactions

The work completed with the soluble and insoluble $[Cu(AcO)_2(L)]_2$ complexes demonstrated that this reaction seems to proceed as well if not better for the insoluble catalysts. The focus of this investigation therefore shifted onto how best to carry out a heterogeneous catalysis using [Cu]/TEMPO and to try to develop an effective system in $scCO_2$. A major advantage of heterogeneous catalysis is the facile separation of the catalyst from product solutions, which can allow the catalyst to be recycled, potentially making much higher TONs possible. In this case however the microcrystalline solid $[Cu(AcO)_2(py)]_2$ would in practice be very difficult to separate from the products. In their work with PDMS functionalised phosphine ligands, Rayner et al.[159] were able to immobilise catalytic metal complexes on silica and then successfully use the supported catalysts in reactions in $scCO_2$. A silica supported catalyst is potentially much more easily separated from reaction products and would even potentially have applications in continuous flow catalysis. Due to the distribution of the [Cu] across the support surface the efficiency of the catalyst per molar quantity should be greatly improved over the pure microcrystalline compound, since in the former a far greater proportion of the [Cu] should be exposed to the reaction medium. The possibility of using silica supported copper acetate was therefore subsequently investigated. It was found that from solution in dichloromethane both **3a** and $[Cu(AcO)_2(py)]_2$ readily adsorbed onto silica gel which was then filtered and dried ready for use in catalytic applications. A series of experiments to test the catalytic activities of the supported catalysts were subsequently run, the results of which are shown below in Table 2.28.

Table 2.28. Oxidation of alcohol substrates using Cu-Silica/TEMPO.[a]

Entry	Catalyst	Solvent	Substrate	Yield (%)
1	None	Acetonitrile [b]	4-Nitrobenzyl alcohol	<1 [d]
2	Silica	Acetonitrile [b]	4-Nitrobenzyl alcohol	<1 [d]
3	**3a**-Silica	Acetonitrile [b]	4-Nitrobenzyl alcohol	21 [d]
4	$[Cu(AcO)_2(py)]$-Silica	Acetonitrile [b]	4-Nitrobenzyl alcohol	26 [d]
5	$[Cu(AcO)_2(py)]$-Silica	Acetonitrile [b]	Benzyl alcohol	2 [e]
6	$[Cu(AcO)_2(py)]$-Silica	Toluene [b]	4-Nitrobenzyl alcohol	100 [d]
7	$[Cu(AcO)_2(py)]$-Silica	Toluene [b]	Benzyl alcohol	100 [e]
8	$[Cu(AcO)_2(py)]$-Silica	$scCO_2$ [c]	4-Nitrobenzyl alcohol	100 [d]
9	$[Cu(AcO)_2(py)]$-Silica	$scCO_2$ [c]	Benzyl alcohol	100 [e]
10	Silica	$scCO_2$ [c]	4-Nitrobenzyl alcohol	6 [d]
11	$[Cu(AcO)_2(py)]$	$scCO_2$ [c]	Benzyl alcohol	46 [e]
12	$[Cu(AcO)_2(py)]$-Silica [f]	$scCO_2$ [c]	4-Nitrobenzyl alcohol	17 [d]
13	$[Cu(AcO)_2(py)]$-Silica	$scCO_2$ [c]	2-Octanol	8 [d]

14 [g]	$[Cu(AcO)_2(py)]$-Silica	$scCO_2$ [c]	2-Octanol	12 [d]
15	$[Cu(AcO)_2(py)]$-Silica	$scCO_2$ [c]	Cyclohexanol	3 [d]
16	$[Cu(AcO)_2(py)]$-Silica	$scCO_2$ [c]	2-(Phenylthio)etanol	0 [d]
17	$[Cu(AcO)_2(py)]$-Silica	$scCO_2$ [c]	3-Phenylpropan-1-ol	0 [d]

[a] 2.0 mmol substrate, 0.5 g silica catalyst (0.015 mmol Cu for copper containing materials), 0.06 mmol TEMPO, T = 80ºC, 1.5 bar O_2, $t_{reaction}$ = 12 h. [b] 10 mL Solvent [c] 150 bar CO_2 [d] Yields determined from weight/^{1}H-NMR of products [e] Yields determined by GC [f] 0.003 mmol silica catalyst, 0.012 mmol TEMPO, 6 mmol alcohol substrate [g] t = 60 h

Working with loadings of 0.03 mmol [Cu] per gram of silica the investigation initially focussed on alcohol oxidations in a relatively polar organic solvent, acetonitrile. This solvent represents a more practical media for many alcohol oxidations than the more non polar solvents examined in the prior studies (i.e. hexane) due to the highly polar nature of many potential alcohol substrates which it thus dissolves more readily. The experiments with silica supported Cu employed lower catalyst loadings than in the study of unsupported catalysts (Table 2.27) with 0.75 % [Cu] and 3.0 % TEMPO (a 1:4 ratio) and 1.5 bar O_2 and 12 h at 80 ºC. In acetonitrile both the supported **3a** and $[Cu(AcO)_2(py)]_2$ were able to convert around 25 % 4-nitrobenzyl alcohol to aldehyde (entries 3 & 4, Table 2.28), indicating that they had similar activities. Since there was apparently no advantage to employing **3a**–silica, which is more complex, expensive and time consuming to synthesise, the simpler $[Cu(AcO)_2(py)]_2$–silica catalyst was preferred in the proceeding studies. Control experiments in the absence of catalyst or plain silica showed that the presence of copper was essential in facilitating the oxidation (entries 1 & 2, Table 2.28). These were positive results, but the conversion was not high and attempts to oxidise the slightly less active benzyl alcohol were unsuccessful (entry 5, Table 2.28), showing that the system was of limited real use. However, when these oxidations, using supported $[Cu(AcO)_2(py)]_2$, were repeated in the less polar solvent toluene (entries 6 & 7, Table 2.28) and in $scCO_2$ (entries 8 & 9, Table 2.28), complete conversions to the aldehyde was observed with no trace of the alcohol detectable by NMR after the 12 h. In $scCO_2$, efficient reaction was again found to depend on the presence of a Cu catalyst, however a low but significant conversion (6 %) was obtained using only silica and TEMPO (entry 10, Table 2.28). This indicates that a slow but significant oxidation mechanism involving only TEMPO was active in $scCO_2$, though not in acetonitrile. This might be evidence that the properties of the $scCO_2$ solvent, such as its perfect miscibility with dioxygen lead to a more efficient oxidative system with the gaseous dioxygen reactant. When unsupported $[Cu(AcO)_2(py)]_2$ was used, incomplete conversion (46 %) was observed (entry 11, Table 2.28). This shows that

supporting the [Cu] on silica improves the efficiency of the catalysis. Probably this is due to the lower quantity of [Cu] exposed to the reaction medium when using the microcrystalline reagent compared to when it is spread over the surface of the silica.

To investigate what sort of TONs might be achievable using this catalytic system, a 60 h experiment was run using only 0.003 mmol of [Cu] catalyst and 6 mmol of the 4-nitrobenzyl alcohol substrate (entry 12, Table 2.28). A 17 % conversion was achieved, corresponding to a TON of 340. However the TOF (5.7 h^{-1}) in this experiment was lower than in the previous experiment under standard conditions (11.1 h^{-1} in entry 8, Table 2.28). This may well indicate that the catalyst lost its potency during the course of the longer reaction due to decomposition, although it should be noted that both experiments were carried out in the same volume (27 mL) of $scCO_2$ but that larger quantity of alcohol substrate (3 x) was used in the longer experiment, and it is very feasible that poorer dissolution of the substrate inhibited the reaction rate.

Lastly, the efficiency of the system in the oxidation of a variety of alcohol substrates was tested, the secondary alkyl alcohol 2-octanol, the cyclic cyclohexanol, the thioether 2-(phenylthio)ethanol and the terminal phenyl functionalised 3-phenylpropan-1-ol (entries 13 & 15-17, Table 2.28). However, none of these substrates converted well. Low conversions were observed for 2-octanol and cyclohexanol (8 and 3 % respectively) whilst the system was completely inactive for the conversion of 2-(phenylthio)ethanol and 3-phenylpropan-1-ol. To see if better conversion might be obtainable by employing longer reaction times the oxidation of 2-octanol was attempted over 60 h. However the yield increased only slightly, from 8 to 12 %. Disappointingly then, the general applicability of this system to a more varied range of alcohol substrates appears to be poor.

2.3.3.1 Recycling the $[Cu(AcO)_4(py)_2]$–silica catalyst

The final part of the oxidation studies with the $[Cu(AcO)_2(py)]_2$–silica catalyst investigated the potential to recycle the catalyst after reaction. Re-use of the catalyst in further cycles in the oxidation of benzyl alcohol was therefore attempted. To do this, after the reaction was completed the reaction products were extracted from the reactor with ether and filtered to capture the solid catalyst. This was then washed with ether, dried and charged to the reactor again for re-use. It was found that TEMPO did not

adsorb well onto silica, in order to observe whether the new addition of TEMPO prior to each catalytic cycle would be necessary catalytic cycles were carried out where TEMPO was and was not added prior to the repeat catalytic cycles. The results are shown in Table 2.29.

Table 2.29. Catalytic cycles with benzyl alcohol [a]

	Yield (%)		
Cycle	**1**	**2**	**3**
Without new addition of TEMPO	100	14	41 [c]
New addition of TEMPO before each run [b]	100	56	46

[a] Experimental conditions: T = 80ºC, 150 bar CO_2, 1.5 bar O_2, $t_{reaction}$ = 12 h, 2.0 mmol benzyl alcohol, 0.5 g $[Cu(AcO)_2(py)]_2$–silica catalyst (0.015 mmol [Cu]), 0.06 mmol TEMPO, Yields determined by GC. [b] 0.06 mmol TEMPO also added prior to cycles 2 and 3. [c] 0.06 mmol TEMPO added prior to cycle 3.

Considering first the results obtained when TEMPO was not added prior to the repeat cycle, the yield was observed to diminish from being complete in the first cycle to only a very low level (14 %) in the second cycle. The two most likely causes of this large decrease in the catalytic activity would be the decomposition of the copper catalyst, and leaching and/or decomposition of the TEMPO co-catalyst, leaching of the adsorbed copper is unlikely simply due to the absence of colour in the ether extracts. Of the possibilities the latter seemed fairly probable as TEMPO is soluble in the ether that was used to extract the reaction products and so probably leached from the system when this extraction was carried out, apparently almost completely. A third cycle was thus run, in this case adding fresh TEMPO to the system, and a yield of 41 % was recorded. Whilst this recovery of activity would seem to indicate that leaching of the TEMPO was responsible for a large part of the loss of catalytic activity in the previous cycle, the fact that the conversion remained significantly lower than in the first cycle indicated that the copper catalyst was less effective, probably due to decomposition. Notably, the previously blue-green catalyst was brown after use in catalysis. In the catalytic cycles run with the addition of copper prior to each subsequent catalytic cycle the yield was also observed to decline, to 56 % and 46 % in the second and third cycles respectively. It is notable that after a presumably large loss in activity between the first and second cycles, the decline in isolated yield between the second and third cycles is relatively slight. However, the significant loss in activity, apparently due to decomposition of the copper species, indicates that this system has only a very limited lifespan, requiring the

addition of fresh TEMPO in order to retain any activity. Its recyclability is therefore only very limited.

2.4 Diacetatopalladium Catalysed Alcohol Oxidations in Apolar Conditions

Continuing the investigations of coordination complexes of the ligand **A** in catalytic processes in apolar media, the preparation of simple complexes of palladium(II) was attempted. A wide range of catalytic processes facilitated by palladium compounds have been developed and extensively studied.[217] PDMS functionalised complexes with high solubilities in very non-polar media might therefore have applications in a wide range of catalytic processes.

2.4.1 Synthesis of PDMS functionalised palladium(II) complexes

2.4.1.1 Preparation of $[Pd(AcO)_2(\mathbf{A})_2]$, **4a**

$[Pd(AcO)_2]$ possesses good solubility in the majority of organic solvents, including halocarbons and toluene. However its solubility in highly apolar media, such as hexane is easily demonstrated to be poor. The preparation of the complex of ligand **A** was therefore interesting, as the PDMS functionalisation could well facilitate much improved solubility in this type of media. Through reaction with **A** the corresponding coordination complex of diacetatopalladium, **4a**, was relatively easily prepared. The product was extracted with hexane, which confirmed its solubility in such low polar solvents, and it appears that due to their insolubility both complexes with a low n and those of the α-addition isomer of **A** are eliminated during this extraction. As discussed previously (Section 2.1.1) ligand **A** consists of a 2:1 mixture of the β and α addition products of the hydrosilylation reaction. This is easily ascertained from the presence and absence of the corresponding peaks on the ^{1}H and ^{13}C-NMR spectra of these compounds. As can be clearly seen in Figure 2.25, only signals corresponding to the β-addition isomer of **A** are present in the coordination compound.

Figure 2.25. ^{1}H-NMR spectrum of **4a**

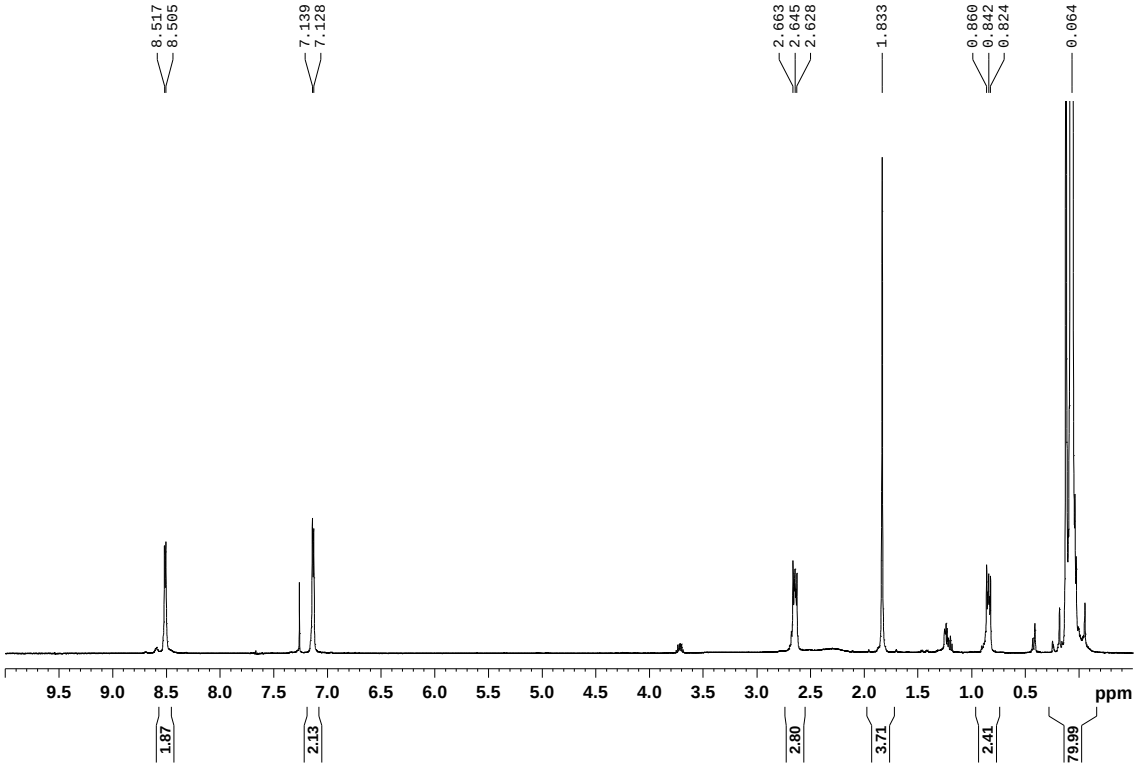

The isomeric purification is made clear by the absence both of the $CHCH_3$ peaks observable at 1.29 and 1.85 ppm in the spectrum of **A** and the presence of only one peak each for the 2,6 and 3,5 protons of the pyridyl ring, indicating only one isomer. Similarly, only signals corresponding to the β-addition isomer are visible on the $^{13}C\{^{1}H\}$-NMR spectrum (see Figure 2.26). Additionally, from the peak integrals of the ^{1}H-NMR spectrum the value of n (n = the number of PDMS monomer units per terminal pyridine, $\{Si(CH_3)_2\text{-}O\}_n$) was calculated to be 13. The sample of **A** from which **4a** was prepared was calculated to have an n of around 5. This indicates that the part of **4a** which formed from fractions of **A** with lower n were eliminated during the workup, presumably due to their insolubility in the very low polar extracting solvent hexane. Evidence indicating that this was the case was obtained in the synthesis of the dichloro analogue, **5a**, discussed below. The compound was thus identified as the complex $[Pd(AcO)_2(\mathbf{A})_2]$.

Figure 2.26. $^{13}C\{^{1}H\}$-NMR spectrum of **4a**

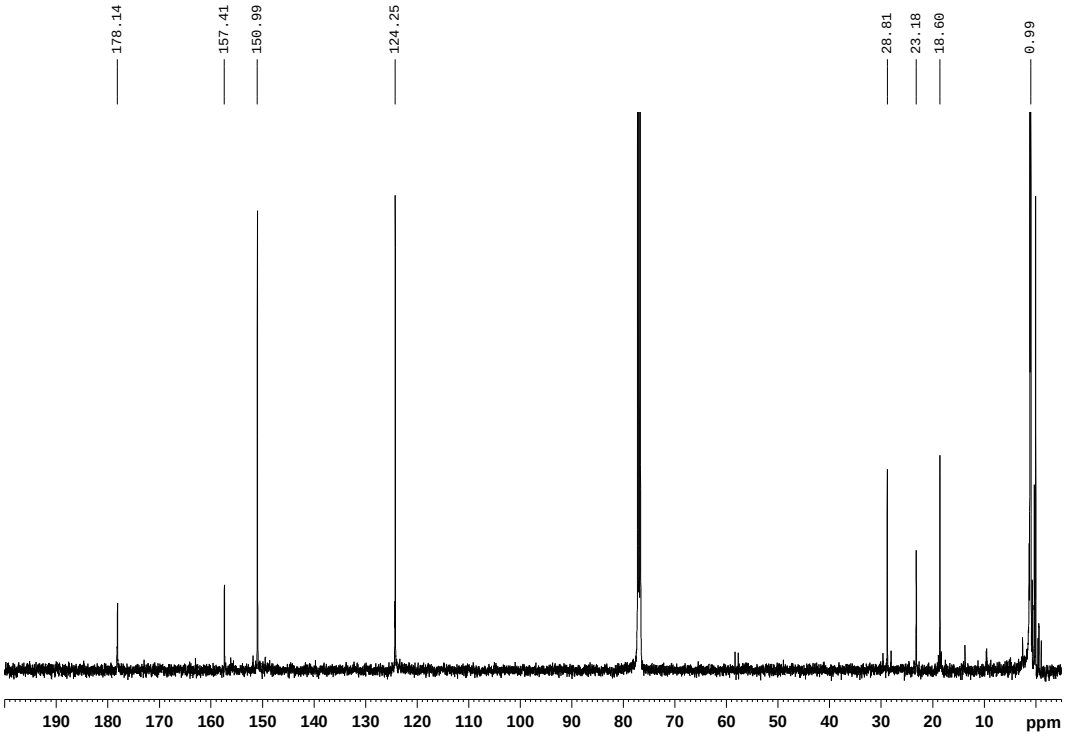

2.4.1.2 Preparation of $[Pd(Cl)_2(\mathbf{A})_2]$, **5a**

Pure dichloropalladium adopts a polymeric structure linked by μ_2-chloride bridges and displays very poor solubility in most media. For synthetic reactions it is typically dissolved by refluxing in a coordinating solvent such as acetonitrile or benzonitrile, consequently forming the corresponding monometallic coordination complex which can then undergo substitution reactions. The synthesis of the dichloropalladium complex of **A**, **5a**, was achieved by heating the two components at 80 ºC in ethanol overnight, followed by hexane extractions of the product. Similar to its diacetato counterpart **4a**, whose synthesis and characterisation was previously discussed (Section 2.4.1.1), only complexes formed from the β-addition complex of **A** were present in the final isolated sample of **5a**, there was no observable trace of the α-addition product which constitutes roughly a third of **A**. Also in common with **4a**, **5a** possessed a far higher value of n, approximately 15, than the sample of **A** from which it was prepared (again n = 5). It was assumed that **5a** complexes formed from the lower n fractions of **A** were being eliminated during the workup, due to their insolubility in hexane. Evidence that this was the case was obtained from ^{1}H-NMR analysis of the last

sediment fraction from which **5a** was separated. Examination of the integrals showed an n value of 4, indicating that the lower polymer lengths in this sample were insufficient for solubilisation in hexane.

2.4.2 Palladium catalysed aerobic alcohol oxidation in highly apolar media

Important aspects of the existing published work on alcohol oxidations catalysed by palladium(II) were discussed in detail in the introduction section. Amongst these, the majority of systems including those of Peterson et al.,[141] Uemura et al.,[145] and Sigman et al.,[149] typically employed organic solvents, for example DMSO, toluene and THF, as reaction media. Sheldon et al. introduced an aqueous system, employing a palladium catalyst with ionic functionalised ligands that was soluble in the highly polar reaction media.[152] This system is highly effective in the conversion of smaller more polar alcohols with sufficient solubilities in water, which formed biphasic reaction systems with the "green" aqueous reaction solvent. This system is a good example of a catalyst being designed to function well in a specific reaction environment. In a similar vein the work described here aimed to facilitate active catalysis in very apolar media, such as "green" $scCO_2$ and solventless conditions. Having developed palladium complexes with good solubilities in very low polar media, their catalytic efficacy in the selective oxidation of alcohol substrates in very apolar reaction conditions was thus examined.

Important aspects of the current mechanistic understanding of palladium(II) catalysed alcohol oxidations were previously covered (see Introduction, Section 1.4.3). Due to the requirement of an adjacent ligand with the capacity to abstract a β-proton during the oxidation mechanism, dichloro complexes are inactive as catalysts in this particular transformation. This has been demonstrated experimentally by Uemura et al.[145] The dichlorocomplex **5a** would therefore not be expected to be catalytically active in this transformation, and thus it was not tested. Carboxylate complexes however are quite capable of facilitating the oxidation mechanism and thus the diacetatopalladium complex **4a** has potential as a catalyst for this process. The intention, as previously stated, was to look for advantages stemming from the solubility of the catalyst in very non-polar media, which might permit homogeneous catalysis under conditions where it would be impossible to use a non PDMS functionalised analogue to obtain decent product yields. The capacity of **4a** to catalyse the oxidation of alcohols to their

corresponding carbonyl products was thus investigated both in solventless conditions and in $scCO_2$.

2.4.2.1 Oxidation of 2-octanol under solventless conditions

The objective of the study being to demonstrate whether **4a** would display improved activity in very low polar conditions, a low polar alcohol substrate, 2-octanol, was chosen for the study of activity in a solventless system. A more polar substrate, e.g. benzyl alcohol, would likely dissolve non-PDMS functionalised analogues of **4a** equally as well. Using standard conditions[145] a solventless study of the oxidation of this substrate employing [$Pd(AcO)_2$] in the absence of a base, and the presence of pyridine or **A** was carried out. The results are shown below in Table 2.30.

Table 2.30. Solventless oxidation of 2-octanol

Entry	Ligand	Alcohol Substrate	Yield
1	-	2-Octanol	69 %
2	Pyridine		28 %
3	**A**		23 %

[a] *$t_{reaction}$ = 18 h, T = 80 ºC, Alcohol Substrate (5.0 mmol), [$Pd(AcO)_2$] (0.05 mmol, 1 %), Ligand (0.25 mmol, 5 %), O_2 (1 bar).*

The presence of a base species was found to inhibit the rate of the oxidation reaction (compare entries 2 & 3 with entry 1, Table 2.30). When no base species was employed a markedly higher yield was obtained whilst pyridine and **A** both reduced the level of conversion to around a third. This is in common with observations made even in early examples of Pd(II) catalysed alcohol oxidations where bases were observed to prevent catalyst decomposition but also reduce the reaction rate. There was little difference in the yields obtained using **A** (entry 3, Table 2.30) or unfunctionalised pyridine (entry 2, Table 2.30), seemingly indicating that using the former did not result in any enhancement of the catalytic system. However, in the reactions which employed base species, the catalyst was observed to retain its yellow orange colour at the end of the reaction time, whilst in the reaction run in the absence of base the palladium had apparently converted completely to palladium black nanoparticles. These observations are in common with those regularly observed in Pd(II) catalysed alcohol oxidations,[144,145] where coordinating bases inhibit the mechanism of the oxidation by

competing for coordination sites, but also inhibit decomposition of the catalyst by preventing agglomeration of the catalyst molecules as palladium black when the Pd(II) is temporarily reduced to Pd(0) during the catalytic cycle. There are two possible reasons for the higher yield observed here when no base species was employed. It may be that the oxidation by the [$Pd(AcO)_2$] proceeded very quickly for a short period with a relatively high yield produced before the catalyst was deactivated by its reduction to palladium black. In this case the less active catalyst species were not able to reach a higher level of conversion during the reaction time despite the greater stability and thus much higher catalyst lifetime in these systems. The other possibility is that the reaction was actually very efficiently catalysed by the palladium black nanoparticles[218] that formed from the catalyst decomposition when no base was employed and that this catalytic system was actually more active than the [$Pd(AcO)_2$]-base systems. Clearly both **A** and pyridine had a fairly equal effect on catalytic activity, the pyridine system even appearing slightly more active. Although **4a** is clearly more soluble in very non-polar media it would appear that in this system this did not result in any catalytic advantage. Overall, with alcohols being by nature relatively polar substrates, the applicability of a specialised, non-polar soluble catalyst in their solventless oxidation would always be fairly limited. Whilst for some very non-polar alcohol substrates an advantage might be demonstrable, even for 2-octanol this was not the case. As such, no advantages from the use of **A** as a catalyst solubilising ligand in solventless oxidations were demonstrated by this study.

2.4.2.2 Oxidation of 2-octanol in $scCO_2$

A detailed discussion of the "greenness" of $scCO_2$ as a reaction solvent was previously presented in the introduction (Section 1.1.1.1). Clearly, as a result of its desirable sustainability credentials, alcohol oxidations which utilised $scCO_2$ as the reaction medium would present advantages from a green perspective. Additionally, with gaseous O_2 as the oxidant, improved reaction rates and selectivities might be obtained due to the perfect mixing with $scCO_2$. Diacetatopalladium complexes of simple bases, i.e. pyridine, should possess negligible solubilities in $scCO_2$. However the PDMS functionalisation of catalyst **4a** could facilitate its dissolution, potentially resulting in an active homogeneous catalytic system. A brief study of the oxidation of 2-octanol in

$scCO_2$ was thus conducted, comparing pyridine and **A** as coordinating base additives. The results are presented in Table 2.31.

Table 2.31. Oxidation of 2-octanol in $scCO_2$

Entry	Ligand	Alcohol Substrate	Yield
1	Pyridine	2-Octanol	26 %
2	**A**		2 %

[a] *$t_{reaction}$ = 18 h, T = 80 ºC, $P(CO_2)$ = 150 bar, $P(O_2)$ = 1 bar, Alcohol Substrate (5.0 mmol), $[Pd(AcO)_2]$ (0.05 mmol, 1 %), Ligand (0.25 mmol, 5 %).*

Using pyridine a limited yield was recovered (entry 1, Table 2.31). However when **A** was used the yield obtained was barely significant (entry 2, Table 2.31). Therefore it can quickly be concluded that **A** did not confer any advantage to the catalytic system through dissolution of the palladium catalyst, as had been hoped. The study was therefore concluded. It is interesting however, to make note of the state of the palladium catalyst following the oxidation in each case. When unsubstituted pyridine was employed the catalyst was completely reduced to palladium black nanoparticles which coated all the internal surfaces of the reactor (see vial (a) in Figure 2.27). In contrast, when **A** was employed the palladium remained in its oxidised state, coating the sides of the reactor as the oily orange coordination compound (see vial (b) in Figure 2.27). This demonstrated that under the reaction conditions **4a** possessed greater stability than its unsubstituted analogue. In analogous fashion, in diacetatopalladium catalysed alcohol oxidations in standard organic media, coordinating bases such as DMSO[143] and pyridine[144] are observed to prevent catalyst decomposition by preventing coagulation as Pd black nanoparticles. The observation of the state of the catalysts after the reaction seems to demonstrate that the palladium black nanoparticles formed in the reaction which employed pyridine were active in the alcohol oxidation. This was previously seen in the reaction where no base was employed under solventless conditions, where a relatively high yield concurrent with the reduction of the catalyst to palladium black was observed (entry 1, Table 2.31). If reduction of the catalyst to this insoluble form is desirable for good catalysis, then the use of solubilising ligands cannot produce any advantage, and the reaction would be cheaper and easier if a Pd(0) catalyst were used from the start. Thus it appears that, in a similar manner to the previously described study employing diacetatocopper catalysts (Section 2.3), the oxidation of alcohols by palladium in $scCO_2$ would actually be best achieved by employing a solid

state heterogeneous catalyst. The investigation of supported palladium black as a catalyst in this system might therefore make for an interesting study. This was not explored in the work covered here however.

Figure 2.27. Visual appearance of (a) $[Pd(AcO)_2]$-py and (b) $[Pd(AcO)_2]$-**A** after 2-octanol oxidations in $scCO_2$

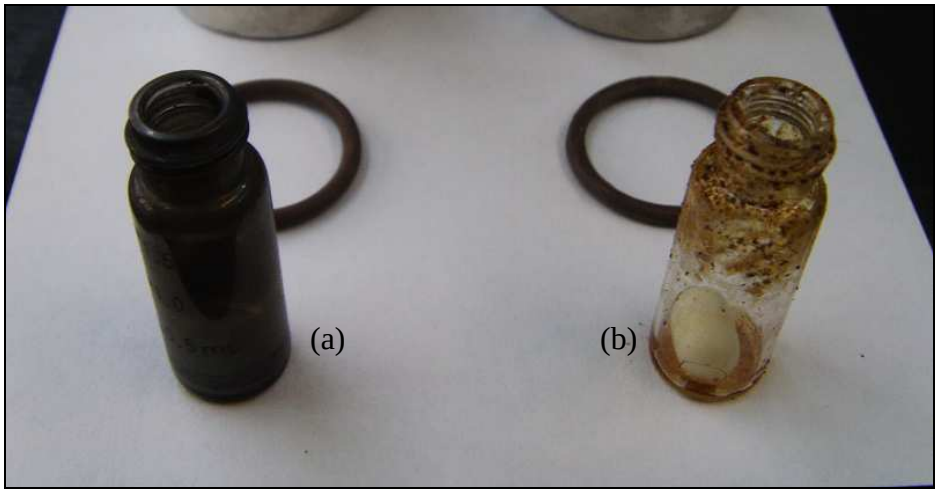

Thus, the PDMS functionalised pyridine ligand **A** did not confer any advantage in alcohol oxidations in the apolar environments of either solventless or $scCO_2$ reactions. However, the catalyst did appear to possess higher stability than its unfunctionalised analogue, which may indicate that in reactions where the catalyst is more active there could be some advantage to its use. With palladium(II) catalysts being active in a wide range of transformations, not limited to oxidation reactions, there may well exist systems in which the functionalised complexes **4a** and **5a** would represent ideal specialised catalysts.

3 Experimental

3 Experimental

3.1 Consideraciones generales

3.1.1 Métodos generales

A menos que se especifique lo contrario, todas las preparaciones de los compuestos, así como el resto de las operaciones, se han realizado utilizando técnicas de manipulación en condiciones secas y aeróbicas. Los disolventes se secaron por los procedimientos habituales, se destilaron y se almacenaron bajo atmósfera de nitrógeno y en presencia de tamiz molecular. Los reactivos empleados se adquirieron de fuentes comerciales (Aldrich) y se usaron sin efectuar una purificación adicional.

3.1.2 Métodos Instrumentales

Los espectros de IR se registraron en un espectrofotómetro Perkin-Elmer modelo BXII. Los espectros de líquidos y aceites se hicieron en pastillas de NaCl y los de sólidos en emulsiones de aceite mineral en pastillas de NaCl o en pastillas de KBr.

Los espectros de UV/Vis se realizaron en un espectrofotómetro Perkin-Elmer, modelo lambda 25.

Los espectros de RMN se obtuvieron en un espectrómetro Bruker, modelos AV-300 y AV-500. El desplazamiento químico en los espectros de RMN de ^{1}H, ^{13}C y ^{29}Si se referenció con respecto al tetrametilsilano, usando como referencia interna la señal de resonancia del disolvente empleado en el caso de los espectros de ^{1}H y ^{13}C.

Los análisis elementales (C, H, N, S), la espectrometría de masas y el análisis ICP se realizaron en los respectivos servicios del Centro de Investigación, Tecnología e Innovación de la Universidad de Sevilla (CITIUS).

Las medidas de cromatografía de gases se llevaron a cabo en un Cromatógrafo Varian CP-3800, equipado con inyector automático Varian modelo CP-8410 y un detector de Ionización de Llama (FID). Se montó una columna capilar Varian modelo CP-8741, utilizando nitrógeno como gas portador. Se utilizó el paquete informático

"Galaxie Workstation" para el control y automatización del sistema, la realización de las medidas y la generación y tratamiento de los datos. Como estándar se empleó alternativamente el dodecano u decano, dependiendo de los analitos a determinar y el programa. Detalles sobre los programas usados se aparecen en los apéndices. En todos los casos, la concentración de analitos se calcula a través de la relación entre el área del pico correspondiente al estándar añadido y las áreas de los picos de los respectivos analitos.

Los estudios de difracción de rayos X incluidos en este trabajo han sido llevados a cabo, de manera independiente al mismo, por el profesor Dr. Eleuterio Álvarez del *Instituto de Investigaciones Químicas* (CSIC).

Otros detalles experimentales relativos a materiales y métodos, que no se incluyen en este momento, se especificarán en los apartados correspondientes donde sean pertinentes.

3.2 Equipamiento de alta presión

La metodología y la mayoría de las técnicas aplicadas en los experimentos de alta presión han sido desarrolladas y utilizadas de forma rutinaria durante los últimos años en el grupo de investigación en el que me encuentro integrado.[219] No obstante, al ser esta memoria la primera en la que se describen estos sistemas, se ha considerado oportuno el realizar una descripción detallada tanto de los sistemas como de los procedimientos.

El sistema de alta presión esencialmente consiste en una línea de alta presión compuesta por tubos de alta presión HiP 1/16'' y un conjunto de conectores y válvulas HiP 1/16'' de tipo on/off que permiten el control de los flujos de gases. A esta línea se acoplan un sistema de bombeo de CO_2, un reactor de alta presión y un sistema de descompresión y recogida de muestras. Asimismo, el sistema consta de los correspondientes controladores de presión y temperatura y está provisto de diferentes elementos de seguridad como válvulas de no-retorno HiP 1/16''y disco de ruptura HiP (presión Max. = 400 bar) (Figura 3.1). La manipulación adecuada de las válvulas on/off permite el llenado del reactor con CO_2 (puro o mezclado con reactivos o co-disolvente), la adición de cualquier otro gas de reacción, la aplicación de vacío, así como la despresurización del mismo.

Figura 3.1. Fotografía (a) y esquema (b) de la línea de alta presión

(a)

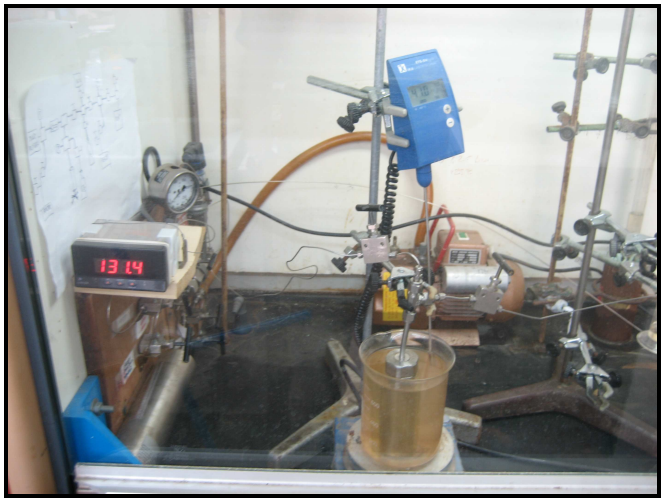

(b)

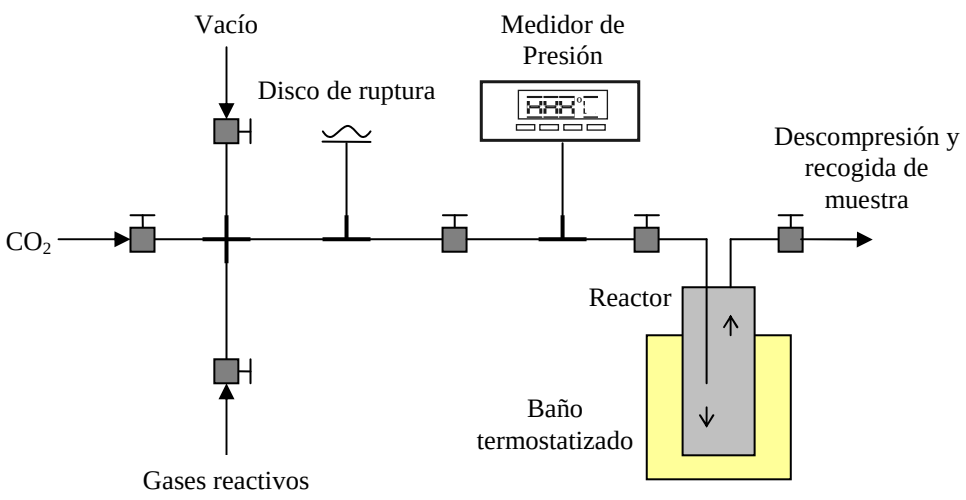

A continuación se describirán más detalladamente alguno de los elementos más importantes del sistema de alta presión.

3.2.1 Sistema de bombeo de CO_2

El dióxido de carbono (Air Liquid, calidad N48, cilindro B50 tipo sifón) utilizado posee unos niveles de oxígeno (< 2 ppm) y de agua (< 3 ppm) que no precisan una purificación adicional. La presión de CO_2 de trabajo habitualmente es superior a la que posee en el cilindro contenedor, de ahí que sea necesario un sistema de bombeo. Se han utilizado dos sistemas de bombeo alternativos, un generador manual de presión HiP (tipo jeringa) modelo 87-6-5 o una bomba de HPLC Jasco modelo PU-1550-CO_2, que permiten alcanzar presiones próximas a los 300 bar. En ambos tipos de sistemas de bombeo se requiere que el CO_2 llegue en estado líquido al compresor, de ahí que se utilice un cilindro contenedor de tipo sifón y sea necesario el enfriamiento previo del CO_2 a temperaturas cercanas a 0 ºC. El sistema de bombeo tipo jeringa se utilizó exclusivamente para experimentos en condiciones de batch, mientras que la bomba HPLC puede usarse tanto para experimentos en batch como en flujo continuo.

3.2.2 Reactores y celdas de alta presión

La mayoría de las reacciones y medidas de solubilidad a alta presión realizadas en el presente trabajo de investigación se han realizado en un reactor en forma de vaso

construido en acero con 27 mL de volumen cuya representación esquemática se muestra en la Figura 3.2. El cierre del reactor se realiza en la parte superior del vaso mediante un tapón de acero que se fija al vaso mediante una contratuerca de acero roscada. El sistema queda totalmente hermetizado mediante una anilla toroidal (o-ring) de Viton colocada en una hendidura en la parte superior del vaso y sobre la que se asienta el tapón. La parte superior del tapón lleva acoplado un tubo de acero de ¼'' que permite la conexión entre el interior y el exterior del reactor. A través de esta conexión se fijan las dos válvulas de tipo on/off que permiten el llenado/vaciado del reactor. Para ello, el tubo de ¼'' se acopla, por su otro extremo, a una conexión en forma de "T" que conecta a las dos válvulas on/off. Una de estas válvulas se conecta a un tubo de 1/16'' que va por el interior del tubo de ¼'' hasta el fondo del reactor y se utiliza para la entrada de gases. La otra válvula permite evacuar los gases del interior del reactor a través del espacio restante entre el exterior del tubo de 1/16'' y el interior del tubo de ¼''. La agitación del reactor se realiza mediante una barra magnética introducida en el interior.

Figura 3.2. Corte transversal del reactor utilizado en las experiencias en $scCO_2$

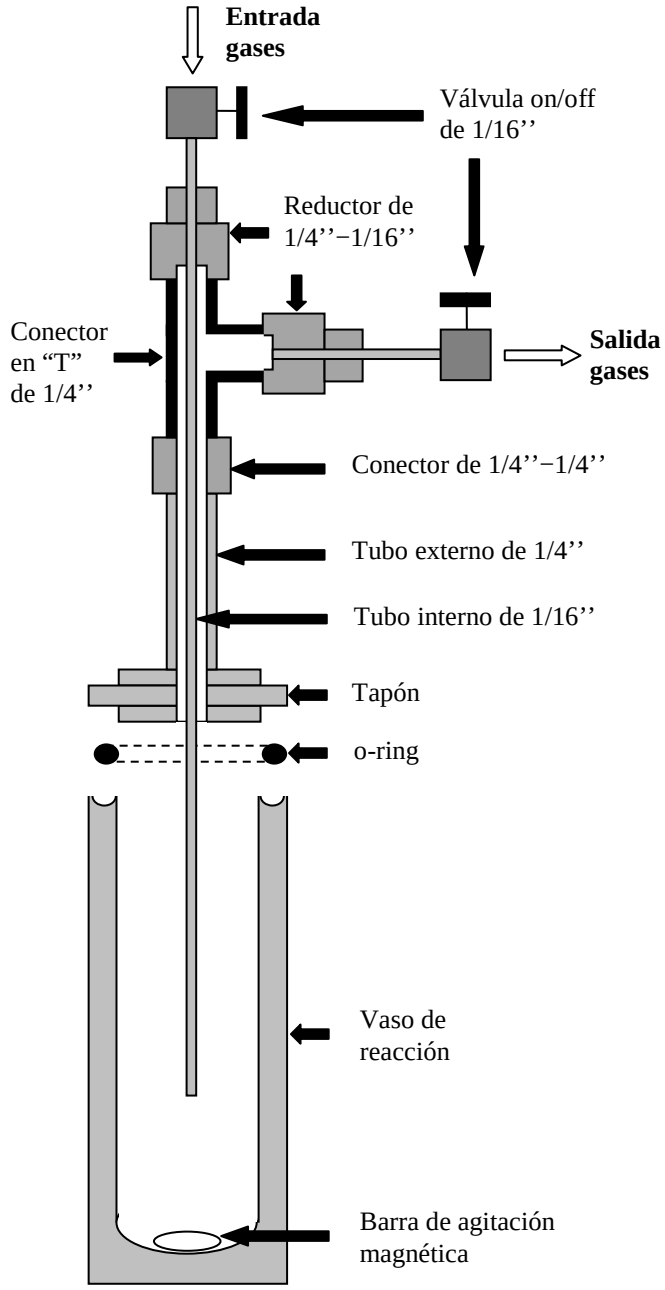

Además del reactor anteriormente descrito, se ha utilizado una celda provista de ventanas de zafiro que permitan un seguimiento visual o espectroscópico (UV, IR) de la mezcla supercrítica (Figura 3.3). La celda esencialmente consta de un cuerpo cilíndrico de acero de 4.4 ml de volumen interno. El cierre del mismo se realiza mediante discos de zafiro colocados en las bases superior e inferior del reactor, que se fijan al cuerpo del reactor mediante una contratuerca de acero roscada. El sistema queda totalmente hermetizado mediante una anilla toroidal (o-ring) de teflón colocada entre el disco de zafiro y el reactor. En el cuerpo de la celda se disponen dos orificios a los que se

acoplan mediante contratuercas HiP sendos tubos de 1/16'' con sus correspondientes válvulas de tipo on/off que permiten el llenado/vaciado del mismo.

Figura 3.3. Fotografías de la celda visual de alta presión (a, b) y corte transversal de la misma (c)

(a)

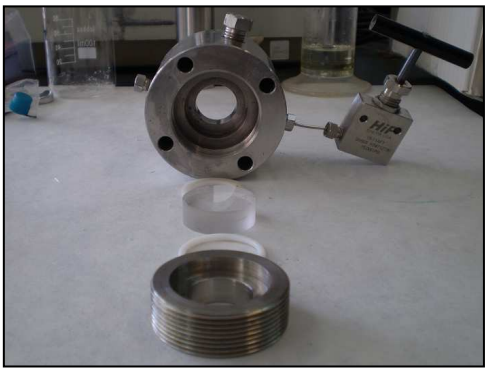

(b)

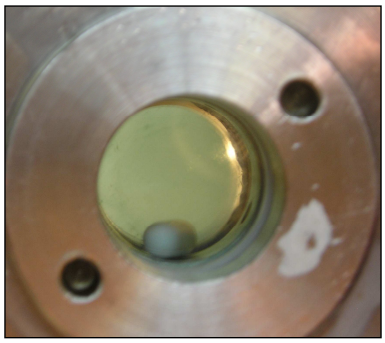

(c)

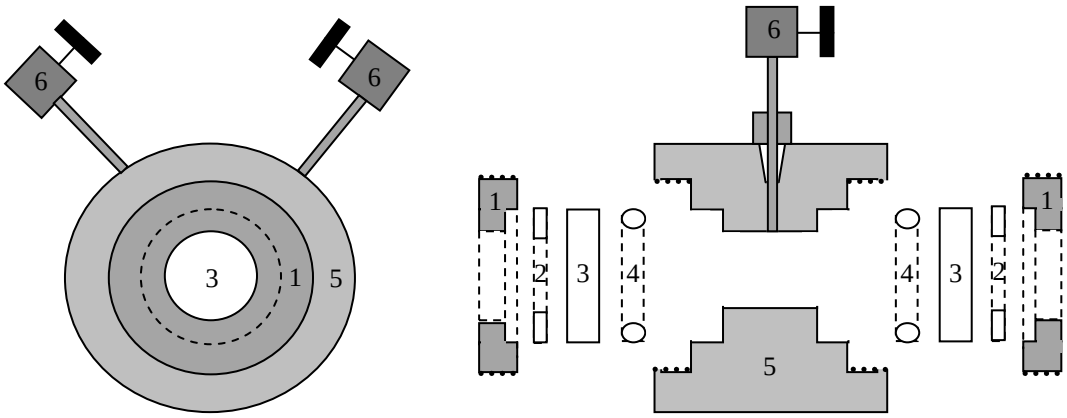

(1) Contratuerca de acero roscada; (2) Anilla plana de teflón; (3) Disco de zafiro; (4) o-ring; (5) Cuerpo de la celda; (6) Válvula on/off HiP 1/16''.

En ambos tipos de celdas de alta presión, el calentamiento se realizó, habitualmente, mediante un baño termostatizado de agua o aceite dependiendo de la temperatura de trabajo. Alternativamente se usó una cinta calentadora Chauvin-Arnoux Statop 4860. Durante las experiencias es conveniente cerrar las válvulas on/off conectadas a la celda para evitar posibles pérdidas por pequeñas fugas. La presión en el interior del reactor se controla mediante un medidor digital de presión.

3.2.3 Descompresión y recogida de muestra

Finalizado el ensayo a alta presión, se retira el reactor o celda de alta presión de la fuente de calentamiento e, inmediatamente, se procede al enfriamiento en un baño de hielo durante 10-15 minutos de forma que el CO_2 abandona el estado supercrítico, dando lugar a la formación de una fase líquida, que contiene disueltos la mayor parte de los solutos, y una fase gaseosa sobrenadante con una presión de 30 bar aproximadamente. La descompresión se realiza desde la fase gaseosa para reducir la perdida de los solutos, tal y como se muestra de forma esquemática en la Figura 3.4.

Figura 3.4. Descompresión del reactor de alta presión

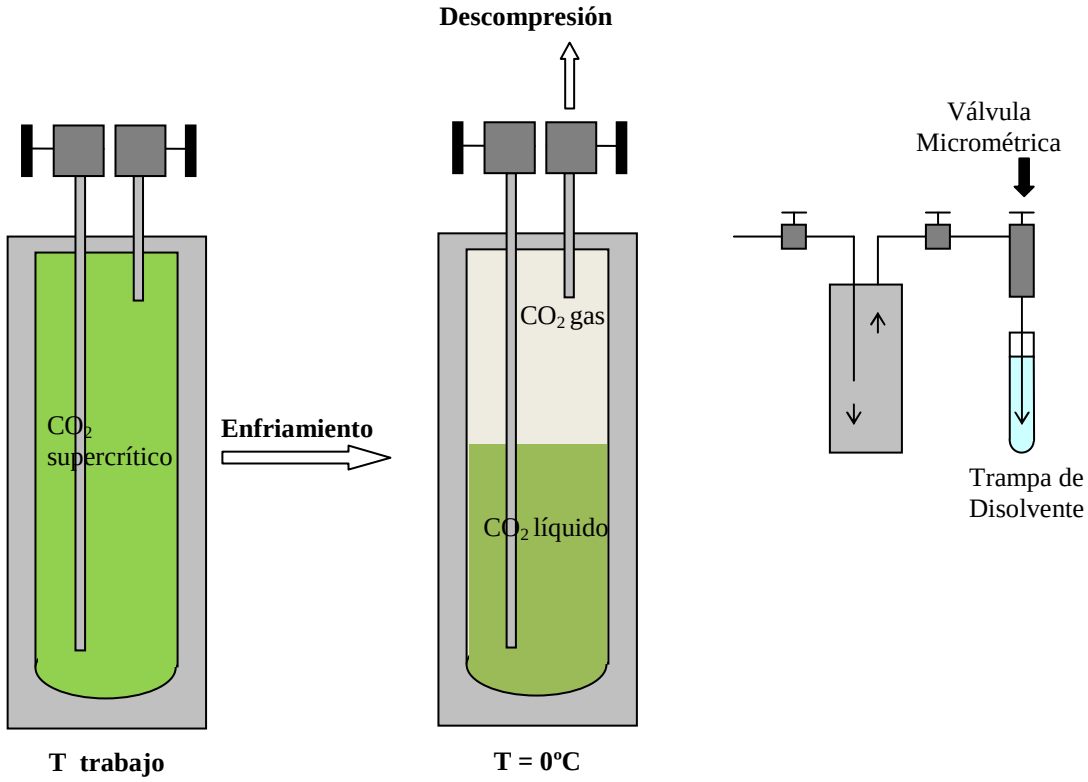

La descompresión se realiza haciendo uso de una válvula micrométrica Swagelok 1/16'', que permite una descompresión lenta mediante el control del flujo de CO_2. El flujo de CO_2 descomprimido procedente del reactor se hace pasar a través de una trampa que contiene un disolvente orgánico que asegura la retención de los productos arrastrados por el gas en su despresurización. Cuando la presión del reactor se iguala a la ambiental, se procede a su apertura para el análisis de la mezcla de reacción.

3.2.4 Estudios de reactividad a HP

Los estudios de reactividad se llevaron a cabo, en la mayoría de los casos, en el reactor de acero descrito en el Apartado 3.2.2. En la mayor parte de los estudios de reactividad realizados se ha optado por introducir de forma separada los reactivos de el(los) catalizador(es), para así evitar el inicio de la reacción antes de homogeneizar la mezcla de reacción en CO_2. Para ello en primer lugar, el reactor, provisto de una barra agitadora magnética, se carga con los correspondientes reactivos. A continuación, se introduce en el reactor un vial, también provisto de una pequeña barra magnética, que contiene el catalizador y el co-catalizador (cuando se requiere) que se emplean en la reacción (Figura 3.5).

Figura 3.5. Introduciendo el vial con el catalizador en el reactor de alta presión

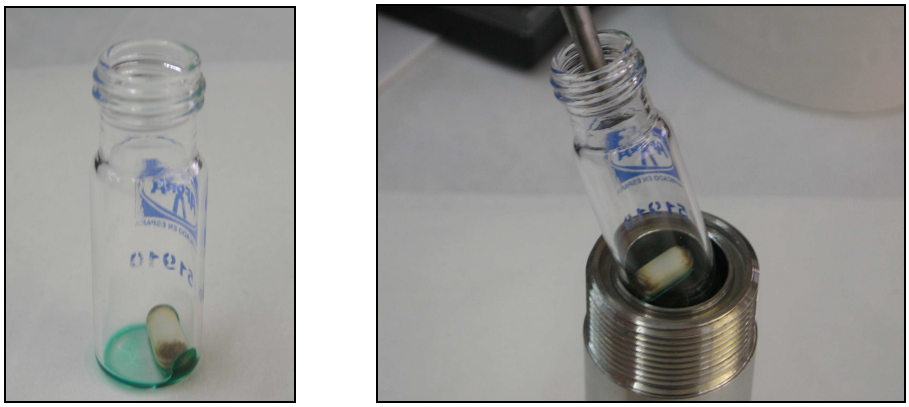

El procedimiento seguido de manera general para los estudios de reactividad en $scCO_2$ se muestra de forma esquemática en la Figura 3.6. Tras sellar el reactor, este se acopla a la línea de alta presión, se aplica vacío en su interior, se calienta a la temperatura de reacción, se introducen reactivos gaseosos (p.e. O_2) en el caso que sea preciso y, finalmente, se introduce CO_2 hasta la presión deseada. Tras la reacción, el sistema se despresuriza tal y como se ha descrito en el apartado anterior. Una vez despresurizado, se adiciona el disolvente orgánico adecuado para extraer los productos de la reacción. La disolución resultante, junto con la mezcla de la trampa, se unen para efectuar el correspondiente análisis mediante RMN o GC.

Figura 3.6. Esquema general para los estudios de reactividad a alta presión

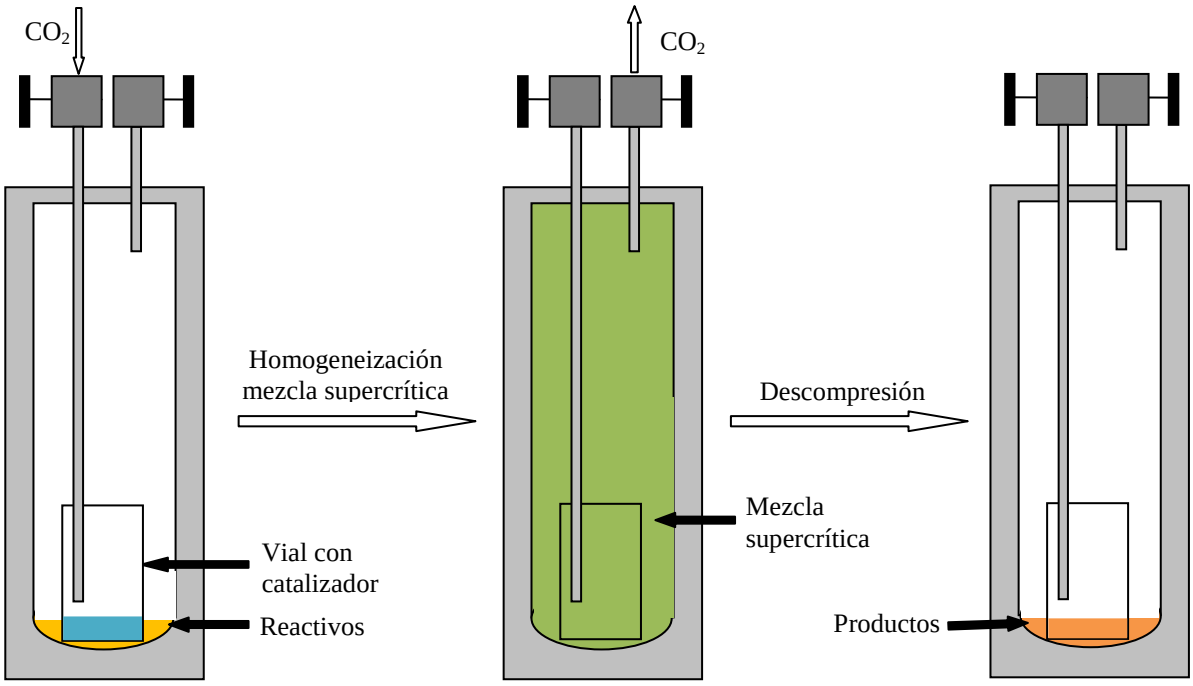

3.2.5 Determinación de solubilidades en $scCO_2$

Habitualmente, el estudio de la actividad catalítica de un precursor metálico en $scCO_2$ requiere una evaluación previa de su solubilidad en dicho medio. Se han empleado dos métodos alternativos para determinar la solubilidad de los complejos metálicos en $scCO_2$.

3.2.5.1 Con sistema de 'loop'

Este procedimiento, mostrado esquemáticamente en la Figura 3.7, permite obtener alícuotas de un volumen conocido de la disolución supercrítica saturada del soluto, cuya concentración se evalúa con posterioridad. Se trata, por tanto, de un procedimiento de medida que altera las condiciones de presión en el interior del reactor. Para ello, se dispone en la celda de alta presión una cantidad suficiente del soluto que permita obtener una disolución saturada en las condiciones supercríticas. A continuación la celda se llena de CO_2 y se alcanzan las condiciones adecuadas de presión y temperatura. Antes de realizar cualquier medida, la mezcla se debe agitar

suficientemente con objeto de garantizar la saturación del complejo en la disolución supercrítica. Para la realización de la medida, se llena con la mezcla supercrítica un 'loop' de volumen conocido mediante la apertura de la correspondiente válvula on/off. A continuación se despresuriza el 'loop' a través de una trampa de disolvente que atrapa los solutos y, finalmente, se lava el 'loop' con disolvente, que se une al resto de disolución de la trampa. La concentración de la disolución resultante se puede analizar empleando espectroscopia de UV-Visible, cromatografía de gases o mediante titulación.

Figura 3.7. Medida de la solubilidad en $scCO_2$ utilizando un 'loop' de volumen conocido

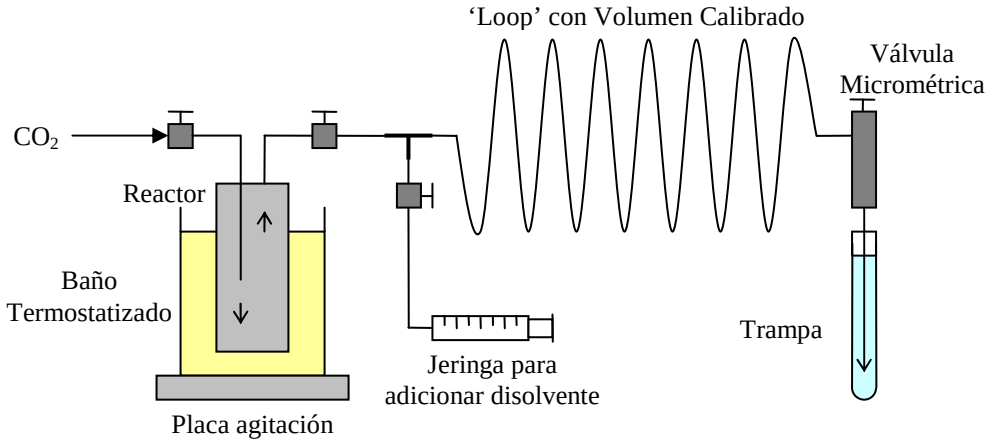

3.2.5.2 Determinación "*in-situ*" de la solubilidad mediante espectroscopia UV-Visible

El segundo método aprovecha las posibilidades que ofrece la celda visual, descrita en el Apartado 3.2.2, para registrar "*in situ*" el espectro de UV-VIS de disoluciones saturadas de un complejo en $scCO_2$. Para ello, al igual que en el procedimiento descrito anteriormente, es necesario obtener una disolución saturada del soluto en $scCO_2$. Para la realización de la medida se dispone la celda en el compartimento interior del espectroscopio UV-visible. El espectro UV/Vis se registra entre 300 y 1000 nm. La absorbancia en $scCO_2$ se calcula por diferencia entre el valor de la absorbancia en una región sin absorción del espectro y el valor de la absorbancia para el pico máximo. La concentración de los analitos en $scCO_2$ se determina usando la ley de Beer-Lambert a través de la utilización de una grafica de calibrado obtenida con disoluciones estándar en un disolvente poco polar, como el hexano. Se asume que estos

disolventes, que tienen aproximadamente la misma polaridad que $scCO_2$, producen cambios solvocromáticos insignificantes y que muestra coeficientes de extinción similares al $scCO_2$.[207,220]

3.3 Síntesis de los Líquidos Iónicos

El avance que se ha producido en las últimas décadas en el área de investigación dedicada al estudio y la utilización de los líquidos iónicos ha sido extraordinario. Por esta razón, en la bibliografía se encuentran descritos los procedimientos de preparación de un número muy elevado de este tipo de compuestos, entre ellos aquellos que se han utilizado en la presente memoria. En la actualidad, el estudio de las posibles mejoras en los procedimientos preparativos de los ILs es una línea activa que tiene como objetivo el obtenerlos de una manera más simple, con un mejor rendimiento, por un procedimiento más "verde", etc. En el caso de los derivados de imidazolio, el procedimiento general consiste en la reacción entre un haluro de alquilo y el derivado adecuado de N-alquilimidazol y, posteriormente, un intercambio de anión mediante una reacción de metátesis.

Esquema 3.1. Síntesis general de ILs de tipo sal de imidazolio

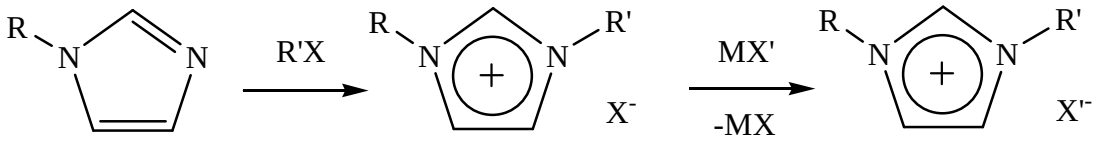

Se ha considerado conveniente incluir los métodos de síntesis de todos los líquidos iónicos utilizados en el presente trabajo ya que han sido preparados utilizando algunas modificaciones de los métodos descritos en la bibliografía. Sin embargo, no se han incluido los datos espectroscópicos de estos compuestos que coinciden con los descritos en la bibliografía.

3.3.1 Haluros de 1-alquil-3-metil-imidazolio, $C_n$mim-X

En un matraz de fondo redondo, equipado con una barra de agitación magnética y un condensador de reflujo provisto de un tubo de cloruro de calcio, se mezclan el 1-metilimidazol (1 equiv.) y el haluro de alquilo correspondiente (1 equiv.). La mezcla de reacción se calienta a 70 ºC durante 24 h, en el caso de bromuros, o durante 72 h para los cloruros. En el caso de la preparación de ILs con cadenas alquílicas de más de 10 átomos de carbono es necesario adicionalmente la presencia de un disolvente, p.e. una

cantidad equivolumétrica de cloroformo, para así disminuir la viscosidad de la mezcla y facilitar la agitación. Finalizada la reacción, el exceso de reactivos se elimina mediante la aplicación de vacío. El producto se obtiene al enfriar como un sólido cristalino con rendimientos prácticamente cuantitativos. En el caso de los ILs con cadenas alquílicas de menos de 6 átomos de carbono, si la cristalización no se inicia espontáneamente, se puede inducir la cristalización mediante solidificación rápida del IL aplicándole baja temperatura y posterior calentamiento a temperatura ambiente que conduce a la formación de cristales.

A través de este procedimiento se prepararon las siguientes sales: cloruro de 1-*n*-butil-3-metilimidazolio, C_4mim-Cl; bromuro de 1-*n*-octil-3-metilimidazolio, C_8mim-Br; bromuro de 1-*n*-dodecil-3-metilimidazolio, C_{12}mim-Br; y bromuro de 1-*n*-octadecil-3-metilimidazolio, C_{18}mim-Br.

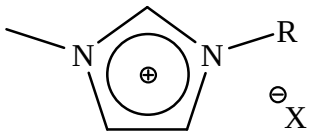

X	**R**	
Cl	*n*-C_4H_9	C_4mim-Cl
Br	*n*-C_8H_{17}	C_8mim-Br
Br	*n*-$C_{12}H_{25}$	C_{12}mim-Br
Br	*n*-$C_{18}H_{37}$	C_{18}mim-Br

3.3.2 Hexafluorofosfatos de 1-alquil-3-metil-imidazolio, $C_n$mim-PF_6

Sobre una disolución acuosa de haluro de 1-alquil-3-metil-imidazolio (1 equiv.) a 0 ºC se añade lentamente (durante 30 minutos aproximadamente) una disolución acuosa de HPF_6 (60 %, 1.05 equiv.). La mezcla resultante se agita durante otros 30 minutos; seguidamente se separa la fase acuosa por decantación, se adiciona a la fase orgánica una cantidad equivolumétrica de diclorometano y ésta se lava varias veces con agua hasta observar pH neutro en las fracciones de lavado. La fase orgánica se recoge en un matraz de fondo redondo, se le añade carbón activo y se deja con agitación manteniendo el sistema cerrado durante al menos tres días. Transcurrido este tiempo, la mezcla se filtra a través de celita y a la disolución resultante se le aplica vacío calentando a 100 ºC durante varias horas para secar totalmente el producto. Tras enfriar a temperatura ambiente, se obtiene el correspondiente IL con un rendimiento superior al 80%.

A través de este procedimiento se prepararon los siguientes ILs: hexafluorofosfato de 1-*n*-butil-3-metilimidazolio, C_4mim-PF_6; hexafluorofosfato de 1-*n*-

octil-3-metilimidazolio, C_8mim-PF_6; hexafluorofosfato de 1-*n*-dodecil-3-metilimidazolio, C_{12}mim-PF_6; y hexafluorofosfato de 1-*n*-octadecil-3-metilimidazolio, C_{18}mim-PF_6.

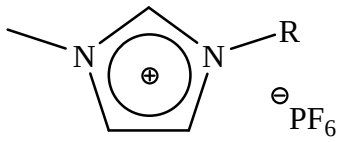

R	IL
n-C_4H_9	C_4mim-PF_6
n-C_8H_{17}	C_8mim-PF_6
n-$C_{12}H_{25}$	C_{12}mim-PF_6
n-$C_{18}H_{37}$	C_{18}mim-PF_6

3.3.3 Tetrafluoroborato de 1-butil-3-metil-imidazolio, C_4mim-BF_4

Los productos $C_n$mim-X (1 equiv.) se disuelven en agua ~200 ml mol^{-1} (o la mínima cantidad posible en el caso de los cadenas alquílicas más largas) y la disolución resultante se enfría en un baño de hielo. Se adiciona a ésta una disolución de tetrafluoroborato de sodio (1.1 equiv.) disuelto en la mínima cantidad de agua. Se observa la formación de dos fases, el líquido iónico debajo, pero gran cantidad del líquido iónico queda disuelto en la fase acuosa. Las fases se separan y la fase acuosa se lava con diclorometano (2 x 1 equivalente volumétrico). La fracción orgánica se combina con el líquido iónico y se adiciona diclorometano hasta que hay 200 ml mol^{-1} líquido iónico. La disolución orgánica se lava varias veces con agua. Tras comprobar la ausencia total de iones haluro en el producto (probando la fase acuosa con una disolución de $AgNO_3$), a la disolución del líquido iónico se le añade una cantidad abundante de carbón activo. La mezcla se deja con agitación durante el mayor tiempo posible (mínimo tres días). Se filtra el disolución a través de celita para eliminar el carbono y se evapora el disolvente mediante vació, con agitación, iniciando la evaporación a temperatura ambiente y terminando a 100 ºC, se calienta a esta temperatura durante 3 h para eliminar las trazas de agua. El producto se lleva a temperatura ambiente bajo nitrógeno y se guarda para ser usado. Rendimientos de ~80 %.

3.4 Preparación de los ligandos N-Donadores

3.4.1 4-(Polidimetilsiloxanil-etil)piridina, A

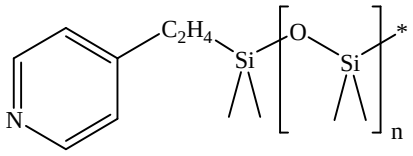

Sobre una disolución del polímero comercial H-(Si(CH_3)$_2$-O)$_n$ (6,0 mL, 16,7 mmol) en Cl_2CH_2 (5 mL) se adiciona, bajo atmósfera de nitrógeno, 4-vinilpiridina (2,4 mL, 21 mmol) en presencia del catalizador de Karstedt's (2 % [Pt] en xilanos) (285 μL, 0,046 mmol). Tras calentar la mezcla de reacción a 60 ºC durante 36 horas, se evapora el disolvente mediante la aplicación de vacío y se realiza un espectro de IR al crudo de la reacción para confirmar la desaparición de la banda a 2126 cm^{-1} correspondiente a la agrupación Si-H del polímero de partida. A continuación, el crudo se disuelve en hexano (15 mL), se seca con sulfato de magnesio y se filtra a través de gel de sílice, para eliminar el catalizador platino. La disolución resultante se centrifuga y posteriormente se lleva a sequedad mediante la aplicación de vacío a 60 ºC durante unas horas. El polímero **A**, que se aísla en forma de aceite amarillo pálido con rendimientos próximos al 70%, se guarda bajo nitrógeno en el frigorífico. Tal y como se discute en la sección de Resultados y Discusión, el polímero **A** se obtiene como una mezcla inseparable de isómeros α y β en una proporción 1:2. Asimismo, se observó que la proporción de agrupaciones Si(CH_3)$_2$ respecto al grupo piridilo variaba entre 5 y 10 en las distintas muestra de **A** que se prepararon. Concretamente, en una de las muestras se calculó, a través de ^{1}H RMN, una proporción de 5,5 grupos Si(CH_3)$_2$ por cada piridilo terminal, lo que correspondía a un peso molecular aproximado de 506 g mol^{-1} para el polímero **A** (5,592 g, rendimiento basado en los grupos piridilo terminales = 66 %).

IR (NaCl, cm^{-1}): 661, 688, 802, 863, 919, 1027, 1092, 1261, 1376, 1414, 1599, 1645, 2963, 3235.

RMN: ^{1}H ($CDCl_3$): δ -0,1 – 0,1 (br s, Si(C***H*****$_3$**)$_2$), isómero α: 1,29 (d, J_{HH} = 7,35 Hz, 3H, py-CH(C***H*****$_3$**)-Si), 1,84 (q, J_{HH} = 8,04 Hz, 1H, py-C***H***(CH_3)-Si), 6,92 (m, 2H, *m*-NC_5H_4), 8,30 (m, 2H, *o*-NC_5H_4); isómero β: 0,82 (t, J_{HH} = 8,7 Hz, 2H, py-CH_2C***H*****$_2$**-Si), 2,57 (t, J_{HH} = 8,6 Hz, 2H, py-C***H*****$_2$**CH_2-Si), 7,05 (m, 2H, *m*-NC_5H_4), 8,37 (m, 2H, *o*-

NC_5H_4). $^{13}C\{^1H\}$ ($CDCl_3$): δ 0-5 (varios s, Si(***C***$H_3)_2$), 13,3 (s, py-CH(***C***H_3), isómero α), 18,9 (s, py-CH_2***C***H_2-Si, isómero β), 28,8 (s, py-***C***H_2CH_2-Si, isómero β), 31,5 py-***C***H(CH_3), isómero α), 122,8 (s, *m*-NC_5H_4, isómero α), 148,8 (s, *o*-NC_5H_4, isómero α), 153,0 (s, *p*-NC_5H_4, isómero α), 123,3 (s, *m*-NC_5H_4, isómero β), 149,4 (s, *o*-NC_5H_4, isómero β), 154,1 (s, *p*-NC_5H_4, isómero β). $^{29}Si\{^1H\}$ ($CDCl_3$): δ –21,6 - –22,1, –21,1, –20,8 (varios s, O-***Si***$(CH_3)_2$-O), –12,9 (s a, C_2H_4-***Si***$(CH_3)_2$-O).

Análisis elemental calculado para una muestra con una proporción de 5,5 grupos Si(CH₃)₂ por cada piridilo terminal ($C_{36}H_{82}N_2O_{10}Si_{11}$): C, 42,73; H, 8,17; N, 2,77. *Experimental:* C, 43,56; H, 8,36; N, 3,23 %.

3.4.2 4-Tridecilpiridina, B

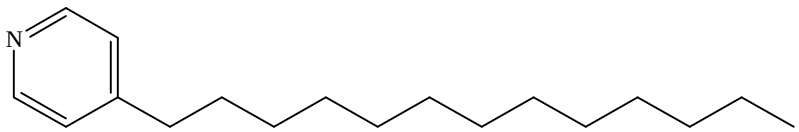

Este procedimiento es análogo al descrito previamente en la bibliografía para la síntesis del 4-heptilpiridina.[221] Sobre una disolución de $^{i}Pr_2NH$ (1,05 equiv., 3 mL, 21 mmol) en THF seco (50 mL) a -78 ºC se adiciona una disolución 1,6 M de ^{n}BuLi en hexano (12,5 mL, 1,05 equiv., 21 mmol), dando lugar a la formación "*in-situ*" de diisopropilamiduro de litio (LDA), que seguidamente se hace reaccionar con 4-picolina (1,00 equiv., 1940 μL, 20,0 mmol). La mezcla de reacción se lleva a 0 ºC mediante el uso de un baño de hielo y se mantiene a esa temperatura durante 5 min. A continuación, se adiciona sobre la mezcla 1-iodododecano (1,00 equiv., 4,9 mL, 20 mmol), manteniéndose la temperatura de 0 ºC durante 5 min. Finalmente, la mezcla de reacción se lleva a temperatura ambiente y se mantiene con agitación durante 36 h. Transcurrido este tiempo, la mezcla se concentra hasta un volumen aproximado de 10 mL, se adiciona Cl_2CH_2 (50 mL) y se lava con agua (3 x 25 mL). Para evitar pérdidas de productos en los lavados, la fracción acuosa se lava con Cl_2CH_2 (3 x 25 mL). Tras combinar todas las fracciones, la disolución orgánica resultante se seca con $MgSO_4$, se filtra y, finalmente, se lleva a sequedad en un rotavapor, dando lugar a un aceite de color marrón. El crudo de reacción se purifica mediante separación cromatográfica en una columna empleando sílica gel y una mezcla 0,5 % de NEt_3 en 1:1 hexano:acetato de

etilo como eluyente. El compuesto se aísla en forma de aceite de color amarillo pálido (3,6 g, 69 %).

IR (NaCl, cm^{-1}): 583, 666, 722, 801, 992, 1048, 1219, 1240, 1373, 1414, 1466, 1559, 1602, 1742, 2853, 2924, 3067

RMN: ^{1}H ($CDCl_3$): δ 0,81 (t, J_{HH} = 3,17 Hz, 3H, C***H*****$_3$**), 0,9 – 1,7 (m, 22H, C***H*****$_2$**), 2,53 (t, J_{HH} = 7,68, 2H, -C***H*****$_2$**-NC_5H_4), 7,03 (m, 2H, *m*-NC_5H_4), δ 8,41 (s, 2H, *o*-NC_5H_4). $^{13}C\{^{1}H\}$ ($CDCl_3$): δ 14,0 (s, ***C***H_3), 20 - 32 (s, ***C***H_2), 35,1 (s, -***C***H_2-NC_5H_4), 123,7 (s, *m*-NC_5H_4), 149,4 (s, *o*-NC_5H_4), 151,6 (s, *p*-NC_5H_4).

Análisis elemental calculado ($C_{18}H_{31}N$): C, 82,69; H, 11,95; N, 5,36. *Experimental*: C, 80,66; H, 11,65; N, 5,33 %.

3.4.3 4-(2,2-Bis-trimetilsilanil-etil)piridina, C

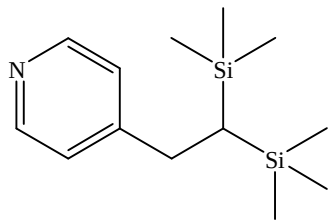

Para la preparación y purificación se sigue un procedimiento similar al descrito en el Apartado 3.4.2 pero utilizando 1-cloro-2,2-bis-trimetilsilanil-etano (1,00 equiv., 650 μL, 3,0 mmol) en lugar de 1-iodododecano con los otros reactivos en propias proporciones con este. Se obtiene el compuesto **C** como un aceite de color amarillo pálido (440 mg, 1.75 mmol, 58 %).

IR (NaCl, cm^{-1}): 500, 685, 755, 774, 839, 981, 1036, 1251, 1415, 1595, 1558, 1598, 2851, 2898, 2952, 3024, 3067

RMN: ^{1}H – ($CDCl_3$): δ 0,00 (s, 18H, Si(C***H*****$_3$**)$_3$), δ 0,32 (t, J_{HH} = 6,78 Hz, 1H, C***H***), δ 2,77 (d, J_{HH} = 6,66, 2H, C***H*****$_2$**), δ 7,13 (m, 2H, *m*-NC_5H_4), δ 8,46 (s, 2H, *o*-NC_5H_4). $^{13}C\{^{1}H\}$ ($CDCl_3$): δ 0,0 (s, Si(***C***H_3)$_3$), 14,6 (s, ***C***H), 31,4 (s, ***C***H_2), 123,7 (s, *m*-NC_5H_4), 149,4 (s, *o*-NC_5H_4), 153,7 (s, *p*-NC_5H_4). $^{29}Si\{^{1}H\}$ ($CDCl_3$): δ 3,8 (s, ***Si***$(CH_3)_3$).

Análisis elemental calculado ($C_{13}H_{25}NSi_2$): C, 62,08; H, 10,02; N, 5,57. *Experimental*: C, 58,45; H, 9,79; N, 4,95 %.

3.4.4 2,6-(Bis-trimetilsilanilmetil)piridina, D

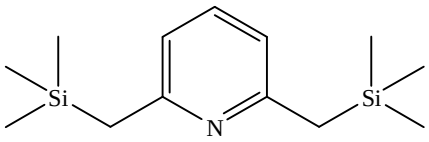

Para la preparación y purificación se sigue un procedimiento similar al descrito en el Apartado 3.4.2 pero utilizando 2,6-lutidina (0,50 equiv., 463 μL, 4,0 mmol) en lugar de 4-picolina y clorotrimetilsilano (1,00 equiv., 1,02 mL, 8,0 mmol) en lugar de 1-iodododecano con los otros reactivos en las adecuadas proporciones. Se obtiene el compuesto **D** como un aceite de color amarillo pálido (520 mg, 2.07 mmol, 52 %).

IR (NaCl, cm^{-1}): 722, 806, 841, 948, 978, 1030, 1093, 1105, 1153, 1184, 1203, 1311, 1378, 1398, 1444, 1466, 1588, 1600, 1622, 2098, 2427, 2489, 2567, 2720, 2760, 2850, 2923, 2960, 3400.

RMN: ^{1}H – ($CDCl_3$): δ 0,00 (s, 18H, Si(C***H*****₃**)$_3$), δ 2,41 (s, 4H, C***H*****₂**), δ 6,68 (m, 2H, *m*-NC_5H_3), δ 7,27 (m, 1H, *p*-NC_5H_3). $^{13}C\{^{1}H\}$ ($CDCl_3$): δ -0,1 (s, Si(***C***H_3)$_3$), 32,8 (s, ***C***H_2), 117,3 (s, *m*-NC_5H_4), 135,4 (s, *p*-NC_5H_4), 157.0 (s, *o*-NC_5H_4). $^{29}Si\{^{1}H\}$ ($CDCl_3$): δ 2,0 (s, ***Si***$(CH_3)_3$).

Análisis elemental calculado ($C_{13}H_{25}NSi_2$): C, 62,08; H, 10,02; N, 5,57. *Experimental*: C, 60,37; H, 10,16; N, 4,97 %.

3.4.5 4,4'-Di(tridecil)-2,2'-bipiridina, E [222]

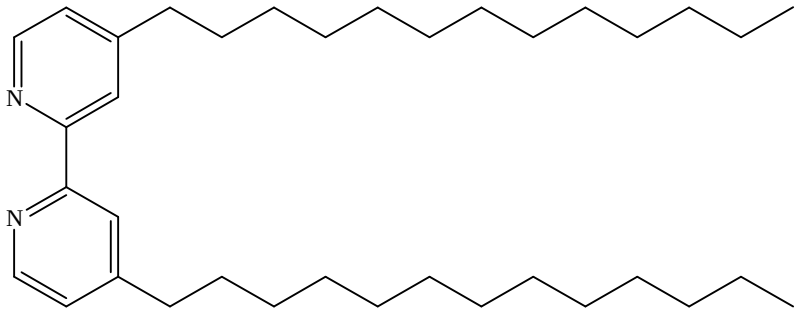

Sobre una disolución de $^{i}Pr_2NH$ (1.05 equiv., 950 μL, 6.7 mmol) en THF seco (~30 mL) a -78 ºC se adiciona una disolución 1,6 M de ^{n}BuLi en hexano (1,05 equiv., 4,0 mL, 6,7 mmol), dando lugar a la formación "*in-situ*" de diisopropilamiduro de litio (LDA), que seguidamente se hace reaccionar con 4,4-dimetil-2,2-bipiridina (1,00

equiv., 590 mg, 3.20 mmol) disuelto en THF (15 mL), observándose la inmediata aparición de una tonalidad rojiza en la mezcla de reacción. La mezcla se lleva a 0 ºC mediante el uso de un baño de hielo y se mantiene a esa temperatura durante 5 min. A continuación, se adicionan 1-yodododecano (1,00 mmol, 1,65 mL, 6,7 mmol), manteniéndose la temperatura de 0 ºC durante 5 min. Finalmente, la mezcla de reacción se lleva a temperatura ambiente y se mantiene con agitación durante 36 h. La purificación del producto se realiza siguiendo un procedimiento similar al descrito en el Apartado 3.4.2. Este producto se recristaliza en metanol, dando lugar a un sólido blanco (900 mg, 70 %).

IR (NaCl, cm^{-1}): 834, 1110, 1547, 1597, 1964.

RMN: ^{1}H ($CDCl_3$): δ 0,80 (t, J_{HH} = 6.42 Hz, 6H, C***H*****$_3$**), 1,1 – 1,7 (m, 44H, C***H*****$_2$**), 2,61 (t, J_{HH} = 7,76 Hz, 4H, -C***H*****$_2$**-NC_5H_3), 7,05 (d, 2H, NC_5H_3 pos-5), 8,16 (s, 2H, NC_5H_3 pos-3), 8,48 (d, 2H, NC_5H_3 pos-6). $^{13}C\{^{1}H\}$ ($CDCl_3$): δ -0,1 (s, ***C***H_3), 12 – 30 (s, ***C***H_2), 33,6 (s, -***C***H_2-NC_5H_3), 119,4, 121,9, 147,0, 150,9, 154,2 (s, NC_5H_3).

Análisis elemental calculado ($C_{36}H_{60}N_2$): C, 83.01; H, 11.61; N, 5.38. *Experimental:* C, 84.23; H, 12.25; N, 5.59 %.

3.4.6 4,4’-Bis-(bistrimetilsilanilmetil)-2,2’-bipiridina, F

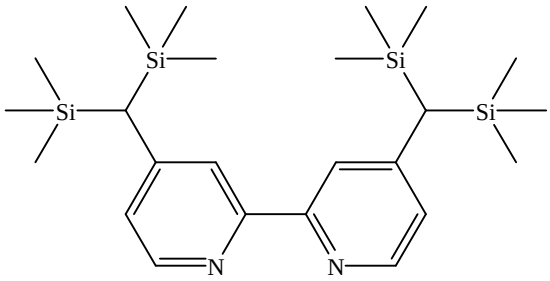

Se sigue un procedimiento similar al descrito en el Apartado 3.4.5, empleando clorotrimetilsilano (1.00 equiv., 770 μL, 5.9 mmol) en lugar de 1-yodododecano con los otros reactivos en las adecuadas proporciones. Se obtiene como cristales finos y blancos, (310 mg, 24 %).

IR (NaCl en nujol, cm^{-1}): 451, 558, 620, 654, 691, 724, 756, 778, 839, 862, 914, 990, 1035, 1069, 1159, 1217, 1247, 1404, 1540, 1580, 3047

RMN: ^{1}H ($CDCl_3$): δ 0.00 (s, 36H, Si(C***H*****₃**)$_3$), 2.16 (s, 4H, C***H*****₂**), 6.89 (d, 2H, NC_5H_3), 8.01 (s, 2H, NC_5H_3), 8.42 (d, 2H, NC_5H_3). $^{13}C\{^{1}H\}$ ($CDCl_3$): δ 0.00 (s, Si(***C***$H_3)_3$), 29.38 (s, ***C***H_2), 122.63, 125.26, 150.51, 153.02, 157.81 (s, NC_5H_3). $^{29}Si\{^{1}H\}$ ($CDCl_3$): δ 2.19 (***Si***$(CH_3)_3$).

Análisis elemental calculado ($C_{24}H_{44}N_2Si_4$): C, 60,95; H, 9,38; N, 5,92. *Experimental:* C, 59,90; H, 10,12; N, 6,07 %.

3.4.7 4,4'-bis-(2,2-bis-trimetilsilanil-etil)-2,2'-bipiridina, G

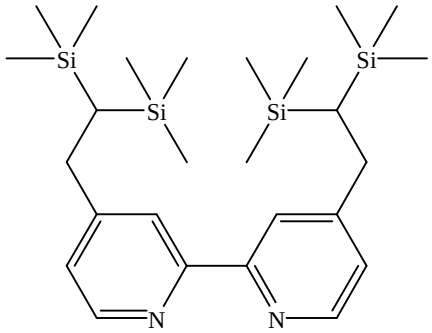

Se sigue un procedimiento similar al descrito en el Apartado 3.4.5, empleando 1-cloro-2,2-bis-trimetilsilanil-etano (1.00 equiv., 1.00g, 5.13 mmol) en lugar de 1-yodododecano con los otros reactivos en las adecuadas proporciones. El producto se recristaliza en metanol obteniendose como cristales de color crema (290 mg, 23 %)

IR (KBr, cm^{-1}): 839, 1036, 1250, 1551, 1590.

RMN: ^{1}H ($CDCl_3$): δ 0.00 (s, 18H, Si(C***H*****₃**)$_3$), 0.47 (t, J_{HH} = 7.00 Hz, 2H, C***H***), 2.87 (d, J_{HH} = 7.02 Hz, 4H, CH_2), 7.14 (d, 2H, NC_5H_3), 8.27 (s, 2H, NC_5H_3), 8.54 (d, 2H, NC_5H_3). $^{13}C\{^{1}H\}$ ($CDCl_3$): δ 0.00 (s, Si(*C*$H_3)_3$), 14.26 (s, *C*H), 31.59 (s, *C*H_2), 121.05 , 123.59, 148.67, 154.57, 155.76 (s, N*C*$_5H_3$). $^{29}Si\{^{1}H\}$ ($CDCl_3$): δ 3.87 ($Si(CH_3)_3$).

Análisis elemental calculado ($C_{26}H_{48}N_2Si_4$): C, 62.33; H, 9.66; N, 5.59. *Experimental:* C, 62.28; H, 10.46; N, 5.84 %.

3.4.8 4-Metil-4'-tridecil-2,2'-bipiridina, H [223]

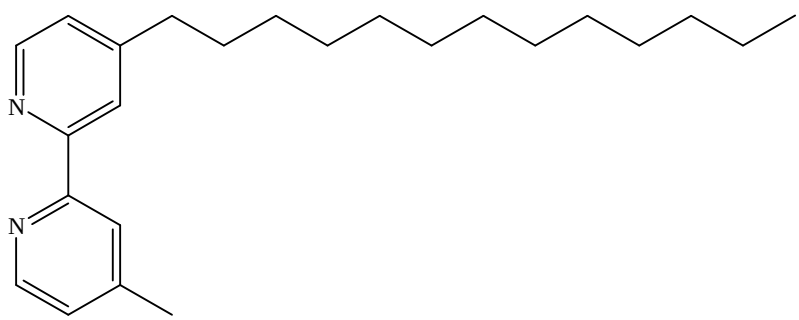

Sobre una disolución de diisopropilamina (461 μL, 3.26 mmol) en THF (3 mL) se adiciona ^{n}BuLi (2.04 mL, 3.26 mmol). Este se agita durante 15 minutos para obtener una disolución amarilla a la que se adiciona por gotas durante 30 minutos una disolución de 4,4'dimetil-2,2'-bipiridina (601 mg, 3.26 mmol) en THF (25 mL). Se obtiene una disolución naranja-marrón que se agita durante 1.5 horas. Se enfría a 0 ºC y se adiciona 1-yodododecano (804 μL, 3.26 mmol). Tras la adición resulta una disolución verde oscuro que rápidamente palidece. Se agita durante 1.5 horas tras las que en la disolución se manifiesta una turbidez. Se añade agua/hielo y la mezcla resultante se extrae con éter dietílico (3 x 50 mL), que se seca ($MgSO_4$), se filtra y se evapora hasta obtener un producto crudo en forma de aceite amarillo. Este se recristaliza tres veces con acetato de etilo hasta conseguir el producto como un sólido blanco (380 mg, 33 %).

IR (KBr, cm^{-1}): 534, 583, 729, 824, 898, 992, 1043, 1107, 1245, 1374, 1462, 1551, 1596, 2849, 2916, 3054

RMN: *^{1}H* – ($CDCl_3$): δ 0.81 (t, J_{HH} = 6.56 Hz, 3H, C**H$_3$** terminal), δ 1.1 – 1.7 (m, 22H, C**H$_2$** intermedios), δ 2.37 (s, 3H, py-4-C**H$_3$**), δ 2.62 (t, J_{HH} = 7.77 Hz, 2H, py-4'-C**H$_2$** contiguo), δ 7.07 (m, 2H, C**H** pos-5), δ 8.17 (m, 2H, C**H** pos-3), δ 8.48 (m, 2H, C**H** pos-6). *RMN $^{13}C^{1}\{H\}$* – ($CDCl_3$): δ 14.0 (**C**H_3 terminal), δ 21.0 (py-4-C**H$_3$**), δ 22-32 (**C**H_2 intermedios), δ 35.4 (py-4'-**C**H_2 contiguo), δ 121.3 (**C**-5'), δ 122.0 (**C**-5), δ 123.8 (**C**-3'), δ 124.5 (**C**-3), δ 148.6 (**C**-4 & 4'), δ 153.0 (**C**-6 & 6'), δ 155.6 (**C**-2 & 2').

Análisis elemental calculado ($C_{24}H_{36}N_2$): C, 81.76; H, 10.29; N, 7.95. *Experimental*: C, 80.94; H, 9.95; N, 7.80 %.

3.5 Complejos de Metiltrioxorenio en la Epoxidación Catalítica de Olefinas bajo Condiciones Apolares

3.5.1 [$Re(CH_3)(O)_3(A)$], 1a

En un tubo de Schlenck que contiene 17.9 mg de MTO (0.07182 mmol) se adiciona, bajo nitrógeno, una disolución del polímero **A** en Cl_2CH_2 (10 ml), originándose una disolución amarilla pálida que se calienta a 40 ºC durante 4 horas. Transcurrido este tiempo se elimina el disolvente mediante la aplicación de vacío dando lugar a un aceite marrón que contiene al compuesto **1a** junto a otras impurezas. La purificación del producto se realiza adicionando etanol seco (10 ml) sobre el aceite y calentando la mezcla resultante a 40 ºC durante 4 horas. Tras la evaporación del etanol, el aceite resultante se extrae con hexano (10 ml), se separan los sólidos insolubles por decantación y se vuelve a llevar a sequedad, dando lugar al complejo de renio **1a** en forma de aceite de color marrón (47.3 mg). El cálculo, a través de RMN de ^1H, indicó una proporción de 16.5 grupos $Si(CH_3)_2$ por cada piridilo terminal y, de éstos, un 75% coordinados a unidades de MTO, lo que significa aproximadamente un rendimiento del 42 %.

IR (cm^{-1}): 3414, 6052, 2962, 2905, 1944, 1638, 1618, 1561, 1498, 1414, 1257, 1016, 912, 795, 703.

RMN: ^1H (C_6D_6): δ 0.39 (s, 84H, $Si(CH_3)_2$), 0.79 (t, J_{HH} = 8.79 Hz, 2H, py-C$H_2$$CH_2$-Si), 1.65 (s, 3H, $ReCH_3$), 2.46 (t, J_{HH} = 8.6 Hz, 2H, py-CH_2CH_2-Si), 6.76 (m, 2H, *m*-NC_5H_4), 8.45 (m, 2H, *o*-NC_5H_4). $^{13}C\{^1H\}$ (C_6D_6): δ 0 - 2 (varios s, $Si(CH_3)_2$), 18.6 (s, py-$CH_2$$CH_2$-Si), 23.9 (s, $ReCH_3$), 28.7 (s, py-$CH_2$$CH_2$-Si), 123.7 (s, *m*-$NC_5H_4$), 148.0 (s, *o*-$NC_5H_4$), 155.1 (s, *p*-$NC_5H_4$). $^{29}Si\{^1H\}$ ($CDCl_3$): δ –21.3 - –22.1, –20.8 (varios s, O-*Si*$(CH_3)_2$-O), –10.7 (s a, CH_2CH_2-*Si*$(CH_3)_2$-O).

Análisis elemental calculado ($C_{41}H_{110}NO_{19}ReSi_{16.5}$): C, 31.35; H, 7.06; N, 0.89. *Experimental:* C, 36.54; H, 7.85; N, 1.45 %.

3.5.2 [Re(CH$_3$)(O)$_3$(B)], 1b

Sobre una disolución de MTO (30.5 mg, 0.122 mmol) en Cl_2CH_2 (5 mL), se adiciona una disolución de 4-tridecilpiridina (**B**) (32 mg, 0.122 mmol) en Cl_2CH_2 (5 mL), observándose un cambio inmediato en el color de la disolución que se torna amarilla pálida. El compuesto **1b** se aísla en forma de sólido amarillo mediante la evaporación del disolvente bajo vacio. El sólido se purifica mediante recristalización, disolviéndolo en la mínima cantidad de Cl_2CH_2 y enfriando la disolución resultante a –23 ºC durante una noche (15.6 mg, 25 %).

IR (KBr, cm^{-1}): 723, 816, 844, 927, 1021, 1066, 1214, 1427, 1465, 1560, 1614, 2852, 2920, 3422

RMN: ^{1}H ($CDCl_3$): δ 0.81 (t, J_{HH} = 6.6 Hz, 3H, C***H*****$_3$**), 1.1 - 1.6 (m, 22H, C***H*****$_2$**), 1.86 (s, 3H, ReC***H*****$_3$**), (t, J_{HH} = 7.8 Hz, 2H, C***H*****$_2$**CH_3), 7.12 (d, J_{HH} = 6.0 Hz, 2H, *m*-NC_5***H***$_4$), 8.15 (d, J_{HH} = 6.3 Hz, 2H, *o*-NC_5***H***$_4$). ^{13}C{^{1}H} ($CDCl_3$): δ 14.1 (s, ***C***H_3), 22 - 32 (s, ***C***H_2 & Re***C***H_3), 125.0 (s, *m*-NC_5H_3), 147.0 (s, *p*-NC_5H_3), 155.0 (s, *o*-NC_5H_3).

Análisis elemental calculado ($C_{19}H_{34}NO_3Re$): C, 44.69; H, 6.71; N, 2.74. *Experimental*: C, 43.88 ; H, 6.76 ; N, 2.52 %.

3.5.3 Procedimiento general de la reacción de epoxidación de olefinas en ausencia de disolvente o en disolvente orgánico

Todas las experiencias que no requieren presión en el interior del reactor se realizaron en ampollas de vidrio de 50 mL provistas de llave de tipo Young. El reactor se carga con correspondiente complejo de renio que actúa como precatalizador, que se adiciona una vez preformado o, alternativamente, se prepara "*in-situ*" en la mezcla de reacción adicionando MTO y el correspondiente ligando nitrogenado. Seguidamente, se adiciona la olefina, el peróxido de hidrógeno (generalmente en disolución acuosa al 30%) y, cuando la reacción lo requiere, el correspondiente disolvente orgánico. Debido a la naturaleza de las reacciones investigadas no es necesaria la utilización de atmósfera inerte; no obstante, para evitar pérdidas de reactivos o productos durante la reacción la ampolla debe permanecer sellada. En los casos en los que se requiere calentamiento se utiliza un baño termostatizado de aceite. Finalizada la reacción, el reactor se enfría durante 5 min. en un baño de hielo antes de proceder a su apertura. Se emplearon dos

métodos analíticos alternativos para calcular el rendimiento de la reacción; mayoritariamente la técnica de cromatografía de gases (GC) y, en ciertas ocasiones, la técnica de resonancia magnética nuclear (RMN).

Para el caso de reacciones analizadas mediante GC, se diluye la mezcla de reacción con Et_2O, se adiciona una cantidad precisa del correspondiente estándar interno y se seca con $MgSO_4$ la disolución resultante, antes del análisis. El análisis se realiza en un Cromatógrafo Varian CP-3800 utilizando el propio Programa descrito en el apartado 3.1.2, utilizando dodecano como estándar interno.

En las reacciones analizadas mediante la técnica de RMN la mezcla de reacción se lleva a sequedad, se adiciona Cl_3CD al crudo de reacción, se adiciona hexametildisiloxano como estándar y se filtra, previamente al análisis. Los rendimientos se calculan mediante comparación de las integrales de ^1H RMN de los protones de C-1 y C-2 en el alqueno y el epóxido, respectivamente, utilizando la integral de los protones estándar interno para calcular los rendimientos.

3.5.4 Procedimiento de la reacción de epoxidación de propileno en octano

Estas reacciones se realizaron en un reactor de vidrio de alta presión modelo Lab Crest®. En el reactor se introduce octano (10 mL) y las cantidades especificadas del MTO, la base nitrogenada (si se emplea), y el H_2O_2 acuoso (30 %). Se sella el reactor y se aplica vacio estático. Después se introduce propileno hasta la presión requerida. Este proceso se debe realizar rápidamente porque el propileno es bastante soluble en el octano y la presión baja rápidamente después de introducirlo. Se agita, notando el descenso de la presión. Finalizada la reacción, el reactor se enfría en hielo antes de abrirse, debido a la alta volatilidad del óxido de propileno. Se abre primero la válvula para quitar la presión de propileno y después el reactor, introduciendo a la disolución dodecano como estándar. De la disolución estandarizada se toma una muestra, que se analiza inmediatamente por cromatografía de gases.

3.6 Oxobisperoxocomplejos de molibdeno en la Epoxidación Catalítica de Olefinas

3.6.1 Disolución del $[Mo(O)(O_2)_2(H_2O)_n]$ en peróxido de hidrógeno acuoso

La disolución del acuocomplejo de oxobisperoxocomplejos de molibdeno $[Mo(O)(O_2)_2(H_2O)_n]$ en peróxido de hidrogeno acuoso, utilizado en este trabajo, ha sido preparada siguiendo el procedimiento de síntesis habitual. Una suspensión de MoO_3 (2,52 g, 17,5 mmol) en 12 ml de peróxido de hidrógeno al 30 % se calienta a 55 ºC durante aproximadamente 1 hora. Transcurrido este tiempo se observa el trióxido de molibdeno completamente disuelto en una disolución amarilla y clara. A ésta se adiciona varias gotas de peróxido de hidrógeno y se adiciona agua destilada hasta un volumen exacto de 25 ml, almacenándose a 4 ºC para evitar la descomposición en la mezcla del peróxido de hidrógeno en exceso. De esta manera se prepara una disolución de concentración 834 mM en [Mo]. La disolución resultante contine varias especies en equilibrio dependiendo de varios factores como concentración, pH y temperatura.[224] En este trabajo se han considerado como una disolución del $[Mo(O)(O_2)_2(H_2O)_n]$ por razón de simplicidad.

3.6.2 $[Mo(O)(O_2)_2(A)_2]$, 2a

A (150 mg, 0,03 mmol) se disuelve en cloroformo (10 mL) y a esta disolución se añade $[Mo(O)(O_2)_2(H_2O)_n]$ acuoso (0.7 M, 0,015 mmol, 21,4 µL). Se forman dos fases y la mezcla se agita durante 30 min. Después se separan los dos fases y la fase orgánica se seca ($MgSO_4$), se filtra y la disolución amarilla resultante se evapora en el rotavapor dejando el producto crudo como un aceite amarillo. Este se purifica por extracción con pentano (2 x 5 mL) que se separa del precipitado empleando una pipeta Pasteur. El disolvente se elimina por aplicación de vacío durante 2 horas obteniéndose el producto como un aceite viscoso de color amarillo. En la cadena PDMS ($[O\text{-}Si(CH_3)_2]_n$) del producto se determina un valor de n de 8,7.

IR (KBr, cm^{-1}): 706, 801, 862, 905, 958, 1023, 1098, 1213, 1262, 1496, 1635, 2963, 3101, 3448.

RMN: ^{1}H ($CDCl_3$): δ 0,00 (s, $Si(CH_3)_2$), 7,07 (a, 2H, *m*-NC_5H_4), 8,09 (a, 2H, *o*-NC_5H_4). $^{13}C\{^{1}H\}$ ($CDCl_3$): δ 0,0 (s, $Si(CH_3)_2$). $^{29}Si\{^{1}H\}$ ($CDCl_3$): δ –22,0 (s, O-*Si*$(CH_3)_2$-O)

Análisis Elemental Calculado (Formula calculada para un valor de n = 8,7: $MoC_{31,4}H_{68,2}N_2O_{13,7}Si_{8,7}$): Mo, 5,18; C, 34,68; H, 7,32; N, 1,51. *Experimental:* Mo, 5,18; C, 30.35; H, 6.85; N, 1.36 %.

3.6.3 [Mo(O)$(O_2)_2(H_2O)$(BO)], 2b

Sobre una disolución de 4-tridecilpiridina (**B**) (50 mg, 0,19 mmol) en metanol (15 ml) se adiciona gota a gota una disolución acuosa del acuocomplejo [Mo(O)$(O_2)_2(H_2O)_n$] (1 equiv., 273 µL, 0,191 mmol) y la mezcla resultante se deja con agitación durante 30 minutos. Transcurrido este tiempo, el precipitado se recoge por filtración, lavando el producto con agua destilada fría. El producto, compuesto **B**, se obtiene en forma de sólido amarillo pulverulento.

IR (KBr, cm^{-1}): 533, 588, 618, 639, 744, 814, 856, 920, 959, 969, 1065, 1213, 1376, 1426, 1467, 1508, 1610, 1639, 2850, 2918, 3085, 3449.

RMN: ^{1}H ($CDCl_3$): δ 0.81 (t, 6H, J_{HH} = 6.6 Hz, C***H*₃**), 1.0 - 1.7 (m, 22H, C***H*₂**), 2.64 (t, 2H, C***H*₂**-CH**₃**), 7.38 (a, 2H, *m*-NC_5H_4), δ 8.67 (a, 2H, *o*-NC_5H_4). $^{13}C\{^{1}H\}$ ($CDCl_3$): δ 14.1 (s, *C*H_3), 22 - 30 (s, *C*H_2), 31.9 (s, *C*H**₂**-CH**₃**).

Análisis elemental calculado ($MoC_{18}H_{33}O_7N$): C, 45.86; H, 7.06; N, 2.94. *Experimental:* C, 45.23; H, 6.61; N, 2.96 %.

3.6.4 [Mo(O)$(O_2)_2$(E)], 2e

Se sigue un procedimiento similar al descrito en el Apartado 3.6.3.

IR (KBr, cm^{-1}): 660, 723, 764, 836, 861, 948, 1031, 1420, 1467, 1610, 2850, 2920, 3058, 3117, 3432.

RMN: ^{1}H ($CDCl_3$): δ 0.80 (t, J_{HH} = 6.32 Hz, 6H, C***H*₃**), 1.1 - 1.9 (m, 44H, C***H*₂**), 2.62, 2.85 (t, J_{HH} = 7.71, 7.76 Hz respectivamente, 4H, py-C***H*₂**-$C_{12}H_{25}$), 7.19, 7.61 (d, 2H, NC_5H_3), 7.81, 8.10 (s, 2H, NC_5H_3), 8.21, 9.36 (d, 2H, NC_5H_3). $^{13}C\{^{1}H\}$ ($CDCl_3$): δ

14.1 (s, *C*CH_3), 22 - 32 (s, *C*CH_2), 35.6, 36.0 (s, py-*C*H_2-$C_{12}H_{25}$), 121.0, 122.8, 126.7, 126.8, 147.4, 147.8, 154.1, 155.1, 156.4, 160.8 (s, N*C*$_5H_3$).

Análisis elemental calculado ($MoC_{36}H_{60}O_5N_2$): C, 62,05; H, 8,68; N, 4,02. *Experimental:* C, 61,56; H, 8.75; N, 3,97 %.

3.6.5 [Mo(O)(O_2)$_2$(F)], 2f

Se sigue un procedimiento similar al descrito en el Apartado 3.6.3.

IR (KBr, cm^{-1}): 622, 655, 691, 776, 843, 866, 946, 1030, 1219, 1252, 1420, 1603, 2899, 2954, 3447.

RMN: ^{1}H ($CDCl_3$): δ 0.00, 0.12 (s, 36H, Si(C***H*****$_3$**)$_3$), 1.68, 1.95 (s, 2H, C***H***), 6.82, 7.22 (m, 2H, NC_5H_3), 7.38, 7.64 (m, 2H, NC_5H_3), 8.00, 9.14 (d, 2H, NC_5H_3).

Análisis elemental calculado ($MoC_{24}H_{44}O_5N_2Si_4$): C, 44.42; H, 6.83; N, 4.32. *Experimental:* C, 43,67; H, 6,66; N, 4,32 %.

3.6.6 [Mo(O)(O_2)$_2$(G)], 2g

Se sigue un procedimiento similar al descrito en el Apartado 3.6.3.

IR (KBr, cm^{-1}): 689, 758, 778, 842, 866, 942, 988, 1036, 1250, 1420, 1610, 2899, 2952, 3447.

RMN: ^{1}H ($CDCl_3$): δ 0.00, 0.08 (s, 36H, Si(C*H*$_3$)$_3$), 0.11, 0.28 (t, J_{HH} = 6.29, 6.42 Hz, 2H, C*H*), 2.75, 2.97 (d, J_{HH} = 6.30, 6.42 Hz, 4H, C*H*$_2$), 7.11, 7.53 (d, 2H, NC_5H_3), 7.69, 7.97 (s, 2H, NC_5H_3), 8.10, 9.25 (d, 2H, NC_5H_3). ^{13}C{^{1}H} ($CDCl_3$): δ 0.0, 0.1 (Si(CH_3)$_3$), δ 14.6, 15.0 (CH), δ 31.8, 32.4 (CH_2), δ 120.6, 122.4 (C-5), δ 126.2, 126.5 (C-3), δ 147.3, 147.5 (C-4), δ 153.7, 158.6 (C-6), δ 154.9, 163.1 (C-2).

Análisis elemental calculado ($MoC_{26}H_{48}O_5N_2Si_4$): C, 46.13; H, 7.15; N, 4.14. *Experimental:* C, 47.13; H, 7.14; N, 4.50 %.

3.6.7 [Mo(O)(O_2)$_2$(H)], 2h

Se sigue un procedimiento similar al descrito en el Apartado 3.6.3.

IR (KBr, cm^{-1}): 661, 723, 836, 863, 947, 1032, 1242, 1308. 1420, 1467, 1610, 2850, 2920, 2956, 3448.

RMN: ^{1}H – ($CDCl_3$): δ 0.88 (t, J_{HH} = 6.0 Hz, 3H, CH_3 terminal), 1.2 – 1.9 (m, 24H, CH_2 intermedios), 2.46, 2.70 (s, 3H, py-4-CH_3), 2.68, 2.91 (t, J_{HH} = 7.7 Hz, 2H, py-4'-CH_2-$C_{12}H_{25}$), 7.18, 7.61 (m, 2H, C*H* pos-5), 7.85, 8.12 (m, 2H, C*H* pos-3), 8.19, 9.34 (m, 2H, C*H* pos-6). RMN $^{13}C^{1}\{H\}$ – ($CDCl_3$): δ 14.0 (*C*H_3 terminal), 22.5 (py-4-*C*H_3), 28-36 (*C*$_{12}H_{24}$-CH_3), 120-161 (*C*-piridilo).

Análisis elemental calculado ($MoC_{24}H_{36}O_5N_2$): C, 54,54; H, 6,87; N, 5,30. *Experimental:* C, 55,15; H, 6,80; N, 5,22 %.

3.6.8 [Mo(O)(O_2)$_2$(H_2O)(pyO)] [178(b)]

Una suspensión de MoO_3 (375 mg, 2.6 mmol) en peróxido de hidrógeno al 30 % (2 mL, ~20 mmol) se calienta a 50 ºC durante una hora originando una disolución amarilla y clara del [$MoO(O)_2(H_2O)_n$]. Sobre esta disolución, enfriada a 0 ºC en un tubo de ensayo, se adiciona piridina (2 equiv., 400 μL, 5.2 mmol). La mezcla de reacción se homogeniza por la aplicación de ultrasonido y posteriormente se adiciona acetona (2.5 mL), mezclándose con la disolución acuosa por ultrasonido. La disolución resultante se deja a cristalizar a 0 ºC observando la precipitación del producto como un sólido amarillo y microcristalino entre 24 h. Esto se filtra, se limpia con agua fría y acetona y se seca en vacio (420 mg, 1.45 mmol, 56 %).

IR (KBr, cm^{-1}): 629, 729, 762, 859, 896, 960, 1006, 1061, 1172, 1204, 1254, 1323, 1387, 1488, 1545, 1635, 2128, 2808, 2966, 3067, 3090, 3406.

Análisis elemental calculado ($C_5H_7MoNO_7$) C, 20,78; H, 2,44; N, 4,85. *Experimental*: C, 20,40; H, 2.83; N, 5,13 %.

3.6.9 [Mo(O)(O_2)$_2$(H_2O)(2pcO)]

Se sigue un procedimiento similar al descrito en el Apartado 3.6.8 obteniéndose el producto como un sólido amarillo y microcristalino (425 mg, 1.40 mmol, 54 %).

IR (KBr, cm^{-1}): 626, 764, 858, 951, 1051, 1116, 1168, 1207, 1291, 1458, 1492, 1539, 1617, 2042, 2730, 3058, 3259, 3453.

Análisis elemental calculado ($MoC_6H_9O_7N$): C, 23,78; H, 2,99, N, 4,62. *Experimental*: C, 25,29; H, 2,87; N, 5,17 %.

3.6.10 [Mo(O)(O$_2$)$_2$(H$_2$O)(3pcO)]

Se sigue un procedimiento similar al descrito en el Apartado 3.6.8 obteniéndose el producto como un sólido amarillo y cristalino (585 mg, 1.93 mmol, 74 %).

IR (KBr, cm^{-1}): 682, 796, 860, 959, 1124, 1188, 1266, 1476, 1616, 3433.

Análisis elemental calculado ($MoC_6H_9O_7N$): C, 23,78; H, 2,99, N, 4,62. *Experimental*: C, 23,08; H, 3,55; N, 4,77 %.

3.6.11 [Mo(O)(O$_2$)$_2$(H$_2$O)(lutO)]

Se sigue un procedimiento similar al descrito en el Apartado 3.6.8 obteniéndose el producto como un sólido crema y cristalino (480 mg, 1.52 mmol, 58 %).

IR (KBr, cm^{-1}): 638, 799, 847, 856, 962, 979, 1052, 1172, 1274, 1377, 1399, 1457, 1539, 1627, 1639, 1656, 1869, 2841, 2895, 2962, 3081, 3190, 3280, 3309, 3446.

Análisis elemental calculado ($MoC_7H_{11}O_7N$): C, 26,51; H, 3,50; N, 4,42. *Experimental*: C, 28,08; H, 3,38; N, 4,98 %.

3.6.12 [Mo(O)(O$_2$)$_2$(H$_2$O)(colO)]

Se sigue un procedimiento similar al descrito en el Apartado 3.6.8 obteniéndose la primera fracción como un sólido amarillo pálido y cristalino (1.63 g, 4.9 mmol, 14 %).

IR (KBr, cm^{-1}): 629, 712, 762, 851, 869, 959, 975, 1001, 1035, 1050, 1161, 1276, 1330, 1371, 1371, 1430, 1473, 1635, 1652, 2588, 2736, 2847, 2882, 3058, 3302, 3446.

Análisis elemental calculado ($MoC_8H_{13}O_7N$): C, 29,02; H, 3,96; N, 4,23. *Experimental*: C, 31,14; H, 4,02; N, 4,66 %.

3.6.13 $[(O)(O_2)_2Mo(\mu^2\text{-}O)Mo(O)(O_2)_2]^{2-} \cdot 2[colH]^+$ [196]

En una matraz Erlenmeyer de 250 mL se mezclan trióxido de molibdeno (5.0 g, 35 mmol) y peróxido de hidrogeno acuoso (30 %) (14 equiv., 50 mL, 490 mmol). Se calienta a 55 ºC manteniendo agitación hasta que todo del molibdeno se ha disuelto, obteniéndose una disolución amarilla y clara que se enfría a 0 ºC. A esta se adiciona lentamente colidina (2 equiv., 9.2 mL, 70 mmol) y la mezcla se agita durante 1 h. Posteriormente se deja a cristalizarse a 4 ºC durante 3 semanas hasta que el producto se obtiene como cristales claros y grandes.

IR (KBr, cm^{-1}): 501, 517, 530, 546, 578, 609, 628, 712, 851, 869, 959, 975, 1001, 1035, 1051, 1276, 1432, 1636, 1653, 2746, 2846, 2883, 3058, 3302.

Análisis elemental calculado ($Mo_2C_{16}H_{24}O_{11}N_2$): Mo, 31,34; C, 31,39; H, 3,95; N, 4,58. *Experimental:* Mo, 29.55; C, 31,03; H, 4,39; N, 4,80 %.

3.6.14 $[Mo(O)(O_2)_2(bpy)]$ [184]

En una matraz Erlenmeyer de 250 mL se mezclan trióxido de molibdeno (5.0 g, 35 mmol) y peróxido de hidrogeno acuoso (30 %) (14 equiv., 50 mL, 490 mmol). Se calienta a 55 ºC manteniendo la agitación hasta que todo el compuesto de molibdeno se ha disuelto, obteniéndose una disolución amarilla y clara que se enfría a 0 ºC. A ésta se adiciona una disolución de 2,2'-bipiridina (1 equiv., 5.47 g, 35 mmol) en metanol (10 mL) y la mezcla resultante se agita durante 10 minutos observándose la precipitación del producto como un sólido amarillo. Después de este tiempo el producto se recoge por filtración, lavándose con agua fría y secándose durante 4 horas bajo vació para obtener el producto como un sólido amarillo pulverulento (10.9 g, 94 %).

IR (KBr, cm^{-1}): 536, 581, 651, 668, 729, 770, 858, 939, 1021, 1032, 1045, 1065, 1103, 1160, 1175, 1220, 1245, 1314, 1444, 1472, 1495, 1569, 1599, 3081.

Análisis elemental calculado ($MoC_{10}H_8O_5N_2$): Mo, 28.89; C, 36.16; H, 2.43; N, 8.43. *Experimental*: Mo, 24.67; C, 36.11; H, 2.51; N, 8.44 %.

3.6.15 [Mo(O)(O_2)$_2$($bpyO_2$)]

En una matraz Erlenmeyer de 25 mL se mezclan trióxido de molibdeno (155 mg, 1.06 mmol) y peróxido de hidrogeno acuoso (30 %) (16 equiv., 1.6 mL, 15.6 mmol). Se calienta a 55 ºC manteniendo la agitación hasta que todo el compuesto de molibdeno se ha disuelto, obteniéndose una disolución amarilla y clara que se enfría a 0 ºC. A ésta se adiciona una suspensión de 2,2'-bipiridina-N,N'-dióxido (1 equiv., 200 mg, 1.06 mmol) en metanol (3 mL) y la mezcla resultante turbia y amarilla se agita durante 10 minutos. Después de este tiempo el producto se recoge por filtración, lavándose con agua fría y secándose durante 4 horas bajo vació para obtener el producto como un sólido amarillo pulverulento (335 mg, 92 %).

IR (KBr, cm^{-1}): 486, 523, 543, 581, 651, 720, 736, 777, 837, 847, 859, 952, 1035, 1100, 1119, 1158, 1200, 1228, 1243, 1258, 1295, 1425, 1445, 1475, 1606, 1622, 3056, 3088.

Análisis elemental calculado ($MoC_{10}H_{10}O_5N_2$): Mo, 26.35; C, 32.99; H, 2.21; N, 7.69. *Experimental*: Mo, 28.86; C, 31.77; H, 2.25; N, 7.48 %.

3.6.16 [Mo(O)(O_2)$_2$(phen)]

Se sigue un procedimiento similar al descrito en el Apartado 3.6.8 pero adicionando solo un equivalente de fenantrolina a la disolución del [Mo(O)(O_2)$_2$(H_2O)$_n$] obteniéndose el producto como un polvo amarillo.

IR (KBr, cm^{-1}): 659, 721, 740, 767, 847, 864, 914, 949, 986, 999, 1035, 1111, 1149, 1199, 1230, 1311, 1345, 1427, 1517, 1581, 1589, 1627, 3051, 3384.

Análisis elemental calculado ($MoC_{12}H_8N_2O_5$): C, 40,47; H, 2,26; N, 7,87. *Experimental*: C, 44,43; H, 2,84; N, 8,87 %.

3.6.17 [Mo(O)(O_2)$_2$(pz)$_2$]

Una suspensión de MoO_3 (5.00 g, 34.7 mmol) en peróxido de hidrógeno al 30 % (14 equiv., 50 mL, 490 mmol) se calienta a 55 ºC durante una hora originando una disolución amarilla y clara del derivado [$MoO(O)_2(H_2O)_n$]. Sobre esta disolución,

enfriada a 0 ºC, se adiciona, lentamente, pirazol (2 equiv., 4,72 g, 69,4 mmol). La mezcla de reacción se deja agitándose a 0 ºC varias horas. Posteriormente el sólido amarillo, pálido y microcristalino se aísla mediante filtración (5.72 g, 16.6 mmol, 48 %). El filtrado se deja a cristalizar durante 2 días obteniendo las siguientes fracciones en la forma de cristales adecuados para la determinación estructural mediante difracción de rayos X. El producto es estable al aire y puede almacenarse durante semanas en un vial sin observarse descomposición apreciable.

IR (KBr, cm^{-1}): 535, 580, 608, 652, 714, 762, 789, 852, 875, 912, 963, 1044, 1055, 1076, 1128, 1146, 1172, 1254, 1284, 1355, 1399, 1466, 2818, 2875, 2924, 2989, 3042, 3127, 3148, 3328.

Análisis elemental calculado ($MoC_6H_8O_5N_4$): Mo, 30.74; C, 23.09; H, 2.58; N, 17.95. *Experimental:* Mo, 29.05; C, 22.27; H, 2.58; N, 18.02 %.

3.6.18 $[Mo(O)(O_2)_2(H_2O)(pz)]$ [180]

Se sigue un procedimiento similar al descrito en el apartado anterior, pero adicionando solo 1 equivalente de pirazol sobre la disolución acuosa de $[MoO(O)_2(H_2O)_n]$. Se filtra la mezcla resultante y la disolución se guarda a 4 ºC durante unas días hasta que se forman cristales amarillos del producto adecuados para la determinación estructural mediante difracción de rayos X (3,23 g, 12.3 mmol, 36 %).

IR (NaCl, cm^{-1}): 577, 654, 781, 830, 951, 1057, 1082, 1142, 1170, 1279, 1355, 1407, 1526, 1628, 2990, 3150, 3418

Análisis elemental calculado ($MoC_3H_6O_6N_2$): Mo, 36,61; C, 13,75; H, 2,31, N, 10,69. *Experimental*: Mo, 34,65; C, 12,91; H, 2,38; N,10,59 %.

3.6.19 $[Mo(O)(O_2)_2(dmpz)_2]$ [181]

Se sigue un procedimiento similar al descrito en el Apartado 3.6.17, Con la adición del 3,5-dimetilpirazol el producto precipita inmediatamente de la mezcla de reacción en forma de sólido pulverulento de color amarillo (6.76 g, 18.4 mmol, 53 %). El compuesto se descompone al aire dando lugar a un sólido marrón. La

descomposición del producto se hace más lenta, pero no se evita, guardándose bajo nitrógeno.

IR (KBr, cm^{-1}): 532, 586, 659, 668, 701, 742, 815, 860, 878, 957, 1023, 1040, 1061, 1096, 1150, 1230, 1276, 1413, 1576, 2872, 2929, 2973, 3039, 3140, 3206, 3325.

Análisis elemental calculado ($MoC_{10}H_{16}O_5N_4$): Mo, 26.06; C, 32.62; H, 4.38; N, 15.22. *Experimental:* Mo, 24.05; C, 32.01; H, 4.36; N, 14.54 %.

3.6.20 $[Mo_8(O)_{22}(O_2)_4(dmpz)_2]^{4-}\cdot 4[(dmpzH)]^{+}\cdot 2H_2O$

El $[Mo(O)(O_2)_2(dmpz)_2]$ se disuelve en una mezcla 1:1 de agua y 2-propanol, dejando la disolución resultante a evaporar lentamente a 4 ºC. Se obtienen cristales pequeñas y amarillos de la recristalización. En contraste con el complejo oxobisperoxo el producto es estable al aire en una vial durante meses.

IR (KBr, cm^{-1}): 505, 558, 596, 629, 676, 852, 893, 952, 1055, 1156, 1286, 1402, 1528, 1570, 1610, 2853, 2925, 3130, 3374.

Análisis elemental calculado ($Mo_8C_{36}H_{108}N_{12}O_{32}$): Mo, 38,59; C, 21,74; H, 5,47; N, 8,45. *Experimental:* C, 20,96; H 3,85; N 9,05 %.

3.6.21 $[Mo_4O_{16}(dmpz)_6].CH_2Cl_2$

Se mezclan disoluciones del $[Mo(O)(O_2)_2(H_2O)_n]$ acuoso y 3,5-dimetilpirazol en diclorometano. Se forma un sistema bifásico que se agita durante 30 minutos, notando la transferencia de color de la fase acuosa a la orgánica. Tras este tiempo la fase orgánica se separa y se seca ($MgSO_4$), se filtra y se deja cristalizar en un tubo de ensayo a aproximadamente -15 ºC. Al cabo de un año, los cristales que se han formado se separan y se lavan con acetona, secándolos al aire. El producto se obtiene como cristales grandes de color naranja.

IR (KBr, cm^{-1}): 631, 668, 745, 853, 903, 956, 967, 1027, 1051, 1151, 1180, 1272, 1299, 1374, 1410, 1472, 1572, 1616, 2856, 2926, 3132, 3420.

Análisis elemental ($Mo_4C_{31}H_{50}N_{12}O_{16}Cl_2$) C, 28,61; H, 3,87; N, 12,91. *Experimental:* C, 28,50; H, 4,25; N, 12,67 %.

3.6.22 Reacción del $[Mo(O)(O)_2(H_2O)_n]/H_2O_2$ acuoso con 4-metilimidazol a 0 ºC

Una suspensión de MoO_3 (2,50 g, 17,4 mmol) en peróxido de hidrógeno al 30 % (14 equiv., 25 mL, 245 mmol) se calienta a 55 ºC durante una hora originando una disolución amarilla y clara del derivado $[MoO(O)_2(H_2O)_n]$. Sobre esta disolución, enfriada a 0 ºC, se adiciona, lentamente, 4-metilimidazol (2 equiv., 2,85 g, 34,7 mmol). Se observa la formación de una disolución de color rojo intenso y un aceite oscuro insoluble. La mezcla de reacción se mantiene a 0 ºC durante varias horas hasta que se observa la desaparición del aceite, momento en el cual se lleva lentamente a 4 ºC. La disolución resultante se deja a cristalizar precipitando un sólido amarillo pulverulento que se aísla mediante filtración (485 mg, 1.9 mmol [Mo], 11 %). El producto presenta una buena solubilidad en agua, pero no ha podido completarse su caracterización.

IR (KBr, cm^{-1}): 520, 537, 572, 616, 740, 855, 869, 948, 1368, 1386, 1405, 1448, 1597, 2852, 3218.

RMN: ^1H (D_2O): δ 8.38 (s)

Análisis elemental calculado ($MoO_5N_5H_{10}$): Mo, 37.92; H, 2.79; N, 27.68. *Experimental*: Mo 37.75, C 2.73, H 2.76, N 27.22 %.

3.6.23 Reacción del $[Mo(O)(O)_2(H_2O)_n]/H_2O_2$ acuoso con 4-metilimidazol a 50 ºC

Una suspensión de MoO_3 (2,50 g, 17,4 mmol) en peróxido de hidrógeno al 30 % (14 equiv., 25 mL, 245 mmol) se calienta a 55 ºC durante una hora originando una disolución amarilla y clara del derivado $[MoO(O)_2(H_2O)_n]$. Sobre esta disolución, enfriada a 0 ºC, se adiciona, lentamente, 4-metilimidazol (2 equiv., 2,85 g, 34,7 mmol). Se observa la formación de una disolución de color rojo intenso y un aceite oscuro insoluble. La mezcla de reacción se mantiene a 0 ºC durante varias horas hasta que se observa la desaparición del aceite, momento en el cual se lleva a 50 ºC durante media hora observándose un cambio de color a amarillo. La disolución resultante se divide en dos. La primera mitad de esta disolución se deja evaporar lentamente a temperatura ambiente, precipitando un sólido blanco cristalino en un aceite amarillo y viscoso, notándose un olor a formaldehido. El sólido se aísla mediante filtración, lavándose con acetona fría y se identifica como 1-acetilurea (62 mg, 0.61 mmol, 7 %). La otra mitad se deja cristalizar durante varias semanas en un recipiente abierto a 4 ºC, precipitando un

sólido amarillo cristalino que se aísla mediante filtración y que se ha caracterizado como una sal que contiene al anión heptamolibdato (356 mg, 1.6 mmol [Mo], 18 %).

1-Acetilurea

IR (KBr, cm^{-1}): 569, 695, 811, 942, 1033, 1098, 1254, 1368, 1418, 1482, 1670, 3226, 3331, 3379.

Análisis elemental calculado ($C_3H_6N_2O_2$): C, 35.29; H, 5.29; N, 27.44. *Experimental:* C, 32.01; H, 5.72; N, 27.22 %.

Cristales del sal heptamolibdato

IR (KBr, cm^{-1}): 470, 566, 626, 685, 784, 839, 893, 945, 1084, 1174, 1195, 1264, 1348, 1399, 1559, 1627, 1653, 1684, 1717, 3169.

Análisis elemental experimental: Mo, 42.52; C, 9.98; H, 2.41; N, 10.84 %.

3.6.24 Reacción del $[MoO(O)_2(H_2O)_n]/H_2O_2$ acuoso con imidazol a 50 ºC

Se sigue un procedimiento similar al descrito en el Apartado 3.6.23. Cuando la disolución se evapora a temperatura ambiente se observa de la misma manera que en el caso de la reacción con 4-metilimidazol, un olor a formaldehido y por evaporación resulta un aceite amarillo, pero en este caso no precipita ningún derivado de urea. Cuando la disolución se evapora lentamente a 4 ºC se forman cristales amarillos.

IR (KBr, cm^{-1}): 463, 556, 626, 673, 838, 893, 957, 1054, 1098, 1184, 1399, 1584, 1623, 1717, 2851, 3144.

Análisis elemental experimental: C, 9,95; H, 2,97; N, 9,54 %.

3.6.25 Procedimiento general de la reacción de epoxidación de olefinas en disolventes convencionales y en ausencia de disolvente.

Todos los ensayos se realizaron en ampollas de vidrio de 50 mL provistas de llave de tipo Young. Se cargan en la ampolla en orden: el disolvente, el ligando nitrogenado, el sustrato olefinico, el catalizador/precursor de molibdeno y el oxidante en las cantidades especificadas y en el mínimo tiempo necesario. Después, la ampolla se

cierra y se calienta a la temperatura especificada (en un baño de aceite con temperatura controlada por termostato) con agitación durante el tiempo de reacción. Cuando se termina la reacción, el reactor se enfría en un baño de hielo durante 5 minutos antes de abrirse para evitar la posibilidad de perder una cantidad significativa de productos volátiles. Si los productos se analizan por GC, el reactor se abre y se prepara una disolución en éter dietílico con un compuesto estándar. Esta disolución se seca ($MgSO_4$) y se analiza empleando una programa apropiado para los correspondientes analitos. Si los productos se analizan por RMN, se prepara y seca la disolución de la misma manera pero sin adicionar el estándar, y se evapora con presión reducida empleando una temperatura apropiada para los analitos. De los residuos resultantes se prepara una disolución en un disolvente deuterado, empleando el hexametilsiloxano como estándar interno. Como catalizador/precursor se emplean oxobisperoxocomplejos de molibdeno sintetizados por los métodos especificados en el Apartado 3.6 o el complejo catalítico se forma *in-situ* por la reacción de un precursor (el trióxido de molibdeno o la disolución acuosa del $[Mo(O)(O_2)_2(H_2O)_n]$) con el oxidante y los correspondientes especies coordinantes. Como oxidante terminal se utiliza peróxido de hidrógeno (en disolución acuosa al 30 %) o el aducto de urea:H_2O_2, UHP.

3.6.26 Procedimiento general de la reacción de epoxidación de olefinas en líquidos iónicos

Todos los ensayos se realizaron en ampollas de vidrio de 50 mL provistas de llave de tipo Young, procediéndose de una manera análoga a la descrita en el apartado anterior para las reacciones de epoxidación catalizadas por derivados de molibdeno en disolventes convencionales. La ampolla se carga, en primer lugar, con el correspondiente líquido iónico que, debido a su alta viscosidad, debe adicionarse con la ayuda de una jeringa. Finalizada la reacción, la mezcla se lleva a 0 ºC y se procede a la extracción de los productos mediante la utilización de un disolvente poco polar, generalmente, el dietil éter o el pentano (3 x 3 mL). Tras secar la disolución resultante con $MgSO_4$, se procede al análisis mediante GC o RMN, siguiendo el procedimiento descrito en el apartado anterior.

3.6.26.1 Reciclado del catalizador/líquido iónico

En algunos de los estudios aquí el líquido iónico junto con el catalizador se reutiliza en varios ciclos catalíticos. En estos experimentos, después de la extracción del producto, se quitan todos los residuos del oxidante no usado, sub-productos y disolventes antes de adicionarse nuevamente sustrato, oxidante y otros aditivos frescos como se especifica en el propio experimento para el próximo ciclo. En experimentos en que se emplea el UHP como oxidante, el UHP no consumido y urea resultante de su uso se quitan disolviendo la media de reacción en CH_2Cl_2 y filtrándoles por la disolución resultante (en que estos compuestos no son solubles). Después, el CH_2Cl_2 se elimina bajo vacio dejándose la disolución IL/[Mo]. En otras reacciones que emplean el H_2O_2 acuoso como oxidante, los residuos se eliminan fácilmente después de la extracción por la aplicación de vacio mediante calentamiento a 60 ºC durante una hora.

3.7 Oxidaciones aeróbicas de alcoholes catalizadas por [Cu]/TEMPO en scCO_2

El $[Cu_2(\mu^2\text{-}AcO)_4(H_2O)_2]$, utilizado en este trabajo se prepara siguiendo el procedimiento habitual de síntesis a través de la reacción del sulfato de cobre(II) con ácido acético. Por su parte, el derivado, también conocido $[Cu_2(\mu^2\text{-}AcO)_4(py)_2]$ se prepara por reacción del complejo $[Cu_2(AcO)_4(H_2O)_2]$ con piridina en etanol.

3.7.1 $[Cu_2(\mu^2\text{-}AcO)_4(4VP)_2]$ [204]

Sobre una disolución de $[Cu_2(AcO)_4(H_2O)_2]$ (0.61 g, 1.52 mmol) en etanol (30 ml) a 80 ºC, bajo atmósfera de nitrógeno, se añaden 0.34 g de 4-vinilpiridina (4VP) (3.05 mmol). Tras la adición, se observa la aparición casi instantánea de un sólido microcristalino de color verde. La suspensión resultante se enfría a temperatura ambiente y después a 0 ºC. El compuesto se aísla por filtración, se lava con etanol frío y se seca a vacío (0.74 g, 1.29 mmol, 85%).

IR (KBr, cm^{-1}): 630, 682, 799, 848, 940, 997, 1012, 1072, 1222, 1347, 1429, 1500, 1608, 1622, 3446.

Análisis elemental calculado ($Cu_2C_{22}H_{26}N_2O_8$): C, 46.07; H, 4.57; N, 4.88. *Experimental:* C, 45.80; H, 4.54; N, 4.93 %.

3.7.2 $[Cu_2(\mu^2\text{-}AcO)_4(A)_2]$, 3a

Una mezcla de $[Cu_2(AcO)_4(H_2O)_2]$ (0.38 g, 0,95 mmol) y **A** (0,89 g, 0,88 mmol) en etanol (15 ml) se calienta a 40 ºC durante 24 horas. El disolvente se elimina mediante vacío hasta obtener un residuo de color oscuro, que posteriormente se extrae con hexano. Los residuos sólidos se separan en primer lugar por filtración y las partículas más finas se eliminan a continuación por centrifugación. El hexano se evapora y se obtiene el producto crudo en forma de un aceite verde-azulado ligeramente turbio. Esta turbidez puede eliminarse definitivamente a través de la disolución del aceite en hexano, centrifugación adicional y evaporación del disolvente. De esta manera se obtiene un aceite transparente de color verde-azulado (0.70 g), que se almacena bajo vacío a 0 ºC.

Por el contenido en cobre determinado por ICP se determinó en una muestra representativa que el grupo PDMS ($[O\text{-}Si(CH_3)_2]_n$) tiene un n = 12,3)

IR (NaCl, cm^{-1}): υ(Si-O) 1092, 1026, υ(Si-CH_3) 1261, υ(O-C-O) 1429, 1615, 1629.

Análisis Elemental Calculado (Formula calculada a partir del contenido en Cu, $Cu_2C_{71}H_{175,1}N_2O_{32,5}Si_{24,5}$): Cu, 5,31; C, 35,64; H, 7,38; N, 1,17. *Experimental:* Cu, 5,31; C, 45,50; H, 9,50; N, 1,21 %.

3.7.2.1 Determinación del contenido de cobre en **3a**

Por espectroscopia UV/Vis: El contenido en cobre en el compuesto **3a** se calculó a través de espectroscopia UV-Vis haciendo uso de una recta de calibrado determinada a través de la medida de la absorbancia a 721 nm de muestras conocidas del compuesto de cobre $[Cu_2(AcO)_4(4VP)_2]$, cuyo contenido en cobre es del 22.16 %, en diclorometano en un rango de concentraciones entre el 0.3 y el 6.5 % de cobre en peso. En este método se asume que los compuestos **3a** y $[Cu_2(AcO)_4(py)_2]$ exhiben similar coeficiente de extinción dada la similitud entre ambos derivados. De esta forma, la medida de la absorbancia a 721 nm de una disolución de peso conocido del complejo **3a** en Cl_2CH_2 permite deducir para éste un porcentaje de cobre variable entre el 4 y el 6 %.

Por titulación iodométrica: Una cantidad conocida (21.3 mg) del complejo **3a** se disuelve en hexano (5 mL) y a esta disolución se adiciona agua (10 mL) y tres gotas de ácido sulfúrico concentrado. La fase acuoso resultante se separa de la fase orgánica y se adiciona NH_3 acuoso 5% gota por gota hasta que la disolución se hace básica. La disolución se reacidifica con ácido acético 10% y se adiciona un exceso de KI y unas gotas de una disolución de almidón como indicador. La titulación de la disolución resultante con una disolución acuosa de tiosulfato de sodio permite calcular el contenido en cobre.

3.7.2.2 Determinación de la solubilidad del derivado **3a** en $scCO_2$

La solubilidad del compuesto **3a** en $scCO_2$ se determinó "*in-situ*" a través de espectroscopia UV/Vis siguiendo el procedimiento experimental descrito en el apartado 3.2.5.2. La medida de la absorbancia a 721 nm permite deducir una concentración máxima de 1.7 mM de Cu^{2+} en $scCO_2$ a la temperatura de 40 ºC y 105 bares de presión.

3.7.3 Preparación de los catalizadores de Cu(II) soportados en sílica

A una suspensión de gel de sílice 60 (0.063 – 0.200 mm) (2.00 g) en CH_2Cl_2 seco (10 mL) se adiciona una disolución del catalizador de cobre (0.015 mmol) también en CH_2Cl_2. Se observa la adsorción instantánea del complejo sobre la sílice, coloreándose de verde-azulado la sílice dejando la disolución clara. La sílica se filtra y se seca bajo vacío durante varias horas.

3.7.4 Procedimiento general de las reacciones de oxidación de alcoholes

3.7.4.1 Procedimiento general de la reacción de oxidación de alcoholes en $scCO_2$

Las reacciones de catálisis en $scCO_2$ se llevaron a cabo, en la mayoría de los casos, en el reactor de acero de 27 mL descrito en el Apartado 3.2.2. En la mayor parte de los estudios de reactividad realizados se ha optado por introducir el alcohol separadamente del catalizador de Cu(II) y el TEMPO, siguiendo el procedimiento descrito en el Apartado 3.2.4, evitando así el inicio de la reacción antes de homogeneizar la mezcla de reacción en $scCO_2$ (ver Figura 3.5 y Figura 3.6). Tras la reacción, el sistema se despresuriza utilizando una trampa que contiene Et_2O, tal y como se describe en el Apartado 3.2.3. Una vez despresurizado el reactor, se adiciona Et_2O para extraer los productos de la reacción que restan en su interior. La disolución resultante, junto con la mezcla de la trampa (aunque en ningún ensayo la disolución de la trampa contenía cantidad detectable de ningún producto), se unen para efectuar el correspondiente análisis mediante RMN o GC. En el caso del análisis mediante GC se adiciona a la disolución etílica una cantidad precisa del correspondiente estándar interno

y se seca con $MgSO_4$ la disolución resultante antes del análisis. En el caso del análisis mediante la integración de las señales de RMN de ^1H de los productos y los reactivos, la disolución etílica se lleva a sequedad, se pesan los productos, se adiciona $CDCl_3$ al crudo de reacción y se filtra, previamente al análisis.

3.7.4.2 Procedimiento general de la reacción de oxidación de alcoholes en disolventes convencionales

Todas las experiencias se realizaron en un reactor de vidrio de alta presión modelo Lab Crest®. El reactor se carga con el complejo de cobre(II) correspondiente, el TEMPO, el disolvente (10 mL) y el alcohol, se sella el reactor, se introduce el oxígeno a la presión de trabajo y se calienta el reactor a la temperatura de reacción durante el tiempo correspondiente. Finalizada la reacción, el reactor se enfría en un baño de hielo, se despresuriza y la disolución resultante se trata depende de si el producto se analiza mediante RMN o GC de una manera similar a la descrita en el apartado anterior.

3.7.4.3 Procedimiento general de la reacción de oxidación de alcoholes en $scCO_2$ empleando los catalizadores soportados en sílica

Siguiendo un procedimiento similar al descrito en el Apartado 3.7.4.1 se introducen los reactivos al reactor, pero en este caso incorporando al reactor el catalizador soportado y el TEMPO e introduciendo el sustrato alcohólico dentro de una vial. Se precede con la reacción en la misma manera que se ha descrito antes, extrayendo los contenidos del reactor y vial con Et_2O después de la reacción y filtrándose la disolución para recuperar el catalizador-sílica. Este se lava con más Et_2O, combinando la disolución con las extracciones y tratándose para análisis en la manera previamente descrita. Si se necesita, el catalizador se puede reciclar, secándose durante una hora bajo presión reducida, volviéndose al reactor y procediendo con el próximo ciclo catalítico de la misma manera.

3.7.4.4 Procedimiento general de la reacción de oxidación de alcoholes en disolventes convencionales empleando los catalizadores soportados en sílica

Todas las experiencias se realizaron en un reactor de vidrio de alta presión modelo Lab Crest®. El reactor se carga con el catalizador de cobre(II) soportado correspondiente, el TEMPO, el disolvente (10 mL) y el alcohol, se sella el reactor, se introduce el oxígeno a la presión de trabajo y se calienta el reactor a la temperatura de reacción durante el tiempo correspondiente. Finalizada la reacción, el reactor se enfría en un baño de hielo, se despresuriza y la disolución resultante se filtra para separar el catalizador-sílica de los productos, lavando con Et_2O que se combina con la disolución anterior. La disolución resultante se trata depende de si el producto se analiza mediante RMN o GC de una manera similar a la descrita en el Apartado 3.7.4.1.

3.8 Oxidación aeróbica de alcohol catalizada por $Pd(AcO)_2$ en condiciones apolares

3.8.1 $[Pd(OAc)_2(4VP)_2]$

Sobre una disolución de diacetato de paladio[225] (112.2 mg, 0.5 mmol) en Cl_2CH_2 (10 mL) se adicionan, bajo nitrógeno, dos equivalentes de 4-vinilpiridina (4VP) (113.5 μL, 1.0 mmol), observándose la precipitación de un sólido de color amarillo. Tras agitar la mezcla durante 6 horas, se elimina el disolvente bajo vacío, para dar lugar a un sólido pulverulento de color amarillo. Tras recristalizar en la mínima cantidad de Cl_2CH_2 se obtiene el compuesto $[Pd(OAc)_2(4VP)_2]$ como un sólido microcristalino amarillo (145.7 mg, 0.335 mmol) con un rendimiento del 67 %.

IR (NaCl, cm^{-1}): 695, 853, 874, 925, 956, 995, 1012, 1033, 1076, 1306, 1377, 1454, 1598, 2853, 2923.

RMN: ^1H ($CDCl_3$): δ 1.86 (s, 3H, CH_3CO_2), 5.62 (m, 1H, Py-$CHCH_{cis}H_{trans}$[†]), 6.03 (m, 1H, Py-$CHCH_{cis}H_{trans}$[†]), 6.65 (m, 1H, Py-$CHCH_2$), 7.29 (m, 2H, *m*-NC_5H_4), 8.61 (m, 2H, *o*-NC_5H_4). $^{13}C\{^1H\}$ ($CDCl_3$): δ 23.3 (CH_3CO_2), 121.7 (Py-$CHCH_2$), δ 121.7 (*m*-NC_5H_4), 133.3 (Py-$CHCH_2$), δ 147.2 (*p*-NC_5H_4), δ 151.5 (*o*-NC_5H_4), δ 178.1 (CH_3CO_2).

Análisis elemental calculado ($PdC_{18}H_{20}N_2O_4$): C, 19.72; H, 4.64; N, 6.44. *Experimental*: C, 19.29; H, 4.76; N, 6.44 %.

3.8.2 $[Pd(AcO)_2(A)_2]$, 4a

Una mezcla de diacetato de paladio (50.0 mg, 0.22 mmol) y el polímero **A** (225 mg, 0.45 mmol) en acetona seca (10 mL) se agita a temperatura ambiente durante toda la noche. Transcurrido este tiempo, la mezcla se lleva a sequedad mediante la aplicación de vacío y el aceite marrón resultante se extrae con hexano (15 mL). La disolución orgánica se separa de los sólidos no disueltos y se deja durante una semana temperatura ambiente, observándose la aparición de un sólido marrón que se separa por filtración.

[†] *cis*/*trans* con respeto al grupo 4-piridil

Después de evaporar el hexano se obtiene el compuesto **4a** en forma de aceite amarillo (40 mg, 8 % en [Pd]).

IR (NaCl, cm^{-1}): 661, 696, 801, 863, 916, 1026, 1092, 1261, 1310, 1366, 1412, 1434, 1502, 1576, 1598, 1619, 2905, 2962, 3351.

RMN: ^{1}H ($CDCl_3$): δ 0.06 (s, ~156H, Si(C***H*****₃**)₂), 0.84 (t, J_{HH} = 5.4 Hz, 4H, Py-CH_2C***H*****₂**-Si), 1.83 (s, 6H, C***H*****₃**CO_2), 2.65 (t, J_{HH} = 5.3 Hz, 4H, Py-C***H*****₂**CH_2-Si), 7.13 (m, 4H, *m*-NC_5H_4), 8.51 (m, 4H, *o*-NC_5H_4). $^{13}C\{^{1}H\}$ ($CDCl_3$): δ 0.00 (Si(***C***$H_3)_2$), 18.60 (Py-CH_2***C***H_2-Si), 23.18 (***C***H_3CO_2), 28.81 (Py-***C***H_2CH_2-Si), 124.30 (*m*-NC_5H_4), 150.99 (*o*-NC_5H_4), 157.41 (*p*-NC_5H_4), 178.14 (CH_3***C***O_2). $^{29}Si\{^{1}H\}$ ($CDCl_3$): δ –21.97 (s, O-***Si***$(CH_3)_2$-O), –20.80 (s, CH_2-***Si***$(CH_3)_2$-O).

Análisis elemental calculado (Formula calculada para n = 13 que se determina a través de las integrales en el espectro ^{1}H RMN: $PdC_{70}H_{176}N_2O_{30}Si_{26})^{*}$: Pd, 4.50; C, 35.58; H, 7.51; N, 1.19. *Experimental*: Pd, 4.47; C, 35.13; H, 7.59; N, 1.35 %.

3.8.3 [Pd(Cl)₂(A)₂], 5a

Dicloruro de paladio (52.0 mg, 0.293 mmol) se mezcla con **A** (300 mg, 0.59 mmol, 2 equiv.) en etanol (15 mL) y se deja agitando a 80 ºC durante la noche. La mezcla resultante se filtra para eliminar el paladio y de esta forma se obtiene una disolución amarilla y clara. El disolvente se evapora hasta dejar un aceite amarillo y turbio. Se extrae con hexano, separando la disolución de los sedimentos por centrifugación. La disolución resultante se deja durante una semana en la que se observa la precipitación de más sólidos[‡] que se eliminan de nuevo por centrifugación. La disolución se decanta y se evapora el disolvente por aplicación de vacío dejando el producto como una pasta amarilla (52.4 mg, 3.3 % en [Pd]).

IR (NaCl, cm^{-1}): 659, 689, 703, 798, 863, 954, 1097, 1261, 1413, 1430, 1617, 2905, 2963.

RMN: ^{1}H ($CDCl_3$): δ 0.09 (s, ~180H, Si(C***H*****₃**)₂), 2.68 (t, J_{HH} = 8.7 Hz, 4H, Py-C***H*****₂**CH_2-Si), 7.17 (m, 4H, *m*-NC_5H_4), 8.67 (m, 4H, *o*-NC_5H_4).

Análisis elemental calculado ($PdC_{74}H_{194}N_2O_{30}Cl_2Si_{30}$): Pd, 4.07; C, 34.02; H, 7.49; N, 1.07. *Experimental*: Pd, 1.97; C, 36.01; H, 7.95; N, 0.99 %.

[‡] Los sedimentos se han caracterizado por ^{1}H RMN, demonstrando que son una fracción de **5a** con un contenido de Si reducido en proporción con la fracción que queda en disolución.

3.8.4 Procedimientos generales de las reacciones de oxidación de alcoholes

3.8.4.1 Procedimiento general de la reacción de oxidación de 2-octanol en $scCO_2$

Las reacciones de catálisis en $scCO_2$ se llevaron a cabo en el reactor de acero de 27 mL descrito en el Apartado 3.2.2. El 2-octanol se introduce separadamente del catalizador, siguiendo el procedimiento descrito en el Apartado 3.2.4, evitando así el inicio de la reacción antes de homogeneizar la mezcla de reacción en $scCO_2$. Tras la reacción, el sistema se despresuriza utilizando una trampa que contiene Et_2O, tal y como se describe en el Apartado 3.2.3. Una vez despresurizado el reactor, se adiciona Et_2O para extraer los productos de la reacción que restan en su interior. La disolución resultante, junto con la mezcla de la trampa (aunque en ningún ensayo la disolución de la trampa contenía una cantidad detectable de ningún producto), se unen, se evaporan, se pesan y se analizan mediante RMN.

3.8.4.2 Procedimiento general de la reacción de oxidación de 2-octanol en la ausencia de disolvente

Todas las experiencias se realizaron en un reactor de vidrio de alta presión modelo Lab Crest®. El reactor se carga con el catalizador, aditivo (si se usa) y el alcohol, se sella el reactor, se introduce el oxígeno a la presión de trabajo y se calienta el reactor a la temperatura de reacción durante el tiempo correspondiente. Finalizada la reacción, el reactor se enfría en un baño de hielo, se despresuriza y los productos se pesan y se analizan directamente por RMN.

4 Conclusions

4 Conclusions

1. 4-(Polydimethylsiloxanyl-ethyl)pyridine (**A**) was isolated and fully characterised. Several complexes of **A** with catalytic transition metal compounds were synthesised and characterised and applications of the ligand in facilitating catalysis in apolar media were investigated with some success.

2. MTO in conjunction with **A** was determined to be a very active, versatile and particularly stable system for the solventless epoxidation of olefins. In comparison to other MTO-base systems the higher stability of the catalyst makes far higher TONs possible.

3. The first reported molybdenum catalysed olefin epoxidation system employing an IL reaction media was developed. The system used simple MoO_3 as catalyst precursor and the dry oxidant UHP limited hydration of the system and thus hydrolytic epoxide opening during the successful epoxidation of *cis*-cyclooctene. However, system recyclability was only limited and application to other substrates gave poorer results.

4. Increasing the length of alkyl chains on the IL cation $C_n$mim reduces hydrolysis of the epoxide product during molybdenum catalysed olefin epoxidations in ILs using aqueous H_2O_2, presumably by limiting the availability of water.

5. The presence of coordinating ligands also reduces hydrolysis probably because they limit access to the acidic metal centre. Pyrazoles, particularly 3,5-dimethylpyrazole, also increase the rate of catalysis and are the best coordinating species.

6. The optimal $[Mo(O)(O_2)_2]$/dmpz/C_8mim-PF_6 epoxidation system was investigated extensively. In the epoxidation of *cis*-cyclooctene its recyclability was excellent providing that fresh dimethylpyrazole was added between catalytic cycles. However, its activity toward other olefin substrates was more limited.

7. A dioxoperoxomolybdenum complex of 3,5-dimethylpyrazole was isolated in crystalline form suitable for x-ray analysis, both the isolation in solid state and the structure of a dioxoperoxomolybdenum complex have yet to be reported in literature.

8. The first copper-TEMPO catalysed aerobic alcohol oxidation system in $scCO_2$ was developed. $[Cu(AcO)_2(\mathbf{A})]_2$ was shown to be significantly soluble in $scCO_2$ and complete oxidation of the 4-nitrobenzyl alcohol substrate was achieved with this catalyst. However, cheaper $[Cu(AcO)_2(py)]_2$ was equally active, showing that solubility of the metal catalyst was not a factor. Subsequently, silica supported [Cu] catalysts were shown to give high conversions for primary aromatic alcohol substrates even with low catalyst loadings.

Bibliografía

Bibliografía

[1] (a) P. T. Anastas, J. C. Warner, *Green Chemistry: Theory and Practice*, Oxford University Press, Oxford, 1998. (b) M. Lancaster, *Green Chemistry: An introductory text*, RSC Paperbacks, Royal Society, 2002. (c) X. Domenech, *Química verde*, Rubes editorial, 2005.

[2] Concepto de economía atómica, ver por ejemplo: B. M. Trost, *Angew. Chem., Int. Ed. Engl.*, 1995, **34**, 259.

[3] D. J. C. Constable, A. D. Curzons, V. L. Cunningham, *Green Chem.*, 2002, **4**, 521.

[4] D. J. Cole-Hamilton, *Science*, 2003, **299**, 1702 y las referencias que ahí aparecen.

[5] R. A. Sheldon, *Green Chem.*, 2005, **7**, 267.

[6] D. J. Adams, P. J. Dyson, S. J. Tavener, *Chemistry in Alternative Reaction Media*, Wiley, 2004.

[7] Edit Székely, "Supercritical Fluid Extraction". Budapest University of Technology and Economics. http://sunny.vemt.bme.hu/sfe/angol/supercritical.html (activa febrero 2009).

[8] R. C. Reid, J. M. Prausnitz, B. E. Poling, *The properties of gases and liquids*, 4ª ed., McGraw-Hill, New York, 1987.

[9] La siguiente revisión consiste en una colección de referencias sobre los principales temas de interés en relación con los fluidos supercríticos: W. H. Hauthal, *Chemosphere*, 2001, **43**, 123.

[10] Ver por ejemplo, la edición especial de la revista *Chem. Rev.*, 1999, **99**, vol. 2, dedicada a los fluidos supercríticos.

[11] Ver por ejemplo: (a) F. Pérez-Caballero, A-L. Peikolainen, M.Uibu, R. Kuusik, O. Volobujeva, M. Koel. *Microporous and Mesoporous Materials*, 2008, **108**, 230-236. (b) F. Pérez-Caballero, A-L Peikolainen, M. Koel, M. Herbert, A. Galindo, F. Montilla, *The Open Petroleum Engineering Journal*, 2008, **1**, 42-46. (c) F. Pérez-Caballero, A-L Peikolainen, M. Koel, *Estonian Pat.*, EE200700032, 2007.

[12] *Chemical synthesis using supercritical fluids*, ed. P. G. Jessop, W. Leitner, Wiley-VCH, 1999.

[13] G. Musie, M. Wei, B. Subramaniam, D. H. Busch, *Coord. Chem. Rev.*, 2001, 219-221, 789.

[14] (a) R. S. Oakes, A. A. Cliford, C. M. Rayner, *J. Chem. Soc., Perkin Trans.* 2001, 917. (b) P. G. Jessop, T. Ikariya, R. Noyori, *Chem. Rev.* 1999, **99**, 475.

[15] (a) D. R. Palo, C. Erkey, *Ind. Eng. Chem. Res.*, 1998, **37**, 4203. (b) D. K. Morita, D. R. Pesiri, S. A. David, W. H. Glaze, W. Tumas, *Chem. Commun.*, 1998, 1397. (c) S. Fujita, K. Yuzawa, B. M. Bhanage, Y. Ikushima, M. Arai, *J. Mol. Catal. A: Chem.*, 2002, **180**, 35. (d) S. Kainz, D. Koch, W. Baumann, W. Leitner, *Angew. Chem., Int. Ed.*, 1997, **36**, 1628. (e) M. A. Carrol, A. B. Holmes, *Chem. Commun.*, 1998, 1395.

[16] (a) M. F. Sellin, I. Bach, J. M. Webster, F. Montilla, V. Rosa, T. Avilés, M. Poliakoff, D. J. Cole-Hamilton, *J. Chem. Soc., Dalton Trans.*, 2002, 4569. (b) F. Montilla, V. Rosa, C. Prevett, T. Avilés, M. Nunes Da Ponte, D. Masi, C. Mealli, *Dalton. Trans.*, 2003, 2170. (c) F. Montilla, A. Galindo, V. Rosa, T. Avilés, *Dalton Trans.*, 2004, 2588.

[17] F. Montilla, A. Galindo, R. Andrés, M. Córdoba, E. de Jesús, C. Bo, *Organometallics*, 2006, **25**, 4138.

[18] (a) P. Wasserscheid, T. Welton, *Ionic liquids in synthesis*, Wiley-VCH, 2003. (b) R. D. Rogers, K. R. Seddon, *Ionic liquids as green solvents: progress and prospects*, ACS Series, American Chemical Society, 2003.

[19] Ver, por ejemplo, las siguientes revisiones: (a) P. Wasserscheid, W. Keim, *Angew. Chem. Int. Ed.*, 2000, **39**, 3772. (b) H. Olivier-Bourbigou, L. Magna, *J. Mol. Catal. A*, 2002, 182-183, 419. (c) M. Picquet, D. Poinsot, S. Stutzmann, I. Tkatchenko, I. Tommasi, P. Wasserscheid, J. Zimmermann, *Topics Catal.*, 2004, **29**, 139. (d) T. Welton, *Coord. Chem. Rev.*, 2004, **248**, 2459. (e) N. Jain, A. Kumar, S. Chauhan, S. M. S. Chauhan, *Tetrahedron*, 2005, **61**, 1015. (f) Z. C. Zhang, *Adv. Catal.*, 2006, **49**, 153. (g) V. I. Pârvulescu, C. Hardacre, *Chem. Rev.*, 2007, **107**, 2615.

[20] (a) A. West, *Chemistry World*, 2005, **2**, 32-36. (b) D. Zhao, Y. Liao, Z. Zhang, *Clean*, 2007, **35**, 42-48. (c) N. Gathergood, M. Teresa Garcia, P. J. Scammells, *Green Chem.*, 2004, **6**, 166-175. (d) M. Teresa Garcia, N. Gathergood, P. J. Scammells, *Green Chem.*, 2005, **7**, 9-14. (e) A. Romero, A. Santos, J. Tojo, A. Rodríguez, *Journal of Hazardous Materials*, 2008, **151**, 268-273.

[21] Ver, por ejemplo: (a) J. Muzart, *Adv. Synth. Catal.*, 2006, **348**, 275. (b) M. Haumann, A. Riisager, *Chem. Rev.*, 2008, **108**, 1474. (c) P. Śledź, M. Mauduit, K. Grela, *Chem. Soc. Rev.*, 2008, **37**, 2433.

[22] (a) C. E. Song, *Chem. Commun.*, 2004, 1033. (b) C. Baudequin, J. Baudoux, J. Levillain, D. Cahard, A.-C. Gaumont, J.-C. Plaquevent, *Tetrahedron: asymmetry*, 2003, **14**, 3081.

[23] N. V. Plechkova, K. R. Seddon, *Chem. Soc. Rev.*, 2008, **37**, 123.

[24] L. A. Blanchard, D. Hancu, E. J. Beckman, J. F. Brenneke, *Nature*, 1999, **399**, 28.

[25] F. M. Kerton, *Alternative Solvents for Green Chemistry*, ed. J. H. Clark, G. A. Kraus, RSC Publishing, 2009, Ch. 2.

[26] T. Welton, *Green Chem.*, 2006, **8**, 13.

[27] G. Kaupp, *CrystEngComm*, 2006, **8**, 794.

[28] B. Rodríguez, A. Bruckmann, T. Rantanen, C. Bolm, *Adv. Synth. Catal.*, 2007, **349**, 2213.

[29] Por ejemplos recientes: (a) G. W. Wang, Y. W. Dong, P. Wu, T. T. Yuan, Y. B. Shen, *J. Org. Chem.*, 2008, **73**, 7088-7095. (b) E. M. C. Gerard, H. Sahin, A. Encinas, S. Braese, *Synlett*., 2008, **17**, 2702-2704. (c) P. R. Patil, K. K. P. Ravindranathan, *Journal of Carbohydrate Chemistry*, 2008, **27**, 411-419.

[30] (a) V. Polshettiwar, R. S. Varma, *Acc. Chem. Res.*, 2008, **41**, 629-639. (b) A. Loupy, *Comptes Rendís Chimie*, 2004, **7**, 103-112. (c) R. S. Varma, *Green Chem.*, 1999, **1**, 43.

[31] S. Puri, B. Kaur, A. Parmar, H. Kumar, *Ultrasonics Sonochemistry*, 2009, **16**, 705-707.

[32] K. Tanaka, F. Toda, *Chem. Rev.*, 2000, **100**, 1025.

[33] Ejemplos recientes incluyen: (a) Diels Alder: C-C. Hsu, C-C. Lai, S-H. Chiu, *Tetrahedron*, 2009, **65**, 2824-2829. (b) Friedel-Crafts: X. Wang, Y. Wang, D-M. Du, J. Xu, *J. Mol. Cat. A: Chem.*, 2006, **255**, 31-35. (c) Fries Rearrangement: J. Cato, H. Kakehata, Y. Maekawa, T. Yamashita, *Chem. Comm.*, 2006, 4498. (d) Wittig: T. Thiemann, *J. Chem. Res.*, 2007, 336. (e) Organometallic Addition: Y. Zhang, X. Jia, J-X. Wang, *Eur. J. Org. Chem.*, 2009, 2983. (f) Beckmann

Rearrangement: M. Hosseini-Sarvari, H. Sharghi, *J. Chem. Res.*, 2006, 205. (g) Claisen Rearrangement: V. K. Sankar, T. K. Raja, *Ind. J. Hetero. Chem.*, 2006, **16**, 195.

[34] Por ejemplo: (a) M. Wang, P. Li, L. Wang, *Eur. J. Org. Chem.*, 2008, 2255. (b) P. A. Robles-Dutenhefner, K. A. de Silva Rocha, E. M. B. Sousa, E. V. Gusevskaya, *J. Catal.*, 2009, **265**, 72. (c) S. R. Ali, V. K. Bansal, A. A. Khan, S. K. Jain, M. A. Ansari, *J. Mol. Cat. A: Chem.*, 2009, **303**, 60. (d) H. R. Shaterian, F. Khorami, A. Amirzadeh, M. Ghashang, *Chinese Journal of Chemistry*, 2009, **27**, 815. (e) G. Rajagopal, H. Lee, S. S. Kim, *Tetrahedron*, 2009, **65**, 4735. (f) X. Chen, J. She, Z-C. Shang, J. Wu, P. Zhang, *Syn. Comm.*, 2009, **39**, 947.

[35] Como ejemplo: C.-H. Jun, J-H. Chung, D-Y. Lee, A. Loupy, S. Chatti, *Tet. Lett.*, 2001, **42**, 4803.

[36] (a) R. A. Sheldon, I Arends, U. Hanefeld, *Green Chemistry and Catalysis*, Wiley-VCH, 2007. (b) *Metal-oxo and Metal-peroxo Species in Catalytic Oxidations*, ed. B. Meunier, A. J. Bard, I. G. Dance, P. Day, J. A. Ibers, Springer-Verlag Berlin and Heidelberg GmbH & Co. K, 2000. (c) *Advances in Catalytic Activation of Dioxygen by Metal Complexes*, ed. L. I. Simándi, Springer, 2003. (d) R. Noyori, M. Aoki, K. Sato, *Chem. Commun.*, 2003, 1977.

[37] (a) R. A. Sheldon, J. K. Kochi, *Metal-Catalyzed Oxidations of Organic Compounds*, Academic Press: New York, 1981. (b) F. Meyer, C. Limberg, *Organometallic Oxidation Catalysis*, Springer, 2007. (c) J. Bäckvall, *Modern Oxidation Methods*, Wiley-VCH, 2004.

[38] *Ullmanns Encyclopedia of Industrial Chemistry*, VCH Verlagsgesellschaft mbH, Weinheim, 1987, A10, 117-135.

[39] (a) *Methoden der organischen Chemie*, ed. E. Müller Houben-Weyl, 4th Ed., Georg Theme Verlag, Stuttgart, 1965, VI/3, 385-397. (b) A. S. Rao, *Comprehensive Organic Synthesis*, Oxford, 1991, 7, 357. (c) N. Prilezhaev, *Ber.*, 1910, **42**, 4811-4815.

[40] Por ejemplo, ver: (a) K. Wada, N. Watanabe, T. Kondo, T. Mitsudo, *Chem. Eng. Sci.*, 2008, **63**, 4917-4923. (b) K. Matsmoto, Y. Sawada, T. Katsuki, *Pure and Applied Chemistry*, 2008, **80**, 1071-1077.

[41] Por ejemplo, ver: (a) K. B. Sharpless, R. C. Michaelson, *J. Am. Chem. Soc.*, 1973, **95**, 6136-6137. (b) S. Tangestaninejad, M. Moghadam, V. Mirkhani, I. Mohammadpoor-Baltork, E. Shams, H. Salavati, *Cat. Comm.*, 2008, **9**, 1001-1009.

[42] Por ejemplo, ver: (a) A. Jimtaisong, R. L. Luck, *Inorg. Chem.*, 2006, **45**, 10391-10402. (b) G. Grigoropoulou, J. H. Clark, J. A. Ellings, *Green Chem.*, 2003, **5**, 1-7. (c) W. Adam, *Peroxide Chemistry – Mechanistic and Preparative Aspects of Oxygen transfer*, Wiley-VCH, Weinheim, FRG, 2000, 355.

[43] (a) W. A. Herrmann, R. W. Fischer, M. U. Rauch, W. Scherer, *J. Mol. Cat.*, 1994, **86**, 243-266. (b) W. A. Herrmann, *Angew. Chem.*, 1988, **100**, 1269; *Angew. Chem. Int. Ed. Engl.*, 1988, 27, 1297. (c) W. A. Herrmann, *J. Organomet. Chem.*, 1990, **382**, 1. (d) W. A. Herrmann, J. G. Kuchler, W. Wagner, J. K. Felixberger, E. Herdtweck, *Angew. Chem.*, 1988, **100**, 420; *Angew. Chem. Int. Ed. Engl.*, 1988, **27**, 394. (e) W. A. Herrmann, J. G. Kuchler, G. Weichselbaumer, E. Herdtweck, P. Kiproff, *J. Organomet. Chem.*, 1989, **372**, 351. (f) W. A. Herrmann, F. E. Kühn, R. W. Fischer, W. R. Thiel, C. C. Romão, *Inorg. Chem.*, 1992, **31**, 4431.

[44] H. Mimoun, I. Seree de Roch, L. Sajus, *Bull. Soc. Chim.*, 1969, 1481.

[45] H. Mimoun, *J. Mol. Cat.*, 1980, **7**, 1-29.

[46] Ver por ejemplo: (a) *Catalytic Oxidations with Hydrogen Peroxide as Oxidant*, ed. G. Strukul Kluwer Academic Publishers, Rotterdam, 1992. (b) K. A. Jørgensen, *Chem. Rev.*, 1989, **89**, 431-458. (c) *Organic Synthesis by Oxidation with Metal Compounds*, ed. W. J. Mijs, C. H. R. I. de Jonge, Plenum Press, New York, 1986. (d) *The Chemistry of Peroxides*, ed. R. A. Sheldon, S. Patai, Wiley, New York, 1983, 161. (e) B. S. Lane, K. Burgess, *Chem. Rev.*, 2003, **103**, 2457-2473.

[47] (a) *Applied Homogeneous Catalysis with Organometallic Compounds Vols. I and II*, ed. B. Cornils, W. A. Herrmann, VCH: Weinheim, 1996. (b) W. A. Herrmann, *J. Organomet. Chem.*, 1995, **500**, 149-174.

[48] A. K. Yudin, K. B. Sharpless, *J. Am. Chem. Soc.*, 1997, **119**, 11536.

[49] I. R. Beattie, P. J. Jones, *Inorg. Chem.*, 1979, **18**, 2318-2319.

[50] (a) J. H. Espenson, *Chem. Commun.*, 1999, 479. (b) W. Herrmann, F. E. Kühn, *Acc. Chem. Res.* 1997, **30**, 169.

[51] (a) W. Adam and C. M. Mitchell, *Angew. Chem., Int. Ed. Engl.*, 1996, **35**, 533. (b) T. R. Boehlow, C. D. Spilling, *Tetrahedron Lett.*, 1996, **37**, 2717. (c) W. Adam, C. M. Mitchell, C. R. Saha-Möller O. Weichold, *J. Am. Chem. Soc.*, 1999, **121**, 2097.

[52] (a) G. Soldaini, F. Cardona, A. Goti, *Tetrahedron Lett.*, 2003, **44**, 5589-5592. (b) A. Omar Bouh, J. H. Espenson, *J. Mol. Cat. A: Chem.*, 2003, **200**, 43-47.

[53] E. P. Carreiro, A. J. Burke, M. J. M. Curto, A. J. R. Teixeira, *J. Mol. Catal. A*, 2004, **217**, 69.

[54] G. S. Owens, M. M. Abu-Omar, *Chem Commun.*, 2000, 1165.

[55] M. M. Abu-Omar, P. J. Hansen, J. H. Espenson, *J. Am. Chem. Soc.*, 1996, **118**, 4966.

[56] (a) J. Rudolph, K. L. Reddy, J. P. Chiang and K. B. Sharpless, *J. Am. Chem. Soc.*, 1997, **119**, 6189-6190. (*b*) H. Adolfsson, A. Converso, K. B. Sharpless, *Tetrahedron Lett.*, 1999, **40**, 3991-3994.

[57] C. Copéret, H. Adolfsson, K. B. Sharpless, *Chem. Commun.*, 1997, 1565-1566.

[58] A. L. Villa de P., D. E. De Vos, C. Montes de C., P. A. Jacobs, *Tetrahedron Letters*, 1998, **39**, 8521.

[59] H. Rudler, J. R. Gregorio, B. Denise, J. M. Brégeault, A. Deloffre, *J. Mol. Cat. A: Chemical*, 1998, **133**, 255-265.

[60] W. A. Herrmann, H. Ding, R. M. Kratzer, F. E. Kühn, J. J. Haider, R. W. Fischer, *J. Organomet. Chem.*, 1997, **549**, 319.

[61] W. A. Herrmann, R. M. Kratzer, H. Ding, W. R. Thiel, H. Glas, *J. Organomet. Chem.*, 1998, **555**, 293-295.

[62] H. Adolfsson, A. Converso, K. B. Sharpless, *Tetrahedron Letters*, 1991, **40**, 3991.

[63] H. Adolfsson, C. Copéret, J. P. Chiang, A. K. Yudin, *J. Org. Chem.*, 2000, **65**, 8651.

[64] W-D. Wang, J. H. Espenson, *J. Am. Chem. Soc.*, 1998, **120**, 11335-11341.

[65] S. Yamazaki, *Org. Biomol. Chem.*, 2007, **5**, 2109-2113.

[66] (a) W.A. Herrmann, F. E. Kühn, M. R. Mattner, G. R. J. Artus, M. R. Geisburger, J. D. G. Correia, *J. Organomet. Chem.*, 1997, **538**, 203. (b) S.-W Park, K.-J. Kim, S. S. Yoon, *Bull. Korean Chem. Soc.*, 2000, **21**, 446. (c) S.-W Park, S. S. Yoon, *J. Korean Chem. Soc.*, 2000, **44**, 81.

[67] M. J. Sabater, M. E. Domine, A. Corma, *J. Catal.*, 2002, **210**, 192.

[68] E. de Palma Carreiro, G. Yong-Em, A. J. Burke, *J. Mol. Catal. A*, 2005, **235**, 285.

[69] J. J. Haider, R. M. Kratzer, W. A. Herrmann, J. Zhao, F. E. Kühn, *J. Organomet. Chem.*, 2004, **689**, 3735.

[70] Ver por ejemplo: *Mechanisms in Homogeneous and Heterogeneous Epoxidation Catalysis*, ed. S. T. Oyama, Elsevier Science, 2008.

[71] A. M. Al-Ajlouni, J. H. Espenson, *J. Am. Chem. Soc.*, 1995, **117**, 9243-9250.

[72] O. Pestovsky, R. van Eldik, P. Huston, J. H. Espenson, *J. Chem. Soc. Dalton Trans.*, 1995, 133.

[73] Z. Zhu, J. H. Espenson, *J. Org. Chem.*, 1995, **60**, 1326.

[74] W. A. Herrmann, R. W. Fischer, D. W. Warz, Angew. *Chem. Int. Ed. Engl.*, 1991, **30**, 1638.

[75] K. A. Vassell, J. H. Espenson, *Inorg. Chem.*, 1994, **33**, 5491.

[76] S. M. Nabavizadeh, M. Rashidi, *J. Am. Chem. Soc.*, 2006, **128**, 351.

[77] S. M. Nabavizadeh, *Inorg. Chem.*, 2003, **42**, 13, 4204.

[78] (a) F. E. Kühn, A. M. Santos, W. A. Herrmann, *Dalton Trans.*, 2005, 2483-2491. (b) R. A. Sheldon J. A. van Doorn, *J. Catal.*, 1973, **31**, 427. (c) R. A. Sheldon J. A. van Doorn, C. W. Schram, H. de Jong, *J. Catal.*, 1973, **31**, 438. (d) B. M. Trost, Y. Masuyama, *Isr. J. Chem.*, 1984, **24**, 134.

[79] H. Mimoun, I. Seree de Roch, L. Sajus, *Tetrahedron*, 1970, **26**, 37-50.

[80] W. R. Thiel, M. Angstl, N. Hansen, *Journal of Molecular Catalysis A: Chemical*, 1995, **103**, 5-10.

[81] C. I. Altinis Kiraz, L. Mora, L. S. Jimenez, *Synthesis*, 2007, **1**, 92-96.

[82] S. K. Maiti, K. M. Abdul Malik, S. Gupta, S. Chakraborty, A. K. Ganguli, A. K. Mukherjee, R. Bhattacharyya, *Inorg. Chem.*, 2006, **45**, 9843-9857.

[83] (a) S. K. Maiti, S. Dinda, N. Gharah, R. Bhattacharyya, *New J. Chem.*, 2006, **30**, 479-489. (b) S. K. Maiti, S. Dinda, S. Banerjee, A. K. Mukherjee, R. Bhattacharyya, *Eur. J. Inorg. Chem.*, 2008, 2038-2051.

[84] (a) N. Gharah, S. Chakraborty, A. K. Mukherjee, R. Bhattacharyya, *Chem. Commun.*, 2004, 2630-2632. (b) S. K. Maiti, S. Dinda, R. Bhattacharyya, *Tetrahedron Lett.*, 2008, **49**, 6205-6208. (c) N. Gharah, M. G. B. Drew, R. Bhattacharyya, *Transition Met. Chem.*, 2009, **34**, 549-557. (d) S. K. Maiti, S. Dinda, M. Nandi, A. Bhaumik, R. Bhattacharyya, *J. Mol. Cat. A: Chem.*, 2008, **287**, 135-141.

[85] (a) D. E. Richardson, H. Yao, K. M. Frank, D. A. Bannett, *J. Am. Chem. Soc.*, 2000, **122**, 1729-1739. (b) B. S. Lane, M. Vogt, V. J. DeRose, K. Burgess, *J. Am. Chem. Soc.*, 2002, **124**, 11946-11954.

[86] J. M. Le Carpentier, A. Mitschler, R. Weiss, *Acta Crystallogr.*, 1972, **B28**, 1288.

[87] B. Booth, R. Hazeldine, G. Neuss, *J. Chem. Soc., Chem. Commun.*, 1972, 1074.

[88] H. Mimoun, R. Charpentier, A. Mitschler, J. Fischer, R. Weiss, *J. Am. Chem. Soc.*, 1980, **102**, 1047-1054.

[89] H. Mimoun, M. Mignard, P. Brechot, L. Saussine, *J. Am. Chem. Soc.*, 1986, **108**, 3711-3718.

[90] P. Chaumette, H. Mimoun, L. Saussine, J. Fischer, A. Mitschler, *J. Organomet. Chem.*, 1983, **250**, 291-310.

[91] K. B. Sharpless, J. M. Townsend, D. R. Williams, *J. Am. Chem. Soc.*, 1972, **94**, 295-296.

[92] K. D. Bingham, G. D. Meakins, G. H. Whitham, *Chem. Commun.*, 1966, 445.

[93] Ver por ejemplo: (a) A. S. Bailey, J. E. White, *J. Chem. Soc. B*, 1966, 819. (b) *The Chemistry of Alkenes*, ed. R. Huisgen, R. Grashey, J. Sauer, S. Patai, Interscience, London, 1964, Ch. 11. (c) R. E. Erickson, R. L. Clark, *Tetrahedron Lett.*, 1969, 3997. (d) A. K. Awasthy, J. Roček, *J. Am. Chem. Soc.*, 1969, **91**, 991. (e) F. Freeman, P. D. McCart, N. J. Yamachika, *ibid.*, 1970, **92**, 4621.

[94] A. M. Al-Ajlouni, J. H. Espenson, *J. Org. Chem.*, 1996, **61**, 3969.

[95] (a) J. Kaloustian, L. Lena, J. Metzger, *Tetrahedron Lett.*, 1975, 599. (b) H. Arakawa, A. Ozaki, *Chem. Lett.*, 1975, 1245.

[96] A. O. Chong, K. B. Sharpless, *J. Org. Chem.*, 1977, **42**, **9**, 1587-1590.

[97] W. R. Thiel, M. Angstl, T. Priermeier, *Chem. Ber.*, 1994, **127**, 2373.

[98] W. R. Thiel, *Journal of Molecular Catalysis A: Chemical*, 1997, **117**, 449-454.

[99] A. Hroch, G. Gemmecker, W. R. Thiel, *Eur. J. Inorg. Chem.*, 2000, **5**, 1107-1114.

[100] W. R. Thiel, J. Eppinger, *Chem. Eur. J.*, 1997, **3**, 696.

[101] Por ejemplo reacción de acetato de cobre con peróxido de hidrogeno; E. Ochiai, *Inorg. Nucl. Chem. Lett.*, 1973, **9**, 987.

[102] F. E. Kühn, J. Zhao, M. Abrantes, W. Sun, C. A. M. Alfonso, L. C. Branco, I. S. Goncalves, M. Pillinger, C. C. Romão, *Tetrahedron Lett.*, 2004, **46**, 47.

[103] A. A. Valente, Ž. Petrovski, L. C. Branco, C. A. M. Afonso, M. Pillinger, A. D. Lopes, C. C. Romão, C. D. Nunes, I. S. Gonçalvez, *J. Mol. Catal. A: Chem.* 2004, **218**, 5.

[104] B. Monteiro, S. Gago, P. Neves, A. A. Valente, I. S. Gonçalvez, C. C. L. Pereira, C. M. Silva, M. Pillinger, *Catal. Lett.* 2009, **129**, 350.

[105] B. Z. Zhan, A. Thompson, *Tetrahedron*, 2004, **60**, 2917-2935.

[106] (a) J. R. Holum, *J. Org. Chem.*, 1961, **26**, 4814-4816. (b) D. G. Lee, U. A. Spitzer, *J. Org. Chem.*, 1970, **35**, 3589-3590. (c) G. Cainelli, G. Cardillo, *Chromium oxidants in organic chemistry*; Springer: Berlin, 1984. (d) J. Muzart, *Chem. Rev.*, 1992, **92**, 113-140.

[107] (a) S. L. Regen, C. Koteel, *J. Am. Chem. Soc.*, 1977, **99**, 3837-3838. (b) F. M. Menger, C. Lee, *Tetrahedron Lett.*, 1981, **22**, 1655-1656.

[108] (a) L. M. Berkowitz, P. N. Rylander, *J. Am. Chem. Soc.*, 1958, **80**, 6682-6684. (b) W. P. Griffith, *Chem. Soc. Rev.*, 1992, **21**, 179-185.

[109] (a) W. P. Griffith, S. V. Ley, G. P. Whitcombe, A. D. White, *J. Chem. Soc., Chem. Commun.*, 1987, 1625-1627. (b) S. V. Ley, J. Norman, W. P. Griffith, S. P. Marsden, *Synthesis*, 1994, 639-666.

[110] T. V. Lee, S. V. Ley, A. Madin, B. M. Trost, I. Fleming, *Comprehensive organic synthesis*; Pergamon: Oxford, 1991, **7**, 291-303. (39b)

[111] D. B. Dess, J. C. Martin, *J. Org. Chem.*, 1983, **48**, 4155-4156.

[112] Ver, por ejemplo: S. Velusamy, T. Punniyamurthy, *Eur. J. Org. Chem.*, 2003, 3913-3915.

[113] Ver, por ejemplo: M. J. Schultz, M. S. Sigman, *Tetrahedron*, 2006, **62**, 8227.

[114] Ver por ejemplo: T. Naota, H. Takaya, S-I. Murahashi, *Chem. Rev.*, 1998, **98**, 2599.

[115] G. T. Musie, M. Wei, B. Subramaniam, D. H. Busch, *Inorg. Chem.*, 2001, **40**, 3336.

[116] G. Maayan, B. Ganchegui, W. Leitner, R. Neumann, *Chem. Commun.*, 2006, 2230.

[117] M. E. González-Nuñez, R. Mello, A. Olmos, R. Acerote, G. Asensio, *J. Org. Chem.*, 2006, **71**, 1039.

[118] R. Ciriminna, P. Hesemann, J. J. E. Moreau, M. Carraro, S. Campestrini, M. Pagliaro, *Chem. Eur. J.* 2006, **12**, 5220.

[119] Ver por ejemplo los artículos de revisión siguientes dedicados a los ILs funcionalizados: (a) S.-G. Lee, *Chem Commun.*, 2006, 1049. (b) Z. fei, T. J. Geldbach, D. Zhao, P. J. Dyson, *Chem. Eur. J.*, 2006, **12**, 2122.

[120] K. R. Seddon, A. Stark, *Green Chem.*, 2002, **4**, 119.

[121] V. Framer, T. Welton, *Green Chem.*, 2002, **4**, 97.

[122] I. A. Ansari, R. Gree, *Org. Lett.*, 2002, **4**, 1507-1509.

[123] N. Jiang, A. J. Ragauskas, *Org. Lett.*, 2005, **7**, 3689-3692.

[124] (a) X. E. Wu, L. Ma, M. X. Ding, L. X. Gao, *Synlett.*, 2005, 607. (b) W. X. Qian, E. L. Jin, W. L. Bo, Y. M. Zhang, *Tetrahedron*, 2006, **62**, 556.

[125] L. Liu, L.-Y. Ji, Y.-Y. Wei, *Monatsh. Chem.*, 2008, **139**, 901.

[126] M. F. Semmelhack, C. R. Schmid, D. A. Corte´s, C. S. Chou, *J. Am. Chem. Soc.*, 1984, **106**, 3374-3376

[127] (a) J. W. Whittaker, *Metal ions in biological systems*; H. Sigel, A. Sigel, Eds.; Marcel Dekker: New York, 1994; **30**, 315-360 (b) P. F. Knowles, N. Ito, *Perspectives in bio-inorganic chemistry*; ed. R. W. Hay, J. R. Dilworth, K. B. Nolan, Jai: London, 1994, Ch. 2, 207-244

[128] M. M. Whittaker, J. W. Whittaker, *J. Biophys.*, 1993, **64**, 762-772.

[129] (a) V. Mahadevan, R. J. M. K. Gebbink, T. D. P. Stack, *Curr. Opin. Chem. Biol.*, 2000, **4**, 228-234. (b) Y. Wang, J. L. DuBois, B. Hedman, K. O. Hodgson, T. D. P. Stack, *Science*, 1998, **279**, 537-540. (c) P. Chaudhuri, M. Hess, U. Flörke, K. Wieghardt, *Angew. Chem., Int. Ed.*, 1998, **37**, 2217-2220. (d) P. Chaudhuri, M. Hess, J. Müller, K. Hildenbrand, E. Bill, T. Weyhermüller, K. Wieghardt, *J. Am. Chem. Soc.*, 1999, **121**, 9599-9610. (e) P. Chaudhuri, M. Hess, T. Weyhermüller, K. Wieghardt, *Angew. Chem., Int. Ed.*, 1999, **38**, 1095-1098. (f) Y. Nagata, C. Miyamoto, Y. Matsushima, S. Matsumoto, *Chem. Pharm. Bull.*, 2000, **48**, 71-76.

[130] Ver por ejemplo: (a) I. E. Markó, P. R. Giles, M. Tsukazaki, S. M. Brown, C. J. Urch, *Science*, 1996, **274**, 2044-2046. (b) I. E. Markó, A. Gautier, I. Chellé-Regnaut, P. R. Giles, M. Tsukazaki, C. J. Urch, S. M. Brown, *J. Org. Chem.*, 1998, **63**, 7576-7577. (c) I. E. Markó, P. R. Giles, M. Tsukazaki, I. Chellé-Regnaut, A. Gautier, S. M. Brown, C. J. Urch, *J. Org. Chem.*, 1999, **64**, 2433-2439

[131] (a) R. A. Sheldon, I. W. C. E. Arends, *J. Mol. Catal. A: Chemical*, 2006, **251**, 200. (b) R. A. Sheldon, I. W. C. E. Arends, *Adv. Synth. Catal.*, 2004, **346**, 1051. (c) J. M. Bobbitt, M. C. L.

Flores, *Heterocycles*, 1988, **27**, 509-533. (d) A. E. J. de Nooy, A. C. Besemer, H. van Bekkum, *Synthesis*, 1996, 1153-1174.

132 P. L. Anelli, C. Biffi, F. Montanari, S. Quici, *J. Org. Chem.*, 1987, **52**, 2559-2562.

133 (a) A. Dijksman, I. W. C. E. Arends, R. A. Sheldon, *Chem. Commun.*, 1999, 1591-1592. (b) A. Dijksman, I. W. C. E. Arends, R. A. Sheldon, *Platinum Met. Rev.*, 2001, **45**, 15-19. (c) A. Dijksman, A. Marino-Gonzalez, A. Mairata i Payeras, I. W. C. E. Arends, R. A. Sheldon, *J. Am. Chem. Soc.*, 2001, **123**, 6826-6833. (d) R. A. Sheldon, I. W. C. E. Arends, G.-J. ten Brink, A. Dijksman, *Acc. Chem. Res.*, 2002, **35**, 774-781.

134 T. Miyazawa, T. Endo, *Journal of Molecular Catalysis*, 1985, **32**, 357-360.

135 P. Gamez, I. W. C. E. Arends, J. Reedijk, R. A. Sheldon, *Chem. Commun.*, 2003, 2414-2415.

136 P. Gamez, I. W. C. E. Arends, R. A. Sheldon, J. Reedijk, *Adv. Synth. Catal.*, 2004, **346**, 805-811.

137 S. Velusamy, A. Srinivasan, T. Punniyamurthy, *Tetrahedron Lett.*, 2006, **47**, 923-926.

138 (a) B. Betzemeier, M. Cavazzini, S. Quici, P. Knochel, *Tetrahedron Lett.*, 2000, **41**, 4343-4346. (b) G. Ragagnin, B. Betzemeier, S. Quici, P. Knochel, *Tetrahedron*, 2002, **58**, 3985-3991.

139 M. Contel, P. R. Villuendas, J. Fernández-Gallardo, P. J. Alonso, J.-M. Vincent, R. H. Fish, *Inorg. Chem.*, 2005, **44**, 9771-9778.

140 T. F. Blackburn, J. Schwartz, *J. Chem. Soc., Chem. Commun.*, 1977, 157.

141 K. P. Peterson, R. C. Larcock, *J. Org. Chem.*, 1998, **63**, 3185-3189.

142 Por ejemplo, ver los citados de Stahl et al (a) J. P. Caradonna, P. R. Reddy, R. H. Holm, *J. Am. Chem. Soc.*, 1988, **110**, 2139-2144. (b) J. C. Bryan, R. E. Stenkamp, T. H. Tulip, J. M. Mayer, *Inorg. Chem.*, 1987, **26**, 2283-2288. (c) J. B. Arterburn, M. C. Perry, S. L. Nelson, B. R. Dible, M. S. Holguin, *J. Am. Chem. Soc.*, 1997, **119**, 9309-9310. (d) M. M. Abu-Omar, S. I. Khan, *Inorg. Chem.*, 1998, **37**, 4979-4985.

143 (a) S. S. Stahl, J. L. Thorman, R. C. Nelson, M. J. Kozee, *Am. Chem. Soc.*, 2001, **123**, 7188-7189. (b) B. A. Steinhoff, S. R. Fix, S. S. Stahl, *J. Am. Chem. Soc.*, 2002, **124**, 766-767.

144 B. A. Steinhoff, S. S. Stahl, *Org. Lett.*, 2002, **4**, 4179-4181.

145 T. Nishimura, T. Onoue, K. Ohe, S. Uemura, *Tetrahedron Lett.*, 1998, **39**, 6011-6014.

146 (a) T. Nishimura, K. Ohe, S. Uemura, *J. Am. Chem. Soc.*, 1999, **121**, 2645-2646. (b) T. Nishimura, N. Kakiuchi, T. Onoue, K. Ohe, S. Uemura, *J. Chem. Soc., Perkin Trans.*, 2000, **1**, 1915-1918.

147 T. Nishimura, Y. Maeda, N. Kakiuchi, S. Uemura, *J. Chem. Soc., Perkin Trans.*, 2000, **1**, 4301-4305.

148 T. Nishimura, T Onoue, K. Ohe, S. Uemura, *J. Org. Chem.*, 1999, **64**, 6750-6755.

149 M. J. Schultz, C. C. Park, M. S. Sigman, *Chem. Commun.*, 2002, 3034-3035.

150 D. R. Jensen, M. J. Schultz, J. A. Mueller, M. S. Sigman, *Agnew. Chem. Int. Ed.*, 2003, **42**, 3810-3813.

151 M. J. Schultz, S. S. Hamilton, D. R. Jensen, M. S. Sigman, *J. Org. Chem.*, 2005, **70**, 3343-3352.

152 G-J. T. Brink, I. W. C. E. Arends, R. A. Sheldon, *Science*, 2000, **287**, 1636-1639.

[153] (a) M. A. McHugh, V. J. Krukonis, *Supercritical Fluid Extraction: Principles and Practice*, Butterworth-Heinemann Ltd., Boston, 1994. (b) V. Chandrasekhar, *Inorganic and Organometallic Polymers*, Springer, 2005, Ch. 6.

[154] D. E. Bergbreiter, J. Tian, C. Hongfa, *Chem. Rev.*, 2009, **109**, 530.

[155] M. A. Grunlan, K. R. Regan, D. E. Bergbreiter, *Chem. Commun.*, 2006, 1715.

[156] (a) A. L. Miller II, N. B. Bowden, *Chem. Commun.*, 2007, 2051. (b) M. T. Mwangi, M. B. Runge, K. M. Hoak, M. D. Schulz, N. B. Bowden, *Chemistry*, 2008, **14**, 6780.

[157] (a) R. F. Parton, I. F. J. Vankelecom, D. Tas, K. B. M. Janssen, P.-P. Knops-Gerrits, P. A. Jacobs, *J. Mol. Catal. A*, 1996, **113**, 283. (b) K. B. M. Janssen, I. Laquiere, W. Dehaen, R. F. Parton, I. F. J. Vankelecom, P. A. Jacobs, *Tetrahedron*: *Asymmetr.*, 1997, **8**, 3481. (c) D. F. C. Guedes, T. C. O. MacLeod, M. C. A. F. Gotardo, M. C. A. F. Schiavon, I. V. P. Yoshida, K. J. Ciuffi, M. D. Assis, *Appl. Catal., A: Gen.*, 2005, **296**, 120. (d) J. R. Pliego Jr., M. A. Schiavon, *J. Phys. Chem. C*, 2008, **112**, 14830.

[158] (a) M. T. Mwangi, M. B. Runge, N. B. Bowden, *J. Am. Chem. Soc.*, 2006, **128**, 14434. (b) M. B. Runge, M. T. Mwangi, N. B. Bowden, *J. Organomet. Chem.*, 2006, **691**, 5278.

[159] S. Saffarzadeh-Matin, C. J. Chuck, F. M. Kerton, C. M. Rayner, *Organometallics*, 2004, **23**, 5176.

[160] F. Tronc, L. Lestel, S. Boileau, *Polymer*, 2000, **41**, 5039.

[161] Both the α and β addition products were also observed in the hydrosilylations of styrene and 4-chlorostyrene with $H[(Si(CH_3)_2O)_n]$ (These results are not part of the studys described here).

[162] See for example: H. N. Cheng, *Modern Methods of Polymer Characterization*, ed. H. G. Barth, J. W. Mays, Wiley 1991, 461.

[163] M. C. DeRosa, P. J. Mosher, G. P. A. Yap, K.-S. Focsaneanu, R. J. Crutchley, C. E. B. Evans, *Inorg. Chem*., 2003, **42**, 4864.

[164] See for example: (a) W. Adam, C. R. Saha-Moeller, O. Weichold, *J. Org. Chem.*, 2000, **65**, 5001. (b) Ref 55.

[165] D. Kahlich, U. Wiechern, J. Lindner, *Propylene Oxide; Ullmann's Encyclopedia of Industrial Chemistry*, Wiley-VCH, Weinheim, 2002, 4-9.

[166] T. Kratz, W. Zeiss, *Peroxide Chemistry*, ed. W. Adam, Wiley-VCH, Weinheim, 2000, 41-59.

[167] N. Ullrich, B. Kolbe, N. Bredemeyer, *Thyssenkrupp Techforum*, 2007, **1**, 38-43.

[168] The theoretical study of MTO derivatives was carried out by Prof. Agustin Galindo of the University of Sevilla. Further details of this study appear in Ref. 199 and the supporting information.

[169] P. D. Vaz, P. J. A. Ribeiro-Claro, *Eur. J. Inorg. Chem.*, 2005, 1836.

[170] W. A. Herrmann, W. Scherer, R. W. Fischer, J. Blümel, M. Kleine, W. Mertin, R. Gruehn, J. Mink, H. Boysen, C. C. Wilson, R. M. Ibberson, L. Bachmann, M. J. Mattner, *J. Am. Chem. Soc.*, 1995, **117**, 3231.

[171] For example see: (a) A. V. Biradar, B. R. Sathe, S. B. Umbarkar, M. K. Dongare, *J. Mol. Cat. A: Chemical*, 2008, **285**, 111-119. (b) D. V. Deubel, J. Sundermeyer, G. Frenking, *Inorg.*

Chem., 2000, **39**, 2314-2320. For an interesting insight into the mechanism of epoxide hydrolysis by methyltrioxorhenium see Ref. 71.

172 M. Herbert, A. Galindo, F. Montilla, *Cat. Comm.*, 2007, **8**, 987-990.

173 E. P. Carreiro, A. J. Burke, *J. Mol. Catal. A: Chem.*, 2006, **249**, 123.

174 O. Bortolini, S. Campestrini, V. Conte, G. Fantin, M. Fogagnolo, S. Maietti, *Eur. J. Org. Chem.*, 2003, 4804.

175 Many of the more active systems are discussed in: *Aziridines and Epoxides in Organic Synthesis*, ed. A. K. Yudin, Wiley-VCH, Weinheim, 2006, Ch. 6. Some effective systems are described in the following: Tungsten: (a) R. Noyori, M. Aoki, K. Sato, *Chem. Commun.*, 2003, 1977-1986. (b) A. L. Villa de P., B. F. Sels, D. E. de Vos, P. A. Jacobs, *J. Org. Chem.*, 1999, **64**, 7267. (c) K. Kamata, K. Yonehara, Y. Sumida, K. Yamaguchi, S. Hikichi, N. Mizuno, *Science*, 2003, **300**, 964. Oxobisperoxotungsten: B. S. Lane, K. Burgess, *Chem. Rev.*, 2003, **103**, 2457–2473 Vanadium: N. Murase, Y. Hoshino, M. Oishi, H. Yamamoto, *J. Org. Chem.*, 1999, **64**, 338. Titanium: B. Notari, *Catal. Today*, 1993, **19**, 163. Manganese/porphyrin: (a) J. T. Groves, M. K. Stern, *J. Am. Chem. Soc.*, 1987, **109**, 3812-3814. (b) C. Ly, D. Vogt, W. Keim, *Chem. Ing. Techn.*, 1989, 61, 646. (c) C. Bolm, *Angew. Chem.*, 1991, **103**, 414-415. Rhenium: See Section 1.3.1 of this document.

176 W. P. Griffith, B. C. Parkin, A. J. P. White, D. J. Williams, *J. Chem Soc. Dalton Trans.*, 1995, 3131-3138.

177 For examples of Mo species acting as catalysts/precursors in the oxidation of tertiary amines see the following: (a) S. L. Jain, J. K. Joseph, B. Sain, *Cat. Lett.*, 2007, **115**, 8-12. (b) J. Kollar, R. S. Barker, *US Pat.*, 3390182, 1968. (c) R. D. Smetana, *US Pat.*, 3657251, 1972.

178 (a) W. P. Griffith, A. M. Z. Slawin, K. M. Thompson, D. J. Williams, *J. Chem. Soc., Chem. Commun.*, 1994, 569-570. (b) F. R. Sensato, Q. B. Cass, E. Longo, J. Zukerman-Schpector, R. Custodio, J. Andrés, M. Z. Hernandes, R. L. Longo, *Inorg. Chem.*, 2001, **40**, 6022-6025.

179 Within this work see the preparation and characterisation of $[Mo(O)(O_2)_2(bpy)]$ (Section 3.6.14) and $[Mo(O)(O_2)_2(bpyO_2)]$ (Section 3.6.15) and the synthesis of the former described in Ref. 184.

180 F. Batigalhia, M. Zaldini-Hernandes, A. G. Ferreira, I. Malvestiti, Q. B. Cass, *Tetrahedron*, 2001, **57**, 9669-9676.

181 S. Das, T. Bhowmick, T. Punniyamurthy, D. Dey, J. Nath, M. K. Chaudhuri, *Tetrahedron Letters*, 2003, **44**, 4915-4917.

182 Regarding imidazole-N-oxides: Discussion of the stable forms of imidazole oxide and some related compounds based on computational models: I. Alkorta, J. Elguero, J. F. Liebman, *Struct. Chem.*, 2006, **17**, 439-444. For preparations of relatively simple imidazole oxide species see: (a) G. Mloston, J. Romanski, M. Jasinski, H. Heimgartner, *Tetrahedron: Asymmetry*, 2009, **20**, 1073-1080. (b) G. Laus, A. Schwaerzler, G. Bentivoglio, M. Hummel, V. Kahlenberg, K. Wurst, E. Kristeva, J. Schutz, H. Kopacka, C. Kreutz, *Zeitschrift fuer Naturforschung, B: Chemical Sciences*, 2008, **63**, 447-464. (c) J. Alcazar, M. Begtrup, A. de la Hoz, *Heterocycles*, 1996, **43**, 1465-1470. (d) J. Alcazar, A. De la Hoz, M. Begtrup, *Mag. Res. Chem.*, 1998, **36**, 296-299. Examples of simple O-metal coordinated imidazole oxide structures

were not apparent in literature though some interesting complexes are described in the following: S. Abuskhuna, M. McCann, J. Briody, M. Devereux, K. Kavanagh, N. Kayal, V. McKee, *Polyhedron*, 2007, **26**, 4573-4580.

183 P. Martín-Zarza, P. Gili, F. V. Rodríguez-Romero, C. Ruiz-Pérez, X. Solans, *Inorg. Chim. Acta*, 1994, **223**, 173-175. The structural data given in this article describes, obviously erroneously, the aqua-pyrazole complex. The bond distances referenced here are assumed to be correct for the aqua-imidazole complex.

184 E. O. Schlemper, G. N. Schrauzer, L. A. Hughes, *Polyhedron*, 1984, **3**, 377-380.

185 For example: Steven D. Burke, Rick L. Danheiser, *Oxidizing and Reducing Agents, Handbook of Reagents for Organic Synthesis*, 1999, Wiley, 84-89; and references therein.

186 P. P. McClellan, *Ind. Eng. Chem.*, 1950, 42, 2402-2407.

187 R. A. Sheldon, *Green Chem.*, 2007, **9**, 1273-1283.

188 R. Wang, Z. Zeng, B. Twamley, M. M. Piekarski, J. M. Shreeve, *Eur. J. Org. Chem.*, 2007, 655-661.

189 M. Nakajima, Y. Sasaki, H. Iwamoto, S. Hashimoto, *Tetrahedron Lett.*, 1998, **39**, 87-88.

190 M. K. Trost, R. G. Bergman, *Organometallics*, 1991, **10**, 1178-1182.

191 H. Mimoun, *Angew. Chem., Int. Ed. Engl.*, 1982, **21**, 734.

192 R. A. Sheldon, J. A. Van Doorn, *J. Organomet. Chem.*, 1975, **94**, 115.

193 (a) K. A. Jørgensen, R. Hoffmann, *Acta, Chem. Scand. B*, 1986, **40**, 411. (b) C. Di Valentin, P. Gisdakis, I. V. Yudanov, N. Rösch, *J. Org. Chem.*, 2000, **65**, 2996. (c) D. V. Deubel, J. Sundermeyer, G. Frenking, *J. Am. Chem. Soc.*, 2000, **122**, 10101.

194 The authors of Ref. 98 present experimental evidence indicating that the discussed bidentate N-donor ligand was poorly dissociating from the oxobisperoxomolybdenum complex. However, note that in later publications from the group this dissociation was determined to probably be rather more facile (see Ref. 99).

195 CSD search (Sep. 2009). An oxobisperoxomolybdenum fragment with two nitrogens bonded to the metal centre, $[Mo(O)(O_2)_2(N)_2]$, encountered nine hits, pertaining only to complexes of bidentate 2,2'-bipyridine, pyrazolylpyridine and oxazolylpyridine type ligands. An oxobisperoxomolybdenum fragment with one nitrogen bonded to the metal centre, $[Mo(O)(O_2)_2(N)]$, encountered a further six new hits, comprising complexes with coordinated imidazole, pyridine, η^2-quinolinate, η^2-salicylaldoximinate and η^2-pyridine carboxylate ligands.

196 All crystal structures described in this work were recorded by Dr. Eleuterio Álvarez of the Instituto de Investigaciones Químicas, CSIC-Universidad de Sevilla, Avda. Américo Vespucio 49, 41092, Sevilla, Spain.

197 L. Vaska, *Acc. Chem. Res.*, 1976, **9**, 175-183.

198 J. A. McGinnety, N. C. Payne, J. A. Ibers, *J. Am. Chem. Soc.*, 1969, **91**, 6301-6310.

199 M. Herbert, A. Galindo, F. Montilla, *Organometallics*, 2009, **28**, 2855-2863.

200 M. Herbert, F. Montilla, A. Galindo, *Inorg. Chem. Commun.*, 2007, **10**, 735-737.

[201] M. Contel, C. Izuel, M. Laguna, P. R. Villuendas, P. F. Alonso and R. H. Fish, *Chem. Eur. J.*, 2003, **9**, 4168.

[202] M. A. McHugh, V. J. Krukonis, *Supercritical Fluid Extraction: Principles & Practice*, Butterworth-Heinemann, Boston, 1994.

[203] SciFinder® Scholar database search (Sep. 2009). Keywords: 'alcohol oxidation' returned almost 79,000 references. Addition of 'supercritical carbon dioxide' reduced this to 111 and subsequent addition of 'copper' to only 3, none of which pertained to copper catalysed alcohol oxidation in $scCO_2$.

[204] During the realization of this work, the X-ray structure of this complex has been reported: F.-Q. Liu, R.-X. Li, L.-S. Sun, G.Y. Liu, *Acta Cryst.*, 2007, E63, m2455.

[205] For example see the assignments for the hydrate complex and relevant discussion in; Y. Mathey, D. R. Greig, D. F. Shriver, *Inorg. Chem.*, 1982, **21**, 3409-3413.

[206] W. J. Evans, J. H. Hain J_r., R. N. R. Broomhall-Dillard, J. W. Ziller, *J. Coord. Chem.*, 1999, **47**, 199-209.

[207] A. F. Lagalante, B. N. Hansen, T. J. Bruno, R. E. Sievers, *Inorg. Chem.*, 1995, **34**, 5781.

[208] See: O. Aschenbrennera, S. Kempera, N. Dahmena, K. Schaberb, E. Dinjusa, *J. Supercrit. Fluids*, 2007, **41**, 179 and references therein.

[209] (a) R. B. Gupta, J.-J. Shim, *Solubility in supercritical carbon dioxide*, CRC Press, 2007. (b) C. Erkey, *J. Supercrit. Fluids*, 2000, **17**, 259. (c) N. G. Smart, T. Carleson, T. Kast, A. A. Clifford, M. D. Burford, C. M. Wai, *Talanta*, 1997, **44**, 137.

[210] W. Cross, Jr., A. Akgerman, C. Erkey, *Ind. Eng. Chem. Res.*, 1996, **35**, 1765.

[211] C. M. Wai, S. Wang, J.-J. Yu, *Anal. Chem.*, 1996, **68**, 3516.

[212] Y. Takeshita, Y. Sato, *J. Supercrit. Fluids*, 2002, **24**, 91.

[213] E. Sais-Galiyev, L. Nikitin, R. Vinokur, M. Gallyamov, M. Kurykin, O. Petrova, B. Lokshin, I. Volkov, A. Khokhlov, K. Schaumburg, *Ind. Eng. Chem. Res.*, 2000, **39**, 4891.

[214] S. Mekki, C. M. Wai, I. Billard, G. Moutiers, C. H. Yen, J. S. Wang, A. Ouadi, C. Gaillard, P. Hesemann, *Green Chem.*, 2000, **57**, 421.

[215] Y. Lin, N. G. Smart, C. M. Wai. *Trends Anal. Chem.*, 1995, **14**, 123.

[216] H. F. Jiang, J.-Y. Tang, A.-Z. Wang, G.-H. Deng, S.-R. Yang, *Synthesis*, 2006, **7**, 1155.

[217] For some examples see: (a) J. Tsuji, *Palladium Reagents and Catalysts*, WileyBlackwell; 2nd revised edition, 2004. (b) J. Tsuji, *Palladium in Organic Synthesis*, Springer, 2005. (c) J.-L. Malleron, J.-C. Fiaud, J.-Y. Legros, *Handbook of Palladium-Catalyzed Organic Reactions*, Elsevier, 1997.

[218] For examples of aerobic alcohol oxidation by Pd(0) nanoparticle catalysts see the following: (a) H. Wu, Q. Zhang, Y. Wang, *Advanced Synthesis & Catalysis*, 2005, **347**, 1356-1360. (b) J. Chen, Q. Zhang, Y. Wang, H. Wan, *Advanced Synthesis & Catalysis*, 2008, **350**, 453-464. (c) Z. Hou, N. Theyssen, W. Leitner, *Green Chem.*, 2007, **9**, 127-132. (d) N. Jamwal, M. Gupta, S. Paul, *Green Chem.*, 2008, **10**, 999-1003. (e) F. Li, Q. Zhang, Y. Wang, *Applied Catalysis, A: General*, 2008, **334**, 217-226; and relevant references therein.

[219] El sistema ha sido descrito en (a): F. Montilla, E. Clara, T. Avilés, T. Casimiro, A. A. Ricardo, M. N. Ponte, *J. Organomet. Chem.*, 2001, **626**, 227. (b) F. Montilla, T. Avilés, T. Casimiro, A. A. Ricardo, M. N. Ponte, *J. Organomet. Chem.*, 2001, **632**, 113.

[220] P. W. Atkins, *Physical Chemistry*, Oxford University Press, 1998.

[221] Cassandra L. Fraser, Natia R. Anastasi, Jaydeep J. S. Lamba, *J. Org. Chem.*, 1997, **62**, 9314-9317.

[222] La síntesis de este producto por otro metodo experimental se encuentra en: U. Kiehne, J. Bunzen, H. Staats, A. Lützen, *Synthesis*, 2007, **7**, 1061-1069.

[223] Basado en la sintesis de 4,4'-diaquil-2,2'-bipiridinas presentado en: D. K. Ellison, R. T. Iwamoto, *Tetrahedron Letters*, 1983, **24**, **1**, 31-32.

[224] Por ejemplo ver: (a) L. J. Csáinyi, *Transition Met. Chem.*, 1989, **14**, 298-302. (b) L. J. Csanyi, I. Horvath, Z. M. Galbacs, *Transition Met. Chem.*, 1989, **14**, 90-94. (c) E. Richardson, *J. Less-Common Mets*, 1960, **2**, 360. (d) G. M. Vol'dman, E. A. Mironova, L. V. Bystrov, *Zhurnal Neorganicheskoi Khimi*, 1990, **35**, 1306-1309.

[225] De hecho hexakisacetatotripaladio en estado solido: A. C. Skapski, M. L. Smart, *Chem. Commun.*, 1970, 658-659.